Inverse scattering problems without phase information

Vladimir Sivkin

INSTITUT POLYTECHNIQUE DE PARIS

NNT : 2023IPPAX062

Thèse de doctorat

Inverse scattering problems without phase information

Thèse de doctorat de l'Institut Polytechnique de Paris
préparée à l'École polytechnique

École doctorale n°574 École doctorale de mathématiques Hadamard (EDMH)
Spécialité de doctorat : Mathématiques appliquées

Thèse présentée et soutenue à Palaiseau, le 6 octobre 2023, par

M. VLADIMIR SIVKIN

Composition du Jury :

Antonin Chambolle Directeur de recherche, Université Paris Dauphine-PSL	Président du jury
Anne de Bouard Directrice de recherche, École polytechnique	Examinatrice
Michael Klibanov Professeur, University of North Carolina at Charlotte	Rapporteur
Roman Novikov Directeur de recherche, École polytechnique	Directeur de thèse
Ozan Öktem Professeur, KTH Royal Institute of Technology, Stockholm	Examinateur
Dimitri Yafaev Professeur émérite, Université Rennes 1	Rapporteur

Remerciements / Acknowledgements

First of all I thank Roman Novikov for his very pedagogical approach in supervising the thesis work. This approach gave me different competences in pure and applied mathematics, presentations, scientific writing, and a lot of other things.

I am very grateful to the members of the jury who have agreed to come to my defense: Antonin Chambolle, Anne de Bouard, and Ozan Öktem. I am also very grateful to the referees Michael Klibanov and Dimitri Yafaev for their reports and for the participation in the thesis jury online. I am extremely honored to have this thesis jury!

I thank very much Antonin Chambolle for supporting my candidature for this PhD position and Nizar Touzi for monitoring the process of the thesis work and for permanent support. I also thank very much Stéphane Nonnenmacher for supporting my thesis work in the framework of EDMH.

I am very grateful to École polytechnique and CMAP already for the internship in 2019 as part of the International Internship Program of École polytechnique. In particular, I thank a lot Elena Murè and Sonia Cordier for managing this international project in my case.

My immense thanks to École polytechnique and CMAP for accepting me for the PhD position and excellent work conditions. I am very grateful to directors of CMAP in the period of my internship and thesis work: Anne de Bouard, Thierry Bodineau, Grégoire Allaire. I am very grateful to Nasséra Naar, Alexandra Liot, and Alexandra Noiret for invaluable administrative help. I thank very much Pierre Straebler for computer support.

I am very thankful to Clothilde Depenoux and Emmanuel Fullenwarth for coordinating my PhD project in EDMH.

I am extremely honored to have a scientific collaboration with Thorsten Hohage within my thesis work.

I thank very much Andrei Shkalikov for valuable scientific discussions and permanent support.

I appreciate very much scientific discussions with Andrey Shurup.

I also appreciate a lot scientific discussions and collaborations with Alexey Agaltsov, Fedor Goncharov, Grigory Sabinin and Rodion Zaytsev.

Beyond the science, I also want to appreciate other important people.

Many thanks to the Darcourt Lezat family for introducing me to traditional french culture and magnificent views of the Pyrenees.

I thank my french teachers Valentina Zhdanova and Elizaveta Nevezhina for wonderful lessons.

Of course, I want to thank my father, my mother, my brother and my sisters for support.

The especial thanks are for my wife Anastasiia Sivkina for motivation to continue and finish this work.

Contents

Préface

Cette thèse consiste en plusieurs articles dans lesquels nous étudions différents aspects du problème de reconstruction de phase pour la transformation de Fourier classique et pour les problèmes de diffusion inverse sans phase pour l'équation de Schrödinger et pour l'équation de Helmholtz.

Cette thèse est basée sur six articles qui peuvent être divisés en deux parties selon la méthode utilisée.

La première partie des articles développe la méthode des diffuseurs de fond dans son application au problème de reconstruction de phase pour la transformation de Fourier classique et à la diffusion inverse sans phase :

I. R.G. Novikov, V. N. Sivkin, Phaseless inverse scattering with background information, Inverse Problems 37.5 (2021): 055011.

II. T. Hohage, R.G. Novikov, V.N. Sivkin, Phase retrieval and phaseless inverse scattering with background information, hal-03806616 (2022).

III. V.N. Sivkin, Approximate Lipschitz stability for phaseless inverse scattering with background information, Journal of Inverse and Ill-posed Problems, https://doi.org/10.1515/jiip-2023-0001 (2023).

La deuxième partie des articles développe l'approche multipoint des problèmes inverses :

IV. R.G. Novikov, V.N. Sivkin, Error estimates for phase recovering from phaseless scattering data, Eurasian Journal of Mathematical and Computer Applications 8.1 (2020): 44-61.

V. R.G. Novikov, V. N. Sivkin, Fixed-distance multipoint formulas for the scattering amplitude from phaseless measurements, Inverse Problems 38.2 (2022): 025012.

VI. R.G. Novikov, V.N. Sivkin, G.V. Sabinin, Multipoint formulas in inverse problems and their numerical implementation, hal-04053473 (2023).

Preface

This thesis consists of several papers in which we study different aspects of phase retrieval problem for the classical Fourier transform and for phaseless inverse scattering problems for the Schrödinger equation and for the Helmholtz equation.

This thesis is based on six papers which can be splitted in two parts depending on the method used.

The first part of articles develops the method of background scatterers in its application to the problem of phase retrieval for the classical Fourier transform and to phaseless inverse scattering:

I. R.G. Novikov, V. N. Sivkin, Phaseless inverse scattering with background information, Inverse Problems 37.5 (2021): 055011.

II. T. Hohage, R.G. Novikov, V.N. Sivkin, Phase retrieval and phaseless inverse scattering with background information, hal-03806616 (2022).

III. V.N. Sivkin, Approximate Lipschitz stability for phaseless inverse scattering with background information, Journal of Inverse and Ill-posed Problems, https://doi.org/10.1515/jiip-2023-0001 (2023).

The second part of articles develops the multipoint approach to inverse problems:

IV. R.G. Novikov, V.N. Sivkin, Error estimates for phase recovering from phaseless scattering data, Eurasian Journal of Mathematical and Computer Applications 8.1 (2020): 44-61.

V. R.G. Novikov, V. N. Sivkin, Fixed-distance multipoint formulas for the scattering amplitude from phaseless measurements, Inverse Problems 38.2 (2022): 025012.

VI. R.G. Novikov, V.N. Sivkin, G.V. Sabinin, Multipoint formulas in inverse problems and their numerical implementation, hal-04053473 (2023).

Chapter 1

Introduction en français

1 Introduction

Les problèmes de diffusion des ondes harmoniques temporelles apparaissent dans de nombreux domaines tels que la théorie quantique, l'imagerie médicale, la géophysique, les contrôles non destructifs, les radars. Le problème de diffusion directe consiste à déterminer la solution de diffusion, compte tenu de l'objet et de son propriété physique, tandis que le problème de diffusion inverse consiste à déterminer l'objet et/ou son propriété physique à partir des informations de mesure de la solution de diffusion.

La théorie standard de la diffusion inverse traite principalement du cas phasé (c'est-à-dire le cas où des mesures de phase sont également disponibles); voir, par exemple, [14], [15], [49].

Cependant, en raison de la règle de Born en mécanique quantique, les valeurs complexes de la fonction d'onde n'ont pas d'interprétation physique directe, alors que les valeurs absolues au carré de cette fonction admettent une interprétation probabiliste et peuvent être directement mesurées.

De même, en optique et en imagerie par rayons X, les détecteurs modernes peuvent mesurer l'intensité des photons (c'est-à-dire des informations sans phase), tandis que les mesures d'informations de phase sont beaucoup plus difficiles (ou actuellement impossibles) en raison de la longueur extrêmement courte de l'onde. Voir, par exemple, [11], [19], [23], [50], [61].

Par conséquent, il est particulièrement important d'étudier les problèmes de reconstruction à partir de données sans phase. Puisqu'il n'y a que «la moitié» des données (c'est-à-dire uniquement l'amplitude, pas de phase), ces problèmes semblent être beaucoup plus compliqués dans différents sens. Par exemple, pour de nombreux problèmes inverses sans phase, il n'y a pas de solution unique même pour le cas linéarisé de l'approximation de Born.

Cette approche remonte, au moins, aux travaux de Perutz sur l'analyse aux rayons X de l'hémoglobine, honorés par le prix Nobel de chimie ; voir [55].

Notons que dans l'approximation de Born, de nombreux problèmes de diffusion inverse sans phase se simplifient en le problème de reconstruction de phase consistant à reconstruire le potentiel à partir de la valeur absolue de sa transformation Fourier. Nos résultats sur le dernier problème de l'analyse de Fourier sont résumés dans la sous-section 2.1. Puis dans la sous-section 2.2 nous présentons les résultats généraux récents dans le domaine de l'analyse asymptotique, où certains de ces résultats ont également été obtenus dans le cadre de cette thèse.

D'autres résultats de thèse utilisent essentiellement les méthodes mathématiques générales résumées dans les sous-sections 2.1 et 2.2. Ces résultats de thèse incluent de nouveaux algorithmes sur les problèmes de diffusion inverse sans phase non-linéarisés et sont résumés dans les sections 4, 5.

La présentation complète de nos résultats est donnée dans les articles I-VI.

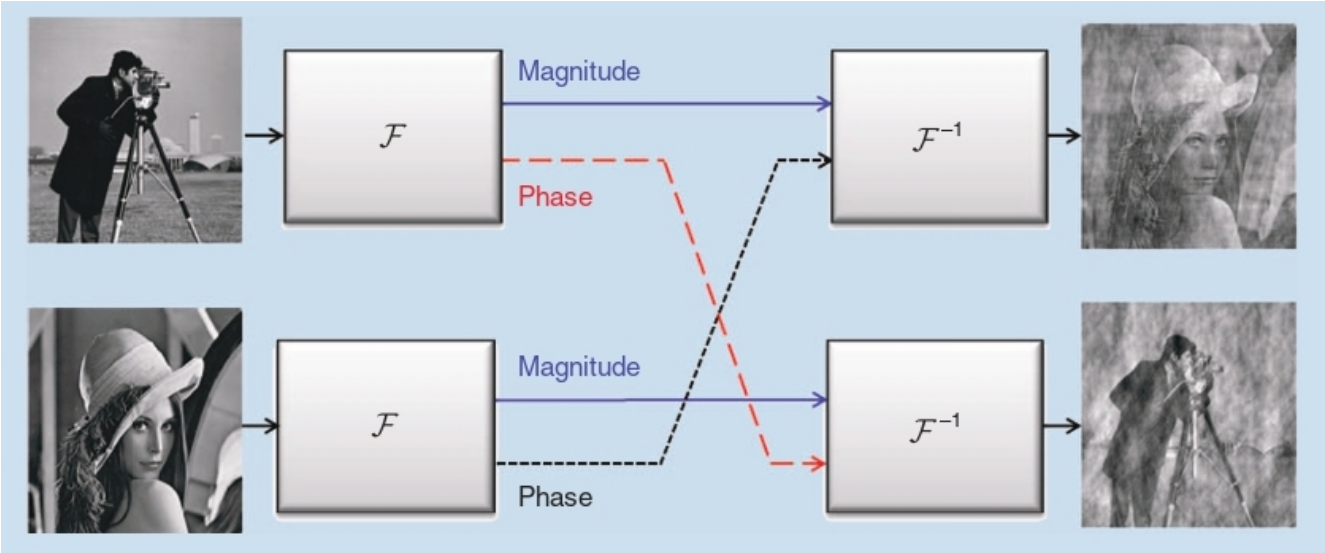

Figure 1.1: [61] L'importance de la phase de Fourier. Deux images, un caméraman et Lenna, sont transformées par Fourier. Après avoir échangé leurs phases, elles sont transformées de Fourier inverse. Le résultat démontre clairement l'importance des informations de phase pour la récupération d'image.

2 Quelques méthodes mathématiques générales

2.1 Problème de reconstruction de phase

Dans cette sous-section, nous discutons du problème de reconstruction de phase pour la transformation de Fourier classique. Ce problème se pose comme une approximation linéaire pour différents problèmes de diffusion inverse sans phase. Ce problème est également d'un grand intérêt indépendant dans le cadre de l'analyse de Fourier.

Nous considérons la transformation de Fourier de la fonction à valeurs complexes v :

$$\widehat{v}(p) = \mathcal{F}v(p) = \frac{1}{(2\pi)^d} \int_{\mathbb{R}^d} e^{ipx} v(x) dx, \quad p \in \mathbb{R}^d. \tag{2.1}$$

Le problème de reconstruction de phase classique est formulé comme suit :

Problem 1. *Trouver v à partir de $|\widehat{v}|^2$.*

Le terme 'problème de reconstruction de phase' signifie que le problème 1 est équivalent à la reconstruction de $Angle(\widehat{v})$ à partir de $Abs(\widehat{v})$.

Le problème 1 est mal posé : il n'a pas de solution unique, même aux translations et aux symétries élémentaires, voir [65] pour les détails. La raison en est le manque d'informations (de phase). Voir aussi Figure 1.1 pour illustration.

Pour compenser les informations de phase manquantes $\widehat{v}/|\widehat{v}|$, on suppose soit des informations a priori sur v ou des données supplémentaires. De telles inversions de la transformée de Fourier à partir de données sans phase sont beaucoup plus compliquées que la inversion de la transformation de Fourier à partir de données phasées. Des exemples d'informations a priori incluent connaissance (approximative) de $supp\, v$, contraintes comme $|v| = 1$ ou $v \geq 0$, et connaissance de v sur une partie du domaine. Dans cette thèse nous concentrez-vous sur la première et la dernière de ces options. Nous nous référons aux monographies [25, 8], aux articles de synthèse [20, 29, 34, 49, 61], aux articles [7], [16], [31] et aux références dedans.

Plus précisément, on considère le problème suivant :

Problem 2. *(A) Reconstruire une fonction v à partir de $|\widehat{v} + \widehat{w}|^2$ sur B_R pour une fonction connue w sous l'hypothèse a priori que $supp\, v$ et $supp\, w$ sont compacts et suffisamment séparés.*

(B) Reconstruire v à partir de $|\widehat{v}|^2$ et $|\widehat{v}+\widehat{w_j}|^2$, $j=1,\dots,n$, sur B_R pour certaines fonctions connues appropriées $w_1,...,w_n$ séparées de v.

Ici

$$B_R=\{x\in\mathbb{R}^d:\quad |x|\le R\}. \tag{2.2}$$

De plus, nous supposons que v et différents diffuseurs de fond non nuls w_1, ..., w_n sont de la forme

$$\begin{aligned} &v,\, w_j\in L^{1,loc}(\mathbb{R}^d),\quad w_j\not\equiv 0,\quad supp\, v\subseteq D,\quad supp\, w_j\subseteq\Omega_j,\\ &D,\,\Omega_j \text{ sont des domaines bornés convexes ouverts dans } \mathbb{R}^d,\quad D\cap\Omega_j=\varnothing. \end{aligned} \tag{2.3}$$

Le problème 2(B) a été considéré notamment dans [43, 45, 3, 5]. De plus, des considérations connexes remontent, au moins, à [55]. Le problème 2(A) a été étudié dans [52, 24]. D'autres recherches liées à ce problème peuvent être trouvées dans [56, 37]. Cette thèse inclut, en particulier, de nouveaux résultats mathématiques et numériques de [52, 24] sur le problème 2(A) et sur le problème 2(B) pour $n=1$.

Soit

$$D-\Omega=\{x-y:\ x\in D,\, y\in\Omega\}, \tag{2.4}$$

et $\chi_{D-\Omega}(x)$ une fonction caractéristique (indicatrice) de l'ensemble $D-\Omega$.

Cette thèse inclut notamment le résultat suivant de [52], pour $d\ge 1$:

Theorem 2.1. *([52]) Soit v et $w=w_1$ satisfait (2.3) avec $\Omega=\Omega_1$, et $dist(D,\Omega)>diam\, D$. Alors $|\widehat{v}+\widehat{w}|^2$ et w déterminent uniquement v par les formules*

$$\begin{aligned} &\widehat{v}(p)=(\overline{\mathcal{F}w(p)})^{-1}\mathcal{F}q(p),\\ &q(x):=\chi_{D-\Omega}(x)\left(u(x)-(2\pi)^{-d}\int_\Omega w(x+y)\overline{w(y)}dy\right),\\ &u(x):=\mathcal{F}^{-1}(|\mathcal{F}(v+w)|^2)(x). \end{aligned} \tag{2.5}$$

Si nous n'avons que $dist(D,\Omega)>0$, alors $|\widehat{v}|^2$, $|\widehat{v}+\widehat{w}|^2$, et w déterminent de manière unique v via la formule (2.5), où u est remplacé par

$$u(x):=\mathcal{F}^{-1}(|\mathcal{F}(v+w)|^2-|\mathcal{F}v|^2)(x). \tag{2.6}$$

En fait, le théorème 2.1 dans sa première partie est une formalisation mathématique appropriée de certaines considérations de [37] lié à la recherche de v et w à partir de $|\widehat{v}+\widehat{w}|^2$, à condition que $supp\, v$ et $supp\, w$ sont suffisamment disjoints, pour $d=2$.

On peut voir que le théorème 2.1 résout, en particulier, le problème 1, si $supp\, v\subseteq(D\cup\Omega)$, où $dist(D,\Omega)>diam\, D$, et v est a priori connu sur Ω.

De plus, les formules du théorème 2.1 conduisent à des reconstructions à partir de données de Fourier sans phase avec une efficacité théorique et numérique similaire à la reconstruction à partir de données de Fourier $\widehat{v}$ avec des informations de phase, voir [52] , [24], [62] et Section 4 pour plus de détails.

La figure 1.2 illustre notre reconstruction numérique de v à partir de $|\widehat{v}+\widehat{w}|^2$ limité à B_R avec un fond connu w.

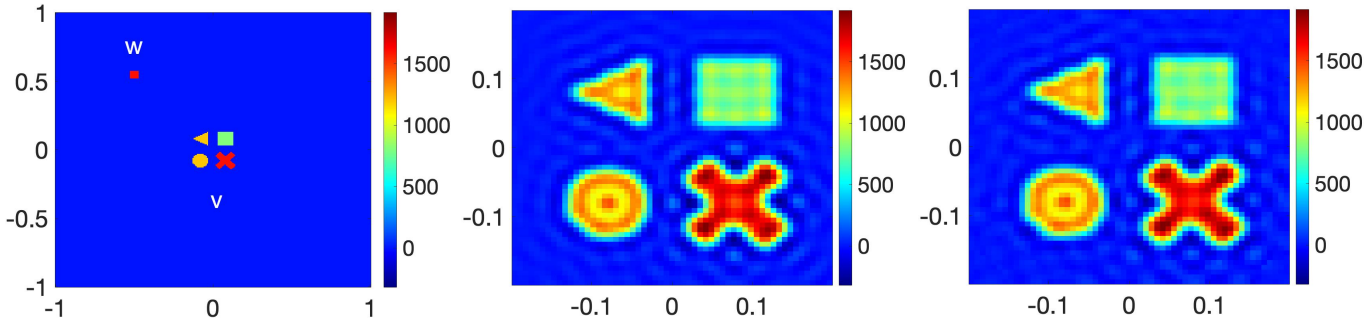

(a) Notre $v + w$.

(b) Reconstruction à partir de données phasées $\widehat{v}$.

(c) Reconstruction à partir de données sans phase $|\widehat{v} + \widehat{w}|^2$.

Figure 1.2: Comparaison des reconstructions de v à partir d'une transformation de Fourier phasée et sans phase.
(a) Constante par morceaux suffisamment séparée v et w.
(b) Reconstruction à partir de données phasées $\widehat{v}$ données sur un certain B_R.
(c) Reconstruction à partir de données sans phase $|\widehat{v} + \widehat{w}|^2$ données sur le même B_R.

2.2 Formules multipoints

De nombreuses fonctions de la théorie du potentiel, de la théorie de la diffusion et d'autres domaines admettent des développements asymptotiques de la forme

$$z(s) = z_{main}(s) + \mathcal{O}(s^{-N}) = \sum_{j=1}^{N} \frac{a_j}{s^{j-1}} + \mathcal{O}(s^{-N}), \text{ lorsque } s \to +\infty, \tag{2.7}$$

où $s \in (\sigma, +\infty)$, pour certains $\sigma > 0$, et a_j sont des nombres complexes ; voir, par exemple, [1], [35], [38], [46], [47], [53], [68]. De plus, dans certains cas, l'information la plus importante est contenue dans a_1 (et/ou certains coefficients principaux suivants), alors que $z(s)$ est mesuré en plusieurs points $s \in (\sigma, +\infty)$.

Pour les fonctions z vérifiant (2.7) le travail [46] considère, en particulier, le problème de trouver a_1 de $z(s)$ donné en n points $s_j \in [r, +\infty)$, $j = 1, ..., n$ de la forme

$$\begin{aligned} &s_j = s + \tau_j, \quad \vec{\tau} := (\tau_1, ..., \tau_n), \\ &0 = \tau_1 < \tau_2 < ... < \tau_n \text{ sont fixés.} \end{aligned} \tag{2.8}$$

Notez aussi qu'il existe une autre géométrie des points de s_j, voir [46].

Supposons que $N \geq 2n - 1$. Alors les formules suivantes sont vraies ([46]) :

$$\begin{aligned} a_1 &= a_{1,n}(s, \vec{\tau}) + \mathcal{O}(s^{-n}), \qquad \text{as } s \to +\infty, \\ a_{1,n}(s, \vec{\tau}) &= \sum_{j=1}^{n} y_j(s, \vec{\tau}) z(s + \tau_j), \end{aligned} \tag{2.9}$$

où

$$y_j(s, \vec{\tau}) = \frac{(-1)^{n-j}(s + \tau_j)^{n-1}}{\alpha_j(\vec{\tau})\beta_{n,j}(\vec{\tau})}, \quad 1 \leq j \leq n, \quad y = (y_1, ..., y_n), \tag{2.10}$$

$$\begin{aligned} &\alpha_j(\vec{\tau}) := \prod_{i=1}^{j-1} (\tau_j - \tau_i) \quad \text{for} \quad 1 < j \leq n, \quad \alpha_1(\vec{\tau}) = 1, \\ &\beta_{n,j}(\vec{\tau}) := \prod_{i=j+1}^{n} (\tau_i - \tau_j) \quad \text{for} \quad 1 \leq j < n, \quad \beta_{n,n}(\vec{\tau}) = 1. \end{aligned} \tag{2.11}$$

Les formules multipoints (2.9) convergent rapidement, pour n assez grand, et ont une structure simple, mais elles sont très instables au bruit pour de grands s. La raison en est que les coefficients $y_j(s,\vec{\tau})$ dans (2.10) se comportent comme

$$y_j(s,\vec{\tau}) = \mathcal{O}(s^{n-1}), \quad \text{lorsque } s \to +\infty. \tag{2.12}$$

La figure 1.3 illustre ces effets sur le plus simple $z(s) = s/(s+1)$. Dans la figure 1.3 nous présentons $\widetilde{a}_{1,n}(s) = a_{1,n}(s-\tau_n,\vec{\tau})$. Notez que pour chaque $n = 1,2,3$, ces $\widetilde{a}_{1,n}(s)$ sont reconstruits à partir de $n = 1,2,3$ points, mais avec le même point maximal s. La figure 1.3(a) montre que les formules à deux et trois points sont plus précises que la reconstruction à un point. La figure 1.3(b) montre que même pour $n = 3$, la reconstruction est très instable même pour s moyen.

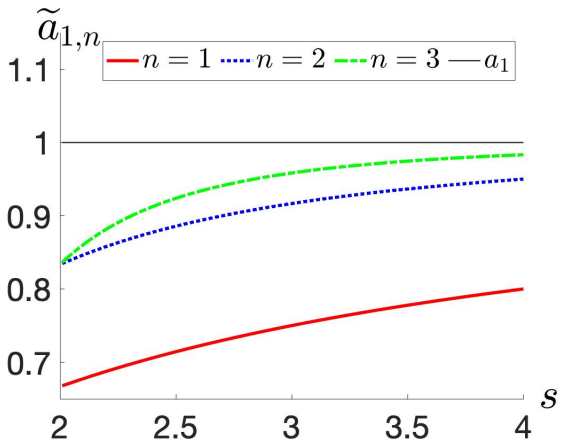

(a) Données exactes. Pas de régularisation.

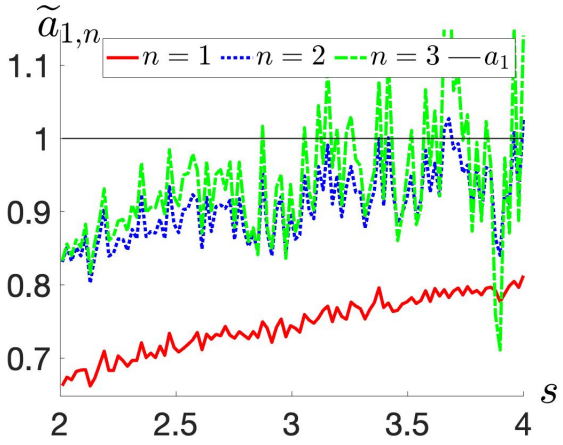

(b) Données bruyantes. Pas de régularisation.

Figure 1.3: ([54]) n-point reconstructions $\widetilde{a}_{1,n}(s) = a_{1,n}(s-\tau_n,\vec{\tau})$ de $a_1 = 1$ pour $z(s) = s/(s+1)$ avec $\tau_j = j-1$, $j = 1,...,n$.
(a) Le cas des données exactes. Les formules à deux et trois points convergent rapidement vers la valeur exacte.
(b) Le cas des données bruitées simulées par la formule (2.13). Les formules à deux et trois points sont instables au bruit.

Compte tenu de l'instabilité susmentionnée, dans [54] nous avons notamment proposé une méthode de régularisation des formules (2.9) pour le cas des données bruitées. Plus précisément, nous supposons que le les données $z(s_j)$ contiennent le bruit aléatoire de la forme

$$\zeta(s) = z_{noisy}(s) = z(s) + \varepsilon N(s), \tag{2.13}$$

où les variables aléatoires $N(s)$ sont i.i.d. pour différents s, l'espérance mathématique est $\mathbb{E}(\zeta(s)) = z(s)$, la dispersion est $\mathbb{D}(\zeta(s)) = \varepsilon^2$.

Afin de rendre applicables les formules multipoints, nous proposons une méthode de régularisation avec un paramètre r. Dans notre régularisation, nous remplaçons la formule (2.9) par

$$\tilde{a}^r_{1,n} = \sum_{j=1}^{n} y^r_j(s,\vec{\tau}) z(s_j(s)), \tag{2.14}$$

où $y^r = (y^r_1,...,y^r_n)$ est construit en [54] et ne dépend que de n et r, et $r \in [n^{-1/2}, \|y\|]$, où y est de (2.10).

Notons que la reconstruction $\tilde{a}^r_{1,n}$ a les propriétés suivantes :

- pour la fonction sans bruit z, la reconstruction régularisée est aussi exacte que possible ;

- la dispersion de reconstruction $a^r_{1,n}$ à partir de données bruitées est bornée par

$$\mathbb{D}(a^r_{1,n}(s,\vec{\tau})) \leq r^2\varepsilon^2 \quad \text{indépendamment de } s. \tag{2.15}$$

Dans notre construction ([54, Section 5]), le paramètre de régularisation $r \in [\frac{1}{\sqrt{n}}, \|y\|]$, pour $y = (y_1, ..., y_n)$ de (2.10). Ici $r = n^{-1/2}$ correspond à la régularisation la plus forte, et $r = \|y\|$ correspond à aucune régularisation.

Figures 1.4(a), 1.4(b) dans leur comparaison avec Figures 2.3(a), 1.3(b) illustrent l'efficacité de notre régularisation (2.14).

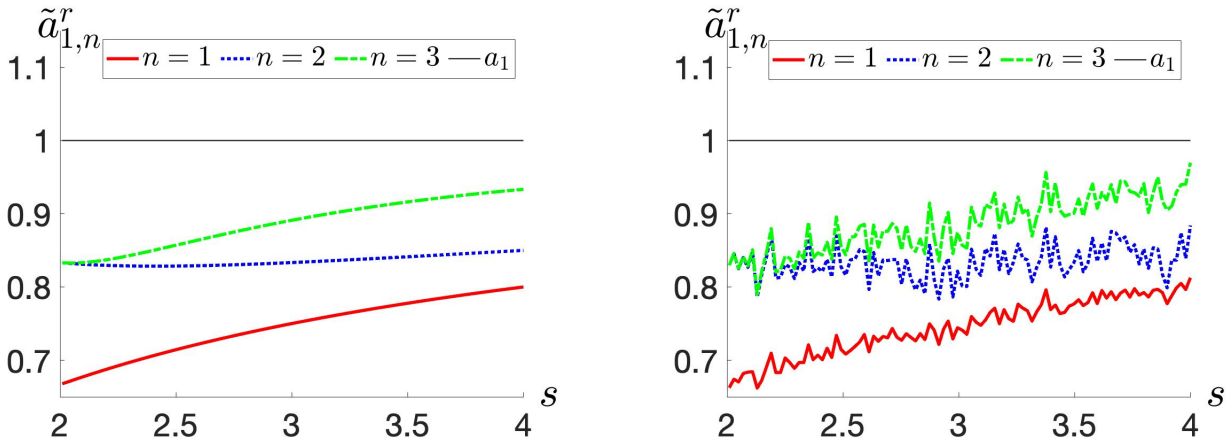

(a) Données exactes. Régularisation. (b) Données bruyantes. Régularisation.

Figure 1.4: ([54]) Reconstructions régularisées n-points $\tilde{a}^r_{1,n}(s) = a^r_{1,n}(s - \tau_n, \vec{\tau})$ de $a_1 = 1$ pour $z(s) = s/(s+1)$ avec $\tau_j = j - 1$, $j = 1, ..., n$. Paramètre de régularisation $r = \sqrt{5}$.
(a) Le cas des données exactes. Les formules régularisées à deux et trois points convergent vers la valeur exacte, mais pas aussi rapidement que sur la figure 1.3(a).
(b) Le cas de données bruitées simulées par la formule (2.13). Les formules régularisées à deux et trois points sont stables au bruit.

Ainsi, dans le cadre de cette thèse, nous avons observé que les formules exactes (2.9) sont très instables au bruit aléatoire (pour $n \geq 2$ et s suffisamment grand) et proposé une régularisation efficace de ces formules multipoints. Cette thèse inclut également des résultats théoriques et numériques sur les applications des formules multipoints précitées à la diffusion inverse phasée et sans phase, voir Section 5.

3 Problèmes de diffusion directe et inverse

3.1 Formulation de problèmes

On considère l'équation de Schrödinger stationnaire

$$-\Delta\psi + v(x)\psi = E\psi, \quad x \in \mathbb{R}^d, \quad d \geq 2, \quad E > 0, \tag{3.1}$$

où Δ est le Laplacien en x, et

$$v \in L^\infty(\mathbb{R}^d), \quad supp\, v \subseteq \mathcal{U}, \quad \mathcal{U} \subset \mathbb{R}^d \text{ est ouvert et borné.} \tag{3.2}$$

L'équation de Schrödinger (3.1), sous hypothèses (3.2), apparaît dans la modélisation de l'interaction d'une particule de mécanique quantique non relativiste à énergie fixe E avec un objet macroscopique contenu dans D, où v est le potentiel de cette interaction. Ici, nous supposons que

$\hbar^2/(2m) = 1$, où $\hbar$ est la constante de Planck réduite et m est la masse de la particule. Pour plus de détails sur un tel modèle dans le cadre de la tomographie électronique, voir par exemple [19].

L'équation (3.1) peut également être considérée comme l'équation de Helmholtz harmonique en temps de l'acoustique et de l'électrodynamique, voir, par exemple, [24], [60] pour plus de détails

Pour l'équation (3.1), sous condition (3.2), on considère les solutions diffusantes $\psi^+ = \psi^+(x,k)$, $k \in \mathbb{R}^d$, $k^2 = E$, spécifié par la condition de rayonnement de Sommerfeld sur $\psi^+(x,k) - e^{ikx}$. Les fonctions ψ^+ ont le développement de type Atkinson (en remontant à [1]) :

$$\psi^+(x,k) = e^{ikx} + \frac{e^{i|k||x|}}{|x|^{(d-1)/2}} \left(\sum_{j=1}^{N} \frac{f_j(k, |k|\frac{x}{|x|})}{|x|^{j-1}} + \mathcal{O}\left(\frac{1}{|x|^N}\right)\right), \quad |x| \to +\infty, \quad N \in \mathbb{N}, \tag{3.3}$$

uniformément dans $x/|x|$. Ici, le coefficient f_1 a une importance physique particulière et est connu comme l'amplitude de diffusion pour l'équation (3.1). Notez que la fonction $f_1 = f_1(k,l)$ est définie sur la variété

$$\mathcal{M}_E = \{k,\, l \in \mathbb{R}^d : \quad k^2 = l^2 = E\} = \mathbb{S}^{d-1}_{\sqrt{E}} \times \mathbb{S}^{d-1}_{\sqrt{E}}, \tag{3.4}$$

où E est l'énergie dans l'équation (3.1). Notez également que dans certaines formules, il est pratique de présenter f_1 comme

$$f_1(k,l) = c(d,|k|) f(k,l), \quad c(d,|k|) = -\pi i(-2\pi i)^{(d-1)/2}|k|^{(d-3)/2} \text{ for } \sqrt{-2\pi i} = \sqrt{2\pi}e^{-i\pi/4}. \tag{3.5}$$

Pour plus d'informations sur ψ^+ et f, voir, par exemple, [10], [44] et leurs références.

En particulier, $\sigma = |f(k,l)|^2$ est connue sous le nom de section efficace de diffusion différentielle pour l'équation (3.1). De manière similaire avec les fonctions d'onde ψ^+, les valeurs complexes de f n'ont pas d'interprétation physique directe, alors que $|f|^2$ admet une interprétation probabiliste et peut être mesuré expérimentalement ; voir, par exemple, [11], [18]. En particulier, la section efficace de diffusion différentielle $\sigma = |f(k,l)|^2$ décrit la densité de probabilité de diffusion d'une particule d'impulsion initiale k dans la direction $l/|l| \neq k/|k|$. De même, dans l'électromagnétisme de l'optique et des rayons X (modélisé dans le cadre de l'équation harmonique de Helmholtz), seuls $|\psi^+|^2$ et $\sigma = |f|^2$ peuvent être mesurés directement par des dispositifs techniques modernes.

L'amplitude de diffusion f contient beaucoup d'informations sur le diffuseur v. En particulier, selon la formule de Born-Faddeev, nous avons ceci :

$$f(k,l) = \widehat{v}(p) + \mathcal{O}(E^{-1/2}) \quad \text{lorsque } E \to +\infty, \quad (k,l) \in \mathcal{M}_E, \quad k - l = p; \tag{3.6}$$

voir, par exemple, [10].

On considère notamment les problèmes suivants :

Problem 3. *Trouver ψ^+ et f à partir de v.*

Problem 4. *(A) Trouver v à partir de f. (B) Trouver f à partir de ψ^+. (C) Trouver v à partir de ψ^+.*

Le problème 3 est le problème de diffusion directe pour l'équation de Schrödinger (3.1). Le problème 4(A) est le problème classique de diffusion inverse en champ lointain. Les problèmes 3 et 4(A) sont étudiés de manière très détaillée dans la littérature ; voir, par exemple, [10], [18], [44]. Et de nouveaux résultats importants sur le Problème 4(A) continuent d'apparaître ; voir, par exemple, [47], [49], [54]. Les problèmes 4(B) et 4(C) sont également étudié dans des publications anciennes et récentes; voir, par exemple, [9], [46], [54] (où [54] est rempli dans le cadre de cette thèse).

Dans cette thèse, nous nous concentrons sur les analogues sans phase des problèmes 4(A)–(C). Plus précisément, nous considérons les problèmes 5 et 6 formulés ci-dessous.

Problem 5. *(A) Trouvez v à partir de ses données de diffusion sans phase $|f[v+w]|^2$ et de son fond w.*

(B) Trouver v à partir des données de diffusion sans phase $|f[v]|^2$, $|f[v+w_1]|^2$, ... $|f[v+w_n]|^2$, et un fond approprié diffuseurs w_1,...,w_n.

Dans le cas linéarisé de l'approximation de Born Le problème 5 se réduit à Problème 2.

Le problème 5(A) avec $w = 0$ est mal posé, de la même manière que le problème 1. Les problèmes 5(A), (B) peuvent être considérés comme des versions non linéaires des problèmes 2(A), (B). Actuellement, les études mathématiques des Problèmes 5(A), (B) ont commencé assez récemment dans [45], [3] , [5], [53] pour le problème 5(B), et dans [52], [24] pour le problème 5(A) (où les travaux [52], [24] sont réalisés dans le cadre de cette thèse).

Problem 6. *(A) Trouver $f(k,l)$ à partir de $|\psi^+(x,k)|^2$ aux points appropriés x tels que $x \in \mathbb{R}^d \setminus D$ et $x/|x| = l/|l|$.*

(B) Trouver v à partir de $|\psi^+|^2$ correctement donné en dehors de D.

Le problème 6(A) est un problème de récupération de phase, tandis que le problème 6(B) est la diffusion inverse sans phase problème en champ proche. Ces problèmes sont notamment traités dans [32, 42, 43, 46, 47, 48, 51, 53, 54] (où des travaux [51, 53, 54] sont réalisés dans le cadre de cette thèse). L'approche multipoint mentionnée dans la sous-section 2.2 admet des applications efficaces à ces problèmes.

En plus des problèmes 5 et 6, il existe également d'autres formulations possibles de phase problèmes de récupération et de diffusion inverse sans phase pour l'équation (3.1) et pour d'autres équations des propagations d'ondes ; voir [30, 28, 33, 57, 58, 59, 67] et leurs références.

3.2 Préliminaires sur la diffusion directe

Les solutions de diffusion ψ^+ satisfaisant (3.1), (3.3) peuvent être trouvées à partir de l'équation intégrale de Lippmann-Schwinger :

$$\psi^+(x,k) = e^{ikx} + \int_D G^+(x-y,k)v(y)\psi^+(y,k)dy, \qquad x,\, k \in \mathbb{R}^d, \quad k^2 = E, \tag{3.7}$$

où

$$G^+(x,k) = -(2\pi)^{-d} \int_{\mathbb{R}^d} \frac{e^{i\xi x}d\xi}{\xi^2 - x^2 - i0}, \tag{3.8}$$

voir, par exemple, [10], [36]. Notons que

$$G^+(x,k) = \frac{e^{i|k||x|}}{2i|k|} \text{ pour } d=1; \quad G^+(x,k) = -\frac{i}{4}H_0^1(|x||k|) \text{ pour } d=2; \tag{3.9}$$
$$G^+(x,k) = -\frac{e^{i|k||x|}}{4\pi|x|} \text{ pour } d=3;$$

où H_0^1 est la fonction de Hankel du premier type.

En fait, en plus de (3.2), on suppose que, pour $E > 0$ fixé,

$$\text{l'équation (3.7) est uniquement résoluble pour } \psi^+(\cdot,k) \in L^\infty(D). \tag{3.10}$$

Si v satisfait (3.2) et est réel, alors (3.10) est satisfait automatiquement.

À son tour, l'amplitude de diffusion f peut être trouvée à partir de v et ψ^+ via

$$f(k,l) = (2\pi)^{-d} \int_D e^{-ily}v(y)\psi^+(y,k)dy, \tag{3.11}$$

où $k,\, l \in \mathbb{R}^d$, $k^2 = l^2 = E > 0$; voir, par exemple, [10].

Le problème 3 peut être résolu en utilisant l'équation (3.7) et la formule (3.11). Certaines des propriétés théoriques importantes de cette solution, y compris (3.6), découlent de l'estimation d'Agmon sur G^+, voir, par exemple [44]. Un algorithme numérique efficace pour résoudre (3.7) est donné en [64].

3.3 Préliminaires en diffusion inverse phasée

On rappelle que dans l'approximation de Born pour un petit v, pour $d \geq 2$, l'amplitude de diffusion f sur $\mathcal{M}_E$ se réduit à la transformation de Fourier $\widehat{v}$ sur la boule $B_{2\sqrt{E}}$ via la formule

$$f(k,l) \approx \widehat{v}(p), \quad (k,l) \in \mathcal{M}_E, \quad p \in B_{2\sqrt{E}}, \quad p = k - l, \tag{3.12}$$

qui est semblable à (3.6).

De plus, pour u_E^1 défini par

$$u_E^1(x) := \int_{B_{2\sqrt{E}}} e^{-ipx} \widehat{v}(p) dp, \tag{3.13}$$

on a que

$$\|v - u_E^1\|_{L^\infty(\mathbb{R}^d)} = \mathcal{O}(E^{-\alpha}), \quad \text{lorsque } E \to +\infty, \quad \text{avec } \alpha := \frac{1}{2}(m-d), \tag{3.14}$$

si $v \in W^{m,1}(\mathbb{R}^d)$, où $W^{m,1}(\mathbb{R}^d)$ dénote les fonctions m-lisses dans $L^1(\mathbb{R}^d)$. Pour plus de détails sur la reconstruction monochromatique linéarisée u_E, voir, par exemple, [49].

La première solution générale du problème 4(A), $d \geq 2$, sans supposer que v est petit, remonte à [17] et est basé sur la formule (3.6).

Cependant, la formule (3.12) ne donne aucune méthode pour reconstruire v à partir de f sur $\mathcal{M}_E$ avec le erreur inférieure à $\mathcal{O}(E^{-1/2})$ même si $v \in \mathcal{S}(\mathbb{R}^d)$, où $\mathcal{S}$ représente la classe Schwartz. En appliquant la transformation de Fourier inverse $\mathcal{F}^{-1}$ aux deux côtés de (3.12), on peut obtenir une formule linéaire explicite pour $u^1 = u_E^1(x)$ en termes de f sur $\mathcal{M}_E$, où

$$\begin{aligned} &u_E^1(x) = v(x) + \mathcal{O}(E^{-\alpha_1}), \quad E \to +\infty, \\ &\alpha_1 = (m-d)/(2m), \quad \text{si } v \in W^{m,1}(\mathbb{R}^d). \end{aligned} \tag{3.15}$$

On peut voir que $\alpha_1 \leq 1/2$ même si $m \to +\infty$.

Un point important est que cette approximation u_1 peut être essentiellement améliorée itérativement en utilisant le lemme suivant :

Lemma 3.1. *([44]). Soit v, v_0 satisfait (3.2), et $v = v_0$ sur $\mathbb{R}^d \setminus D$, où D est un sous-domaine de $\mathcal{U}$. Soit v_{appr}^E une approximation de v telle que :*

$$\begin{cases} |v_{appr}^E(x) - v(x)| = \mathcal{O}(E^{-\alpha}), & x \in D, \quad \textit{pour certain } \alpha > 0, \\ v_{appr}^E(x) = v_0(x), & x \in \mathbb{R}^d \setminus D. \end{cases} \tag{3.16}$$

Donc, pour $(k,l) \in \mathcal{M}_E$,

$$\left| f[v](k,l) - f[v_{appr}^E](k,l) + \widehat{v}_{appr}^E(k-l) - \widehat{v}(k-l) \right| = \mathcal{O}(E^{-\alpha - \frac{1}{2}}). \tag{3.17}$$

Ici, $f[v]$ et $f[v_{appr}^E]$ désignent l'amplitude de diffusion pour v et v_{appr}^E (respectivement) ; $\widehat{v}_{appr}^E$ est la transformation de Fourier de v_{appr}^E.

Notons que les conditions (3.2) sont plus fortes que les hypothèses utilisées dans [44].

Le fait est que le taux de convergence dans (3.17) est plus élevé que dans (3.16) comme $E \to +\infty$. Cela conduit au schéma suivant de [44] pour les reconstructions itératives u_E^j de v à partir de $f[v]$:

$$f[v] \xrightarrow{(3.6)} u_E^1 \xrightarrow{(3.7),(3.11)} f[u_E^1] \xrightarrow{(3.17)} \widehat{u}_E^2 := \widehat{u}_E^1 + f[v] - f[\widehat{u}_E^1] \xrightarrow{(3.7),(3.11)} f[u_E^2] \to u_E^3 \to \dots \tag{3.18}$$

De plus, si

$$v - v_0 \in W^{m,1}(\mathbb{R}^d), \tag{3.19}$$

donc ([44]):

$$\begin{aligned} &\|v - u_E^j\|_{L^\infty(D)} = \mathcal{O}(E^{-\alpha_j}) \quad \text{lorsque } E \to +\infty, \\ &\alpha_1 := \frac{m-d}{2m}, \quad \alpha_j := \left(1 - \left(\frac{m-d}{m}\right)^j\right) \frac{m-d}{2d}, \quad j \geq 1. \end{aligned} \tag{3.20}$$

De plus, on peut voir que

$$\begin{aligned} &\alpha_j \to \alpha_\infty := \frac{m-d}{2d} \quad \text{lorsque } j \to +\infty, \\ &\alpha_j \to \frac{j}{2} \quad \text{lorsque } m \to +\infty, \\ &\alpha_\infty \to +\infty \quad \text{lorsque } m \to +\infty. \end{aligned} \tag{3.21}$$

Donc, la convergence de u_E^j vers v dans (3.15), (3.20), comme $E \to +\infty$, est considérablement meilleur pour $j > 1$ que pour $j = 1$, au moins, pour les gros m et j.

Notons que seul $f|_{\Gamma_E}$ est utilisé dans les résultats de reconstruction mentionnés ci-dessus. Ici, Γ_E est un sous-ensemble $d-$dimensionnel approprié de $\mathcal{M}_E$, voir [52] pour plus de détails.

La reconstruction monochromatique itérative de [44] est implémentée numériquement dans [6], [63] pour $d = 2$ et $v_0 \equiv 0$. Pour d'autres reconstructions de diffusion inverse de phase monochromatique pour l'équation (3.1) et l'équation de Helmholtz, voir, par exemple, [4], [12], [22], [49].

Notons que les algorithmes de reconstruction de [52], [24] réalisés dans le cadre des études de cette thèse sur le Problème 5 peuvent être considérés comme de propres analogues sans phase de formule (3.6) et l'approche itérative susmentionnée de [44].

4 Diffusion inverse sans phase avec information de fond

4.1 Préliminaires historiques

Le problème 5(B) pour $d = 1$, $n = 1$ est considéré dans [2]. Problème 5(B) en dimension $d \geq 2$ est considéré dans [3, 5, 43, 45, 52, 24, 62] (où [52, 24, 62] sont remplis dans le cadre de cette thèse). En particulier, pour le problème 5(B), pour $d \geq 2$, $n = 2$, analogues de formule (3.6) et mondial connexe les résultats d'unicité sont donnés dans [43, 45]. Résultats de la reconstruction de [43, 45] sur le problème 5(B), pour $d \geq 2$, $n = 2$, sont fortement développés dans [3, 5]. En particulier, pour le cas sans phase avec bruit de fond diffuseurs, les résultats de [3] incluent un analogue de l'algorithme itératif de [44], mentionné dans la sous-section 3.3. Numérique associé l'implémentation est également donnée dans [3].

En particulier, pour les reconstructions itératives u_E^j à partir des données sans phase non surdéterminées du problème 5(B) pour $n = 2$, $d \geq 2$, à E, fixe le travail [3] donne les estimations

$$\|u_E^j - v\|_{L^\infty(D)} = \mathcal{O}(E^{-\alpha_j}), \quad \text{lorsque } E \to +\infty, \tag{4.1}$$

où

$$\begin{aligned} &\alpha_j \to \frac{j}{2} \quad \text{lorsque } m \to +\infty, \\ &\alpha_\infty \to +\infty \quad \text{lorsque } m \to +\infty, \quad \text{où} \quad \alpha_\infty = \lim_{j \to +\infty} \alpha_j, \end{aligned} \tag{4.2}$$

sous l'hypothèse que v, w_1, w_2 satisfont (2.3), $v \in W^{m,1}(\mathbb{R}^d)$, $m > d$, w_1, $w_2 \in C(\mathbb{R}^d)$, et, en particulier,

$$|\widehat{w}_j(p)| \geq c(1 + |p|)^{-\beta}, \quad j = 1, 2, \quad \beta > d. \tag{4.3}$$

Nous nous référons au [5, Lemme 1] et à [66] en relation avec des exemples de réels non négatifs à support compact w satisfaisant (4.3).

Notons que α_j dans ces résultats de [3] se comportent de manière similaire à α_j dans le résultat de [44] mentionné dans la sous-section 3.3, bien que α_j dans [3] sont plus petits.

Pour les problèmes 5(A) et 5(B), $n = 1$, pour $d \geq 2$, analogues de la formule (3.6) et les résultats d'unicité globale associés sont donnés dans le travail récent [52]. Ces résultats sont présentés dans la sous-section 4.2. Résultats de la reconstruction de [52] sur les problèmes 5(A), 5(B), $n = 1$, sont fortement développés théoriquement et implémentés numériquement dans les travaux récents [24]. Ces résultats sont présentés dans la sous-section 4.3. Les estimations de stabilité Lipschitz approximatives associées sont données dans l'ouvrage récent [62] et sont présentées dans la sous-section 4.4.

Notons également que les travaux [43, 45] et les travaux ultérieurs précités utilisent essentiellement, notamment, la version sans phase suivante de la formule (3.6):

$$|f(k,l)|^2 = |\widehat{v}(p)|^2 + \mathcal{O}(E^{-1/2}), \quad \text{as } E \to +\infty, \quad (k,l) \in \mathcal{M}_E, \quad k - l = p, \tag{4.4}$$

qui est utilisé pour v lui-même et pour v remplacé par $v + w_j$.

L'avantage clé des travaux [52], [24] (réalisés dans le cadre de cette thèse) consiste à résoudre le problème 5(A), où les données sont étonnamment limitées, et pas seulement problème 5(B).

4.2 Diffuseur de fond unique : la première approximation

L'ouvrage [52] traite du cas d'un seul diffuseur de fond, c'est-à-dire avec des problèmes 5(A) et 5 (B), $n = 1$, for $d \geq 2$. L'approche de [52] à ces problèmes de diffusion inverse sans phase est basée sur la formule (4.4) et les résultats de [52] présentés dans la sous-section 2.1 sur les problèmes de reconstruction de phase 2(A), (B).

En particulier, dans [52], en dimension $d \geq 2$, on montre que $|f[v + w]|^2$ aux hautes énergies détermine de manière unique v via des formules explicites, où $f[v+w]$ est l'amplitude de diffusion pour $v + w$, w est un diffuseur de fond non nul connu a priori, sous la condition que $supp\, v$ et $supp\, w$ soient suffisamment disjoints. Si cette condition est relâché, alors nous donnons des formules similaires pour trouver v à partir de $|f[v]|^2$ et $|f[v + w]|^2$.

De plus, pour les données de diffusion sans phase susmentionnées données à une énergie fixe E, dans [52] nous construisons des approximations u_E^1 à v telles que dans l'espace de Fourier

$$\begin{aligned} &|\widehat{u}_E^1(p) - \widehat{v}(p)| = |\widehat{w}(p)|^{-1}\mathcal{O}(E^{-1/2}), \quad \text{lorsque } E \to +\infty, \quad p \in B_{(2-\delta)\sqrt{E}}, \\ &\widehat{u}_E^1(p) = 0, \quad p \in \mathbb{R}^d \setminus B_{(2-\delta)\sqrt{E}}, \quad \text{pour fixe } \delta \in (0,2). \end{aligned} \tag{4.5}$$

De plus, dans l'espace de configuration, nous avons que

$$\|u_E^1 - v\|_{L^\infty(D)} = \mathcal{O}(E^{-\frac{1}{2}\frac{m-d}{m+\beta}}), \quad \text{as } E \to +\infty, \tag{4.6}$$

sous les hypothèses supplémentaires que $v \in W^{m,1}(\mathbb{R}^d)$, $m > d$, et w satisfait (4.3) avec $beta > d$.

Néanmoins, la convergence en (4.5), (4.6) est lente. Il ne dépasse pas $\mathcal{O}(E^{-1/2})$ même pour v. infiniment lisse À cet égard, les reconstructions approchées u_E^1 de [52] sont considérablement améliorées itérativement dans [24], voir sous-section 4.3.

4.3 Diffuseur de fond unique : itérations et implémentation numérique

Le travail [24] dans sa partie théorique améliore drastiquement la première approximation u_E^1 mentionnée dans la sous-section 4.2 via les itérations, $d \geq 2$. Ces itérations sont basées sur l'analogue sans phase suivant du lemme 3.1:

Lemma 4.1. *([24]) Sous les hypothèses du lemme 3.1, l'estimation suivante est vérifiée :*

$$\left| |f[v](k,l)|^2 - |f[v^E_{appr}](k,l)|^2 + |\widehat{v}^E_{appr}(k-l)|^2 - |\widehat{v}(k-l)|^2 \right| = \mathcal{O}(E^{-\alpha-1/2}), \tag{4.7}$$

lorsque $E \to +\infty$, *pour* $(k,l) \in \mathcal{M}_E$.

Pour le problème 5(A), l'étape itérative consiste à construire u_E^{j+1} à l'aide de la formule

$$\begin{aligned} &|\mathcal{F}(u_E^{j+1}+w)(p)|^2 = |\mathcal{F}(u_E^j+w)(p)|^2 + |f[v+w](k,l)|^2 - |f[u_E^j+w](k,l)|^2, \\ &\text{où } \ p \in B_{(2-\delta)\sqrt{E}}, \quad k-l=p, \quad k^2=l^2=E, \end{aligned} \tag{4.8}$$

et en utilisant les résultats sur la reconstruction de phase mentionnée dans la sous-section 2.1. Les propriétés théoriques de ces itérés u_E^j sont formalisées dans le théorème suivant.

Theorem 4.2. *([24]) Soient* v, $w = w_1$ *vérifiant les hypothèses (2.3), où* $dist(D,\Omega) > diam\, D$, $v \in W^{m,1}(\mathbb{R}^d)$, $m > d$, $w \in C(\mathbb{R}^d)$ *and* w *satisfy (4.3). Donc*

$$\|v - u_E^j\|_{L^\infty(D)} = \mathcal{O}(E^{-\alpha_j}) \quad \textit{lorsque } E \to +\infty, \tag{4.9}$$

où

$$\alpha_j = \frac{1}{2}\frac{m-d}{\beta+d}\left(1 - \left(\frac{m-d}{m+\beta}\right)^j\right). \tag{4.10}$$

Pour α_j du théorème 4.2, on a que

$$\begin{aligned} &\alpha_j \to \alpha_\infty := \frac{1}{2}\frac{m-d}{\beta+d} && \text{lorsque } j \to +\infty, \\ &\alpha_j \to \frac{j}{2} && \text{lorsque } m \to +\infty, \\ &\alpha_\infty \to +\infty && \text{lorsque } m \to +\infty. \end{aligned} \tag{4.11}$$

Des résultats similaires sont valables pour le problème 5(B), $n = 1$; voir [24].

On peut voir que la convergence en (4.9) est drastiquement meilleure qu'en (4.6), du moins, pour les gros m et j. De plus, la convergence en (4.9) (avec un seul w_1) est encore meilleure qu'en (4.1) (avec deux diffuseurs de fond w_1, w_2) . La convergence en (4.9), est similaire à la convergence un peu plus rapide en (3.20) pour le cas phasé.

Notons que seules les données de diffusion sans phase limitées à Γ_E sont utilisées dans les reconstructions mentionnées ci-dessus. Ici, Γ_E est le même sous-ensemble $d-$dimensionnel de $\mathcal{M}_E$ que dans sous-section 3.3.

Figure 1.5 illustre notre reconstruction numérique de v à valeur réelle non lisse pour le problème 4(A), où v, w sont représentés sur figure 1.2(a) ; voir [24, Section 4.3]. Les données de diffusion sans phase consistent en la seule section efficace de diffusion différentielle $|f[v+w]|^2$. Les figures 1.5(a), 1.5(c) illustrent la première approximation u_E^1 à v comme une fonction à valeurs complexes. Les figures 1.5(b), 1.5(d) illustrent notre approximation itérative u_E^{10}. Notons que la qualité de u_E^{10} est similaire à la solution de récupération de phase montrée dans la figure 1.2(c) et est bien meilleure que la première approximation u_E^1.

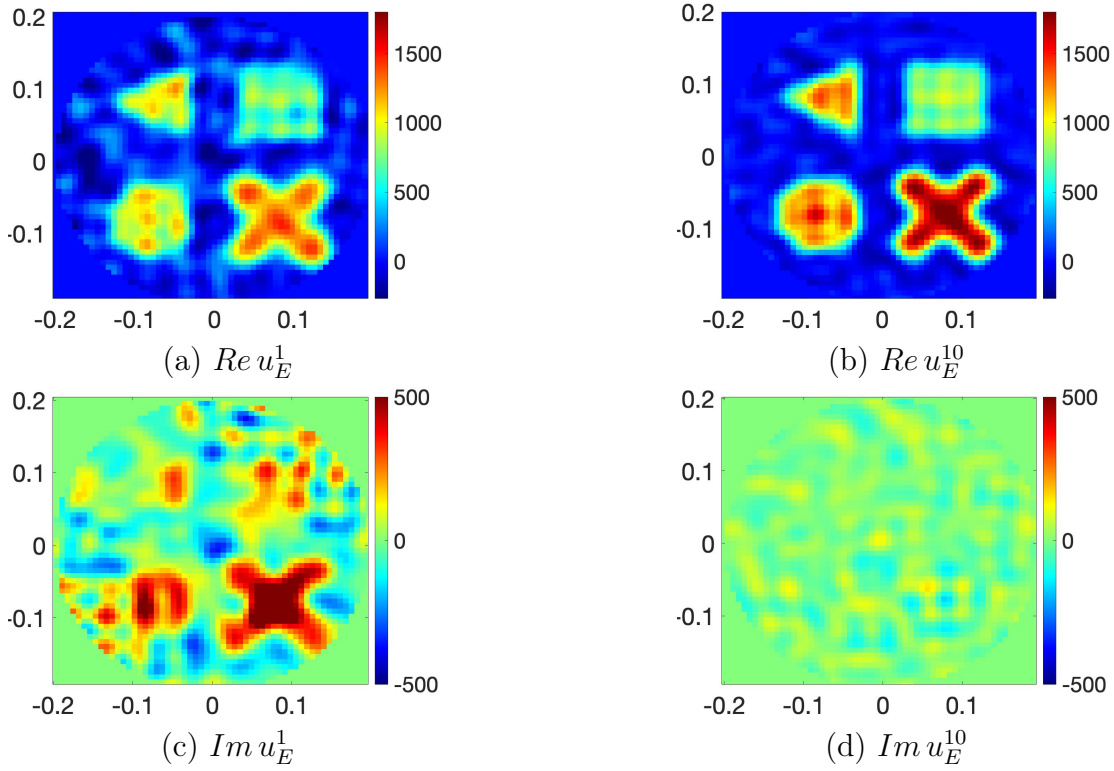

(a) $Re\, u_E^1$ (b) $Re\, u_E^{10}$

(c) $Im\, u_E^1$ (d) $Im\, u_E^{10}$

Figure 1.5: ([24]) Reconstructions u_E^J, de v à valeur réelle non lisse pour problème 5(A); voir Fig. 1.2. Rangée du haut : pièces réelles. Rangée du bas : parties imaginaires.

Notons que dans les problèmes de diffusion, les données $|f[v+w]|^2$ considérées comme une approximation de $|\widehat{v}+\widehat{w}|^2$ apparaissent sur une grille très non uniforme. Cela conduit à des difficultés numériques importantes, notamment dans le cadre du problème 5(A). Cela a nécessité une régularisation numérique avancée développée dans [24].

Il est remarquable que notre méthode reconstruise approximativement deux fonctions à valeurs réelles $Re\, v$ et $Im\, v$ sur D à partir d'une fonction à valeurs réelles $|f[v+w]|^2|_{\Gamma_E}$ à E fixe pour un fond connu w, sous l'hypothèse supplémentaire que v et w sont suffisamment séparés. Γ_E est le même sous-ensemble $d-$dimensionnel de $\mathcal{M}_E$ que dans la sous-section 3.3.

4.4 Estimations de stabilité

La stabilité est l'un des problèmes les plus importants dans les problèmes inverses. En particulier, la stabilité signifie que les données proches ne peuvent être produites que par des paramètres internes proches. Donc, sans de tels résultats on ne peut s'attendre à ce que la reconstruction reste adéquate pour des données bruitées (ou légèrement perturbées).

Le problème de la stabilité de Lipschitz pour le problème phasé 4(A) a été étudié dans [41], où l'estimation suivante a été donnée

$$\|v_1 - v_2\|_{L^\infty(D)} \leq A_1 E^{\frac{1}{2}} \|f[v_1] - f[v_2]\|_{C(\Gamma_E)} + A_2 E^{-\frac{1}{2}\frac{m-d}{d}}, \tag{4.12}$$

où $E \geq 1$, v_1, v_2 satisfont (3.2), $v_1 - v_2 \in W^{m,1}(\mathbb{R}^d)$, $d \geq 2$, et A_1, A_2 ne dépendent que des bornes pour les normes de v_1, v_2. Ici Γ_E est le même sous-ensemble $d-$dimensionnel de $\mathcal{M}_E$ que dans sous-sections 3.3, 4.3.

L'estimation (4.12) est une estimation approximative de la stabilité Lipschitz dans la terminologie de [41].

Dans le travail récent [62] (réalisé dans le cadre de cette thèse) nous avons obtenu des estimations similaires pour les problèmes sans phase 5(A), 5(B), $n = 1$. En particulier, pour le problème 5(A) nous avons prouvé que

$$\|v_1 - v_2\|_{L^\infty(D)} \leq C_1 E^{\frac{1}{2}-\varepsilon} \| |f[v_1+w]|^2 - |f[v_2+w]|^2 \|_{C(\Gamma_E)} + C_2 E^{-(\frac{1}{2}-\varepsilon)\frac{m-d}{\beta+d}}, \tag{4.13}$$

pour un grand E, où v_1, v_2, w satisfont les hypothèses (3.2), (4.3), $v_1 - v_2 \in W^{m,1}(\mathbb{R}^d)$, et $dist(D, \Omega) > diam\, D$, et $\varepsilon \in (0, 1/2)$ est fixe, C_1, C_2 sont similaires à A_1, A_2.

Des estimations similaires à (4.13) sont également valables pour problem 5(B), $n = 1$; voir [62].

Des estimations similaires à (4.13) sont également valables pour les problèmes de reconstruction de phase 2(A), (B); voir [62].

On peut voir que les membres droits de (4.12), (4.13) sont des sommes de deux termes. Le premier est Lipschitz terme par rapport à la différence de données, et le second est approximatif mais décroissant pour les hautes énergies. En outre, sa décroissance est très rapide pour les grands m, c'est-à-dire pour les $v_1 - v_2$ lisses. On peut voir qu'à énergie fixe E, le membre de droite dans les estimations (4.12), (4.13) tendent vers des constantes positives si les différences de données tendent vers zéro. Cependant, ces constantes devenir très petit pour un grand E. Ceci est tout à fait suffisant du point de vue de l'analyse numérique : les reconstructions ne sont jamais absolument précises. Il est donc tout à fait naturel d'étudier les reconstructions (dont la stabilité) jusqu'à quelques petites constantes (c'est-à-dire des reconstructions approximatives).

L'algorithme de diffusion inverse lié à l'estimation de stabilité (4.12) a été donné dans [44], implémenté numériquement dans [6], [63], et mentionné dans la sous-section 3.3. À son tour, le l'algorithme de diffusion inverse lié à l'estimation de stabilité (4.13) a été donné et implémenté numériquement dans [24].

Notons également que, sous nos hypothèses, Lipschitz et Hölder estimations de stabilité à énergie fixe E sont impossibles ; voir [38], [26], [27], pour de tels résultats d'instabilité pour plus ou problèmes inverses non linéaires et linéaires moins similaires.

5 Formules multipoints en théorie de la diffusion

Comme il est déjà mentionné dans la sous-section 2.2, des développements de la forme (2.7) surviennent, en particulier, pour différentes fonctions de la théorie de la diffusion. Ci-dessous dans cette section, nous décrivons les applications des formules multipoints mentionnées dans la sous-section 2.2 à la diffusion directe et inverse pour l'équation (3.1).

5.1 Approche multipoint de la diffusion inverse depuis le champ lointain

L'approche générale la plus simple du problème 4(A) et des problèmes 5(A), (B) consiste en des formules (3.6), (4.4) pour l'amplitude de diffusion f aux hautes énergies et reconstruction ultérieure à partir de transformées de Fourier en phase ou sans phase. Pour le cas des transformées de Fourier sans phase, certains de ces résultats de reconstruction sont obtenus dans le cadre de cette thèse et sont mentionnés dans la sous-section 2.1.

L'un des principaux inconvénients de cette approche la plus simple des problèmes 4(A), 5(A), (B) consiste en une lente convergence des formules (3.6), (4.4) lorsque $E \to +\infty$. Dans ce respect, les formules (3.6), (4.4) sont drastiquement améliorées dans [47], [54], au moins, pour v lisse (où le travail [54] est réalisé dans le cadre de cette thèse). Cette avancée surprenante est basée sur des développements asymptotiques de la forme (2.7) pour l'amplitude de diffusion f aux hautes énergies (voir [13], [38], [68]) et la formules multipoints mentionnées dans la sous-section 2.2.

Soit, par exemple, $v \in \mathcal{C}_c^\infty(\mathbb{R}^d)$, où $\mathcal{C}_c^\infty$ désigne les fonctions infiniment lisses avec support compact. Alors (voir [54])

$$f(k(s), l(s)) = \sum_{j=1}^{N} \frac{a_j(p, \omega)}{s^{j-1}} + \mathcal{O}(s^{-N}) \quad \text{lorsque } s \to +\infty, \tag{5.1}$$

où

$$\begin{aligned} &k(p) = p/2 + (E - p^2/4)^{1/2}\omega, \quad l(p) = -p/2 + (E - p^2/4)^{1/2}\omega, \quad E = E(s) = s^2, \\ &p \in \mathbb{R}^d, \quad p \cdot \omega = 0, \quad \omega \in \mathbb{S}^{d-1}, \end{aligned} \tag{5.2}$$

et

$$a_1(p,\omega) = \widehat{v}(p), \tag{5.3}$$

où $\widehat{v}$ est défini par (2.1). Notons que la formule (5.1), pour $N = 1$, découle de (3.6).

On peut voir que le développement (5.1) est de la forme (2.7). Ainsi, l'approche multipoint mentionnée dans la sous-section 2.2 conduit notamment au résultat suivant sur le problème 4(A) (voir [54]):

Theorem 5.1. *Soit $v \in \mathcal{C}_c^\infty(\mathbb{R}^d)$. Donc*

$$\begin{aligned}
&\widehat{v}(p) = \widehat{v}_n(p,s,\vec{\tau}) + \mathcal{O}(s^{-n}), \quad \text{lorsque} \quad s \to +\infty,\\
&\widehat{v}_n(p,s,\vec{\tau}) = \sum_{j=1}^{n} \frac{(-1)^{n-j}(s+\tau_j)^{n-1} f(k_j(s), l_j(s))}{\alpha_j(\vec{\tau})\beta_{n,j}(\vec{\tau})},\\
&|k_j(s)|^2 = |l_j(s)|^2 = E_j(s) = (s+\tau_j)^2, \quad s > 0,\\
&\vec{\tau} = (\tau_1, \dots, \tau_n), \ \tau_1 = 0, \ \tau_{j_1} < \tau_{j_2} \quad \text{for} \quad j_1 < j_2,
\end{aligned} \tag{5.4}$$

où

$$\begin{aligned}
&k_j(s) = p/2 + (E_j - p^2/4)^{1/2}\omega, \quad l_j(s) = -p/2 + (E_j - p^2/4)^{1/2}\omega, \quad E_j = E(s_j) = s_j^2,\\
&p \in \mathbb{R}^d, \quad p \cdot \omega = 0, \quad \omega \in \mathbb{S}^{d-1},
\end{aligned} \tag{5.5}$$

et α_j, $\beta_{n,j}$ sont définis dans (2.11).

Le théorème 5.1 est un résultat multi-énergie (polychromatique) sur la diffusion inverse pour l'équation (3.1). Le fait est que la convergence dans (5.4), pour $n > 1$, est beaucoup plus rapide que dans (3.6).

Les résultats de diffusion inverse polychromatique d'un tel type remontent à [47]. Cependant, les formules du théorème 5.1 sont bien plus pratiques que les formules apparentées de [47], notamment, pour les implémentations numériques ; voir [54] pour plus de détails.

L'analogue sans phase du théorème 5.1 est le suivant (voir [54]):

Theorem 5.2. *Sous les hypothèses du théorème 5.1, on a aussi que*

$$\begin{aligned}
&|\widehat{v}(p)|^2 = |\widehat{v}|^{2,n}(p,s,\vec{\tau}) + \mathcal{O}(s^{-n}), \quad \text{lorsque} \quad s \to +\infty,\\
&|\widehat{v}|^{2,n}(p,s,\vec{\tau}) = \sum_{j=1}^{n} \frac{(-1)^{n-j}(s+\tau_j)^{n-1} |f(k_j(s), l_j(s))|^2}{\alpha_j(\vec{\tau})\beta_{n,j}(\vec{\tau})}.
\end{aligned} \tag{5.6}$$

Comme il est déjà mentionné ci-dessus, les théorèmes 5.1, 5.2 et la reconstruction résultent des transformations de Fourier phasées et sans phase donner des méthodes théoriques avancées pour les problèmes 4(A), 5(A), (B).

Les premières implémentations numériques des formules (5.4), (5.6) sont données dans [54]. Dans le cadre de cette implémentation pour le cas bruité, nous utilisons également les formules multipoints régularisées mentionnées dans la sous-section 2.2.

La figure 1.6 montre des exemples d'implémentation numérique des formules (5.6) pour le potentiel lisse v (illustré à la figure 5(a) de [24]), où $d = 2$. L'image précise de v n'est pas essentielle pour ces exemples. La figure 1.6(a) est une fonction exacte $|\widehat{v}|^2$. Les figures 2.6(b)–(d) sont différentes reconstructions de $|\widehat{v}|^2$ à partir de l'amplitude de diffusion sans phase $|f[v]|^2$ donnée sur $\mathcal{M}_E$ pour différentes énergies E en utilisant les formules (5.6) et leurs versions régularisées (voir sous-section 2.2). Figure 1.6(b) : $n = 3$, $E = 25^2$, 30^2, 35^2, et la régularisation est appliquée; Figure 1.6(c) : $n = 1$, $E = 35^2$, et la régularisation n'est pas nécessaire ; Figure 1.6(d) : $n = 3$, $E = 25^2$, 30^2, 35^2, et la régularisation n'est pas appliquée.

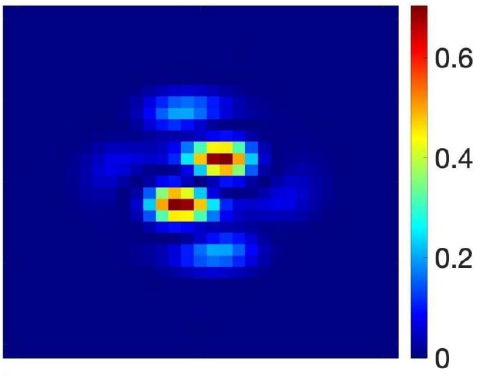

(a) Exact $|\widehat{v}|^2$.

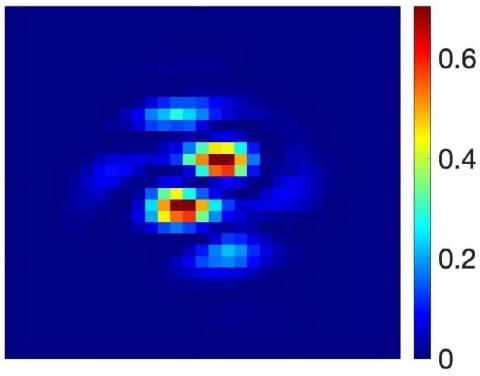

(b) Noisy data. Three-point reconstruction with regularization.

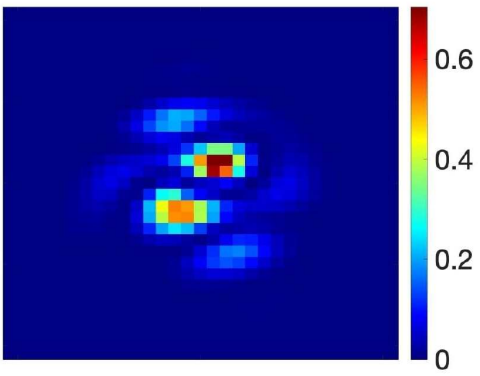

(c) Exact data. One-point reconstruction.

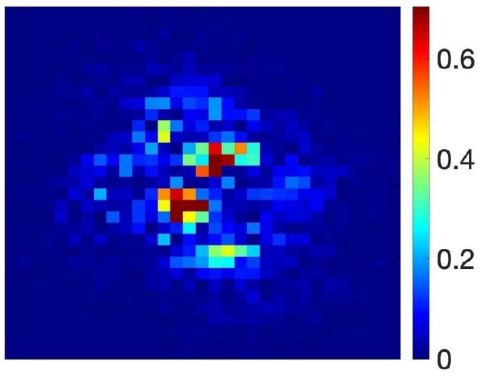

(d) Noisy data. Three-point reconstruction without regularization.

Figure 1.6: ([54]) Exact $|\widehat{v}|^2$ et ses reconstructions polychromatiques sans phase ; voir les sous-sections 2.2 et 5.1 (et [54] pour plus de détails). (a) Exact $|\widehat{v}|^2$.
(b) Reconstruction régularisée en trois points à partir du $|f|^2$ bruitée à $E = 25^2, 30^2, 35^2$. Paramètre de régularisation $r = \sqrt{10}$.
(c) Reconstruction en un point à partir de $|f|^2$ à $E = 35^2$.
(d) Reconstruction en trois points à partir du $|f|^2$ bruitée à $E = 25^2, 30^2, 35^2$ sans régularisation.

5.2 Approche multipoint pour la diffusion inverse à partir du champ proche

Dans cette sous-section, nous présentons les résultats de [54] sur le problème 4(C).

Considérons les solutions de diffusion ψ^+ satisfaisant (3.1), (3.2). Pour $v \in \mathcal{C}_c^\infty(\mathbb{R}^d)$, on a que

$$\begin{aligned} \psi^+(x,k) &= e^{ikx}\left(1 + \sum_{j=1}^{N-1} \frac{b_j(x,\theta)}{s^j} + \mathcal{O}(s^{-N})\right), \text{ lorsque } s \to +\infty, \\ b_1(x,\theta) &= \frac{1}{2i} Dv(x,-\theta), \quad Dv(x,\theta) := \int_0^{+\infty} v(x+\tau\theta)d\tau, \end{aligned} \tag{5.7}$$

où $x \in \mathbb{R}^d$, $s = |k|$, $\theta = k/|k|$ (x et θ sont fixés); voir [68], [54]. Notons que Dv est connu comme la transformée de faisceau divergente de v; voir, par exemple, [39].

En utilisant les formules multipoints (2.9) pour la fonction

$$z(x,k) = 2i|k|(e^{-ikx}\psi^+(x,k) - 1), \tag{5.8}$$

Nous obtenons le résultat suivant (voir [54]):

Theorem 5.3. *Soit $v \in \mathcal{C}_c^\infty(\mathbb{R}^d)$. Donc*

$$\begin{aligned} Dv(x,-\theta) &= a_{1,n}(x,\theta,s,\vec{\tau}) + \mathcal{O}(s^{-n}), \ \textit{lorsque } s \to +\infty, \\ a_{1,n}(x,\theta,s,\vec{\tau}) &:= \sum_{j=1}^{n} y_j(s,\vec{\tau}) z(x, s_j(s)\theta), \end{aligned} \tag{5.9}$$

où s_j sont définis par (2.8), y_j sont définis par (2.10).

Les formules de reconstruction (5.9), (5.8) sont nouvelles pour $n \geq 2$.

Supposons que $supp\, v \subset \Omega$, où Ω est un domaine convexe borné ouvert dans $\mathbb{R}^d$ avec une frontière lisse $\partial\Omega$. Soit

$$\Sigma = \{(x,\theta) : x \in \partial\Omega,\ \theta \in \mathbb{S}^{d-1},\ \nu_x \theta > 0\}, \tag{5.10}$$

où ν_x désigne la normale extérieure à $\partial\Omega$ au point x. Alors $2ib_1(x,\theta) = Dv(x,-\theta)$, $(x,\theta) \in \Sigma$, peut être considérée comme la transformation en rayons X de v.

Les méthodes de reconstruction de v à partir de sa transformée X sont très développées ; voir, par exemple, [39].

Les formules (5.8),(5.9) et les formules d'inversion pour la transformation des rayons X (voir, par exemple, [39]) donnent une méthode de diffusion inverse à partir des valeurs limites $\psi^+(x, s\theta)$, $(x,\theta) \in \Sigma$ à plusieurs grands s (c'est-à-dire à plusieurs grandes énergies).

5.3 Approches de l'application champ proche-lointain

Dans cette sous-section, nous rappelons quelques résultats connus anciens et récents sur le problème 4(B).

La première formule de résoudre du problème 4(B) a été donnée dans le théorème 3.3 de [9] pour le cas $d = 3$. Cette formule donne $f_1(k,l)$ à $k \in \mathbb{S}^2_{\sqrt{E}}$ it terme d'une somme infinie de intégrales de $\psi^+(x,k) - e^{ikx}$, $x \in \partial D$, pour le cas où $D = B_R$ pour un certain $R > 0$, $d = 3$, où B_r est de (2.2).

Notons que le problème 4(B), pour $d \geq 1$, peut aussi être résolu via

$$f(k,l) = (2\pi)^{-d} \int_{\partial D} \left(e^{-ilx} \frac{\partial}{\partial \nu_x} \psi^+(x,k) - \psi^+(x,k) \frac{\partial}{\partial \nu_x} e^{-ilx} \right) dx, \tag{5.11}$$

où $k,\ l \in \mathbb{R}^d$, $k^2 = l^2 = E > 0$, ν_x est la normale extérieure à ∂D en $x \in D$; voir [40].

Un inconvénient des formules bien connues susmentionnées pour résoudre le problème 4(B) pour $d > 1$ consiste en ce qui suit : pour trouver $f_1(k,l)$ à $kfixe, l \in \mathbb{S}^{d-1}_{\sqrt{E}}$ valeurs de $\psi^+(x,k)$ le long la limite entière ∂D est nécessaire. De plus, la formule de [9] est compliquée, alors que la formule (5.11) requiert non seulement ψ^+ sur ∂D mais aussi sa dérivée normale sur ∂D.

En revanche, l'approche multipoint de [46], donne notamment pour fixe $(k,l) \in \mathcal{M}_E$,

$$\begin{aligned} &\text{formules explicites pour trouver } f_1(k,l) \text{ précis à } \mathcal{O}(s^{-n}), \text{ lorsque } s \to +\infty, \\ &\text{de } \psi^+(x,k) \text{ donné à } n \text{ points } x_1(s), ..., x_n(s), \end{aligned} \tag{5.12}$$

où

$$\begin{aligned} &x_j(s) = (s + \tau_j)\hat{l}, \quad j = 1, ..., n, \quad \hat{l} = l/|l|, \\ &s > 0, \quad 0 = \tau_1 < ... < \tau_n. \end{aligned} \tag{5.13}$$

Cette approche est basée sur le développement asymptotique (3.3) pour ψ^+, le fait que la fonction

$$z(|x|, k, x/|x|) = |x|^{(d-1)/2} e^{-i|k||x|} \left(\psi^+(x,k) - e^{ikx} \right), \tag{5.14}$$

pour k fixe, $x/|x|$ est de la forme (2.7), et les formules multipoints présentées dans la sous-section 2.2.

De plus, dans les sous-sections 5.4, (5.5), nous discutons des analogues de formules (5.12) pour le cas du problème 6(A).

5.4 Formules à deux points pour l'application sans phase du champ proche-lointain

Historiquement, l'approche multipoint remonte aux formules à deux points de [42], [43] pour résoudre le problème 6(A).

Soit

$$a(x,k) = |x|^{(d-1)/2}(|\psi^+(k,x)|^2 - 1). \tag{5.15}$$

En particulier, les travaux [42], [43] donnent

$$\begin{aligned} &\text{formules explicites pour trouver } f(k,l) \text{ précis à } \frac{\mathcal{O}\left(s^{-\sigma}\right)}{\sin(\tau(|k| - k\hat{l}))}, \text{ lorsque } s \to +\infty, \\ &\text{de } a(x,k) \text{ donné à deux points } x_1(s),\, x_2(s), \end{aligned} \tag{5.16}$$

où $x_1(s) = s\hat{l}$, $x_2(s) = (s+\tau)\hat{l}$, $\hat{l} = l/|l|$, et

$$\sigma = \begin{cases} 1/2, & \text{pour} \quad d = 2, \\ 1, & \text{pour} \quad d \geq 3. \end{cases} \tag{5.17}$$

Estimations détaillées du terme d'erreur en (5.16), pour $d = 2$ et $d = 3$, sont donnés en [51] réalisé dans le cadre de cette thèse.

Le principal inconvénient des formules (5.16) est un taux de convergence lent comme $s \to +\infty$. Cet inconvénient a motivé d'autres études multipoints données dans [46], [48], [53], où [53] est réalisé dans le cadre de cette thèse.

5.5 Formules multipoints pour l'application sans phase du champ proche-lointain

Dans cette sous-section nous présentons les résultats des travaux [53] sur problème 6(A).

En particulier, dans ce travail nous donnons, pour fixes $(k,l) \in \mathcal{M}_E$, $l \neq k$, for $d \geq 2$,

$$\begin{aligned} &\text{formules explicites pour trouver } f_1(k,l) \text{ précis à } \mathcal{O}\left(s^{-n}\right), \text{ lorsque } s \to +\infty, \\ &\text{de } |\psi^+(x,k)|^2 \text{ donné à } m \text{ points } x_1(s), ..., x_m(s), \end{aligned} \tag{5.18}$$

où m dépend linéairement de n, et

$$\begin{aligned} &x_j(s) = (s+\tau_j)\hat{l}, \quad j = 1, ..., m, \quad \hat{l} = l/|l|, \\ &s > 0, \quad \tau_1 = 0, \quad \tau_{j_1} < \tau_{j_2}, \quad j_1 < j_2. \end{aligned} \tag{5.19}$$

On peut voir que dans les formules (5.18) et (5.19) les points de mesure $x_j = x_j(s)$ sont sur le rayon commençant à l'origine dans la direction $\hat{l}$, où s est la distance entre l'origine et l'ensemble des ces points, et les distances $\tau_{j+1} - \tau_j = |x_{j+1} - x_j|$ est fixé. De plus, la reconstruction les formules mentionnées dans (5.18) sont asymptotiques, où n peut être considéré comme leur convergence taux en termes de $\mathcal{O}(s^{-n})$ comme $s \to +\infty$, c'est-à-dire lorsque les points $x_j = x_j(s)$ se déplacent vers l'infinité.

L'idée principale est d'appliquer les approches des sous-sections 2.2, 5.4 à la fonction sans phase a définie par (5.15) en termes de $|\psi^+|^2$.

Dans le résultat le plus simple de [53], on suppose que dans les formules (5.18) et (5.19) $d = 3$, $m = 2n$ et que

$$\tau_j = \begin{cases} (j-1)\tau, & j = 1, ..., n, \\ \sigma + (j-1-n)\tau, & j = n+1, ..., 2n, \end{cases} \tag{5.20}$$

$$\tau = \tau(k,l) = \frac{2\pi}{\kappa}, \qquad 0 < \sigma \neq 0 \,(\mathrm{mod}\frac{\pi}{\kappa}), \quad \kappa = |k| - k\hat{l}. \tag{5.21}$$

Alors nos formules (5.18) sont spécifiées comme suit :

$$
\begin{aligned}
f_1(k,l) &= \frac{e^{-i(s+\sigma)\kappa}a_1(s) - e^{-is\kappa}a_2(s) + \mathcal{O}(s^{-n})}{-2i\sin(\sigma\kappa)}, \quad \text{lorsque } s \to +\infty, \\
a_1(s) = a_1(k,l,s) &= \sum_{j=1}^{n} \frac{(-1)^{n-j}(s+\tau_j)^{n-1}}{(j-1)!(n-j)!\tau^{n-1}} a(x_j(s),k), \\
a_2(s) = a_2(k,l,s) &= \sum_{j=n+1}^{2n} \frac{(-1)^{n-j}(s+\tau_j)^{n-1}}{(j-1-n)!(2n-j)!\tau^{n-1}} a(x_j(s),k),
\end{aligned}
\tag{5.22}
$$

où $(k,l) \in \mathcal{M}_E$, $l \neq k$, $d = 3$, $a(x,k)$ est défini par (5.15). De plus, $\kappa \neq 0$, for $l \neq k$.

Le fait que les formules (5.22) nécessitent $2n$ points au lieu de n points dans (5.12) pour une même précision $\mathcal{O}(s^{-n})$ est lié à l'absence d'information de phase dans les données utilisées dans (5.22). De plus, les formules (5.22), pour $n = 1$, se réduisent à des formules à deux points (5.16).

Notons que les formules (5.22) sont complètement explicites ! Un autre avantage de cette formule est relativement faible ($m = 2n$) nombre de points de mesure pour chaque (k,l). Un inconvénient possible de la formule (5.22) est que le pas $\tau = \tau(k,l)$ est fixé a priori, et dépend de (k,l). De plus, la formule (5.22) n'est pas valide pour $d = 2$ (à cause d'asymptotiques différentes (3.3) pour ψ^+).

Les inconvénients susmentionnés de (5.22) ont motivé d'autres résultats dans [53].

Dans ces résultats, on considère $|\psi^+(x,k)|^2$ pour k fixe, donné en m points x_j de la forme (5.19), où

$$
\tau_j = (j-1)\tau, \quad \tau \neq 0 \ (\mathrm{mod}\, \frac{\pi}{\kappa}).
\tag{5.23}
$$

Pour ces points x_j on a les résultats suivants :

- pour le cas des petits potentiels ('cas linéaire'), pour $d = 2$, 3, on a

  formules explicites pour trouver $f_1(k,l)$ précis à $\mathcal{O}(s^{-n})$, lorsque $s \to +\infty$, de $a(x,k)$ donné à $2n$ points $x_1(s), ..., x_{2n}(s)$, (5.24)

- pour les potentiels généraux, $d = 3$, on a

  formules explicites pour trouver $f_1(k,l)$ précis à $\mathcal{O}(s^{-n})$, lorsque $s \to +\infty$, de $a(x,k)$ donné à $3n-1$ points $x_1(s), ..., x_{3n-1}(s)$, (5.25)

- pour les potentiels généraux, $d = 2$, on a

  formules explicites pour trouver $f_1(k,l)$ précis à $\mathcal{O}(s^{-n})$, lorsque $s \to +\infty$, de $a(x,k)$ donné à $3n$ points $x_1(s), ..., x_{3n}(s)$. (5.26)

Notons que:

- il y a une différence entre $d = 2$ et $d = 3$ du fait de l'asymptotique (3.3) de ψ^+, le cas $d = 2$ est plus difficile ;
- pour le cas général, $d = 2$, 3, les formules (5.25), (5.26) nécessitent plus de points que les formules (5.22) ou (5.24);
- contrairement à (5.22), formules (5.24), (5.25) et (5.26) ne nécessitent pas de fixer τ a priori en fonction de (k,l). A cet égard, les formules (5.24), (5.25) et (5.26) sont plus pratiques pour les applications ;
- apparemment, pour les cas généraux de (5.25), (5.26) il existe des formules qui nécessitent moins de points de mesure pour une même précision.

Notons que les formules de [42, 43, 48, 53] peuvent également être utilisées pour le problème 6(A), (B) lorsque le coefficient v dans l'équation (3.1) est remplacé, par exemple, par un obstacle impénétrable (voir, par exemple, [15] pour la définition des obstacles impénétrables).

6 Conclusion

Cette thèse contribue aux études sur la reconstruction de phase, la diffusion inverse sans phase et les formules multipoints dans les problèmes inverses, et inclut les résultats suivants :

1 Nous donnons des formules de reconstruction de phase à partir d'une seule transformation de Fourier sans phase avec des informations de fond appropriées. En partant de ces formules, nous obtenons différents résultats théoriques et numériques sur le problème de reonstruction de phase pour la transformation de Fourier classique.

2 Nous proposons un algorithme itératif pour la diffusion inverse à partir d'une seule section efficace de diffusion différentielle avec un diffuseur de fond approprié. Cela inclut les estimations d'erreur, les estimations de stabilité et l'implémentation numérique.

3 Nous donnons la première implémentation numérique de la méthode des formules multipoints dans les problèmes inverses, incluant une régularisation efficace de ces formules pour le cas bruité. Par cette méthode, nous obtenons également de nouveaux résultats théoriques sur les problèmes de diffusion inverse polychromatique (à partir de données de champ lointain, de données de champ lointain sans phase et de données de champ proche).

Les sujets d'études futures comprennent:

1 Implémentation numérique des algorithmes mentionnés ci-dessus pour les problèmes de reconstruction de phase et de diffusion inverse sans phase pour $d = 3$.

2 Poursuite de l'implémentation numérique des formules multipoints en diffusion inverse pour les équations de Schrödinger et Helmholtz.

3 Extensions théoriques et numériques des résultats de la thèse aux cas d'autres équations de la physique mathématique.

4 Reconstruction à partir de données réelles, par exemple en analyse aux rayons X ou en tomographie électronique.

Chapter 2

Introduction in english

1 Introduction

Problems of scattering of time-harmonic waves appear in many areas such as quantum theory, medical imaging, geophysics, nondestructive testing, radars. The direct scattering problem is to determine the scattering solution, given the object and its physical property, while the inverse scattering problem is to determine the object and/or its physical property from the measurement information of the scattering solution.

The standard inverse scattering theory mostly deals with the phased case (i.e., the case when phase measurements are also available); see, e.g., [14], [15], [21], [49].

However, due to Born's rule in quantum mechanics, the complex values of wave function have no direct physical interpretation, whereas the squared absolute values of this function admit probabilistic interpretation and can be directly measured. Similarly, in optics and in X-ray imaging, modern detectors can measure the photon intensity (i.e. phaseless information), while the measurements of phase information are much more difficult (or currently impossible) due to extremely short length of the wave. See, for example, [11], [19], [23], [50], [61].

Therefore, it is especially important to study problems of reconstruction from phaseless data. Since there is only 'a half' of data (that is, only amplitude, no phase), these problems appear to be much more complicated in different senses. For example, for many phaseless inverse problems, there is no unique solution even for the linearized case of the Born approximation.

This approach goes back, at least to the work of Perutz on X-ray analysis of hemoglobin, honored by Nobel prize; see [55].

Note that in the Born approximation many phaseless inverse scattering problems simplify to the phase retrieval problem of reconstructing the potential from the absolute value of its Fourier transform. Our results on the later problem of Fourier analysis are summarized in Subsection 2.1. Then in Subsection 2.2 we present recent general results in the domain of asymptotic analysis, where some of these results were also obtained in the framework of this thesis.

Further thesis results essentially use the general mathematical methods summarized in Subsections 2.1 and 2.2. These thesis results include new algorithms on non-linearized phaseless inverse scattering problems and are summarized in Sections 4, 5.

Complete presentation of our results is given in Articles I-VI.

2 Some general mathematical methods

2.1 Phase retrieval problem

In this subsection we discuss the phase retrieval problem for the classical Fourier transform. This problem arises as a linear approximation for different phaseless inverse scattering problems. This problem is also of great independent interest in the framework of Fourier analysis.

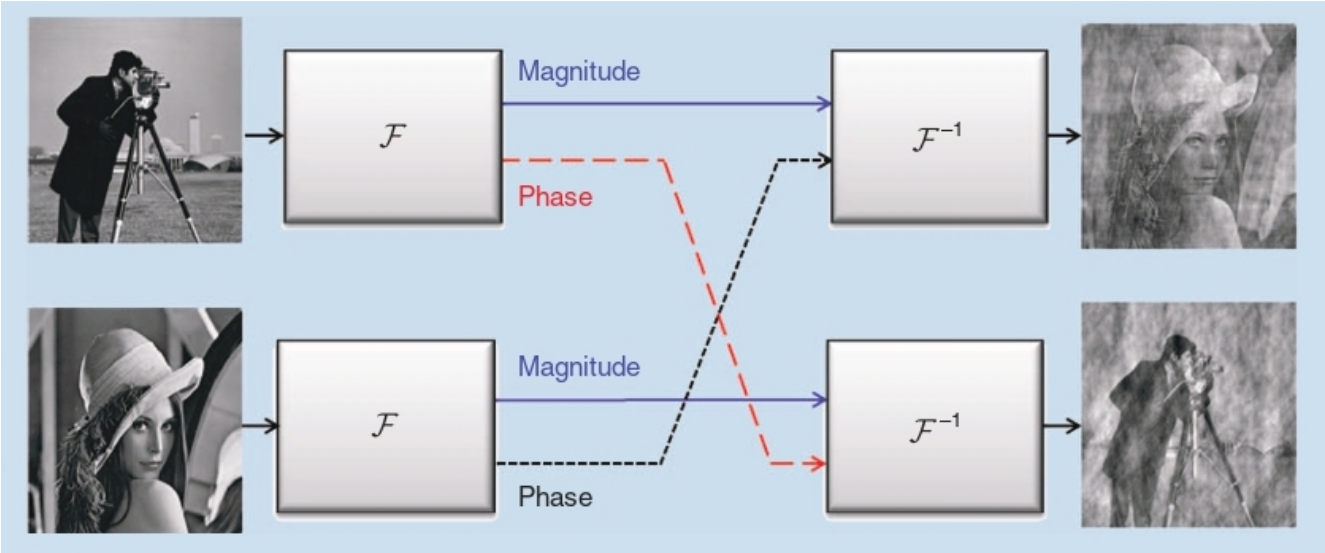

Figure 2.1: [61] The importance of Fourier phase. Two images, a cameraman and Lenna, are Fourier transformed. After swapping their phases, they are inverse Fourier transformed. The result clearly demonstrates the importance of phase information for image recovery.

We consider the Fourier transform of complex-valued function v :

$$\widehat{v}(p) = \mathcal{F}v(p) = \frac{1}{(2\pi)^d} \int_{\mathbb{R}^d} e^{ipx} v(x)dx, \quad p \in \mathbb{R}^d. \tag{2.1}$$

The classical phase retrieval problem is formulated as follows:

Problem 1. *Find v from $|\widehat{v}|^2$.*

The term 'phase retrieval problem' means that Problem 1 is equivalent to the reconstruction of $Angle(\widehat{v})$ from $Abs(\widehat{v})$.

Problem 1 is ill-posed: it does not have a unique solution, even up to translations and elementary symmetries, see [65] for details. The reason is the lack of (phase) information. See also Figure 2.1 for illustration.

To compensate for the missing phase information $\widehat{v}/|\widehat{v}|$, one either assumes a-priori information on v or additional data. Such inversions of the Fourier transform from phaseless data are much more complicated than the inversion of the Fourier transform from phased data. Examples of a-priori informations include (approximate) knowledge of $supp\, v$, constraints like $|v| = 1$ or $v \geq 0$, and knowledge of v on part of the domain. In this thesis we focus on the first and the last of these options. We refer to the monographs [25, 8], the review papers [20, 29, 34, 49, 61], the articles [7], [16], [31] and references therein.

More precisely, we consider the following problem:

Problem 2. *(A) Reconstruct a function v from $|\widehat{v}+\widehat{w}|^2$ on B_R for some known function w under the a-priori assumption that $supp\, v$ and $supp\, w$ are compact and sufficiently separated.*

(B) Reconstruct v from $|\widehat{v}|^2$ and $|\widehat{v} + \widehat{w_j}|^2$, $j = 1, \ldots, n$, on B_R for some appropriate known functions $w_1, ..., w_n$ separated from v.

Here

$$B_R = \{x \in \mathbb{R}^d : \quad |x| \leq R\}. \tag{2.2}$$

In addition, we assume that v and different non-zero background scatterers w_1, ..., w_n are of the form

$$\begin{aligned} &v,\, w_j \in L^{1,loc}(\mathbb{R}^d), \quad w_j \not\equiv 0, \quad supp\, v \subseteq D, \quad supp\, w_j \subseteq \Omega_j, \\ &D,\, \Omega_j \text{ are open convex bounded domain in } \mathbb{R}^d, \quad D \cap \Omega_j = \varnothing. \end{aligned} \tag{2.3}$$

Problem 2(B) was considered, in particular, in [43, 45, 3, 5]. In addition, related considerations go back, at least, to [55]. Problem 2(A) was studied in [52, 24]. Other investigations related to this problem can be found in [56, 37]. This thesis includes, in particular, new mathematical and numerical results of [52, 24] on Problem 2(A) and on Problem 2(B) for $n = 1$.

Let

$$D - \Omega = \{x - y : \, x \in D, \, y \in \Omega\}, \tag{2.4}$$

and $\chi_{D-\Omega}(x)$ be a characteristic (indicator) function of the set $D - \Omega$.

This thesis includes, in particular, the following result of [52], for $d \geq 1$:

Theorem 2.1. *([52]) Let v and $w = w_1$ satisfy (2.3) with $\Omega = \Omega_1$, and $dist(D, \Omega) > diam\, D$. Then $|\widehat{v} + \widehat{w}|^2$ and w uniquely determine v by the formulas*

$$\begin{aligned} &\widehat{v}(p) = (\overline{\mathcal{F}w(p)})^{-1}\mathcal{F}q(p), \\ &q(x) := \chi_{D-\Omega}(x)\left(u(x) - (2\pi)^{-d}\int_{\Omega} w(x+y)\overline{w(y)}dy\right), \\ &u(x) := \mathcal{F}^{-1}(|\mathcal{F}(v+w)|^2)(x). \end{aligned} \tag{2.5}$$

If we have only that $dist(D, \Omega) > 0$, then $|\widehat{v}|^2$, $|\widehat{v} + \widehat{w}|^2$, and w uniquely determine v via formula (2.5), where u is replaced by

$$u(x) := \mathcal{F}^{-1}(|\mathcal{F}(v+w)|^2 - |\mathcal{F}v|^2)(x). \tag{2.6}$$

Actually, Theorem 2.1 in its first part is a proper mathematical formalization of some of considerations of [37] related with finding v and w from $|\widehat{v} + \widehat{w}|^2$, under the condition that $supp\, v$ and $supp\, w$ are sufficiently disjoint, for $d = 2$.

One can see that Theorem 2.1 solves, in particular, Problem 1, if $supp\, v \subseteq (D \cup \Omega)$, where $dist(D, \Omega) > diam\, D$, and v is a priori known on Ω.

In addition, formulas of Theorem 2.1 lead to reconstructions from phaseless Fourier data with theoretical and numerical efficiency similar to reconstruction from Fourier data $\widehat{v}$ with phase information, see [52], [24], [62] and Section 4 for details.

Figure 2.2 illustrates our numerical reconstruction of v from $|\widehat{v}+\widehat{w}|^2$ limited to B_R with known background w.

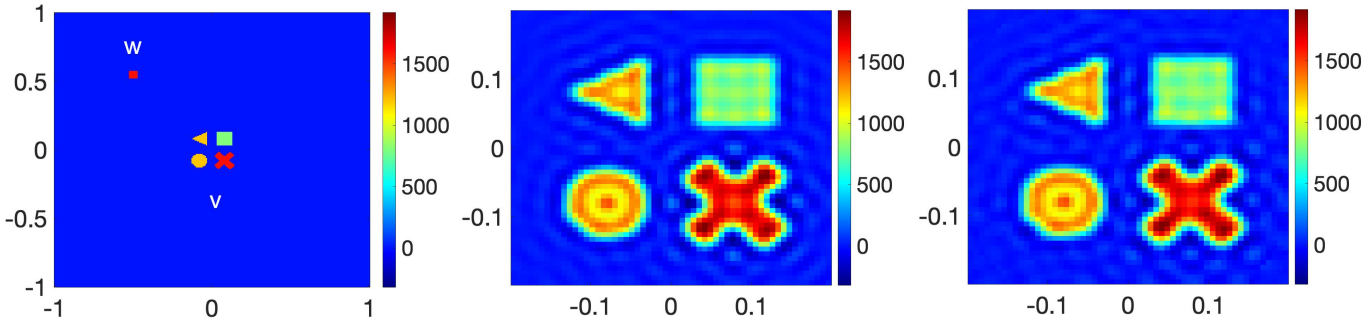

(a) Our $v + w$.

(b) Reconstruction from phased data $\widehat{v}$.

(c) Reconstruction from phaseless data $|\widehat{v} + \widehat{w}|^2$.

Figure 2.2: Comparison of reconstructions of v from phased and phaseless Fourier transform.
(a) Piecewise constant sufficiently separated v and w.
(b) Reconstruction from phased data $\widehat{v}$ given on some B_R.
(c) Reconstruction from phaseless data $|\widehat{v} + \widehat{w}|^2$ given on the same B_R.

2.2 Multipoint formulas

Many functions of potential theory, scattering theory, and other fields admit asymptotic expansions of the form

$$z(s) = z_{main}(s) + \mathcal{O}(s^{-N}) = \sum_{j=1}^{N} \frac{a_j}{s^{j-1}} + \mathcal{O}(s^{-N}), \text{ as } s \to +\infty, \tag{2.7}$$

where $s \in (\sigma, +\infty)$, for some $\sigma > 0$, and a_j are complex numbers; see, for example, [1], [35], [38], [46], [47], [53], [68]. In addition, in some cases, the most important information is contained in a_1 (and/or some next leading coefficients), whereas $z(s)$ is measured in several points $s \in (\sigma, +\infty)$.

For functions z satisfying (2.7) the work [46] considers, in particular, the problem of finding a_1 from $z(s)$ given at n points $s_j \in [r, +\infty)$, $j = 1, ..., n$ of the form

$$\begin{aligned} &s_j = s + \tau_j, \quad \vec{\tau} := (\tau_1, ..., \tau_n), \\ &0 = \tau_1 < \tau_2 < ... < \tau_n \text{ are fixed.} \end{aligned} \tag{2.8}$$

Note also that there is another geometry of points of s_j, see [46].

Suppose that $N \geq 2n - 1$. Then the following formulas hold ([46]):

$$\begin{aligned} a_1 &= a_{1,n}(s, \vec{\tau}) + \mathcal{O}(s^{-n}), \qquad \text{as } s \to +\infty, \\ a_{1,n}(s, \vec{\tau}) &= \sum_{j=1}^{n} y_j(s, \vec{\tau}) z(s + \tau_j), \end{aligned} \tag{2.9}$$

where

$$y_j(s, \vec{\tau}) = \frac{(-1)^{n-j}(s + \tau_j)^{n-1}}{\alpha_j(\vec{\tau})\beta_{n,j}(\vec{\tau})}, \quad 1 \leq j \leq n, \quad y = (y_1, ..., y_n), \tag{2.10}$$

$$\begin{aligned} \alpha_j(\vec{\tau}) &:= \prod_{i=1}^{j-1} (\tau_j - \tau_i) \quad \text{for} \quad 1 < j \leq n, \quad \alpha_1(\vec{\tau}) = 1, \\ \beta_{n,j}(\vec{\tau}) &:= \prod_{i=j+1}^{n} (\tau_i - \tau_j) \quad \text{for} \quad 1 \leq j < n, \quad \beta_{n,n}(\vec{\tau}) = 1. \end{aligned} \tag{2.11}$$

Multipoint formulas (2.9) rapidly converge, for n large enough, and have a simple structure, but they are very unstable to noise for large s. The reason is that the coefficients $y_j(s, \vec{\tau})$ in (2.10) behave as

$$y_j(s, \vec{\tau}) = \mathcal{O}(s^{n-1}), \quad \text{as } s \to +\infty. \tag{2.12}$$

Figure 2.3 illustrates these effects on the simplest $z(s) = s/(s + 1)$. In Figure 2.3 we present $\widetilde{a}_{1,n}(s) = a_{1,n}(s - \tau_n, \vec{\tau})$. Note that for every $n = 1, 2, 3$, these $\widetilde{a}_{1,n}(s)$ are reconstructed from $n = 1, 2, 3$ points, but with the same maximal point s. Figure 2.3(a) shows that two- and three-point formulas are more accurate than one-point reconstruction. Figure 2.3(b) shows that even for $n = 3$, the reconstruction is very instable even for medium s.

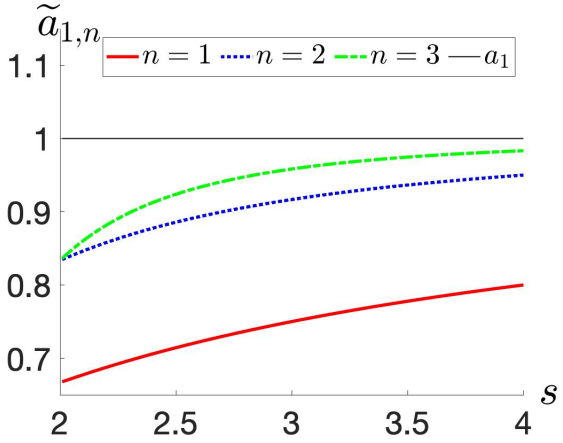

(a) Exact data. No regularization.

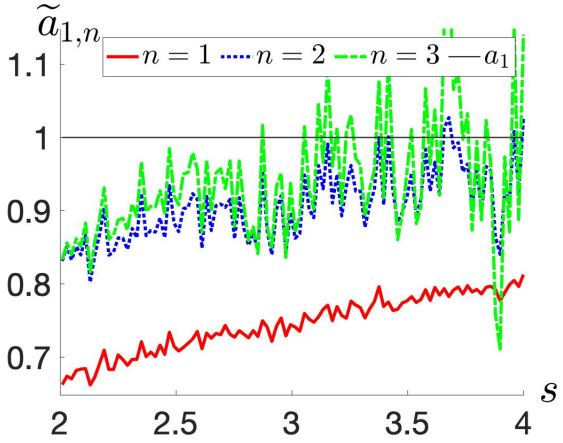

(b) Noisy data. No regularization.

Figure 2.3: ([54]) n-point reconstructions $\widetilde{a}_{1,n}(s) = a_{1,n}(s - \tau_n, \vec{\tau})$ of $a_1 = 1$ for $z(s) = s/(s+1)$ with $\tau_j = j - 1$, $j = 1, ..., n$.
(a) The case of exact data. Two- and three-point formulas rapidly converge to exact value.
(b) The case of noisy data simulated using formula (2.13). Two- and three-point formulas are unstable to noise.

In view of the aforementioned instability, in [54] we proposed, in particular, a regularization method for formulas (2.9) for the case of noisy data. More precisely, we assume that the data $z(s_j)$ contain the random noise of the form

$$\zeta(s) = z_{noisy}(s) = z(s) + \varepsilon N(s), \tag{2.13}$$

where the random variables $N(s)$ are i.i.d. for different s, mathematical expectation is $\mathbb{E}(\zeta(s)) = z(s)$, the dispersion is $\mathbb{D}(\zeta(s)) = \varepsilon^2$.

In order to make multipoint formulas applicable, we propose a regularisation method with a parameter r. In our regularization, we replace formula (2.9) by

$$\tilde{a}^r_{1,n} = \sum_{j=1}^{n} y^r_j(s, \vec{\tau}) z(s_j(s)), \tag{2.14}$$

where $y^r = (y^r_1, ..., y^r_n)$ is constructed in [54] and depends only on n and r, and $r \in [n^{-1/2}, \|y\|]$, where y is of (2.10).

Note that, the reconstruction $\tilde{a}^r_{1,n}$ has the following properties:

- for the noiseless function z, the regularized reconstruction is as exact as possible;
- the dispersion of reconstruction $a^r_{1,n}$ from noisy data is bounded by

$$\mathbb{D}(a^r_{1,n}(s, \vec{\tau})) \le r^2 \varepsilon^2 \quad \text{independently of } s. \tag{2.15}$$

In our construction ([54, Section 5]), the regularization parameter $r \in [\frac{1}{\sqrt{n}}, \|y\|]$, for $y = (y_1, ..., y_n)$ of (2.10). Here $r = n^{-1/2}$ corresponds to the strongest regularization, and $r = \|y\|$ corresponds to no regularization.

Figures 2.4(a), 2.4(b) in their comparison with Figures 2.3(a), 2.3(b) illustrate efficiency of our regularization (2.14).

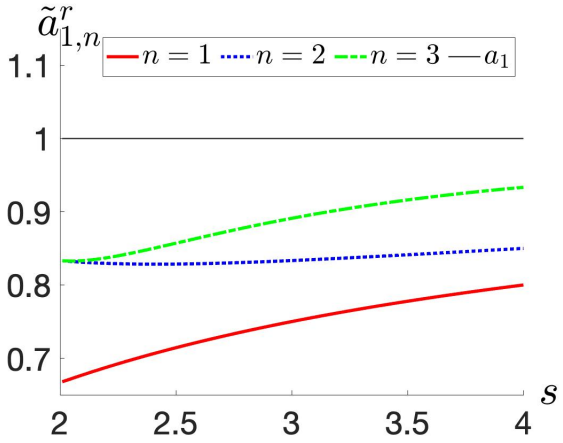

(a) Exact data. Regularization.

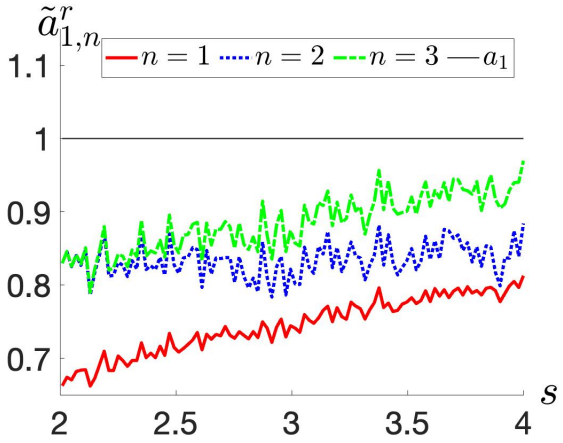

(b) Noisy data. Regularization.

Figure 2.4: ([54]) n-point regularized reconstructions $\tilde{a}^r_{1,n}(s) = a^r_{1,n}(s-\tau_n, \vec{\tau})$ of $a_1 = 1$ for $z(s) = s/(s+1)$ with $\tau_j = j-1$, $j = 1, ..., n$. Regularization parameter $r = \sqrt{5}$.
(a) The case of exact data. Two- and three-point regularized formulas converge to exact value, but not so rapid as in Figure 2.3(a).
(b) The case of noisy data simulated using formula (2.13). Two- and three-point regularized formulas are stable to noise.

Thus, in the framework of this thesis, we observed that the exact formulas (2.9) are very unstable to random noise (for $n \geq 2$ and sufficiently large s) and suggested an efficient regularization of these multipoint formulas. This thesis also includes theoretical and numerical results on applications of the aforementioned multipoint formulas to phased and phaseless inverse scattering, see Section 5.

3 Direct and inverse scattering problems

3.1 Formulations of problems

We consider the stationary Schrödinger equation

$$-\Delta\psi + v(x)\psi = E\psi, \quad x \in \mathbb{R}^d, \quad d \geq 2, \quad E > 0, \tag{3.1}$$

where Δ is the Laplacian in x, and

$$v \in L^\infty(\mathbb{R}^d), \quad supp\, v \subseteq \mathcal{U}, \quad \mathcal{U} \subset \mathbb{R}^d \text{ is open and bounded.} \tag{3.2}$$

The Schrödinger equation (3.1), under assumptions (3.2), arises in modelling interaction of a non-relativistic quantum mechanical particle at fixed energy E with a macroscopic object contained in D, where v is the potential of this interaction. Here, we assume that $\hbar^2/(2m) = 1$, where $\hbar$ is the reduced Planck's constant, and m is the mass of the particle. For more details on such a model in the framework of electron tomography, see, for example, [19].

Equation (3.1) can be also considered as time-harmonic Helmholtz equation of acoustics and electrodynamics, see, for example, [24], [60] for details.

For equation (3.1), under condition (3.2), we consider the scattering solutions $\psi^+ = \psi^+(x,k)$, $k \in \mathbb{R}^d$, $k^2 = E$, specified by the Sommerfeld radiation condition on $\psi^+(x,k) - e^{ikx}$. Functions ψ^+ have the Atkinson-type expansion (going back to [1]):

$$\psi^+(x,k) = e^{ikx} + \frac{e^{i|k||x|}}{|x|^{(d-1)/2}} \left(\sum_{j=1}^{N} \frac{f_j(k, |k|\frac{x}{|x|})}{|x|^{j-1}} + \mathcal{O}\left(\frac{1}{|x|^N}\right) \right), \quad |x| \to +\infty, \quad N \in \mathbb{N}, \tag{3.3}$$

uniformly in $x/|x|$. Here, the coefficient f_1 is of special physical importance and is known as the scattering amplitude for equation (3.1). Note that the function $f_1 = f_1(k,l)$ is defined on the manifold

$$\mathcal{M}_E = \{k,\, l \in \mathbb{R}^d : \quad k^2 = l^2 = E\} = \mathbb{S}^{d-1}_{\sqrt{E}} \times \mathbb{S}^{d-1}_{\sqrt{E}}, \tag{3.4}$$

where E is the energy in equation (3.1). Note also that in some formulas it is convenient to present f_1 as

$$f_1(k,l) = c(d,|k|)f(k,l), \quad c(d,|k|) = -\pi i(-2\pi i)^{(d-1)/2}|k|^{(d-3)/2} \text{ for } \sqrt{-2\pi i} = \sqrt{2\pi}e^{-i\pi/4}. \tag{3.5}$$

For more information on ψ^+ and f, see, for example, [10], [44] and references therein.

In particular, $\sigma = |f(k,l)|^2$ is known as the differential scattering cross section for equation (3.1). In a similar way with the wave functions ψ^+, the complex values of f have no direct physical interpretation, whereas $|f|^2$ admits a probabilistic interpretation and can be measured in experiments; see, for example, [11], [18]. In particular, the differential scattering cross section $\sigma = |f(k,l)|^2$ describes the probability density of scattering of a particle with initial impulse k into direction $l/|l| \neq k/|k|$. Similarly, in the electromagnetism of optics and X-rays (modeled in the framework of the time-harmonic Helmholtz equation) only $|\psi^+|^2$ and $\sigma = |f|^2$ can be measured directly by modern technical devices.

The scattering amplitude f contains a lot of information about scatterer v. In particular, according to the Born-Faddeev formula we have that:

$$f(k,l) = \widehat{v}(p) + \mathcal{O}(E^{-1/2}) \quad \text{as } E \to +\infty, \quad (k,l) \in \mathcal{M}_E, \quad k - l = p; \tag{3.6}$$

see, for example, [10].

We consider, in particular, the following problems:

Problem 3. *Find ψ^+ and f from v.*

Problem 4. *(A) Find v from f. (B) Find f from ψ^+. (C) Find v from ψ^+.*

Problem 3 is the direct scattering problem for the Schrödinger equation (3.1). Problem 4(A) is the classical inverse scattering problem from far-field. Problems 3 and 4(A) are studied in many details in the literature; see, e.g., [10], [18], [44]. And new important results on Problem 4(A) continue to appear; see, e.g., [47], [49], [54]. Problems 4(B) and 4(C) are also studied in old and recent publications; see, e.g., [9], [46], [54] (where [54] is fulfilled in the framework of this thesis).

In this thesis we focus on phaseless analogs of Problems 4(A)–(C). More precisely, we consider Problems 5 and 6 formulated below.

Problem 5. *(A) Find v from its phaseless scattering data $|f[v+w]|^2$ and background w.*

(B) Find v from the phaseless scattering data $|f[v]|^2$, $|f[v+w_1]|^2$, ... $|f[v+w_n]|^2$, and some appropriate background scatterers w_1,...,w_n.

In the linearized case of the Born approximation Problem 5 reduces to Problem 2.

Problem 5(A) with $w = 0$ is ill-posed, in a similar way with Problem 1. Problems 5(A), (B) can be considered as non-linear versions of Problems 2(A), (B). Actually, mathematical studies of Problems 5(A), (B) are started rather recently in [45], [3], [5], [53] for Problem 5(B), and in [52], [24] for Problem 5(A) (where works [52], [24] are fulfilled in the framework of this thesis).

Problem 6. *(A) Find $f(k,l)$ from $|\psi^+(x,k)|^2$ at appropriate points x such that $x \in \mathbb{R}^d \setminus D$ and $x/|x| = l/|l|$.*

(B) Find v from $|\psi^+|^2$ appropriately given outside of D.

Problem 6(A) is a phase recovering problem, whereas Problem 6(B) is the phaseless inverse scattering problem from near-field. These problems are considered, in particular, in [32, 42, 43, 46, 47, 48, 51, 53, 54] (where works [51, 53, 54] are fulfilled in the framework of this thesis). The multipoint approach mentioned in Subsection 2.2 admits efficient applications to these problems.

In addition to Problems 5 and 6, there are also other possible formulations of phase retrieval and phaseless inverse scattering problems for equation (3.1) and for other equations of wave propagations; see [30, 28, 33, 57, 58, 59, 67] and references therein.

3.2 Preliminaries on direct scattering

The scattering solutions ψ^+ satisfying (3.1), (3.3) can be found from the Lippmann-Schwinger integral equation:

$$\psi^+(x,k) = e^{ikx} + \int_D G^+(x-y,k)v(y)\psi^+(y,k)dy, \qquad x,\, k \in \mathbb{R}^d, \quad k^2 = E, \tag{3.7}$$

where

$$G^+(x,k) = -(2\pi)^{-d}\int_{\mathbb{R}^d} \frac{e^{i\xi x}d\xi}{\xi^2 - x^2 - i0}, \tag{3.8}$$

see, e.g., [10], [36]. Note that

$$G^+(x,k) = \frac{e^{i|k||x|}}{2i|k|} \text{ for } d=1; \quad G^+(x,k) = -\frac{i}{4}H_0^1(|x||k|) \text{ for } d=2; \tag{3.9}$$
$$G^+(x,k) = -\frac{e^{i|k||x|}}{4\pi|x|} \text{ for } d=3;$$

where H_0^1 is the Hankel function of the first type.

Actually, in addition to (3.2), we assume that, for fixed $E > 0$,

$$\text{equation (3.7) is uniquely solvable for } \psi^+(\cdot,k) \in L^\infty(D). \tag{3.10}$$

If v satisfies (3.2) and is real-valued, then (3.10) is fulfilled automatically.

In turn, the scattering amplitude f can be found from v and ψ^+ via

$$f(k,l) = (2\pi)^{-d}\int_D e^{-ily}v(y)\psi^+(y,k)dy, \tag{3.11}$$

where $k,\, l \in \mathbb{R}^d$, $k^2 = l^2 = E > 0$; see, e.g., [10].

Problem 3 can be solved using equation (3.7) and formula (3.11). Some of important theoretical properties of this solution, including (3.6), follow from the Agmon estimate on G^+, see, e.g. [44]. An efficient numerical algorithm for solving (3.7) is given in [64].

3.3 Preliminaries on phased inverse scattering

We recall that in the Born approximation for small v, for $d \geq 2$, the scattering amplitude f on $\mathcal{M}_E$ reduces to the Fourier transform $\widehat{v}$ on the ball $B_{2\sqrt{E}}$ via the formula

$$f(k,l) \approx \widehat{v}(p), \quad (k,l) \in \mathcal{M}_E, \quad p \in B_{2\sqrt{E}}, \quad p = k - l, \tag{3.12}$$

which is similar to (3.6).

Moreover, for u_E^1 defined by

$$u_E^1(x) := \int_{B_{2\sqrt{E}}} e^{-ipx}\widehat{v}(p)dp, \tag{3.13}$$

we have that

$$\|v - u_E^1\|_{L^\infty(\mathbb{R}^d)} = \mathcal{O}(E^{-\alpha}), \quad \text{as } E \to +\infty, \quad \text{with } \alpha := \frac{1}{2}(m-d), \tag{3.14}$$

if $v \in W^{m,1}(\mathbb{R}^d)$, where $W^{m,1}(\mathbb{R}^d)$ denotes m-times smooth functions in $L^1(\mathbb{R}^d)$. For more details on the linearised monochromatic reconstruction u_E, see, for example, [49].

The first general solution of Problem 4(A), $d \geq 2$, without assumption that v is small, goes back to [17] and is based on formula (3.6).

However, formula (3.12) gives no method to reconstruct v from f on $\mathcal{M}_E$ with the error smaller than $\mathcal{O}(E^{-1/2})$ even if $v \in \mathcal{S}(\mathbb{R}^d)$, where $\mathcal{S}$ stands for the Schwartz class. Applying the inverse Fourier transform $\mathcal{F}^{-1}$ to both sides of (3.12), one can obtain an explicit linear formula for $u^1 = u_E^1(x)$ in terms of f on $\mathcal{M}_E$, where

$$\begin{aligned} &u_E^1(x) = v(x) + \mathcal{O}(E^{-\alpha_1}), \quad E \to +\infty, \\ &\alpha_1 = (m-d)/(2m), \quad \text{if } v \in W^{m,1}(\mathbb{R}^d). \end{aligned} \tag{3.15}$$

One can see that $\alpha_1 \leq 1/2$ even if $m \to +\infty$.

An important point is that this approximation u_1 can be essentially improved iteratively using the following lemma:

Lemma 3.1. *([44]). Let v, v_0 satisfy (3.2), and $v = v_0$ on $\mathbb{R}^d \setminus D$, where D is a subdomain of $\mathcal{U}$. Let v_{appr}^E be an approximation to v such that:*

$$\begin{cases} |v_{appr}^E(x) - v(x)| = \mathcal{O}(E^{-\alpha}), & x \in D, \quad \text{for some } \alpha > 0, \\ v_{appr}^E(x) = v_0(x), & x \in \mathbb{R}^d \setminus D. \end{cases} \tag{3.16}$$

Then, for $(k,l) \in \mathcal{M}_E$,

$$\left| f[v](k,l) - f[v_{appr}^E](k,l) + \widehat{v}_{appr}^E(k-l) - \widehat{v}(k-l) \right| = \mathcal{O}(E^{-\alpha-\frac{1}{2}}). \tag{3.17}$$

Here, $f[v]$ and $f[v_{appr}^E]$ denote the scattering amplitude for v and v_{appr}^E (respectively); $\widehat{v}_{appr}^E$ is the Fourier transform of v_{appr}^E.

Note that conditions (3.2) are more strong than the assumptions used in [44].

The point is that the rate of convergence in (3.17) is higher than in (3.16) as $E \to +\infty$. This leads to the following scheme of [44] for iterative reconstructions u_E^j of v from given $f[v]$:

$$f[v] \xrightarrow{(3.6)} u_E^1 \xrightarrow{(3.7),(3.11)} f[u_E^1] \xrightarrow{(3.17)} \widehat{u}_E^2 := \widehat{u}_E^1 + f[v] - f[\widehat{u}_E^1] \xrightarrow{(3.7),(3.11)} f[u_E^2] \to u_E^3 \to \dots \tag{3.18}$$

In addition, if

$$v - v_0 \in W^{m,1}(\mathbb{R}^d), \tag{3.19}$$

then ([44]):

$$\begin{aligned} &\|v - u_E^j\|_{L^\infty(D)} = \mathcal{O}(E^{-\alpha_j}) \quad \text{as } E \to +\infty, \\ &\alpha_1 := \frac{m-d}{2m}, \quad \alpha_j := \left(1 - \left(\frac{m-d}{m}\right)^j\right) \frac{m-d}{2d}, \quad j \geq 1. \end{aligned} \tag{3.20}$$

In addition, one can see that

$$\begin{aligned} &\alpha_j \to \alpha_\infty := \frac{m-d}{2d} && \text{as } j \to +\infty, \\ &\alpha_j \to \frac{j}{2} && \text{as } m \to +\infty, \\ &\alpha_\infty \to +\infty && \text{as } m \to +\infty. \end{aligned} \tag{3.21}$$

Therefore, the convergence of u_E^j to v in (3.15), (3.20), as $E \to +\infty$, is drastically better for $j > 1$ than for $j = 1$, at least, for large m and j.

Note that only $f|_{\Gamma_E}$ is used in the reconstruction results mentioned above. Here Γ_E is a proper $d-$dimensional subset of $\mathcal{M}_E$, see [52] for details.

The iterative monochromatic reconstruction of [44] is implemented numerically in [6], [63] for $d = 2$ and $v_0 \equiv 0$. For other monochromatic phased inverse scattering reconstructions for equation (3.1) and the Helmholtz equation, see, for example, [4], [12], [22], [49].

Note that the reconstruction algorithms of [52], [24] fulfilled in the framework of studies of this thesis on Problem 5 can be considered as proper phaseless analogs of formula (3.6) and the aforementioned iterative approach of [44].

4 Phaseless inverse scattering with background information

4.1 Historical preliminaries

Problem 5(B) for $d = 1$, $n = 1$ is considered in [2]. Problem 5(B) in dimension $d \geq 2$ is considered in [3, 5, 43, 45, 52, 24, 62] (where [52, 24, 62] are fulfilled in the framework of this thesis). In particular, for Problem 5(B), for $d \geq 2$, $n = 2$, analogs of formula (3.6) and related global uniqueness results are given in [43, 45]. Reconstruction results of [43, 45] on Problem 5(B), for $d \geq 2$, $n = 2$, are strongly developed in [3, 5]. In particular, for the phaseless case with background scatterers, results of [3] include an analog of the iterative algorithm of [44], mentioned in Subsection 3.3. Related numerical implementation is also given in [3].

In particular, for the iterative reconstructions u_E^j from the non-overdetermined phaseless data of Problem 5(B) for $n = 2$, $d \geq 2$, at fixed E, the work [3] gives the estimates

$$\|u_E^j - v\|_{L^\infty(D)} = \mathcal{O}(E^{-\alpha_j}), \quad \text{as } E \to +\infty, \tag{4.1}$$

where

$$\begin{aligned} &\alpha_j \to \frac{j}{2} \qquad \text{as } m \to +\infty, \\ &\alpha_\infty \to +\infty \quad \text{as } m \to +\infty, \quad \text{where} \quad \alpha_\infty = \lim_{j \to +\infty} \alpha_j, \end{aligned} \tag{4.2}$$

under the assumptions that v, w_1, w_2 satisfy (2.3), $v \in W^{m,1}(\mathbb{R}^d)$, $m > d$, w_1, $w_2 \in C(\mathbb{R}^d)$, and, in particular,

$$|\widehat{w}_j(p)| \geq c(1 + |p|)^{-\beta}, \quad j = 1, 2, \quad \beta > d. \tag{4.3}$$

We refer to [5, Lemma 1] and to [66] in connection with examples of non-negative real compactly supported w satisfying (4.3).

Note that α_j in these results of [3] behave similarly to α_j in the result of [44] mentioned in Subsection 3.3, althought α_j in [3] are smaller.

For Problems 5(A) and 5(B), $n = 1$, for $d \geq 2$, analogs of formula (3.6) and related global uniqueness results are given in the recent work [52]. These results are presented in Subsection 4.2. Reconstruction results of [52] on Problems 5(A), 5(B), $n = 1$, are strongly developed theoretically and implemented numerically in the recent work [24]. These results are presented in Subsection 4.3. Related approximate Lipschitz stability estimates are given in the recent work [62] and are presented in Subsection 4.4.

Note also that the works [43, 45] and the aforementioned subsequent works essentially use, in particular, the following phaseless version of formula (3.6):

$$|f(k,l)|^2 = |\widehat{v}(p)|^2 + \mathcal{O}(E^{-1/2}), \quad \text{as } E \to +\infty, \quad (k,l) \in \mathcal{M}_E, \quad k - l = p, \tag{4.4}$$

which is used for v itself and for v replaced by $v + w_j$.

The key advantage of works [52], [24] (fulfilled in the framework of this thesis) consists in solving of Problem 5(A), where the data are surprisingly limited, and not only Problem 5(B).

4.2 Single background scatterer: the first approximation

The work [52] deals with the case of a single background scatterer, that is, with Problems 5(A) and 5(B), $n = 1$, for $d \geq 2$. The approach of [52] to these phaseless inverse scattering problems is based on formula (4.4) and the results of [52] presented in Subsection 2.1 on the phase retrieval Problems 2(A), (B).

In particular, in [52], in dimension $d \geq 2$, we show that $|f[v + w]|^2$ at high energies uniquely determines v via explicit formulas, where $f[v + w]$ is the scattering amplitude for $v + w$, w is an a priori known nonzero background scatterer, under the condition that $supp\, v$ and $supp\, w$ are sufficiently disjoint. If this condition is relaxed, then we give similar formulas for finding v from $|f[v]|^2$ and $|f[v + w]|^2$.

In addition, for the aforementioned phaseless scattering data given at a fixed energy E, in [52] we construct approximations u_E^1 to v such that in the Fourier space

$$\begin{aligned} &|\widehat{u}_E^1(p) - \widehat{v}(p)| = |\widehat{w}(p)|^{-1}\mathcal{O}(E^{-1/2}), \quad \text{as } E \to +\infty, \quad p \in B_{(2-\delta)\sqrt{E}}, \\ &\widehat{u}_E^1(p) = 0, \quad p \in \mathbb{R}^d \setminus B_{(2-\delta)\sqrt{E}}, \quad \text{for fixed } \delta \in (0, 2). \end{aligned} \tag{4.5}$$

Besides, in the configuration space, we have that

$$\|u_E^1 - v\|_{L^\infty(D)} = \mathcal{O}(E^{-\frac{1}{2}\frac{m-d}{m+\beta}}), \quad \text{as } E \to +\infty, \tag{4.6}$$

under the additional assumptions that $v \in W^{m,1}(\mathbb{R}^d)$, $m > d$, and w satisfies (4.3) with $\beta > d$.

Nevertheless, the convergence in (4.5), (4.6) is slow. It does not exceed $\mathcal{O}(E^{-1/2})$ even for infinitely smooth v. In this respect, approximate reconstructions u_E^1 of [52] are drastically improved iteratively in [24], see Subsection 4.3.

4.3 Single background scatterer: iterations and implementation

The work [24] in its theoretical part drastically improves the first approximation u_E^1 mentioned in Subsection 4.2 via iterations, $d \geq 2$. These iterations are based on the following phaseless analogue of Lemma 3.1:

Lemma 4.1. *([24]) Under the assumptions of Lemma 3.1, the following estimate holds:*

$$\left||f[v](k,l)|^2 - |f[v_{appr}^E](k,l)|^2 + |\widehat{v}_{appr}^E(k-l)|^2 - |\widehat{v}(k-l)|^2\right| = \mathcal{O}(E^{-\alpha-1/2}), \tag{4.7}$$

as $E \to +\infty$, for $(k,l) \in \mathcal{M}_E$.

For Problem 5(A), the iterative step consists in constructing u_E^{j+1} using the formula

$$\begin{aligned} &|\mathcal{F}(u_E^{j+1} + w)(p)|^2 = |\mathcal{F}(u_E^j + w)(p)|^2 + |f[v + w](k,l)|^2 - |f[u_E^j + w](k,l)|^2, \\ &\text{where } p \in B_{(2-\delta)\sqrt{E}}, \quad k - l = p, \quad k^2 = l^2 = E, \end{aligned} \tag{4.8}$$

and using results on the phase retrieval mentioned in Subsection 2.1. Theoretical properties of these iterates u_E^j are formalized in the following theorem.

Theorem 4.2. *([24]) Let v, $w = w_1$ satisfy assumptions (2.3), where $dist(D, \Omega) > diam\, D$, $v \in W^{m,1}(\mathbb{R}^d)$, $m > d$, $w \in C(\mathbb{R}^d)$ and w satisfy (4.3). Then*

$$\|v - u_E^j\|_{L^\infty(D)} = \mathcal{O}(E^{-\alpha_j}) \quad \text{as } E \to +\infty, \tag{4.9}$$

where

$$\alpha_j = \frac{1}{2}\frac{m-d}{\beta+d}\left(1 - \left(\frac{m-d}{m+\beta}\right)^j\right). \tag{4.10}$$

For α_j of Theorem 4.2, we have that

$$\begin{aligned} &\alpha_j \to \alpha_\infty := \frac{1}{2}\frac{m-d}{\beta+d} && \text{as } j \to +\infty, \\ &\alpha_j \to \frac{j}{2} && \text{as } m \to +\infty, \\ &\alpha_\infty \to +\infty && \text{as } m \to +\infty. \end{aligned} \tag{4.11}$$

Similar results hold for Problem 5(B), $n = 1$; see [24].

One can see that convergence in (4.9) is drastically better than in (4.6), at least, for large m and j. Moreover, the convergence in (4.9) (with single w_1) is even better than in (4.1) (with two background scatterers w_1, w_2). The convergence in (4.9), is similar to the somewhat more rapid convergence in (3.20) for the phased case.

Note that only the phaseless scattering data limited to Γ_E are used in the reconstructions mentioned above. Here Γ_E is the same $d-$dimensional subset of $\mathcal{M}_E$ as in Subsection 3.3.

Figure 2.5 illustrates our numerical reconstruction of non-smooth real-valued v for Problem 4(A), where v, w are shown in Figure 2.2(a); see [24, Section 4.3]. The phaseless scattering data consist of the single differential scattering cross section $|f[v+w]|^2$. Figures 2.5(a), 2.5(c) illustrate the first approximation u_E^1 to v as a complex-valued function. Figures 2.5(b), 2.5(d) illustrate our iterative approximation u_E^{10}. Note that the quality of u_E^{10} is similar to the phase retrieval solution shown in Figure 2.2(c) and is much better than the first approximation u_E^1.

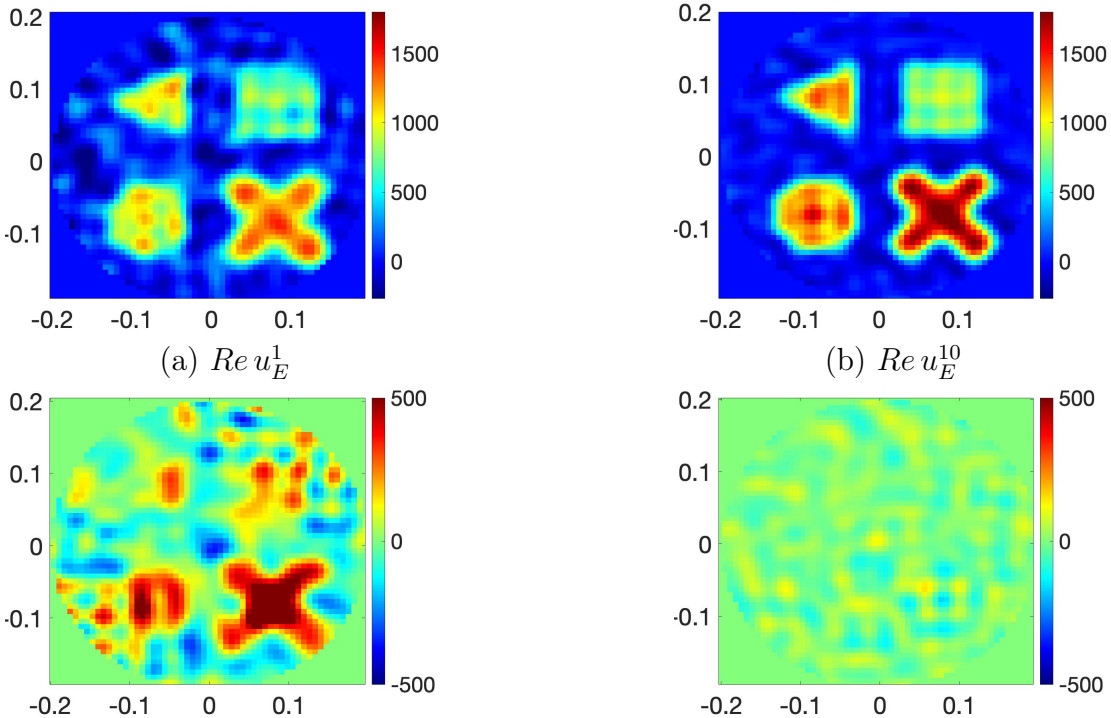

(a) $Re\, u_E^1$ (b) $Re\, u_E^{10}$

(c) $Im\, u_E^1$ (d) $Im\, u_E^{10}$

Figure 2.5: ([24]) Reconstructions u_E^J, of non-smooth real-valued v for Problem 5(A); see Fig. 2.2. Top row: Real parts. Bottom row: Imaginary parts.

Note that in scattering problems, the data $|f[v+w]|^2$ considered as an approximation to $|\widehat{v}+\widehat{w}|^2$ arise on a very non-uniform grid. This leads to significant numerical difficulties, especially in the framework of Problem 5(A). This required advanced numerical regularisation developed in [24].

It is remarkable that our method approximately reconstructs two real-valued functions $Re\, v$ and $Im\, v$ on D from one real-valued function $|f[v+w]|^2|_{\Gamma_E}$ at fixed E for known background w, under the additional assumption that v and w are sufficiently separated. Γ_E is the same $d-$dimensional subset of $\mathcal{M}_E$ as in Subsection 3.3.

4.4 Stability estimates

Stability is one of the most important issues in inverse problems. In particular, stability means that the close data can be produced only by close inner parameters. Therefore, without such results one cannot expect that the reconstruction remains adequate for noisy (or slightly perturbed) data.

The problem of Lipschitz stability for the phased Problem 4(A) was studied in [41], where the following estimate was given

$$\|v_1 - v_2\|_{L^\infty(D)} \leq A_1 E^{\frac{1}{2}} \|f[v_1] - f[v_2]\|_{C(\Gamma_E)} + A_2 E^{-\frac{1}{2}\frac{m-d}{d}}, \tag{4.12}$$

where $E \geq 1$, v_1, v_2 satisfy (3.2), $v_1 - v_2 \in W^{m,1}(\mathbb{R}^d)$, $d \geq 2$, and A_1, A_2 depend only on bounds for norms of v_1, v_2. Here Γ_E is the same $d-$dimensional subset of $\mathcal{M}_E$ as in Subsections 3.3, 4.3.

Estimate (4.12) is an approximate Lipschitz stability estimate in terminology of [41].

In the recent work [62] (fulfilled in the framework of this thesis) we obtained similar estimates for the phaseless Problems 5(A), 5(B), $n = 1$. In particular, for Problem 5(A) we proved that

$$\|v_1 - v_2\|_{L^\infty(D)} \leq C_1 E^{\frac{1}{2}-\varepsilon} \| |f[v_1 + w]|^2 - |f[v_2 + w]|^2 \|_{C(\Gamma_E)} + C_2 E^{-(\frac{1}{2}-\varepsilon)\frac{m-d}{\beta+d}}, \tag{4.13}$$

for large E, where v_1, v_2, w satisfy assumptions (3.2), (4.3), $v_1 - v_2 \in W^{m,1}(\mathbb{R}^d)$, and $dist(D, \Omega) > diam\, D$, and $\varepsilon \in (0, 1/2)$ is fixed, C_1, C_2 are similar to A_1, A_2.

Estimates similar to (4.13) also hold for Problem 5(B), $n = 1$; see [62].

Estimates similar to (4.13) also hold for the phase retrieval Problems 2(A), (B); see [62].

One can see that the right hand sides of (4.12), (4.13) are sums of two terms. The first one is Lipschitz term with respect to data difference, and the second one is approximate but decaying for high energies. In addition, its decay is very fast for large m, that is for smooth $v_1 - v_2$. One can see that, at fixed energy E, the right-hand side in estimates (4.12), (4.13) tend to positive constants if data differences tend to zero. However, these constants become very small for large E. This is completely sufficient from the point of view of numerical analysis: numerical reconstructions are never absolutely precise. Therefore, it is very natural to study reconstructions (including stability) up to some small constants (that is, approximate reconstructions).

The inverse scattering algorithm related with the stability estimate (4.12) was given in [44], implemented numerically in [6], [63], and mentioned in Subsection 3.3. In turn, the inverse scattering algorithm related with the stability estimate (4.13) was given and implemented numerically in [24].

Note also that, under our assumptions, exact Lipschitz and Hölder stability estimates at fixed energy E are impossible; see [38], [26], [27], for such instability results for more or less similar non-linear and linear inverse problems.

5 Multipoint formulas in scattering theory

As it is already mentioned in Subsection 2.2, expansions of the form (2.7) arise, in particular, for different functions of the scattering theory. Below in this section we describe applications of multipoint formulas mentioned in Subsection 2.2 to direct and inverse scattering for equation (3.1).

5.1 Multipoint approach to inverse scattering from far-field

The simplest general approach to Problem 4(A) and Problems 5(A), (B) consists in formulas (3.6), (4.4) for the scattering amplitude f at high energies and subsequent reconstruction from phased or phaseless Fourier transforms. For the case of phaseless Fourier transforms, some of these reconstruction results are obtained in the framework of this thesis and are mentioned in Subsection 2.1.

One of the main drawbacks of this simplest approach to Problems 4(A), 5(A), (B) consists in slow convergence in formulas (3.6), (4.4) as $E \to +\infty$. In this respect, formulas (3.6), (4.4) are drastically improved in [47], [54], at least, for smooth v (where work [54] is fulfilled in the framework of this thesis). This surprising advancement is based on asymptotic expansions of the form (2.7) for the scattering amplitude f at high energies (see [13], [38], [68]) and the multipoint formulas mentioned in Subsection 2.2.

Let, for example, $v \in \mathcal{C}_c^\infty(\mathbb{R}^d)$, where $\mathcal{C}_c^\infty$ denotes compactly supported infinitely smooth functions. Then (see [54])

$$f(k(s), l(s)) = \sum_{j=1}^{N} \frac{a_j(p,\omega)}{s^{j-1}} + \mathcal{O}(s^{-N}) \text{ as } s \to +\infty, \tag{5.1}$$

where

$$\begin{aligned} &k(p) = p/2 + (E - p^2/4)^{1/2}\omega, \quad l(p) = -p/2 + (E - p^2/4)^{1/2}\omega, \quad E = E(s) = s^2, \\ &p \in \mathbb{R}^d, \quad p \cdot \omega = 0, \quad \omega \in \mathbb{S}^{d-1}, \end{aligned} \tag{5.2}$$

and

$$a_1(p,\omega) = \widehat{v}(p), \tag{5.3}$$

where $\widehat{v}$ is defined by (2.1). Note that formula (5.1), for $N = 1$, follows from (3.6).

One can see that expansion (5.1) is of the form (2.7). Therefore, the multipoint approach mentioned in Subsection 2.2 leads, in particular, to the following result on Problem 4(A) (see [54]):

Theorem 5.1. *Let $v \in \mathcal{C}_c^\infty(\mathbb{R}^d)$. Then*

$$\begin{aligned} &\widehat{v}(p) = \widehat{v}_n(p, s, \vec{\tau}) + \mathcal{O}(s^{-n}), \quad \text{as} \quad s \to +\infty, \\ &\widehat{v}_n(p, s, \vec{\tau}) = \sum_{j=1}^{n} \frac{(-1)^{n-j}(s+\tau_j)^{n-1} f(k_j(s), l_j(s))}{\alpha_j(\vec{\tau})\beta_{n,j}(\vec{\tau})}, \\ &|k_j(s)|^2 = |l_j(s)|^2 = E_j(s) = (s+\tau_j)^2, \quad s > 0, \\ &\vec{\tau} = (\tau_1, \dots, \tau_n), \ \tau_1 = 0, \ \tau_{j_1} < \tau_{j_2} \ \text{ for } \ j_1 < j_2, \end{aligned} \tag{5.4}$$

where

$$\begin{aligned} &k_j(s) = p/2 + (E_j - p^2/4)^{1/2}\omega, \quad l_j(s) = -p/2 + (E_j - p^2/4)^{1/2}\omega, \quad E_j = E(s_j) = s_j^2, \\ &p \in \mathbb{R}^d, \quad p \cdot \omega = 0, \quad \omega \in \mathbb{S}^{d-1}, \end{aligned} \tag{5.5}$$

and α_j, $\beta_{n,j}$ are defined in (2.11).

Theorem 5.1 is a multi-energy (polychromatic) result on inverse scattering for equation (3.1). The point is that the convergence in (5.4), for $n > 1$, is much faster than in (3.6).

Polychromatic inverse scattering results of such a type go back to [47]. However, the formulas of Theorem 5.1 are much more convenient than the related formulas of [47], especially, for numerical implementations; see [54] for details.

The phaseless analogue of Theorem 5.1 is as follows (see [54]):

Theorem 5.2. *Under the assumptions of Theorem 5.1, we have also that*

$$\begin{aligned} &|\widehat{v}(p)|^2 = |\widehat{v}|^{2,n}(p, s, \vec{\tau}) + \mathcal{O}(s^{-n}), \quad \text{as} \quad s \to +\infty, \\ &|\widehat{v}|^{2,n}(p, s, \vec{\tau}) = \sum_{j=1}^{n} \frac{(-1)^{n-j}(s+\tau_j)^{n-1} |f(k_j(s), l_j(s))|^2}{\alpha_j(\vec{\tau})\beta_{n,j}(\vec{\tau})}. \end{aligned} \tag{5.6}$$

As it is already mentioned above, Theorems 5.1, 5.2 and reconstruction results from phased and phaseless Fourier transforms give advanced theoretical methods for Problems 4(A), 5(A), (B).

The first numerical implementations of formulas (5.4), (5.6) is given in [54]. In the framework of this implementation for the noisy case, we also use the regularised multipoint formulas mentioned in Subsection 2.2.

Figure 2.6 shows examples of numerical implementation of formulas (5.6) for smooth potential v (shown in Figure 5(a) of [24]), where $d = 2$. The precise image of v is not essential for these examples. Figure 2.6(a) is an exact function $|\widehat{v}|^2$. Figures 2.6(b)–(d) are different reconstructions of $|\widehat{v}|^2$ from phaseless scattering amplitude $|f[v]|^2$ given on $\mathcal{M}_E$ for some different energies E using formulas (5.6) and their regularized versions (see Subsection 2.2). Figure 2.6(b): $n = 3$, $E = 25^2, 30^2, 35^2$, and regularisation is applied; Figure 2.6(c): $n = 1$, $E = 35^2$, and regularisation is not required; Figure 2.6(d): $n = 3$, $E = 25^2, 30^2, 35^2$, and regularisation is not applied.

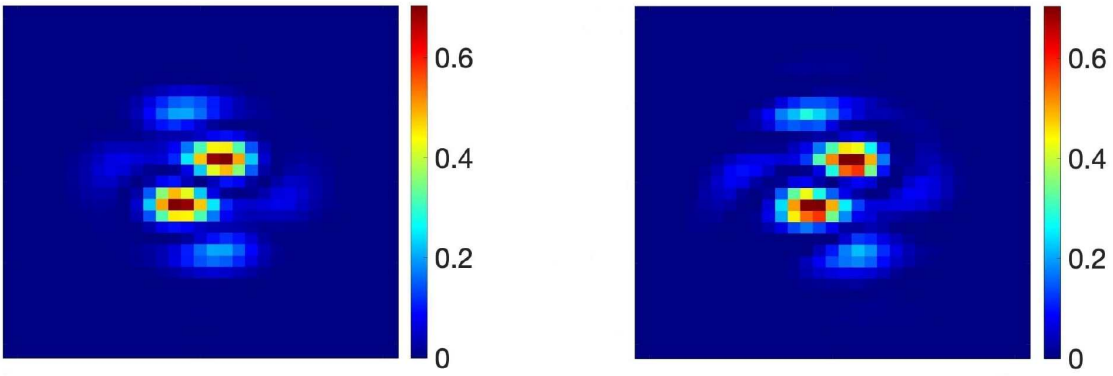

(a) Exact $|\widehat{v}|^2$.

(b) Noisy data. Three-point reconstruction with regularization.

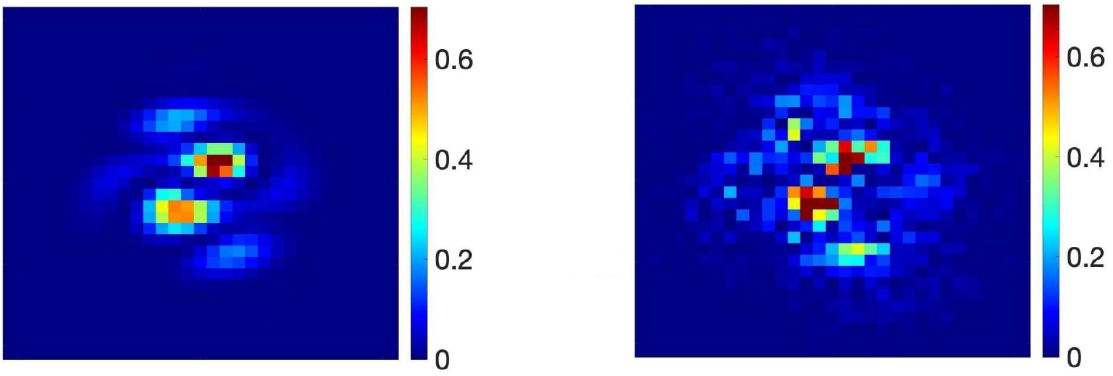

(c) Exact data. One-point reconstruction.

(d) Noisy data. Three-point reconstruction without regularization.

Figure 2.6: ([54]) Exact $|\widehat{v}|^2$ and its polychromatic phaseless reconstructions; see Subsections 2.2 and 5.1 (and [54] for details). (a) Exact $|\widehat{v}|^2$.
(b) Three-point regularized reconstruction from noisy $|f|^2$ at $E = 25^2, 30^2, 35^2$. Regularization parameter $r = \sqrt{10}$.
(c) One-point reconstruction from $|f|^2$ at $E = 35^2$.
(d) Three-point reconstruction from noisy $|f|^2$ at $E = 25^2, 30^2, 35^2$ without regularization.

5.2 Multipoint approach for inverse scattering from near-field

In this subsection we present the results of [54] on Problem 4(C).

Consider the scattering solutions ψ^+ satisfying (3.1), (3.2). For $v \in \mathcal{C}_c^\infty(\mathbb{R}^d)$, we have that

$$\begin{aligned} &\psi^+(x,k) = e^{ikx}\left(1 + \sum_{j=1}^{N-1} \frac{b_j(x,\theta)}{s^j} + \mathcal{O}(s^{-N})\right), \text{ as } s \to +\infty, \\ &b_1(x,\theta) = \frac{1}{2i} Dv(x,-\theta), \quad Dv(x,\theta) := \int_0^{+\infty} v(x+\tau\theta)d\tau, \end{aligned} \tag{5.7}$$

where $x \in \mathbb{R}^d$, $s = |k|$, $\theta = k/|k|$ (x and θ are fixed); see [68], [54]. Note that Dv is known as the divergent beam transform of v; see, for example, [39].

Using the multipoint formulas (2.9) for the function

$$z(x,k) = 2i|k|(e^{-ikx}\psi^+(x,k) - 1), \tag{5.8}$$

we obtain the following result (see [54]):

Theorem 5.3. *Let $v \in \mathcal{C}_c^\infty(\mathbb{R}^d)$. Then*

$$\begin{aligned} &Dv(x,-\theta) = a_{1,n}(x,\theta,s,\vec{\tau}) + \mathcal{O}(s^{-n}), \text{ as } s \to +\infty, \\ &a_{1,n}(x,\theta,s,\vec{\tau}) := \sum_{j=1}^{n} y_j(s,\vec{\tau}) z(x, s_j(s)\theta), \end{aligned} \tag{5.9}$$

where s_j are defined by (2.8), y_j are defined by (2.10).

The reconstruction formulas (5.9), (5.8) are new for $n \geq 2$.

Suppose that $supp\, v \subset \Omega$, where Ω is an open bounded convex domain in $\mathbb{R}^d$ with smooth boundary $\partial\Omega$. Let

$$\Sigma = \{(x,\theta) : x \in \partial\Omega,\ \theta \in \mathbb{S}^{d-1},\ \nu_x\theta > 0\}, \tag{5.10}$$

where ν_x denotes the outward normal to $\partial\Omega$ at point x. Then $2ib_1(x,\theta) = Dv(x,-\theta)$, $(x,\theta) \in \Sigma$, can be considered as the X-ray transform of v.

The methods for reconstructing v from its X-ray transform are developed in very details; see, for example, [39].

Formulas (5.8)-(5.9) and inversion formulas for the X-ray transform (see, e.g., [39]) give a method for inverse scattering from the boundary values $\psi^+(x,s\theta)$, $(x,\theta) \in \Sigma$ at several large s (that is, at several large energies).

5.3 Approaches to near-to-far field mapping

In this subsection we recall some old and recent known results on Problem 4(B).

The first formula for solving Problem 4(B) was given in theorem 3.3 of [9] for the case $d = 3$. This formula gives $f_1(k,l)$ at fixed $k \in \mathbb{S}^2_{\sqrt{E}}$ it term of an infinite sum of integrals of $\psi^+(x,k) - e^{ikx}$, $x \in \partial D$, for the case when $D = B_R$ for some $R > 0$, $d = 3$, where B_r is of (2.2).

Note that Problem 4(B), for $d \geq 1$, can be also solved via

$$f(k,l) = (2\pi)^{-d} \int_{\partial D} \left(e^{-ilx}\frac{\partial}{\partial\nu_x}\psi^+(x,k) - \psi^+(x,k)\frac{\partial}{\partial\nu_x}e^{-ilx}\right) dx, \tag{5.11}$$

where k, $l \in \mathbb{R}^d$, $k^2 = l^2 = E > 0$, ν_x is the outward normal to ∂D at $x \in D$; see [40].

A disadvantage of the aforementioned well-known formulas for solving Problem 4(B) for $d > 1$ consists in the following: for finding $f_1(k,l)$ at fixed $k, l \in \mathbb{S}^{d-1}_{\sqrt{E}}$ values of $\psi^+(x,k)$ along the whole boundary ∂D are necessary. In addition, the formula of [9] is complicated, whereas formula (5.11) requires not only ψ^+ on ∂D but also its normal derivative on ∂D.

In contrast, the multipoint approach of [46], gives, in particular, for fixed $(k,l) \in \mathcal{M}_E$,

$$\begin{aligned} &\text{explicit formulas for finding } f_1(k,l) \text{ up to } \mathcal{O}(s^{-n}), \text{ as } s \to +\infty, \\ &\text{from } \psi^+(x,k) \text{ given at } n \text{ points } x_1(s), ..., x_n(s), \end{aligned} \tag{5.12}$$

where

$$\begin{aligned} &x_j(s) = (s+\tau_j)\hat{l}, \quad j = 1, ..., n, \quad \hat{l} = l/|l|, \\ &s > 0, \quad 0 = \tau_1 < ... < \tau_n. \end{aligned} \tag{5.13}$$

This approach is based on asymptotic expansion (3.3) for ψ^+, the fact that the function

$$z(|x|, k, x/|x|) = |x|^{(d-1)/2} e^{-i|k||x|} \left(\psi^+(x,k) - e^{ikx}\right), \tag{5.14}$$

for fixed k, $x/|x|$ is of the form (2.7), and multipoint formulas presented in the Subsection 2.2.

Further, in Subsections 5.4, (5.5), we discuss analogs of formulas (5.12) for the case of Problem 6(A).

5.4 Two-point formulas for phaseless near-to-far field mapping

Historically, the multipoint approach goes back to two-point formulas of [42], [43] for solving Problem 6(A).

Let

$$a(x,k) = |x|^{(d-1)/2}(|\psi^+(k,x)|^2 - 1). \tag{5.15}$$

In particular, works [42], [43] give

$$\begin{aligned} &\text{explicit formulas for finding } f(k,l) \text{ up to } \frac{\mathcal{O}\left(s^{-\sigma}\right)}{\sin(\tau(|k| - k\hat{l}))}, \text{ as } s \to +\infty, \\ &\text{from } a(x,k) \text{ given at two points } x_1(s),\ x_2(s), \end{aligned} \tag{5.16}$$

where $x_1(s) = s\hat{l}$, $x_2(s) = (s+\tau)\hat{l}$, $\hat{l} = l/|l|$, and

$$\sigma = \begin{cases} 1/2, & \text{for} \quad d = 2, \\ 1, & \text{for} \quad d \geq 3. \end{cases} \tag{5.17}$$

Detailed estimates for the error term in (5.16), for $d = 2$ and $d = 3$, are given in [51] fulfilled in the framework of this thesis.

The main drow-back of formulas (5.16) is a slow rate of convergence as $s \to +\infty$. This disadvantage motivated further multipoint studies given in [46], [48], [53], where [53] is fulfilled in the framework of this thesis.

5.5 Multipoint formulas for phaseless near-to-far field mapping

In this subsection we present results of work [53] on Problem 6(A).

In particular, in this work we give, for fixed $(k,l) \in \mathcal{M}_E$, $l \neq k$, for $d \geq 2$,

$$\begin{aligned} &\text{explicit formulas for finding } f_1(k,l) \text{ up to } \mathcal{O}\left(s^{-n}\right), \text{ as } s \to +\infty, \\ &\text{from } |\psi^+(x,k)|^2 \text{ given at } m \text{ points } x_1(s), ..., x_m(s), \end{aligned} \tag{5.18}$$

where m depends linearly on n, and

$$\begin{aligned} &x_j(s) = (s+\tau_j)\hat{l}, \quad j = 1, ..., m, \quad \hat{l} = l/|l|, \\ &s > 0, \quad \tau_1 = 0, \quad \tau_{j_1} < \tau_{j_2}, \quad j_1 < j_2. \end{aligned} \tag{5.19}$$

One can see that in formulas (5.18) and (5.19) the measurement points $x_j = x_j(s)$ are on the ray starting at the origin in direction $\hat{l}$, where s is the distance between the origin and the set of these points, and the distances $\tau_{j+1} - \tau_j = |x_{j+1} - x_j|$ are fixed. In addition, the reconstruction formulas mentioned in (5.18) are asymptotic, where n can be considered as their convergence rate in terms of $\mathcal{O}(s^{-n})$ as $s \to +\infty$, that is when the points $x_j = x_j(s)$ move to infinity.

The main idea is to apply the approaches of Subsections 2.2, 5.4 to the phaseless function a defined by (5.15) in terms of $|\psi^+|^2$.

In the simplest result of [53], we assume that in formulas (5.18) and (5.19) $d = 3$, $m = 2n$ and that

$$\tau_j = \begin{cases} (j-1)\tau, & j = 1, ..., n, \\ \sigma + (j-1-n)\tau, & j = n+1, ..., 2n, \end{cases} \tag{5.20}$$

$$\tau = \tau(k,l) = \frac{2\pi}{\kappa}, \qquad 0 < \sigma \neq 0 \,(\mathrm{mod}\frac{\pi}{\kappa}), \quad \kappa = |k| - k\hat{l}. \tag{5.21}$$

Then our formulas (5.18) are specified as follows:

$$\begin{aligned} f_1(k,l) &= \frac{e^{-i(s+\sigma)\kappa}a_1(s) - e^{-is\kappa}a_2(s) + \mathcal{O}(s^{-n})}{-2i\sin(\sigma\kappa)}, \quad \text{as } s \to +\infty, \\ a_1(s) &= a_1(k,l,s) = \sum_{j=1}^{n} \frac{(-1)^{n-j}(s+\tau_j)^{n-1}}{(j-1)!(n-j)!\tau^{n-1}} a(x_j(s),k), \\ a_2(s) &= a_2(k,l,s) = \sum_{j=n+1}^{2n} \frac{(-1)^{n-j}(s+\tau_j)^{n-1}}{(j-1-n)!(2n-j)!\tau^{n-1}} a(x_j(s),k), \end{aligned} \tag{5.22}$$

where $(k,l) \in \mathcal{M}_E$, $l \neq k$, $d = 3$, $a(x,k)$ is defined by (5.15). In addition $\kappa \neq 0$, for $l \neq k$.

The fact that formulas (5.22) require $2n$ points in place of n points in (5.12) for the same precision $\mathcal{O}(s^{-n})$ is related to absence of phase information in data used in (5.22). In addition, formulas (5.22), for $n = 1$, reduce to two-point formulas (5.16).

Note that formulas (5.22) are completely explicit! Another advantage of this formula is relatively small ($m = 2n$) number of measurement points for every (k,l). A possible inconvenience of formula (5.22) is that the step $\tau = \tau(k,l)$ is fixed a priori, and depends on (k,l). Besides, formula (5.22) is not valid for $d = 2$ (because of different asymptotics (3.3) for ψ^+).

The aforementioned disadvantages of (5.22) motivated further results in [53].

In these results, we consider $|\psi^+(x,k)|^2$ for fixed k, given at m points x_j of the form (5.19), where

$$\tau_j = (j-1)\tau, \quad \tau \neq 0 \ (\mathrm{mod}\,\frac{\pi}{\kappa}). \tag{5.23}$$

For these points x_j we have the following results:

- for the case of small potentials ('linear case'), for $d = 2$, 3, we have

$$\begin{aligned} &\text{explicit formulas for finding } f_1(k,l) \text{ up to } \mathcal{O}(s^{-n}), \text{ as } s \to +\infty, \\ &\text{from } a(x,k) \text{ given at } 2n \text{ points } x_1(s), ..., x_{2n}(s), \end{aligned} \tag{5.24}$$

- for general potentials, $d = 3$, we have

$$\begin{aligned} &\text{explicit formulas for finding } f_1(k,l) \text{ up to } \mathcal{O}(s^{-n}), \text{ as } s \to +\infty, \\ &\text{from } a(x,k) \text{ given at } 3n-1 \text{ points } x_1(s), ..., x_{3n-1}(s), \end{aligned} \tag{5.25}$$

- for general potentials, $d = 2$, we have

$$\begin{aligned} &\text{explicit formulas for finding } f_1(k,l) \text{ up to } \mathcal{O}(s^{-n}), \text{ as } s \to +\infty, \\ &\text{from } a(x,k) \text{ given at } 3n \text{ points } x_1(s), ..., x_{3n}(s). \end{aligned} \tag{5.26}$$

Note that:

- there is a difference between $d = 2$ and $d = 3$ due to asymptotics (3.3) of ψ^+, the case $d = 2$ is more difficult;
- for the general case, $d = 2, 3$, formulas (5.25), (5.26) require more points than formulas (5.22) or (5.24);
- in contrast to (5.22), formulas (5.24), (5.25) and (5.26) do not require to fix τ a priori as a function of (k, l). In this respect, formulas (5.24), (5.25) and (5.26) are more convenient for applications;
- apparently, for the general cases of (5.25), (5.26) there are formulas that require less measurement points for the same precision.

Note that formulas of [42, 43, 48, 53] can be also used for Problem 6(A), (B) when coefficient v in equation (3.1) is replaced, e.g., by an impenetrable obstacle (see, e.g., [15] for definition of impenetrable obstacles).

6 Conclusions

This thesis contributes to studies on phase retrieval, phaseless inverse scattering, and multipoint formulas in inverse problems, and includes the following results:

1 We give phase retrieval formulas from a single phaseless Fourier transform with appropriate background information. Proceeding from these formulas we obtain different theoretical and numerical results on the phase retrieval problem for the classical Fourier transform.

2 We propose an iterative algorithm for inverse scattering from a single differential scattering cross section with appropriate background scatterer. This includes error estimates, stability estimates, and numerical implementation.

3 We give the first numerical implementation of the method of multipoint formulas in inverse problems, including an efficient regularization of these formulas for the noisy case. By this method we also obtain new theoretical results on polychromatic inverse scattering problems (from far-field data, phaseless far-field data, and from near-field data).

Topics of future studies include:

1 Numerical implementation of the aforementioned algorithms for the phase retrieval and phaseless inverse scattering problems for $d = 3$.

2 Further numerical implementation of multipoint formulas in inverse scattering for the Schrödinger and Helmholtz equations.

3 Theoretical and numerical extensions of the thesis results to the cases of other equations of mathematical physics.

4 Reconstruction from real data, e.g., in X-ray analysis or in electron tomography.

Bibliography

[1] F.V. Atkinson, *On Sommerfeld's 'radiation condition'*, London, Edinburgh Dublin Phil. Mag. J. Sci. 40 645–651 (1949)

[2] T. Aktosun, P.E. Sacks, *Inverse problem on the line without phase information,* Inverse Problems 14 211–24 (1998)

[3] A.D. Agaltsov, T. Hohage, R.G. Novikov, *An iterative approach to monochromatic phaseless inverse scattering*, Inverse Problems 35, 24001 (24 pp.) (2019)

[4] N.V. Alexeenko, V.A. Burov, O.D. Rumyantseva, *Solution of the three-dimensional acoustical inverse scattering problem. The modified Novikov algorithm,* Acoust. Phys. 54(3), 407–419 (2008)

[5] A.D. Agaltsov, R.G. Novikov, *Error Estimates for Phaseless Inverse Scattering in the Born Approximation at High Energies,* J Geom Anal 30, 2340–2360 (2020)

[6] J. A. Barceló, C. Castro, and J. M. Reyes, *Numerical approximation of the potential in the two-dimesional inverse scattering problem,* Inverse Problems, 32(1), 015006 (19pp) (2016)

[7] A. Barnett et al., *Geometry of the phase retrieval problem,* Inverse Problems 36.9 : 094003 (2020)

[8] A.H. Barnett, Ch.L. Epstein, L.F. Greengard, J.F. Magland, *Geometry of the phase retrieval problem—graveyard of algorithms*, Cambridge University Press, Cambridge (2022)

[9] Yu.M. Berezanskii, *On the uniqueness theorem in the inverse problem of spectral analysis for the Schrödinger equation,* Tr. Mosk. Mat. Obshch. 7, 3-62 (1958) (in Russian)

[10] F.A. Berezin, M.A. Shubin, *The Schrödinger Equation*, Mathematics and Its Applications, Vol. 66, Kluwer Academic, Dordrecht (1991)

[11] M. Born, *Quantenmechanik der Stossvorgange*, Zeitschrift fur Physik 38 (11-12), 803-827 (1926)

[12] V.A. Burov, N.V. Alekseenko, O.D. Rumyantseva, *Multifrequency generalization of the Novikov algorithm for the two-dimensional inverse scattering problem,* Acoust. Phys. 55(6), 843–856 (2009)

[13] V.S. Buslaev, *Trace formulas and certain asymptotic estimates of the resolvent kernel for the Schrödinger operator in three-dimensional space*, Topics in Mathematical Physics, Vol. 1, Plenum Press, Oxford (1967)

[14] K. Chadan, P.C. Sabatier, *Inverse Problems in Quantum Scattering Theory*, 2nd edn. Springer, Berlin, (1989)

[15] D. Colton, R. Kress, *Inverse Acoustic and Electromagnetic Scattering Theory (Applied Mathematical Sciences)* vol 93 4th edn (Berlin: Springer) (2019)

[16] K. Engel, B. Laasch, *The modulus of the Fourier transform on a sphere determines 3-dimensional convex polytopes*, J. Inverse Ill-Posed Probl., https://doi.org/10.1515/jiip-2020-0103

[17] L.D. Faddeev, *Uniqueness of the solution of the inverse scattering problem,* Vestn. Leningrad Univ. 7, 126–130 (1956) (in Russian)

[18] L.D. Faddeev, S.P. Merkuriev, *Quantum Scattering Theory for Multi-particle Systems*, Mathematical Physics and Applied Mathematics, 11. Kluwer Academic Publishers Group, Dordrecht, 1993

[19] D. Fanelli, O. Öktem, *Electron tomography: a short overview with an emphasis on the absorption potential model for the forward problem,* Inverse Problems, 24(1), 013001 (51 pp.) (2008)

[20] A. Fannjiang, T. Strohmer, *The numerics of phase retrieval,* Acta Numerica, 29, 125-228 (2020).

[21] P. G. Grinevich, *Scattering transformation at fixed non-zero energy for the two-dimensional Schrödinger operator with potential decaying at infinity*, Uspekhi Mat. Nauk, 55:6(336) (2000), 3–70; Russian Math. Surveys, 55:6 (2000), 1015–1083

[22] P. Hähner, T. Hohage, *New stability estimates for the inverse acoustic inhomogeneous medium problem and applications,* SIAM J. Math. Anal., 33(3):670–685, (2001)

[23] T. Hohage, R.G. Novikov, *Inverse wave propagation problems without phase information*, Inverse Problems 35, 070301 (4 pp.)(2019)

[24] T. Hohage, R.G. Novikov, V.N. Sivkin, *Reconstruction from differential scattering cross section with background information*, hal-03806616 (2022)

[25] N.E. Hurt, *Phase retrieval and zero crossings*, Kluwer Academic Publishers Group, Dordrecht (1989)

[26] M. I. Isaev, *Exponential instability in the inverse scattering problem on the energy interval*, Functional Analysis and Its Applications, vol. 47, 187–194 (2013)

[27] M. I. Isaev, R. G. Novikov, *Hölder-logarithmic stability in Fourier synthesis*, Inverse Problems, 36 (12), 125003 (2020)

[28] O. Ivanyshyn, R. Kress, R. Kress, *Identification of sound-soft 3D obstacles from phaseless data,* Inverse Problems Imaging 4 131–49 (2010)

[29] K. Jaganathan, Y. C. Eldar, B. Hassibi, *Phase retrieval: An overview of recent developments*, Optical Compressive Imaging, 279-312 (2016)

[30] A. Jesacher, W. Harm, S. Bernet, M. Ritsch-Marte, *Quantitative single-shot imaging of complex objects using phase retrieval with a designed periphery,* Opt. Express 20 5470–80 (2012)

[31] M.V. Klibanov, *On the recovery of a 2-D function from the modulus of its Fourier transform,* J. of Mathematical Analysis and Applications, 323, 818-843 (2006)

[32] M.V. Klibanov, *Phaseless inverse scattering problems in three dimensions,* SIAM J. Appl. Math. 74 392–410 (2014)

[33] M.V. Klibanov, V.G. Romanov, *Reconstruction procedures for two inverse scattering problems without the phase information* SIAM J. Appl. Math. 76 178–96 (2016)

[34] M.V. Klibanov, P.E. Sacks, A.V. Tikhonravov, *The phase retrieval problem*, Inverse Problems 11, 1–28 (1995)

[35] L.D. Landau, E.M. Lifschitz, *The classical theory of fields,* Pergamon press, chapter 5.41 (1971)

[36] B.A. Lippmann, J. Schwinger, *Variational principles for scattering processes,* I. Physical Review, 79(3), 469 (1950)

[37] B. Leshem, R. Xu, Y. Dallal, J. Miao, B. Nadler, D. Oron, N. Dudovich, O. Raz, *Direct single-shot phase retrieval from the diffraction pattern of separated objects,* Nature Communications 7(1), 1-6 (2016)

[38] N. Mandache, *Exponential instability in an inverse problem for the Schrödinger equation*, Inverse Problems, 17:5, 1435–1444 (2001)

[39] F. Natterer, *The Mathematics of Computerized Tomography*, Society for Industrial Mathematics, 184 pp. (2001)

[40] R.G. Novikov, *Multidimensional inverse spectral problem for the equation* $-\Delta\psi + (v(x) - Eu(x))\psi = 0$, Functional Analysis and Its Applications, 22(4), 263-272 (1988)

[41] R. G. Novikov, *Approximate Lipschitz stability for non-overdetermined inverse scattering at fixed energy*, Journal of Inverse and Ill-posed Problems. 21(6), 813–823 (2013)

[42] R.G. Novikov, *Formulas for phase recovering from phaseless scattering data at fixed frequency,* Bulletin des Sciences Mathematiques 139(8), 923-936 (2015)

[43] R.G. Novikov, *Inverse scattering without phase information,* Seminaire Laurent Schwartz - EDP et applications Exp. No16, 13p (2014-2015)

[44] R. G. Novikov, *An iterative approach to non-overdetermined inverse scattering at fixed energy,* Sbornik: Mathematics 206(1), 120-134 (2015)

[45] R. G. Novikov, *Explicit formulas and global uniqueness for phaseless inverse scattering in multidimensions*, J. Geom. Anal. 26(1), 346-359 (2016), e-print: https://hal.archives-ouvertes.fr/hal-01095750v1

[46] R. G. Novikov, *Multipoint formulas for scattered far field in multidimensions,* Inverse Problems, 36 (9), 095001(12 pp.) (2020)

[47] R. G. Novikov, *Multipoint formulae for inverse scattering at high energies,* Uspekhi Mat. Nauk, 76:4(460) , 177–178 (2021); Russian Math. Surveys, 76:4, 723–725 (2021)

[48] R.G Novikov, *Multipoint Formulas for Phase Recovering from Phaseless Scattering Data* J Geom Anal 31, 1965–1991 (2021)

[49] R.G. Novikov, *Multidimensional inverse scattering for the Schrödinger equation*, In: Cerejeiras, P., Reissig, M. (eds) Mathematical Analysis, its Applications and Computation. ISAAC 2019. Springer Proceedings in Mathematics & Statistics, vol 385, pp 75-98 (2022).Springer, Cham.

[50] R.G. Novikov, B.L. Sharma, *Phase recovery from phaseless scattering data for discrete Schrödinger operators,* arXiv preprint arXiv:2307.06041 (2023)

[51] R.G. Novikov, V.N. Sivkin, *Error estimates for phase recovering from phaseless scattering data,* Eurasian Journal of Mathematical and Computer Applications 8(1): 44-61 (2020)

[52] R.G. Novikov, V.N. Sivkin, *Phaseless inverse scattering with background information*, Inverse Problems 37(5), 055011 (2021)

[53] R.G. Novikov, V.N. Sivkin, *Fixed-distance multipoint formulas for the scattering amplitude from phaseless measurements*, Inverse Problems 38(2), 025012 (2022)

[54] R.G. Novikov, V.N. Sivkin, G.V. Sabinin, *Multipoint formulas in inverse problems and their numerical implementation,* hal-04053473 (2023)

[55] M.F. Perutz, *X-ray Analysis of Hemoglobin: The results suggest that a marked structural change accompanies the reaction of hemoglobin with oxygen,* Science, 140(3569), 863-869 (1963)

[56] S.G. Podorov, K.M. Pavlov, D.M. Paganin, *A non-iterative reconstruction method for direct and unambiguous coherent diffractive imaging*, Optics Express, 15(16), 9954-9962 (2007)

[57] V.G. Romanov, *Phaseless inverse problems that use wave interference,* Sib. Math. J. 59 494–504 (2018)

[58] V.G. Romanov, *Phaseless inverse problems for Schrödinger, Helmholtz, and Maxwell equations,* Comput. Math. Math. Phys. 60 1045–62 (2020)

[59] V.G. Romanov, *A phaseless inverse problem for electrodynamic equations in the dispersible medium,* Appl. Anal. https://doi.org/10.1080/00036811.2020.1846721 (2020)

[60] T. Salditt, A.-L. Robisch, *Coherent X-ray Imaging,* Nanoscale Photonic Imaging (eds. T. Salditt, A. Egner, R. Luke), pp. 35–70, Springer Int'l Publishing, https://doi.org/10.1007/978-3-030-34413-9_2 (2020)

[61] Y. Shechtman, Y.C. Eldar, O. Cohen, H.N. Chapman, J. Miao, J. M. Segev, *Phase retrieval with application to optical imaging: a contemporary overview,* IEEE signal processing 32, 87–109 (2015)

[62] V.N. Sivkin, *Approximate Lipschitz stability for phaseless inverse scattering with background information,* Journal of Inverse and Ill-posed Problems, https://doi.org/10.1515/jiip-2023-0001 (2023)

[63] A.S. Shurup, *Numerical comparison of iterative and functional-analytic algorithms for inverse acoustic scattering,* Eurasian Journal of Mathematical and Computer Applications **10**(1), 79-99 (2022)

[64] G. Vainikko, *Fast Solvers of the Lippmann-Schwinger equation,* Direct and Inverse Problems of Mathematical Physics (eds R.P. Gilbert, J. Kajiwara, Y.S. Xu) Kluwer, Dordrecht (2000)

[65] A. Walther, *The question of phase retrieval in optics,* Optica Acta: International Journal of Optics, 10(1), 41-49 (1963)

[66] H. Wendland, *Error estimates for interpolation by compactly supported radial basis functions of minimal degree,* J. Approx. Theory 93, 258–72 (1998)

[67] X. Xu, B. Zhang, H. Zhang, *Uniqueness in inverse electromagnetic scattering problem with phaseless far-field data at a fixed frequency,* IMA J. Appl. Math. 85 823–39 (2020)

[68] D. Yafaev, *High-energy and smoothness asymptotic expansion of the scattering amplitude,* Journal of Functional Analysis 202(2), 526-570 (2003)

Article I

Phaseless inverse scattering with background information

R.G. Novikov, V.N.Sivkin

We consider phaseless inverse scattering for the multidimensional Schrödinger equation with unknown potential v using the method of known background scatterers. In particular, in dimension $d \geq 2$, we show that $|f_1|^2$ at high energies uniquely determines v via explicit formulas, where f_1 is the scattering amplitude for $v + w_1$, w_1 is an a priori known nonzero background scatterer, under the condition that $supp\, v$ and $supp\, w_1$ are sufficiently disjoint. If this condition is relaxed, then we give similar formulas for finding v from $|f|^2, |f_1|^2$, where f is the scattering amplitude for v. In particular, we continue studies of [Novikov, J. Geom. Anal. 26(1), 346–359, 2016], [Leshem et al, Nature Communications 7(1), 1–6, 2016].

Keywords: Schrödinger equation, Helmholtz equation, phaseless inverse scattering, phase retrieval problem

1 Introduction

We consider the scattering problem for the stationary Schrödinger equation

$$-\Delta\psi + v(x)\psi = E\psi, \quad x \in \mathbb{R}^d, \ d \geq 1, \ E > 0, \tag{1.1}$$

where Δ is the standard Laplacian in x,

$$\begin{aligned} &v \in L^\infty(\mathbb{R}^d), \ v \text{ is complex–valued}, \ \ supp\ v \subset D, \\ &D \text{ is an open bounded domain in } \mathbb{R}^d. \end{aligned} \tag{1.2}$$

The Schrödinger equation (1.1), under assumptions (1.2), describes a non-relativistic quantum mechanical particle at fixed energy E interacting with a macroscopic object contained in D, where v is the potential of this interaction (and we assume that $\frac{\hbar^2}{2m} = 1$, where $\hbar$ is the reduced Planck's constant, m is the mass of the particle).

Equation (1) at fixed E can be also considered as the Helmholtz equation of electrodynamics or acoustics at fixed frequency ω. In this context v and E are interpreted as follows:

$$v(x) = (1 - n^2(x))E, \quad E = \left(\frac{\omega}{c_0}\right)^2, \tag{1.3}$$

where $n(x)$ is a scalar index of refraction, $n(x) \equiv 1$ on $\mathbb{R}^d \setminus D$, c_0 is a reference speed of wave propagation; and in the simplest case $n(x) = c_0/c(x)$, where $c(x)$ is a speed of wave propagation.

For equation (1.1) we consider the classical scattering solutions $\psi^+ = \psi^+(x,k)$, $x \in \mathbb{R}^d$, $k \in \mathbb{R}^d$, $k^2 = E$, specified by the following asymptotics as $|x| \to \infty$:

$$\psi^+(x,k) = e^{ikx} + \frac{e^{i|k||x|}}{|x|^{(d-1)/2}} A(k, |k|\frac{x}{|x|}) + O\left(\frac{1}{|x|^{(d+1)/2}}\right), \tag{1.4}$$

for some a priori unknown A. The function $\psi^+ = \psi^+(x,k)$ describes scattering of the incident plane waves described by e^{ikx} on the scatterer described by v. The second term on the right–hand side of (1.4) describes the leading scattered spherical waves. The function A arising with this term is the scattering amplitude for equation (1.1) for fixed E. This function is defined on

$$\mathcal{M}_E = \{k,\, l \in \mathbb{R}^d : \quad k^2 = l^2 = E\} = S^{d-1}_{\sqrt{E}} \times S^{d-1}_{\sqrt{E}}. \tag{1.5}$$

It is convenient to present A as follows:

$$A(k,l) = c(d,|k|) f(k,l),\ (k,l) \in \mathcal{M}_E, \tag{1.6}$$

$$c(d,|k|) = -\pi i (-2\pi i)^{(d-1)/2} |k|^{(d-3)/2},\ \text{for}\ \sqrt{-2\pi i} = \sqrt{2\pi} e^{-i\pi/4};$$

see formulas (1.9), (2.2), (2.5). We also use the terminology "scattering amplitude" for f arising in (1.4), (1.6).

In order to study ψ^+ and f one can use the Lippmann–Schwinger integral equation (2.1) for ψ^+ and the integral formula (2.2) for f; see Section 2.

We recall that in quantum mechanics the complex (phased) values of the functions ψ^+ and f have no direct physical sense, whereas the phaseless values of $|\psi^+|^2$ and $|f|^2$ have probabilistic interpretation (the Born's principle) and can be obtained in experiments; see [6], [11]. On the other hand, in acoustics or electrodynamics the complex values of ψ^+ and f can be directly measured, at least, in principle. However, in many important cases of monochromatic electro–magnetic wave propagation described using the model (1.1), (1.3) (e.g., X–rays and lasers) the frequency ω is so great that only phaseless values of $|\psi^+|$ and $|f|$ can be measured in practice by modern technical devices; see, e.g., [13] and references therein.

Let

$$\mathcal{M}_\Lambda = \cup_{E\in\Lambda} \mathcal{M}_E, \quad \text{where}\ \Lambda \subset \mathbb{R}_+ = (0,+\infty). \tag{1.7}$$

We consider, in particular, the following inverse scattering problems for equation (1):

Problem 1.1. Reconstruct potential v on $\mathbb{R}^d$ from its scattering amplitude f on some appropriate $\mathcal{M}' \subseteq \mathcal{M}_{\mathbb{R}_+}$.

Problem 1.2. Reconstruct potential v on $\mathbb{R}^d$ from its phaseless scattering data $|f|^2$ on some appropriate $\mathcal{M}' \subseteq \mathcal{M}_{\mathbb{R}_+}$.

Let $\mathcal{F}$ denote the Fourier transform defined by the formula

$$\hat{\nu}(p) = \mathcal{F}\nu(p) = (2\pi)^{-d} \int_{\mathbb{R}^d} e^{ipx} \nu(x) dx,\ p \in \mathbb{R}^d, \tag{1.8}$$

where ν is a test function.

In particular, for Problem 1.1, for $d \geq 2$, it is well known that the scattering amplitude f at high energies uniquely determines v via the formula

$$\hat{v}(p) = f(k,l) + O(E^{-1/2}) \ \text{ as } \ E \to +\infty, \ \ (k,l) \in \mathcal{M}_E, \ \ k - l = p \in \mathbb{R}^d; \tag{1.9}$$

see, for example, [10], [22]. For many other important results on Problem 1.1, see, for example, [7], [9], [26] and references therein.

On the other hand, for Problem 1.2 it is well known that the phaseless scattering data $|f|^2$ on $\mathcal{M}_{\mathbb{R}_+}$ do not determine v uniquely, in general; see, for example, [23].

In view of the aforementioned nonuniqueness for Problem 1.2 we also consider Problem 1.3 formulated below.

Let f be the initial scattering amplitude for v satisfying (1.2) and f_j be the scattering amplitude for

$$v_j = v + w_j, \quad j = 1, \dots, n, \tag{1.10}$$

where $w_1, \dots, w_n$ are additional a priori known background scatterers such that

$$\begin{aligned} &w_j \in L^\infty(\mathbb{R}^d), \;\; w_j \neq 0 \text{ in } L^\infty(\mathbb{R}^d), \quad supp\, w_j \subset \Omega_j, \\ &\Omega_j \;\text{ is an open bounded domain in }\; \mathbb{R}^d, \; \Omega_j \cap D = \varnothing, \\ &w_{j_1} \neq w_{j_2} \;\text{ for }\; j_1 \neq j_2 \;\text{ in }\; L^\infty(\mathbb{R}^d), \\ &j, \; j_1, \; j_2 \in \{1, \dots, n\}. \end{aligned} \tag{1.11}$$

Problem 1.3. Reconstruct potential v on $\mathbb{R}^d$ from the phaseless scattering data $|f|^2$, $|f_1|^2, ..., |f_n|^2$ on some appropriate $\mathcal{M}' \subseteq \mathcal{M}_{\mathbb{R}_+}$, for some appropriate background scatterers $w_1, \dots, w_n$.

Problem 1.3 in dimension $d = 1$ was considered in [1] for $n = 1$. Problem 1.3 in dimension $d \geq 2$ was considered in [2], [3], [23], [24].

In particular, for Problem 1.3, for $d \geq 2$, $n = 2$, analogs of formula (1.9) and related global uniqueness results were given in [23], [24]. Reconstruction results of [23], [24] on Problem 1.3, for $d \geq 2$, $n = 2$, were strongly developed in [2], [3]. In particular, for the phaseless case with background scatterers, results of [2] include an analog of the algorithm of [22]. Related numerical implementation is also given in [2].

In the previous works [2], [3], [22], [23], [24] for uniqueness and efficiency of reconstruction in Problem 1.3, for $d \geq 2$, the phaseless scattering data $|f|^2$, $|f_1|^2$, $|f_2|^2$ at high energies and background w_1, w_2 were necessary. In the present work we show that these data can be reduced considerably. In particular, we show that already $|f_1|^2$ at high energies and w_1 uniquely determine v via explicit formulas, under the condition that $supp\, v$ and $supp\, w_1$ are sufficiently disjoint ! If the latter condition is relaxed, we give similar formulas for finding v from $|f|^2$, $|f_1|^2$ at high energies and w_1. These formulas and related global uniqueness results are given in detail in Sections 3–6; see Theorems 4.1, 4.2, Corollaries 4.1, 4.2, Propositions 4.1, 4.2, Theorems 5.1, 5.2 and Theorems 6.1, 6.2. Note that our aforementioned reconstruction formulas include approximate reconstructions at fixed E and related error estimates; see Sections 4.2, 5, 6.

Remark 1.1. The aforementioned results on Problem 1.3 consisting in finding v from $|f_1|^2$ and w_1 can be also considered as results on Problem 1.2 with v supported in $D \cup \Omega_1$, where v is unknown in D and $v = w_1$ in Ω_1.

In addition, the present work involves considerations of the following problem of reconstruction from phaseless Fourier transforms, under assumptions (2), (9)–(11) (with L^1 in place of L^∞ for more generality).

Problem 1.4. Reconstruct v from the phaseless Fourier transforms $|\mathcal{F}v|^2$, $|\mathcal{F}v_1|^2, ..., |\mathcal{F}v_n|^2$ and background $w_1, ..., w_n$.

Problem 1.4 can be considered as Problem 1.3 in the Born approximation at high energies or/and for small $v, w_1, ..., w_n$; see formulas (2.5), (2.7).

In the literature the problem of finding v from $|\mathcal{F}v|^2$ is known as the phase retrieval problem; see [20], [4], [8] and references therein. The problem of finding v from $|\mathcal{F}v_1|^2$ and w_1 was considered, in particular, in [28], [21]. Problem 1.4 in the framework of solving Problem 1.3 was considered in [3], [2], [23], [24] and we continue such considerations in the present work.

The results of the present work on Problem 1.4 are given in Section 3 and consist in Theorems 3.1 and 3.2. Actually, Theorem 3.1 is a proper mathematical formalization of some of considerations of [21] related with finding v from $|\mathcal{F}v_1|^2$ and w_1, under the condition that $supp\, v$ and $supp\, w_1$ are sufficiently disjoint.

In addition to Problems 1.2, 1.3, 1.4, there are also other possible formulations of phaseless inverse scattering problems for equation (1.1) and for other equations of wave propagation. In connection with such formulations and related results, see, for example, [12]–[14], [17]–[19], [23], [25]–[27], [29]–[32] and references therein.

Finally, note that the further structure of the present article is as follows. In Section 2 we recall some known results on direct scattering for equation (1.1) under assumptions (1.2) (or when v is replaced by v_j of (1.10), (1.11)). The results of the present work on Problem 1.4 are given in

Section 3. The results of the present work on Problem 1.3 (and on Problem 1.2, see Remark 1.1) are given in Sections 4, 5, 6. In addition, estimates of Sections 5 and 6 are proved in Sections 7 and 8.

2 Preliminaries on direct scattering for equation (1.1)

For equation (1.1), under assumptions (1.2), we consider the scattering solutions ψ^+ specified by (1.4) and the scattering amplitude f arising in (1.4), (1.6). We recall that ψ^+ satisfy the Lippmann–Schwinger integral equation

$$\begin{aligned} \psi^+(x,k) &= e^{ikx} + \int_D G^+(x-y,k)v(y)\psi^+(y,k)dy, \\ G^+(x,k) &= -(2\pi)^{-d}\int_{\mathbb{R}^d} \frac{e^{i\xi x}d\xi}{\xi^2 - k^2 - i0} = G_0^+(|x|,|k|,d), \end{aligned} \tag{2.1}$$

where x, $k \in \mathbb{R}^d$, $k^2 = E$, and for f the following formula holds:

$$f(k,l) = (2\pi)^{-d}\int_D e^{-ily}v(y)\psi^+(y,k)dy, \tag{2.2}$$

where k, $l \in \mathbb{R}^d$, $k^2 = l^2 = E > 0$; see, for example, [5], [26] and references therein.

We also recall that for any $s > 1/2$, the following Agmon estimate holds:

$$\| < x >^{-s} G^+(k) < x >^{-s} \|_{L^2(\mathbb{R}^d)\to L^2(\mathbb{R}^d)} = a_0(d,s)|k|^{-1},\ |k| \geq 1, \tag{2.3}$$

where $< x >$ denotes the multiplication operator by the function $(1+|x|^2)^{1/2}$, $G^+(k)$ denotes the integral operator such that

$$G^+(k)u(x) = \int_{\mathbb{R}^d} G^+(x-y,k)u(y)dy, \tag{2.4}$$

where $G^+(x,k)$ is defined in (2.1), u is a test function. See, for example, the proof of (2.3) given in [9]; following this proof an explicit estimate for $a_0(d,s)$ can be given.

Using (2.1), (2.2), (2.3) one can show that, under assumptions (1.2), (1.10), (1.11), formula (1.9) is valid and the following formulas hold:

$$|\mathcal{F}v_j(p)|^2 = |f_j(k,l)|^2 + O(E^{-1/2}) \text{ as } E \to +\infty,\ (k,l) \in \mathcal{M}_E,\ k-l = p \in \mathbb{R}^d, \tag{2.5}$$

where f_j is the scattering amplitude for v_j, $j = 0, ..., n$, and $v_0 = v$, $f_0 = f$, $v_j = v + w_j$, $j \geq 1$; see, for example, [22], [24] and references therein.

We recall that formulas (1.9), (2.5) hold for any fixed $p \in \mathbb{R}^d$ for $d \geq 2$.

Suppose that, in addition to (1.2), (1.10), (1.11), we have that

$$\max(\|v\|_\infty, \|w_j\|_\infty) \leq \eta, \tag{2.6}$$

where $j = 1, ..., n$, $\|\cdot\|_\infty = \|\cdot\|_{L^\infty(\mathbb{R}^d)}$. Then the following more precise version of (2.5) holds (see formula (2.15) in [24]):

$$\begin{aligned} &||\mathcal{F}v_j(p)|^2 - |f_j(k,l)|^2| \leq c(D\cup\Omega_j)\eta^3 E^{-1/2},\ (k,l) \in \mathcal{M}_E,\ k-l = p \\ &\text{for } E^{1/2} \geq \rho(D\cup\Omega_j,\eta), \end{aligned} \tag{2.7}$$

where $j = 0, ..., n$, $\Omega_0 = \varnothing$, and $c > 0$, $\rho \geq 1$ are the constants defined by the formulas:

$$\rho(\mathcal{U},\eta) = \max(2a_0(d,\sigma/2)c_2(\mathcal{U},\sigma)\eta, 1), \tag{2.8}$$

$$c(\mathcal{U}) = 6(2\pi)^{-2d}a_0(d,\sigma/2)(c_1(d,\sigma))^4(c_2(\mathcal{U},\sigma))^3, \tag{2.9}$$

$$c_1(d,\sigma) = \left(\int_{\mathbb{R}^d} \frac{dx}{(1+|x|^2)^{\sigma/2}}\right)^{1/2}, \tag{2.10}$$

$$c_2(\mathcal{U},\sigma) = \sup_{x\in\mathcal{U}}(1+|x|^2)^{\sigma/2}, \tag{2.11}$$

for some fixed $\sigma > d$, $a_0(d,\sigma)$ is the constant of (2.3), $\mathcal{U}$ is an open bounded domain in $\mathbb{R}^d$.

Remark 2.1. The constants c, ρ have the following monotonicity properties:

$$c(\mathcal{U}_1 \cup \mathcal{U}_2) \geq c(\mathcal{U}_1), \tag{2.12}$$

$$\rho(\mathcal{U}_1 \cup \mathcal{U}_2, \eta) \geq \rho(\mathcal{U}_1, \eta), \quad \rho(\mathcal{U}, \eta_2) \geq \rho(\mathcal{U}, \eta_1) \text{ for } \eta_2 > \eta_1, \tag{2.13}$$

where $\mathcal{U}$, $\mathcal{U}_1$, $\mathcal{U}_2$ are bounded domains in $\mathbb{R}^d$, η, $\eta_1, \eta_2 > 0$.

3 Reconstruction from phaseless Fourier transforms

We consider v and w such that

$$v, w \in L_{1,loc}(\mathbb{R}^d),\ w \neq 0,\ d \geq 1, \tag{3.1}$$

$$supp\, v \subset D,\ supp\, w \subset \Omega, \tag{3.2}$$

$$D,\ \Omega \text{ are open convex and bounded domains in } \mathbb{R}^d. \tag{3.3}$$

Let

$$diam\, \mathcal{U} = \sup_{x,y \in \mathcal{U}} |x - y|, \tag{3.4}$$

$$-\mathcal{U} := \{-x :\ x \in \mathcal{U}\}, \tag{3.5}$$

$$\mathcal{U}_1 + \mathcal{U}_2 := \{x + y :\ x \in \mathcal{U}_1,\ y \in \mathcal{U}_2\}, \tag{3.6}$$

where $\mathcal{U}$, $\mathcal{U}_1$, $\mathcal{U}_2$ are bounded sets in $\mathbb{R}^d$.
Note that

$$\begin{aligned} &B_{r_1}(a_1) + B_{r_2}(a_2) = B_{r_1+r_2}(a_1 + a_2), \text{ where} \\ &B_r(a) = \{x \in \mathbb{R}^d :\ |x - a| < r\},\ a \in \mathbb{R}^d,\ r > 0. \end{aligned} \tag{3.7}$$

We suppose that the Fourier transformation $\mathcal{F}$ is defined by formula (1.8).
In this case $\mathcal{F}^{-1}$ is given by the formula

$$\mathcal{F}^{-1}\varphi(x) := \int_{\mathbb{R}^d} e^{-ipx}\varphi(p)dp, \tag{3.8}$$

where φ is a test function.
Let $\chi_{D-\Omega}$ denote the characteristic function of the set $D - \Omega$.

Theorem 3.1. *Let v, w satisfy (3.1)–(3.3), where $dist(D, \Omega) > diam\, D$. Then $|\mathcal{F}(v + w)|^2$ and w uniquely determine v by the formulas*

$$\mathcal{F}v(p) = (\overline{\mathcal{F}w}(p))^{-1}\mathcal{F}q(p),\ p \in \mathbb{R}^d, \tag{3.9}$$

$$q(x) := \chi_{D-\Omega}(x)\left(u(x) - (2\pi)^{-d}\int_{y \in \Omega} w(x + y)\overline{w(y)}dy\right), \tag{3.10}$$

$$u(x) := \mathcal{F}^{-1}(|\mathcal{F}(v + w)|^2)(x),\ x \in \mathbb{R}^d. \tag{3.11}$$

As it was already mentioned in Introduction, Theorem 3.1 can be considered as a proper mathematical formalization of some of considerations of [21] related with finding v from $|\mathcal{F}(v+w)|^2$ and w, under the condition that $supp\, v$ and $supp\, w$ are sufficiently disjoint.

Theorem 3.2. *Let v, w satisfy (3.1)–(3.3), where $dist(D, \Omega) > 0$. Then $|\mathcal{F}(v)|^2$, $|\mathcal{F}(v+w)|^2$ and w uniquely determine v by the formulas*

$$\mathcal{F}v(p) = (\overline{\mathcal{F}w}(p))^{-1}\mathcal{F}q(p),\ p \in \mathbb{R}^d, \tag{3.12}$$

$$q(x) := \chi_{D-\Omega}(x)\left(u(x) - (2\pi)^{-d}\int_{y \in \Omega} w(x + y)\overline{w(y)}dy\right), \tag{3.13}$$

$$u(x) := \mathcal{F}^{-1}(|\mathcal{F}(v + w)|^2)(x) - \mathcal{F}^{-1}(|\mathcal{F}v|^2)(x),\ x \in \mathbb{R}^d. \tag{3.14}$$

Under our assumptions on w, we have that

$$\mu\left(\{p \in \mathbb{R}^d \,:\, \mathcal{F}w(p) = 0\}\right) = 0, \tag{3.15}$$

where $\mu(\mathcal{A})$ denotes the d–dimentional Lebesgue measure of a set $\mathcal{A}$. Therefore, formulas (3.9), (3.12) are correctly defined inspite of the factor $(\overline{\mathcal{F}w}(p))^{-1}$.

In order to prove Theorems 3.1 and 3.2 we use, in particular, that

$$\mathcal{F}^{-1}(\varphi_1\varphi_2) = (2\pi)^{-d}(\mathcal{F}^{-1}\varphi_1) * (\mathcal{F}^{-1}\varphi_2), \tag{3.16}$$

$$(\nu_1 * \nu_2)(x) := \int_{\mathbb{R}^d} \nu_1(x-y)\nu_2(y)dy, \tag{3.17}$$

$$\overline{\mathcal{F}\nu} = \mathcal{F}\widetilde{\nu}, \;\; \widetilde{\nu}(x) = \overline{\nu(-x)}, \tag{3.18}$$

$$(2\pi)^{-d}\mathcal{F}(\nu_1 * \nu_2) = \mathcal{F}\nu_1\mathcal{F}\nu_2, \tag{3.19}$$

where φ_1, φ_2, ν, ν_1, ν_2 are test functions.

Proof of Theorem 3.1. Using formulas (3.16), (3.17), (3.18) for $\varphi_1 = \mathcal{F}(v+w)$, $\varphi_2 = \overline{\mathcal{F}(v+w)}$, $\nu = \nu_1 = v + w$, $\nu_2 = \widetilde{v} + \widetilde{w}$, we obtain that

$$\begin{aligned} I &= (2\pi)^d\mathcal{F}^{-1}(|\mathcal{F}(v+w)|^2) = (v+w) * (\widetilde{v} + \widetilde{w}) = \\ &= \int_{\mathbb{R}^d} (v(x-y) + w(x-y))\overline{(v(-y) + w(-y))}dy = \\ &= \int_{\mathbb{R}^d} v(x-y)\overline{v(-y)}dy + \int_{\mathbb{R}^d} w(x-y)\overline{v(-y)}dy + \int_{\mathbb{R}^d} v(x-y)\overline{w(-y)}dy + \\ &+ \int_{\mathbb{R}^d} w(x-y)\overline{w(-y)}dy =: I_1 + I_2 + I_3 + I_4. \end{aligned} \tag{3.20}$$

Let

$$B_r = \{x \in \mathbb{R}^d : |x| < r\}. \tag{3.21}$$

Note that

$$I_1(x) = \int_{y \in -D} v(x-y)\overline{v(-y)}dy, \tag{3.22}$$

$$supp\, I_1 \subset B_{diam D}, \tag{3.23}$$

$$I_2(x) = \int_{y \in -D} w(x-y)\overline{v(-y)}dy, \tag{3.24}$$

$$supp\, I_2 \subset \Omega - D, \tag{3.25}$$

$$I_3(x) = \int_{-y \in \Omega} v(x-y)\overline{w(-y)}dy, \tag{3.26}$$

$$supp\, I_3 \subset D - \Omega, \tag{3.27}$$

$$I_4(x) = \int_{-y \in \Omega} w(x-y)\overline{w(-y)}dy, \tag{3.28}$$

$$supp\, I_4(x) \subset B_{diam\,\Omega}, \tag{3.29}$$

where $\Omega - D$, $D - \Omega$, B_r are defined according to (3.5), (3.6), (3.21).

Property (3.23) follows from the observation that if $y \in D$, $x + y \in D$, then $x \in B_{diam\, D}$; property (3.25) follows from the observation that if $y \in D$, $x + y \in \Omega$, then $x \in \Omega - D$; and the derivation of (3.27), (3.29) is similar.

Using (3.3) and the assumption that $dist(D, \Omega) > diam\, D$ one can see that

$$dist(D,\Omega) > diam\, D \Leftrightarrow \forall x \in D,\, y \in \Omega : |x-y| > diam\, D \Leftrightarrow B_{diam\, D} \cap (D - \Omega) = \varnothing. \tag{3.30}$$

Since D and Ω are convex, the sets $D-\Omega$ and $\Omega-D$ are also convex and reciprocally symmetric. Therefore, if their intersection is nonempty, it contains the point 0. But formula (3.30) implies that $0 \notin D-\Omega$. Thus, we have that

$$(D-\Omega)\cap(\Omega-D)=\varnothing. \tag{3.31}$$

From (3.30), (3.31) we conclude that

$$(D-\Omega)\cap(B_{diam\,D}\cup(\Omega-D))=\varnothing, \tag{3.32}$$
$$(\Omega-D)\cap(B_{diam\,D}\cup(D-\Omega))=\varnothing. \tag{3.33}$$

Formulas (3.20), (3.23), (3.25), (3.27), (3.32), (3.33) imply that

$$I_2(x)=\chi_{\Omega-D}(x)(I(x)-I_4(x)), \tag{3.34}$$
$$I_3(x)=\chi_{D-\Omega}(x)(I(x)-I_4(x)). \tag{3.35}$$

Using (3.19), (3.24), (3.26) we have that

$$(2\pi)^{-d}\mathcal{F}I_2=\mathcal{F}\widetilde{v}\mathcal{F}w, \tag{3.36}$$

$$(2\pi)^{-d}\mathcal{F}I_3=\mathcal{F}v\mathcal{F}\widetilde{w}. \tag{3.37}$$

The formulas (3.9)–(3.11) follow from (3.18), (3.20), (3.35), (3.37). This completes the proof of Theorem 3.1.

Proof of Theorem 3.2. Formulas (3.20)–(3.29), (3.36), (3.37) remain valid under the assumptions of Theorem 3.2.

The assumption $dist(D,\,\Omega)>0$ implies that

$$0\notin D-\Omega. \tag{3.38}$$

Using formula (3.38) and the proof of formula (3.31) we obtain that formula (3.31) also remains valid under the assumptions of Theorem 3.2.

Formulas (3.20), (3.25), (3.27) and (3.31) imply that

$$I_2(x)=\chi_{\Omega-D}(x)(I(x)-I_1(x)-I_4(x)), \tag{3.39}$$
$$I_3(x)=\chi_{D-\Omega}(x)(I(x)-I_1(x)-I_4(x)). \tag{3.40}$$

The formulas (3.12)–(3.14) follow from (3.20), (3.37), (3.40). This completes the proof of Theorem 3.2.

Remark 3.1. Under the assumptions of Theorem 3.1, there exist $\varepsilon>0$, an open ε–neighbourhood $\mathcal{N}_\varepsilon(D-\Omega)$ of $D-\Omega$, and a function $\chi_{D-\Omega,\varepsilon}\in C^\infty(\mathbb{R}^d)$, such that

$$\chi_{D-\Omega,\varepsilon}(x)=1,\ x\in D-\Omega, \tag{3.41}$$
$$\chi_{D-\Omega,\varepsilon}(x)=0,\ x\in\mathbb{R}^d\setminus\mathcal{N}_\varepsilon(D-\Omega), \tag{3.42}$$
$$(\Omega-D)\cap\mathcal{N}_\varepsilon(D-\Omega)=\varnothing, \tag{3.43}$$
$$B_{diam\,D}\cap\mathcal{N}_\varepsilon(D-\Omega)=\varnothing. \tag{3.44}$$

In addition, formulas (3.9)–(3.11) remain valid with $\chi_{D-\Omega}$ replaced by $\chi_{D-\Omega,\varepsilon}$.

Remark 3.2. Under the assumptions of Theorem 3.2, there exist $\varepsilon>0$, an open ε–neighbourhood $\mathcal{N}_\varepsilon(D-\Omega)$ of $D-\Omega$, and a function $\chi_{D-\Omega,\varepsilon}\in C^\infty(\mathbb{R}^d)$, such that properties (3.41)–(3.43) are fulfilled. In addition, formulas (3.12)–(3.14) remain valid with $\chi_{D-\Omega}$ replaced by $\chi_{D-\Omega,\varepsilon}$.

Note that Remarks 3.1 and 3.2 are used in estimates of Sections 5 and 6.

4 Reconstruction formulas and uniqueness results for Problem 1.3

In this section we give reconstruction formulas and global uniqueness results for Problem 1.3, for $d \geq 2$, $n = 1$, and for Problem 1.2, for $d \geq 2$ (see Remark 1.1). These reconstruction formulas and global uniqueness results develop considerably related studies of [23], [24] on Problem 1.3, for $d \geq 2$, $n = 2$ and $n = 1$.

4.1 Uniqueness results

Theorem 4.1. *Let v, w_1 satisfy (1.2), (1.11), where D, $\Omega = \Omega_1$ satisfy (3.3), $dist(D, \Omega_1) > diam\, D$, and $d \geq 2$. Then $|f_1|^2$ and w_1 uniquely determine v via formulas (3.9)–(3.11), where $w = w_1$, and formula (2.5) for $j = 1$.*

Theorem 4.2. *Let v, w_1 satisfy (1.2), (1.11), where D, $\Omega = \Omega_1$ satisfy (3.3), $dist(D, \Omega_1) > 0$, and $d \geq 2$. Then $|f|^2$, $|f_1|^2$ and w_1 uniquely determine v via formulas (3.12)–(3.14), where $w = w_1$, and formula (2.5) for $j = 0, 1$.*

Theorems 4.1 and 4.2 follow directly from formula (2.5) and Theorems 3.1 and 3.2.
In addition to f, f_1 on $\mathcal{M}_E$, we also consider $f|_{\Gamma_E}$, $f_1|_{\Gamma_E}$, where

$$\begin{aligned} &\Gamma_E = \left\{k = k_E(p),\, l = l_E(p)\ : p \in \overline{B}_{2\sqrt{E}}\right\}, \\ &k_E(p) = p/2 + (E - p^2/4)^{1/2}\gamma(p),\ l_E(p) = -p/2 + (E - p^2/4)^{1/2}\gamma(p), \end{aligned} \tag{4.1}$$

$$B_r = \{p \in \mathbb{R}^d : |p| < r\},\ \ \overline{B}_r = \{r \in \mathbb{R}^d : |p| \leq r\},\ r > 0, \tag{4.2}$$

where γ is a piecewise continuous vector–function on $\mathbb{R}^d$, $d \geq 2$, such that

$$|\gamma(p)| = 1,\ \gamma(p)p = 0,\ p \in \mathbb{R}^d. \tag{4.3}$$

We recall that

$$\Gamma_E \subset \mathcal{M}_E,\ dim\, \Gamma_E = d,\ dim\, \mathcal{M}_E = 2d - 2,\ E > 0,\ d \geq 2. \tag{4.4}$$

We also consider

$$\mathcal{M}_\Lambda = \cup_{E\in\Lambda}\mathcal{M}_E,\ \Gamma_\Lambda = \cup_{E\in\Lambda}\Gamma_E, \tag{4.5}$$

where $\Lambda \subseteq \mathbb{R}_+ = (0, +\infty)$.

Let, for example, Λ be of the following form

$$\Lambda = \{E_j \in \mathbb{R}_+ : j \in \mathbb{N},\ E_j \to \infty,\ \text{ as } j \to \infty\}. \tag{4.6}$$

Theorems 4.1 and 4.2, where we use formula (2.5) with $k = k_{E_j}(p)$, $l = l_{E_j}(p)$, imply the following corollaries:

Corollary 4.1. *Let the assumptions of Theorem 4.1 hold. Let Λ be of the form (4.6). Then $|f_1|^2$ on Γ_Λ and background w_1 uniquely determine v in $L^\infty(\mathbb{R}^d)$.*

Corollary 4.2. *Let the assumptions of Theorem 4.2 hold. Let Λ be of the form (4.6). Then $S = \{|f|^2, |f_1|^2\}$ on Γ_Λ and background w_1 uniquely determine v in $L^\infty(\mathbb{R}^d)$.*

We also consider Λ of the form

$$\Lambda = \{E_j \in \mathbb{R}_+ : j \in \mathbb{N},\ E_{j_1} \neq E_{j_2} \text{ for } j_1 \neq j_2,\ E_j \to E_*,\ \text{ as } j \to \infty\},\ E_* > 0. \tag{4.7}$$

Proceeding from Theorems 4.1 and 4.2 we obtain the following results:

Proposition 4.3. *Let the assumptions of Theorem 4.1 hold, and v, w_1 be real–valued. Let Λ be of the form (4.7). Then $|f_1|^2$ on Γ_Λ and background w_1 uniquely determine v.*

Proposition 4.4. *Let the assumptions of Theorem 4.2 hold, and v, w_1 be real–valued. Let Λ be of the form (4.7). Then $S = \{|f|^2, |f_1|^2\}$ on Γ_Λ and background w_1 uniquely determine v.*

The proof of Propositions 4.1, 4.2 is similar to the proof of Theorem 2.2 of [24].

Remark 4.1 Corollary 4.2 and Proposition 4.2 of the present work develop the result of Proposition 2.2 of [24], where it was show that:

(A) There are not more than two different complex–valued potentials v satisfying (1.2) with given $S = \{|f|^2, |f_1|^2\}$ on Γ_Λ and background complex–valued potential w_1 satisfying (1.11), $w_1 \neq 0$ in $L^\infty(\mathbb{R}^d)$, where Λ is defined as in (4.6);

(B) There are not more than two different real–valued potentials v satisfying (1.2) with given $S = \{|f|^2, |f_1|^2\}$ on Γ_Λ and background real–valued potential w_1 satisfying (1.11), $w_1 \neq 0$ in $L^\infty(\mathbb{R}^d)$, where Λ is defined as in (4.7).

In addition, the reconstruction of Corollary 4.2 (based on formulas mentioned in Theorem 4.2) of the present work does not involve an analytic continuation in contrast with item (A) of Proposition 2.2 of [24].

4.2 Approximate reconstruction formulas

Suppose that the assumptions of Theorem 4.1 are valid. Then, at fixed E, proceeding from Theorem 4.1 and Remark 3.1 we reconstruct $v(x)$ as $v_{appr}(x, E)$, where

$$v_{appr}(x, E) := (\mathcal{F}^{-1}\hat{v}_{appr})(x, E),\ x \in D, \tag{4.8}$$

$$\hat{v}_{appr}(p, E) := \begin{cases} (\overline{\mathcal{F}w_1(p)})^{-1}(\mathcal{F}q_{appr})(p) \text{ for } p \in B_{(2-\delta)\sqrt{E}}, \\ 0 \text{ for } p \in \mathbb{R}^d \setminus B_{(2-\delta)\sqrt{E}}, \end{cases} \tag{4.9}$$

$$q_{appr}(x, E) := \chi_{D-\Omega,\varepsilon}(x)(u_{appr}(x, E) - (2\pi)^{-d}\int_{y\in\Omega} w_1(x+y)\overline{w_1(y)}dy), \tag{4.10}$$

$$u_{appr}(x, E) := (\mathcal{F}^{-1}h)(x), \tag{4.11}$$

$$h(p, E) := \begin{cases} |f_1(k_E(p), l_E(p))|^2 \text{ for } p \in B_{2\sqrt{E}}, \\ |\mathcal{F}w_1(p, E)|^2 \text{ for } p \in \mathbb{R}^d \setminus B_{2\sqrt{E}}, \end{cases} \tag{4.12}$$

where $k_E(p), l_E(p)$ are defined in (4.1), $\chi_{D-\Omega,\,\varepsilon}$ is the function of Remark 3.1, and $\delta \in (0, 2)$.

Suppose that the assumptions of Theorem 4.2 are valid. Then, at fixed E, proceeding from Theorem 4.2 and Remark 3.2 we reconstruct $v(x)$ as $v_{appr}(x, E)$, where $v_{appr}(x, E)$ is given by formulas (4.8)–(4.11) with

$$h(p, E) := \begin{cases} |f_1(k_E(p), l_E(p))|^2 - |f(k_E(p), l_E(p))|^2 \text{ for } p \in B_{2\sqrt{E}}, \\ |\mathcal{F}w_1(p, E)|^2 \text{ for } p \in \mathbb{R}^d \setminus B_{2\sqrt{E}}. \end{cases} \tag{4.13}$$

In Sections 5 and 6 we give error estimates for $\hat{v}_{appr}$ and v_{appr}. These error estimates develop considerably related studies of [23], [24], and [3] on Problem 1.3, for $d \geq 2$, $n \geq 2$.

5 Error estimates for $\hat{v}_{appr}$

In this section we estimate $|\hat{v}(p) - \hat{v}_{appr}(p, E)|$ for $p \in B_{(2-\delta)\sqrt{E}}$, where $\hat{v}_{appr}$ is defined in Subsection 4.2, $\hat{v} = \mathcal{F}v$.

Note that the following estimate holds:

$$|\mathcal{F}\chi_{D-\Omega,\varepsilon}(p)| \le \frac{C_1(\sigma)}{(1+|p|)^\sigma},\ p\in\mathbb{R}^d,\ \sigma\ge 0, \tag{5.1}$$

where $\chi_{D-\Omega,\varepsilon}$ is the function of Remarks 3.1, 3.2, $C_1(\sigma)=C_1(\sigma,\chi_{D-\Omega,\varepsilon})$ is a positive constant.

Let

$$C_2(\sigma)=\int_{\mathbb{R}^d}\frac{dp}{(1+|p|)^\sigma},\ \sigma>d. \tag{5.2}$$

Let $\mu(\mathcal{U})$ denote the Lebesgue measure of a bounded domain $\mathcal{U}\subset\mathbb{R}^d$.

Theorem 5.1. *Suppose that the assumptions of Theorem 4.1 are valid, and v, w_1 satisfy (2.6). Let $\hat v_{appr}$ be defined via (4.9)–(4.12). Then:*

$$|\hat v(p)-\hat v_{appr}(p,E)|\le|\hat w_1(p)|^{-1}\left(C_3E^{-1/2}\eta^3+\frac{C_4\eta^2}{(1+\delta E^{1/2})^{\sigma-d-\alpha}}\right) \tag{5.3}$$

for $p\in B_{(2-\delta)\sqrt{E}}$, $E^{1/2}\ge\rho(D\cup\Omega,\eta)$,

$$C_3=c(D\cup\Omega)C_1(\sigma_1)C_2(\sigma_1),\ \sigma_1>d, \tag{5.4}$$

$$C_4=(2\pi)^{-2d}(\mu(D)^2+2\mu(D)\mu(\Omega))C_1(\sigma)C_2(d+\alpha),\ \alpha>0,\ \sigma-d-\alpha>0, \tag{5.5}$$

where c, ρ are the constants of (2.7), C_1, C_2 are the constants of (5.1), (5.2), $\delta\in(0,2)$ is fixed.

Theorem 5.2. *Suppose that the assumptions of Theorem 4.2 are valid, and v, w_1 satisfy (2.6). Let $\hat v_{appr}$ be defined via (4.9)–(4.11), (4.13). Then:*

$$|\hat v(p)-\hat v_{appr}(p,E)|\le|\hat w_1(p)|^{-1}\left(C_5E^{-1/2}\eta^3+\frac{C_6\eta^2}{(1+\delta E^{1/2})^{\sigma-d-\alpha}}\right) \tag{5.6}$$

for $p\in B_{(2-\delta)\sqrt{E}}$, $E^{1/2}\ge\rho(D\cup\Omega,\eta)$,

$$C_5=(c(D)+c(D\cup\Omega))C_1(\sigma_1)C_2(\sigma_1),\ \sigma_1>d, \tag{5.7}$$

$$C_6=2(2\pi)^{-2d}\mu(D)\mu(\Omega)C_1(\sigma)C_2(d+\alpha),\ \alpha>0,\ \sigma-d-\alpha>0, \tag{5.8}$$

where c, ρ are the constants of (2.7), C_1, C_2 are the constants of (5.1), (5.2), $\delta\in(0,2)$ is fixed.

The estimates of Theorems 5.1, 5.2 can be considered as error estimates for $\hat v_{appr}(p,E)$ at high energies E.

Theorems 5.1, 5.2 are proved in Section 7.

In addition, it may be of interest to consider estimates (5.3), (5.6) for small v, w_1, that is for small η. In this case it is convenient to suppose also that

$$|\mathcal{F}w_1(p)|\ge\eta|\hat w_0(p)|,\ \forall p\in\mathbb{R}^d, \tag{5.9}$$

where $\hat w_0$ is independent of η, and

$$\hat w_0(p)=\mathcal{F}w_0(p), \tag{5.10}$$

$$w_0\in L^\infty(\mathbb{R}^d),\ supp\, w_0\subset\Omega=\Omega_1,\ w_0\ne 0. \tag{5.11}$$

Then estimate (5.3) takes the form

$$|\hat v(p)-\hat v_{appr}(p,E)|\le|\hat w_0(p)|^{-1}\left(C_3E^{-1/2}\eta^2+\frac{C_4\eta}{(1+\delta E^{1/2})^{\sigma-d-\alpha}}\right) \tag{5.12}$$

for $p\in B_{(2-\delta)\sqrt{E}}$, $E^{1/2}\ge\rho(D\cup\Omega,\eta)$, $\alpha>0$, $\sigma>d+\alpha$,

and estimate (5.6) takes the form

$$|\hat{v}(p) - \hat{v}_{appr}(p,E)| \le |\hat{w}_0(p)|^{-1}\left(C_5 E^{-1/2}\eta^2 + \frac{C_6\eta}{(1+\delta E^{1/2})^{\sigma-d-\alpha}}\right)$$
$$\text{for } p \in B_{(2-\delta)\sqrt{E}},\ E^{1/2} \ge \rho(D\cup\Omega,\eta),\ \alpha>0,\ \sigma > d+\alpha. \tag{5.13}$$

One can see that estimates (5.12), (5.13) are very efficient for small η and large E, because in this case $E^{-1/2}\eta^2$ and $\eta(1+\delta E^{1/2})^{-\sigma+d+\alpha}$ are very small.

Remark 5.1. The background w_1 can be chosen as real–valued non–negative continuous compactly supported function on $\mathbb{R}^d$ such that

$$\widehat{w_1}(p) = \overline{\widehat{w_1}(p)} \ge c_3(1+|p|)^{-\beta},\ p\in\mathbb{R}^d, \tag{5.14}$$

for $\beta > d$ and $c_3 > 0$; see, for example, Lemma 1 in [3]. Property (5.14) can be convenient in the framework of applications of the error estimates (5.3), (5.6).

Remark 5.2. If $\widehat{w_1}(p)$ in (4.9), (5.3), (5.6) has zeros, then the definition of $\hat{v}_{appr}(p,E)$ can be modified in neighborhoods of these zeros in a similar way with interpolations of Section 4 of [3].

6 Error estimates for v_{appr}

In this section we estimate $|v(x) - v_{appr}(x,E)|$ for $x\in D$, where v_{appr} is defined as in Subsection 4.2 with δ depending on E, and v, w_1 satisfy the assumptions of Theorem 5.1 or 5.2. In addition, for simplicity, we assume that $v\in W^{m,1}(\mathbb{R}^d)$, $m>d$, and w_1 satisfies (5.14), where

$$W^{m,1}(\mathbb{R}^d) = \{u : \partial^J u \in L^1(\mathbb{R}^d),\ |J|\le m\},$$
$$\|u\|_{m,1} = \max_{|J|\le m}\|\partial^J u\|_{L^1(\mathbb{R}^d)},\ m\in\mathbb{N}\cup 0. \tag{6.1}$$

Next, we assume that

$$v_{appr}(x,E) = \int_{B_{r_1(E)}} e^{-ixp}\hat{v}_{appr}(p,E)dp,\ x\in D,$$
$$r_1(E) = (2-\delta(E))\sqrt{E} = 2\tau E^{\gamma},\ \gamma = \frac{1}{2}\frac{1}{m+\beta}, \tag{6.2}$$

where $E \ge \rho^2(D\cup\Omega,\eta)\ge 1$ as in Theorems 5.1, 5.2, β is the number of (5.14), $\tau\in(0,1)$ is fixed. One can see that $\delta(E)\in(0,2)$ under the assumptions of formula (6.2).

Note that if $v\in W^{m,1}(\mathbb{R}^d)$, $m\ge 0$, then the following estimate holds:

$$|\hat{v}(p)| \le \frac{C_7(m)}{(1+|p|)^m},\ p\in\mathbb{R}^d, \tag{6.3}$$

where $C_7(m) = C_7(m,d,\|v\|_{m,1})$ is a positive constant.

Let

$$\gamma_1 = \frac{1}{2}\frac{m-d}{m+\beta},\quad \gamma_2 = \frac{\sigma-d-\alpha-1}{2}, \tag{6.4}$$

where $\alpha>0$, $\sigma-d-\alpha>1$, $\beta>d$, $m>d$.

Let $|S^{d-1}|$ denotes the $(d-1)$–dimentional Lebesgue measure of the unit sphere.

Theorem 6.1. *Let v, w_1 satisfy the assumptions of Theorem 5.1, where $\alpha>0$, $\sigma-d-\alpha>1$. Suppose also that $v\in W^{m,1}(\mathbb{R}^d)$, where $m>d$, and w_1 satisfies (5.14), where $\beta>d$. Let v_{appr} be defined by (4.9)–(4.12), (6.2). Then:*

$$|v(x) - v_{appr}(x,E)| \le A_1 E^{-\gamma_1} + A_2 E^{-\gamma_2},\ x\in D, \tag{6.5}$$

$$A_1 = \frac{|S^{d-1}|C_7(m)}{(2\tau)^{m-d}(m-d)} + (1+2\tau)^{\beta}(2\tau)^d c_3 C_3\eta^3\mu(B_1), \tag{6.6}$$

$$A_2 = \frac{(1+2\tau)^{\beta}(2\tau)^d}{(2-2\tau)^{\sigma-d-\alpha}}\mu(B_1)c_3C_4\eta^2, \tag{6.7}$$

where γ_1, γ_2 are given by (6.4), C_3, C_4, C_7 are given by (5.4), (5.5), (6.3), τ is the number of (6.2).

Theorem 6.2. *Let v, w_1 satisfy the assumptions of Theorem 5.2, where $\alpha > 0$, $\sigma - d - \alpha > 1$. Suppose also that $v \in W^{m,1}(\mathbb{R}^d)$, where $m > d$, and w_1 satisfies (5.14), where $\beta > d$. Let v_{appr} be defined by (4.9)–(4.11), (4.13), (6.2). Then:*

$$|v(x) - v_{appr}(x, E)| \le A_3 E^{-\gamma_1} + A_4 E^{-\gamma_2},\ x \in D, \tag{6.8}$$

$$A_3 = \frac{|S^{d-1}| C_7(m)}{(2\tau)^{m-d}(m-d)} + (1+2\tau)^{\beta}(2\tau)^d c_3 C_5 \eta^3 \mu(B_1), \tag{6.9}$$

$$A_4 = \frac{(1+2\tau)^{\beta}(2\tau)^d}{(2-2\tau)^{\sigma-d-\alpha}} \mu(B_1) c_3 C_6 \eta^2, \tag{6.10}$$

where γ_1, γ_2 are given by (6.4), C_5, C_6, C_7 are given by (5.7), (5.8), (6.3), τ is the number of (6.2).

The proofs of Theorems 6.1, 6.2 are given in Section 8. In these proofs we proceed from Theorems 5.1, 5.2, formula (6.2) and estimates (5.14), (6.3).

Remark 6.1. If the assumption that $v \in W^{m,1}(\mathbb{R}^d)$, $m > d$, is not fulfilled, then the considerations of the present section can be developed for apodized (smoothed) v in a similar way with considerations of Section 6.1 of [15] and Theorem 3.2, Remark 3.3 of [16].

7 Proofs of Theorems 5.1 and 5.2

Recall that

$$\mathcal{F}(\varphi_1\varphi_2)(p) = (\mathcal{F}\varphi_1 * \mathcal{F}\varphi_2)(p) = \int_{\mathbb{R}^d} \mathcal{F}\varphi_1(p-p')\mathcal{F}\varphi_2(p')dp',\ p \in \mathbb{R}^d, \tag{7.1}$$

where φ_1, φ_2 are test functions.

7.1 Proof of Theorem 5.1

We consider

$$\Delta h(p, E) = |\mathcal{F}(v + w_1)(p)|^2 - h(p, E),\ p \in \mathbb{R}^d, \tag{7.2}$$

$$\Delta u(x, E) = u(x) - u_{appr}(x, E),\ x \in \mathbb{R}^d, \tag{7.3}$$

$$\Delta q(x, E) = q(x) - q_{appr}(x, E),\ x \in \mathbb{R}^d, \tag{7.4}$$

$$\Delta \hat{v}(p, E) = \hat{v}(p) - \hat{v}_{appr}(p, E),\ p \in B_{(2-\delta)E}, \tag{7.5}$$

where $\hat{v} = \mathcal{F}v$, q, u are the functions of (3.9)–(3.11) with $\chi_{D-\Omega,\varepsilon}$ in place of $\chi_{D-\Omega}$, and $\hat{v}_{appr}$, q_{appr}, u_{appr}, h are the functions of (4.9)–(4.12). We have that

$$\Delta u(\cdot, E) = \mathcal{F}^{-1}\Delta h(\cdot, E),\ \ \Delta q(\cdot, E) = \chi_{D-\Omega,\varepsilon}\,\mathcal{F}^{-1}\Delta h(\cdot, E), \tag{7.6}$$

$$\Delta \hat{v}(p, E) = (\overline{\mathcal{F}w_1}(p))^{-1}\mathcal{F}\Delta q(p, E), \tag{7.7}$$

$$\mathcal{F}\Delta q(p, E) = \int_{\mathbb{R}^d} \mathcal{F}\chi_{D-\Omega,\varepsilon}(p-p')\Delta h(p', E)dp',\ p \in B_{(2-\delta)\sqrt{E}}, \tag{7.8}$$

where in (7.8) we used (7.1) and (7.6).

First, we estimate Δh. Definition (7.2) can be rewritten as

$$\Delta h(p, E) = |\mathcal{F}(v + w_1)(p)|^2 - |f_1(k_E(p), l_E(p))|^2,\ p \in B_{2\sqrt{E}}, \tag{7.9}$$

$$\Delta h(p, E) = |\mathcal{F}(v + w_1)(p)|^2 - |\mathcal{F}w_1(p)|^2,\ p \in \mathbb{R}^d \setminus B_{2\sqrt{E}}. \tag{7.10}$$

Due to (2.7), (7.9), we have that

$$|\Delta h(p,E)| \le c(D\cup\Omega)\eta^3 E^{-1/2},\ p\in B_{2\sqrt{E}},\ \text{ for } E^{1/2}\ge \rho(D\cup\Omega,\eta). \tag{7.11}$$

In addition, we have that

$$|\Delta h(p,E)| \le (2\pi)^{-2d}\eta^2(\mu(D)^2+2\mu(D)\mu(\Omega)),\ p\in\mathbb{R}^d\setminus B_{2\sqrt{E}}. \tag{7.12}$$

Estimate (7.12) follows from the following estimates

$$\begin{aligned}&\left||\mathcal{F}(v+w_1)|^2-|\mathcal{F}w_1|^2\right| \le \left||\mathcal{F}(v+w_1)|-|\mathcal{F}w_1|\right|\left(|\mathcal{F}(v+w_1)|+|\mathcal{F}w_1|\right)\le\\ &\le |\mathcal{F}v|^2+2|\mathcal{F}v||\mathcal{F}w_1|, \qquad (7.13)\\ &|\mathcal{F}v|\le(2\pi)^{-d}\eta\mu(D),\ |\mathcal{F}w_1|\le(2\pi)^{-d}\eta\mu(\Omega). \qquad (7.14)\end{aligned}$$

In (7.13) we used the inequalities

$$-|a|\le|a+b|-|b|\le|a|,\ a=\mathcal{F}v,\ b=\mathcal{F}w_1. \tag{7.15}$$

In view of (7.7), (7.8), estimating $\Delta\hat{v}$ consists of the following. We have that

$$\begin{aligned}&|\mathcal{F}\Delta q(p,E)|\le\int_{B_{2\sqrt{E}}}|\mathcal{F}\chi_{D-\Omega,\varepsilon}(p-p')|\,|\Delta h(p',E)|dp'+\\ &+\int_{\mathbb{R}^d\setminus B_{2\sqrt{E}}}|\mathcal{F}\chi_{D-\Omega,\varepsilon}(p-p')|\,|\Delta h(p',E)|dp'=I_1(p,E)+I_2(p,E),\end{aligned} \tag{7.16}$$

where $p\in B_{(2-\delta)\sqrt{E}}$.

Using (5.1), (7.11) we estimate I_1 as follows:

$$|I_1(p,E)|\le c(D\cup\Omega)\eta^3E^{-1/2}\int_{B_{2\sqrt{E}}}|\mathcal{F}\chi_{D-\Omega,\varepsilon}(p-p')|dp', \tag{7.17}$$

$$\begin{aligned}&\int_{B_{2\sqrt{E}}}|\mathcal{F}\chi_{D-\Omega,\varepsilon}(p-p')|dp'\le\int_{\mathbb{R}^d}|\mathcal{F}\chi_{D-\Omega,\varepsilon}(p')|dp'\le\\ &\le C_1(\sigma_1)\int_{\mathbb{R}^d}\frac{dp'}{(1+|p'|)^{\sigma_1}}=C_1(\sigma_1)C_2(\sigma_1),\ \sigma_1>d,\end{aligned} \tag{7.18}$$

where $p\in B_{(2-\delta)\sqrt{E}}$, C_1, C_2 are the constants of (5.1), (5.2).

Using (5.1), (7.12) we estimate I_2 as follows:

$$|I_2(p,E)|\le(2\pi)^{-2d}\eta^2(\mu(D)^2+2\mu(D)\mu(\Omega))C_1(\sigma)\int_{\mathbb{R}^d\setminus B_{2\sqrt{E}}}\frac{dp'}{(1+|p-p'|)^{\sigma}}, \tag{7.19}$$

$$\begin{aligned}&\int_{\mathbb{R}^d\setminus B_{2\sqrt{E}}}\frac{dp'}{(1+|p-p'|)^{\sigma}}=\int_{\mathbb{R}^d\setminus B_{2\sqrt{E}}}\frac{dp'}{(1+|p-p'|)^{\sigma-d-\alpha}(1+|p-p'|)^{d+\alpha}}\le\\ &\le\frac{1}{(1+\delta E^{1/2})^{\sigma-d-\alpha}}\int_{\mathbb{R}^d\setminus B_{2\sqrt{E}}}\frac{dp'}{(1+|p-p'|)^{d+\alpha}}\le\\ &\le\frac{1}{(1+\delta E^{1/2})^{\sigma-d-\alpha}}\int_{\mathbb{R}^d}\frac{dp'}{(1+|p-p'|)^{d+\alpha}}\le\frac{C_2(d+\alpha)}{(1+\delta E^{1/2})^{\sigma-d-\alpha}},\end{aligned} \tag{7.20}$$

where $p\in B_{(2-\delta)\sqrt{E}}$, $\alpha>0$, $\sigma-d-\alpha>0$, C_1, C_2 are the constants of (5.1), (5.2).

Formulas (5.3)–(5.5) follow from (7.5), (7.7), (7.16)–(7.20).

Theorem 5.1 is proved.

7.2 Proof of Theorem 5.2

We consider

$$\Delta h(p,E) = |\mathcal{F}(v+w_1)(p)|^2 - |\mathcal{F}v(p)|^2 - h(p,E),\ p \in \mathbb{R}^d, \tag{7.21}$$

where h is defined in (4.13). We also consider Δu, Δq, $\Delta\hat{v}$ defined as in (7.3)–(7.5), where u, q, $\hat{v} = \mathcal{F}v$ are defined by (3.12)–(3.14), u_{appr}, q_{appr}, $\hat{v}_{appr}$ are defined by (4.9)–(4.11), (4.13).

Note that formulas (7.6)–(7.8) remain valid with Δh given by (7.21).

First, we estimate Δh. Definition (7.21) can be rewritten as

$$\begin{aligned}&\Delta h(p,E) = (|\mathcal{F}(v+w_1)(p)|^2 - |f_1(k_E(p),l_E(p))|^2) - (|\mathcal{F}v(p)|^2 - |f(k_E(p),l_E(p))|^2),\\ &p \in B_{2\sqrt{E}},\end{aligned} \tag{7.22}$$

$$\Delta h(p,E) = |\mathcal{F}(v+w_1)(p)|^2 - |\mathcal{F}v(p)|^2 - |\mathcal{F}w_1(p)|^2,\ p \in \mathbb{R}^d \setminus B_{2\sqrt{E}}. \tag{7.23}$$

Due to (2.7), (7.22), we have that

$$\begin{aligned}&|\Delta h(p,E)| \le (c(D\cup\Omega)+c(D))\eta^3 E^{-1/2},\ p \in B_{2\sqrt{E}},\\ &\text{for } E^{1/2} \ge \rho(D\cup\Omega,\eta).\end{aligned} \tag{7.24}$$

In addition, we have that

$$|\Delta h(p,E)| \le 2(2\pi)^{-2d}\eta^2\mu(D)\mu(\Omega),\ p \in \mathbb{R}^d \setminus B_{2\sqrt{E}}. \tag{7.25}$$

Estimate (7.25) follows from (7.14) and the following estimate

$$||\mathcal{F}(v+w_1)|^2 - |\mathcal{F}v|^2 - |\mathcal{F}w_1|^2| \le 2|\mathcal{F}v||\mathcal{F}w_1|. \tag{7.26}$$

Estimate (7.16) for $\mathcal{F}\Delta q$ remains valid with Δh given by (7.21).

In addition: using (7.24) we have that

$$|I_1(p,E)| \le (c(D)+c(D\cup\Omega))\eta^3 E^{-1/2}\int_{B_{2\sqrt{E}}} |\mathcal{F}\chi_{D-\Omega,\varepsilon}(p-p')|dp',\ p \in B_{(2-\delta)\sqrt{E}}; \tag{7.27}$$

using (7.25) we have that

$$|I_2(p,E)| \le 2(2\pi)^{-2d}\eta^2\mu(D)\mu(\Omega)C_1(\sigma)\int_{\mathbb{R}^d\setminus B_{2\sqrt{E}}} \frac{dp'}{(1+|p-p'|)^\sigma},\ p \in B_{(2-\delta)\sqrt{E}},\ \sigma > d. \tag{7.28}$$

Formulas (5.6)–(5.8) follow from (7.5), (7.7), (7.16), (7.18), (7.20), (7.27), (7.28).

Theorem 5.2 is proved.

8 Proof of Theorems 6.1 and 6.2

The following formulas hold:

$$v(x) = \int_{\mathbb{R}^d} e^{-ixp}\hat{v}(p)dp,\ \ v_{appr}(x,E) = \int_{B_{(2-\delta)\sqrt{E}}} e^{-ixp}\widehat{v}_{appr}(p,E)dp,\ x \in D, \tag{8.1}$$

$$|v(x) - v_{appr}(x,E)| \le \int_{B_{(2-\delta)\sqrt{E}}} |\hat{v}(p) - \hat{v}_{appr}(p,E)|dp + \int_{\mathbb{R}^d\setminus B_{(2-\delta)\sqrt{E}}} |\hat{v}(p)|dp, \tag{8.2}$$

where in (8.1) we used the inversion formula for the Fourier transform and the definition of v_{appr}.

Recall that according to (6.2) we have that

$$(2-\delta(E))\sqrt{E} = 2\tau E^\gamma,\ \gamma = \frac{1}{2}\frac{1}{m+\beta}. \tag{8.3}$$

Using (6.3), (8.3) we have that

$$I_0 := \int_{\mathbb{R}^d \setminus B_{(2-\delta)\sqrt{E}}} |\hat{v}(p)|dp \le C_7(m)|S^{d-1}| \int_{(2-\delta)\sqrt{E}}^{\infty} \frac{dr}{r^{m-d+1}} = \\ = \frac{C_7(m)|S^{d-1}|}{(m-d)((2-\delta)\sqrt{E})^{m-d}} = \frac{C_7(m)|S^{d-1}|}{(m-d)(2\tau)^{m-d}} E^{-\gamma(m-d)}. \tag{8.4}$$

From Theorem 5.1 we have that

$$|\hat{v}(p) - \hat{v}_{appr}(p,E)| \le |\hat{w}_1(p)|^{-1}(C_3 E^{-1/2}\eta^3 + \frac{C_4\eta^2}{(1+\delta E^{1/2})^{\sigma-d-\alpha}}),\ p \in B_{(2-\delta)\sqrt{E}}. \tag{8.5}$$

From (5.14), (8.3) and (8.5) we obtain

$$\int_{B_{(2-\delta)\sqrt{E}}} |\hat{v}(p) - \hat{v}_{appr}(p,E)|dy \le c_3 \int_{B_{(2-\delta)\sqrt{E}}} (1+|p|)^{\beta} \left(C_3\eta^3 E^{-1/2} + \frac{C_4\eta^2}{(1+\delta E^{1/2})^{\sigma-d-\alpha}} \right) dp = \\ = c_3(C_3\eta^3 I_1 + C_4\eta^2 I_2), \tag{8.6}$$

$$I_1 := E^{-1/2} \int_{B_{(2-\delta)\sqrt{E}}} (1+|p|)^{\beta} dp \le E^{-1/2}(1+(2-\delta)\sqrt{E})^{\beta}\mu(B_1)((2-\delta)\sqrt{E})^d \le \\ \le E^{-1/2+d/2}(2-\delta)^d(1+(2-\delta)\sqrt{E})^{\beta}\mu(B_1) = E^{-1/2}(2\tau)^d E^{\gamma d}(1+2\tau E^{\gamma})^{\beta}\mu(B_1), \tag{8.7}$$

$$I_2 := \frac{\int_{B_{(2-\delta)\sqrt{E}}}(1+|p|)^{\beta}dp}{(1+\delta E^{1/2})^{\sigma-d-\alpha}} \le \frac{(1+(2-\delta)\sqrt{E})^{\beta}(2-\delta)^d E^{d/2}\mu(B_1)}{(1+\delta E^{1/2})^{\sigma-d-\alpha}} = \\ = \frac{(1+2\tau E^{\gamma})^{\beta}(2\tau)^d E^{\gamma d}\mu(B_1)}{(1+\delta E^{1/2})^{\sigma-d-\alpha}}. \tag{8.8}$$

Using (8.3), (8.7), (8.8), for $E \ge 1$ as in (6.2), we have that

$$I_1 \le (1+2\tau)^{\beta}\mu(B_1)(2\tau)^d E^{-1/2+\gamma d+\gamma\beta}, \tag{8.9}$$

$$I_2 \le \frac{(1+2\tau)^{\beta}(2\tau)^{\beta}\mu(B_1)E^{\gamma\beta+\gamma d}}{(\delta E^{1/2})^{\sigma-d-\alpha}} \le \frac{(1+2\tau)^{\beta}(2\tau)^{\beta}\mu(B_1)E^{\gamma\beta+\gamma d}}{(2\sqrt{E}(1-\tau E^{\gamma-1/2}))^{\sigma-d-\alpha}} \le \\ \le \frac{(1+2\tau)^{\beta}(2\tau)^{\beta}\mu(B_1)E^{\gamma\beta+\gamma d}}{2^{\sigma-d-\alpha}E^{(\sigma-d-\alpha)/2}(1-\tau E^{\gamma-1/2})^{\sigma-d-\alpha}} \le \frac{(1+2\tau)^{\beta}(2\tau)^{\beta}\mu(B_1)E^{\gamma\beta+\gamma d}}{2^{\sigma-d-\alpha}E^{(\sigma-d-\alpha)/2}(1-\tau)^{\sigma-d-\alpha}}, \tag{8.10}$$

where in the last inequality we used that $\gamma < 1/2$.

In addition, taking into account the value of γ we have that, for $E \to +\infty$:

$$I_0 = \mathcal{O}(E^{-\frac{1}{2}\frac{m-d}{m+\beta}}) = \mathcal{O}(E^{-\gamma_1}), \tag{8.11}$$

$$I_1 = \mathcal{O}(E^{-\frac{1}{2}+\frac{1}{2}\frac{d+\beta}{m+\beta}}) = \mathcal{O}(E^{-\frac{1}{2}\frac{m-d}{m+\beta}}) = \mathcal{O}(E^{-\gamma_1}), \tag{8.12}$$

$$I_2 = \mathcal{O}(E^{\frac{1}{2}\frac{\beta+d}{\beta+m}-\frac{\sigma-d-\alpha}{2}}) = \mathcal{O}(E^{-\frac{\sigma-d-\alpha-1}{2}}) = \mathcal{O}(E^{-\gamma_2}). \tag{8.13}$$

Estimate (6.5) follows from formulas (8.2), (8.4), (8.6), (8.9)–(8.13).

Theorem 6.1 is proved.

The proof of Theorem 6.2, proceeding from formula (6.2) and Theorem 5.2, is similar to the proof of Theorem 6.1, proceeding from formula (6.2) and Theorem 5.1.

Bibliography

[1] T. Aktosun, P. E. Sacks, *Inverse problem on the line without phase information*, Inverse Problems 14, 211–224 (1998)

[2] A.D. Agaltsov, T. Hohage, R.G. Novikov, *An iterative approach to monochromatic phaseless inverse scattering*, Inverse Problems 35, 24001 (24 pp.) (2019)

[3] A. D. Agaltsov, R.G. Novikov, *Error estimates for phaseless inverse scattering in the Born approximation at high energies*, J. Geom. Anal. (2017), https://doi.org/10.1007/s12220-017-9872-6, e-print: https://hal.archives-ouvertes.fr/hal-01303885v2

[4] A.H. Barnett, Ch.L. Epstein, L.F. Greengard, J.F. Magland, *Geometry of the phase retrieval problem*, Inverse Problems 36, 094003 (2020)

[5] F.A. Berezin, M.A. Shubin, *The Schrödinger Equation*, Mathematics and Its Applications, Vol. 66, Kluwer Academic, Dordrecht, 1991

[6] M. Born, *Quantenmechanik der Stossvorgange*, Zeitschrift fur Physik 38 (11-12), 803-827 (1926)

[7] K. Chadan, P.C. Sabatier, *Inverse Problems in Quantum Scattering Theory*, 2nd edn. Springer, Berlin, 1989

[8] K. Engel, B. Laasch, *The modulus of the Fourier transform on a sphere determines 3-dimensional convex polytopes*, J. Inverse Ill-Posed Probl., https://doi.org/10.1515/jiip-2020-0103

[9] G. Eskin, *Lectures on Linear Partial Differential Equations*, Graduate Studies in Mathematics, Vol. 123, American Mathematical Society, 2011

[10] L.D. Faddeev, *Uniqueness of the solution of the inverse scattering problem,* Vestn. Leningrad Univ. 7, 126–130 (1956) (in Russian)

[11] L.D. Faddeev, S.P. Merkuriev, *Quantum Scattering Theory for Multi-particle Systems*, Mathematical Physics and Applied Mathematics, 11. Kluwer Academic Publishers Group, Dordrecht, 1993

[12] A.A. Govyadinov, G.Y. Panasyuk, J.C. Schotland, *Phaseless three-dimensional optical nanoimaging*, Phys. Rev. Lett. 103, 213901 (2009)

[13] T. Hohage, R.G. Novikov, *Inverse wave propagation problems without phase information*, Inverse Problems 35, 070301 (4 pp.)(2019)

[14] O. Ivanyshyn, R. Kress, *Inverse scattering for surface impedance from phase-less far field data*, J. Comput. Phys. 230(9), 3443-3452 (2011)

[15] M. Isaev, R.G. Novikov, *Hölder-logarithmic stability in Fourier synthesis*, Inverse Problems 36, 125003 (2020)

[16] M. Isaev, R.G. Novikov , *Stability estimates for reconstruction from the Fourier transform on the ball*, J. Inverse Ill-Posed Probl., https://doi.org/10.1515/jiip-2020-0106

[17] M.V. Klibanov, *Phaseless inverse scattering problems in three dimensions*, SIAM J.Appl. Math. 74(2), 392-410 (2014)

[18] M.V. Klibanov, N.A. Koshev, D.-L. Nguyen, L.H. Nguyen, A. Brettin, V.N. Astratov, *A numerical method to solve a phaseless coefficient inverse problem from a single measurement of experimental data*, SIAM J. Imaging Sci. 11(4), 2339-2367 (2018)

[19] M.V. Klibanov, V.G. Romanov, *Reconstruction procedures for two inverse scattering problems without the phase information*, SIAM J. Appl. Math. 76(1), 178-196 (2016)

[20] M.V. Klibanov, P.E. Sacks, A.V. Tikhonravov, *The phase retrieval problem*, Inverse Problems 11, 1–28 (1995)

[21] B. Leshem, R. Xu, Y. Dallal, J. Miao, B. Nadler, D. Oron, N. Dudovich, O. Raz, *Direct single-shot phase retrieval from the diffraction pattern of separated objects,* Nature Communications 7(1), 1-6 (2016)

[22] R. G. Novikov, *An iterative approach to non-overdetermined inverse scattering at fixed energy*, Sbornik: Mathematics 206(1), 120-134 (2015)

[23] R. G. Novikov, *Inverse scattering without phase information*, Seminaire Laurent Schwartz - EDP et applications (2014-2015), Exp. No16, 13p

[24] R. G. Novikov, *Explicit formulas and global uniqueness for phaseless inverse scattering in multidimensions*, J. Geom. Anal. 26(1), 346-359 (2016), e-print: https://hal.archives-ouvertes.fr/hal-01095750v1

[25] R. G. Novikov, *Multipoint formulas for phase recovering from phaseless scattering data*, J. Geom. Anal. (2019), https://doi.org/10.1007/s12220-019-00329-6

[26] R.G. Novikov, *Multidimensional inverse scattering for the Schrödinger equation*, Book series: Springer Proceedings in Mathematics and Statistics. Title of volume: Mathematical Analysis, its Applications and Computation - ISAAC 2019, Aveiro, Portugal, July 29-August 2; Editors: P. Cerejeiras, M. Reissig (to appear), e-preprint: https://hal.archives-ouvertes.fr/hal-02465839v1

[27] R. G. Novikov, V. N. Sivkin, *Error estimates for phase recovering from phaseless scattering data*, Eurasian Journal of Mathematical and Computer Applications, vol. 8(1), 44–61, (2020)

[28] S.G. Podorov, K.M. Pavlov, D.M. Paganin, *A non-iterative reconstruction method for direct and unambiguous coherent diffractive imaging*, Optics Express, 15(16), 9954-9962 (2007)

[29] V. G. Romanov, *Inverse problems without phase information that use wave interference*, Sib. Math. J. 59(3), 494-504 (2018)

[30] V.G. Romanov, *A phaseless inverse problem for electrodynamic equations in the dispersible medium*, Applicable Analysis (2020), https://doi.org/10.1080/00036811.2020.1846721

[31] X. Xu, B. Zhang, H. Zhang, *Uniqueness in inverse electromagnetic scattering problem with phaseless far–field data at a fixed frequency*, IMA Journal of Applied Mathematics 85(6), 823-839 (2020)

[32] Y. Ziyang, H. Wang, *Phase retrieval with background information*, Inverse Problems 35, 054003 (20pp.) (2019)

Article II

Phase retrieval and phaseless inverse scattering with background information

T. Hohage, R.G. Novikov, V.N. Sivkin

We consider the problem of finding a compactly supported potential in the multidimensional Schrödinger equation from its differential scattering cross section (squared modulus of the scattering amplitude) at fixed energy. In the Born approximation this problem simplifies to the phase retrieval problem of reconstructing the potential from the absolute value of its Fourier transform on a ball. To compensate for the missing phase information we use the method of a priori known background scatterers. In particular, we propose an iterative scheme for finding the potential from measurements of a single differential scattering cross section corresponding to the sum of the unknown potential and a known background potential, which is sufficiently disjoint. If this condition is relaxed, then we give similar results for finding the potential from additional monochromatic measurements of the differential scattering cross section of the unknown potential without the background potential. The performance of the proposed algorithms is demonstrated in numerical examples.

Keywords: Schrödinger equation, Helmholtz equation, monochromatic scattering, phaseless inverse scattering, phase retrieval problem, numerical reconstructions

1 Introduction

In this work we contribute to the study of phase retrieval problems and phaseless inverse scattering problems. These problems naturally arise in quantum mechanics, optics, and related areas such as electron tomography and X-ray imaging; see, for example, [20] and references therein. In particular, according to Born's rule in quantum mechanics complex (phased) values of a particle wave function have no direct physical interpretation, whereas their (phaseless) squared modulus admits a probabilistic interpretation and can be measured; see [9]. Similarly, in optics modern technical devices such as CCD cameras measure the intensity, i.e. the squared modulus, but it is very hard or impossible to measure the phase of time-harmonic electromagnetic waves in the frequency range of visible light or even X-rays.

In general, phase retrieval problems consist in finding a function $v : \mathbb{R}^d \to \mathbb{C}$ from the magnitude $|\widehat{v}|$ of its Fourier transform

$$\widehat{v}(p) = \mathcal{F}v(p) = \frac{1}{(2\pi)^d} \int_{\mathbb{R}^d} e^{ip\cdot x} v(x)\, dx, \tag{1.1}$$

often given only for p in some bounded subset of $\mathbb{R}^d$, e.g., $B_r := \{x \in \mathbb{R}^d : |x|_2 \le r\}$. To compensate for the missing phase information $\widehat{v}/|\widehat{v}|$, one either assumes a-priori information on v or additional data. Such inversions of the Fourier transform from phaseless data are much more complicated than the inversion of the Fourier transform from phased data. Examples of a-priori

informations include (approximate) knowledge of $\operatorname{supp} v$, constraints like $|v| = 1$ or $v \geq 0$, and knowledge of v on part of the domain. In this paper we will focus on the first and the last of these options. Such problems arise directly in phaseless linearized inverse scattering problems in quantum mechanics, optics and related areas such as electron tomography and X-ray imaging. We refer to the monographs [21, 7], the review papers [32, 39, 47], the article [12], and references therein.

We now give the precise formulation of the phase retrieval problems studied in this paper:

Problem 7. *(A) Reconstruct a function v from $|\widehat{v}+\widehat{w}|^2$ on B_R for some known function w under the a-priori assumption that $\operatorname{supp} v$ and $\operatorname{supp} w$ are compact and sufficiently separated.*

(B) Reconstruct v from $|\widehat{v}|^2$ and $|\widehat{v} + \widehat{w_j}|^2$, $j = 1, \dots, n$, on B_R for some appropriate known functions $w_1, ..., w_n$ separated from v.

Problem 7(B) was considered, in particular, in [36, 37, 1, 2]. In addition, related considerations go back, at least, to [43]. Problem 7(A) was studied in [41]. Other investigations related to this problem can be found in [44, 37]. In the present work we give, in particular, new mathematical and numerical results on Problem 7(A) and on Problem 7(B) for $n = 1$.

Inverse scattering problems consist in finding functions describing a scattering object from data on scattered waves, usually at large distances from the scatterer. These problems are similar in many respects to reconstructing a function from its Fourier transform and, moreover, are reduced to such a Fourier inversion by the Born approximation, i.e. linearization around a zero background. Of course, also in situations where linearizations are not valid, only amplitudes can be measured for the same reasons as described above. This motivates the study of phaseless inverse scattering problems.

We consider the stationary Schrödinger equation of quantum mechanics:

$$-\Delta\psi + v(x)\psi = E\psi, \qquad x \in \mathbb{R}^d,\ d \geq 1,\ E > 0, \tag{1.2}$$

where

$$v \in L^\infty(\mathbb{R}^d),\ \operatorname{supp} v \subseteq D,\ \ D \subset \mathbb{R}^d \text{ is open and bounded.} \tag{1.3}$$

Equation (1.2), under assumptions (1.3), arises in modelling interaction of a non-relativistic quantum mechanical particle at fixed energy E with a macroscopic object contained in D, where v is the potential of this interaction. Here, we assume that $\hbar^2/(2m) = 1$, where $\hbar$ is the reduced Planck's constant, and m is the mass of the particle. For more details on such a model in the framework of electron tomography, see, for example, [15].

We also consider the time harmonic Helmholtz equation of electrodynamics and acoustics:

$$\Delta\psi + \kappa^2 n^2(x)\psi = 0, \qquad \kappa = \omega/c_0, \tag{1.4}$$

where ω is the frequency, c_0 is a reference speed of wave propagation, $n(x)$ is a scalar index of refraction, $n(x) \equiv 1$ for $x \in \mathbb{R}^d \setminus D$, and D is as in (1.3). We recall that in the simplest case $n(x) = c_0/c(x)$, where $c(x)$ is a speed of wave propagation. For more details on such a model in the framework of X-ray imaging, see, for example, [49]. We recall that the Helmholtz equation (1.4) at fixed ω can be written in the form of the Schrödinger equation (1.2), (1.3), where

$$v(x) = (1 - n^2(x))E, \quad E = \left(\frac{\omega}{c_0}\right)^2. \tag{1.5}$$

For equation (1.2), under condition (1.3), we consider the scattering solutions $\psi^+ = \psi^+(x, k)$, $k \in \mathbb{R}^d$, $k^2 = E$, specified by the conditions

$$\psi^+(x, k) = e^{ikx} + \psi^{\mathrm{sc}}(x, k); \tag{1.6}$$

$$|x|^{(d-1)/2}\left(\frac{\partial}{\partial|x|} - i|k|\right)\psi^{\mathrm{sc}}(x, k) \to 0 \ \text{ as } |x| \to +\infty, \tag{1.7}$$

uniformly in $x/|x|$. The Sommerfeld radiation condition (1.7) implies that

$$\psi^{\rm sc}(x,k)=\frac{e^{i|k||x|}}{|x|^{(d-1)/2}}A\left(k,|k|\frac{x}{|x|}\right)+O\left(\frac{1}{|x|^{(d+1)/2}}\right)\quad\text{as } |x|\to+\infty, \tag{1.8}$$

where $A=A[v]$ is the scattering amplitude for equation (1.2). For more information on the definitions of ψ^+ and A, see, for example, [8], [39] and references therein.

In turn, $\sigma[v](k,l)=|A[v](k,l)|^2$ is known as the differential scattering cross section for equation (1.2). We will suppress v in $\sigma[v]$ and $A[v]$ if there is no ambiguity. As for particle wave functions, A admits no direct physical interpretation whereas $|A|^2$ is the expected value of quantities that can be measured in experiments; see, for example, [9], [16]. In particular, the differential scattering cross section $\sigma(k,l)$ describes the probability density of scattering of a particle with initial impulse k into direction $l/|l|\neq k/|k|$. Similarly, in the electromagnetism of optics and X-rays only $|\psi^+|^2$ and $\sigma=|A|^2$ can be measured directly by modern technical devices.

Note that the aforementioned functions A and $\sigma=|A|^2$ are defined on

$$\mathcal{M}_E=\{k,\,l\in\mathbb{R}^d:\quad k^2=l^2=E\}=\mathbb{S}^{d-1}_{\sqrt{E}}\times\mathbb{S}^{d-1}_{\sqrt{E}}. \tag{1.9}$$

We consider the following monochromatic phaseless inverse scattering problems which reduce to Problem 7 in the Born approximation:

Problem 8. *(A) Reconstruct a compactly supported potential v in (1.2) from the differential scattering cross section $\sigma[v+w]$ on some appropriate $\mathcal{M}'\subseteq\mathcal{M}_E$ for some known compactly supported background potential w sufficiently separated from v.*

(B) Reconstruct v from $\sigma[v]$ and $\sigma[v+w_j]$, $j=1,\dots,n$ on some appropriate $\mathcal{M}'\subseteq\mathcal{M}_E$ (see (1.9)) for some appropriate known background potentials $w_1,...,w_n$ separated from v.

Phaseless inverse scattering problems are much more difficult than usual inverse scattering problems with phase information, and until recently very little results have been known for such problems (see, e.g., [1, 11, 39, 41] and references therein). In particular, it is well known that $\sigma=|A|^2$ on $\mathcal{M}_{\mathbb{R}_+}=\bigcup_{E\in\mathbb{R}_+}\mathcal{M}_E$ does not determine v uniquely, in general; see, for example, [39].

In addition to Problem 8 there are also other possible formulations of phaseless inverse scattering problems for equation (1.2) and for other equations of wave propagation. In connection with such formulations and related results, see, for example, [5], [11], [17], [20], [22], [23], [27], [29]–[31], [36], [38]–[40], [42], [45], [46], [52], [53] and references therein.

Following previous works of the authors, our general approach for "solving" Problems 7 and 8 is to provide explicit reconstruction formulas only for the stable part of the solution defined roughly in terms of the classical diffraction limit. These reconstruction formulas only provide a smoothed version of the unknown function v. They do not converge to the true solution v as the noise level tends to zero, but only as the energy (or wave number) tends to infinity. On the other hand, in contrast to regularization methods, they are Lipschitz stable with respect to data noise, they do not require a sufficiently good initial guess, and they are cheaper to compute. For small noise levels, our reconstructions can be improved by using them as initial guess for iterative regularization methods. Probably, our reconstructions can be also improved using the approach of [26], but this issue requires additional studies.

Our main results can be summarized as follows:

We propose an iterative reconstruction algorithm for Problem 8(A) in dimension $d\geq 2$ under the condition that $\operatorname{supp} v$ and $\operatorname{supp} w$ are sufficiently disjoint. If this condition is relaxed, then we give similar results just for Problem 8(B) with $d\geq 2$ and $n=1$. This iterative monochromatic reconstruction is analogous to the algorithm suggested in [35] for inverse scattering problems with phase information at fixed sufficiently large energy E. This reconstruction is considerably simpler than the algorithm developed in [1] for Problem 8(B) with $d\geq 2$ and $n=2$. This reconstruction

proceeds from results of [41], which provide, in particular, the first approximation. In addition, for our iterates u_E^j, $j = 1, 2, ...$, we have that

$$\|v - u_E^j\|_{L^\infty} = \mathcal{O}(E^{-\alpha_j}) \text{ as } E \to +\infty, \tag{1.10}$$

with α_j tending to $+\infty$ as $j \to \infty$, for infinitely smooth v. See Section 3.2.

We implement numerically the aforementioned iterative monochromatic reconstruction, at least, for $d = 2$; see Sections 4 and 5.

In connection with the aforementioned monochromatic reconstruction v_E in the Born approximation our study also includes new results on Problem 7(A) and Problem 7(B) for $n = 1$. In particular, in this case proceeding from [41] we show that

$$\|v - v_E\|_{L^\infty} = \mathcal{O}(E^{-\alpha}) \text{ as } E \to +\infty,\ \alpha = \frac{1}{2}(m - d), \tag{1.11}$$

where v is m-times smooth in $L^1(\mathbb{R}^d)$; see Section 3.1. Note that estimate (1.11) is an analog for the phaseless case of estimate (2.16) for the phased case. In addition, in numerical reconstruction of v_E from the data on discrete Ewald grid in $B_{2\sqrt{E}}$, we modified the related conjugate gradient approach of [1]; see Section 4.3.

The further structure of the present article is as follows. In Section 2 we recall some known results on direct and inverse scattering for equation (1.2) under assumptions (1.3), including results on Problems 7 and 8. Our main new theoretical results on Problems 7 and 8 are given in Section 3. Our numerical results on these problems are presented in Sections 4, 5. In conclusion, we discuss the results of the present work, previous results, and natural further research directions; see Section 6. Some proofs are also given in Sections 7 and 8 of Appendix.

2 Preliminaries

2.1 Direct scattering

For equation (1.2), under condition (1.3), we consider the scattered field ψ^+, its scattering amplitude A, and its scattering cross section $\sigma = |A|^2$ mentioned in the Introduction; see formulas (1.6), (1.7), and (1.8). For finding these functions from v one can use the Lippmann-Schwinger integral equation

$$\begin{aligned} \psi^+(x,k) &= e^{ikx} + \int_{\mathbb{R}^d} G^+(x-y,k)v(y)\psi^+(y,k)dy, \\ G^+(x,k) &= -(2\pi)^{-d}\int_{\mathbb{R}^d} \frac{e^{i\xi x}d\xi}{\xi^2 - k^2 - i0} = G_0^+(|x|,|k|,d), \end{aligned} \tag{2.1}$$

for ψ^+ with $x,\ k \in \mathbb{R}^d$, $k^2 = E$ and the following formulas for A:

$$\begin{aligned} &A(k,l) := c(d,|k|)f(k,l),\ (k,l) \in \mathcal{M}_E, \\ &c(d,|k|) := -\pi i(-2\pi i)^{(d-1)/2}|k|^{(d-3)/2},\ \text{for } \sqrt{-2\pi i} = \sqrt{2\pi}e^{-i\pi/4}, \end{aligned} \tag{2.2a}$$

$$f(k,l) := (2\pi)^{-d}\int_{\mathbb{R}^d} e^{-ily}v(y)\psi^+(y,k)dy, \tag{2.2b}$$

We will use the term 'scattering amplitude' also for f arising in (2.2).

Note that one can also use equation (2.1) and formula (2.2b) for the case when

$$v \in L_s^\infty(\mathbb{R}^d),\ \text{ for some } s > d, \tag{2.3}$$

where

$$L_s^\infty(\mathbb{R}^d) = \{u \in L^\infty(\mathbb{R}^d) : \|u\|_s < \infty\}, \tag{2.4}$$

$$\|u\|_s = \operatorname{ess\,sup}_{\mathbb{R}^d}(1 + |x|^2)^{s/2}|u(x)|,\ s \geq 0; \tag{2.5}$$

see, for example, [8], [39] and references therein.

Let

$$B_r = \{x \in \mathbb{R}^d : |x| \le r\}. \tag{2.6}$$

In addition to A, σ, and f on $\mathcal{M}_E$, we also consider their restrictions to lower-dimensional subsets $\Gamma_E \subset \mathcal{M}_E$ for which the function

$$\tilde{\Phi} : \Gamma_E \to B_{2\sqrt{E}}, \qquad \tilde{\Phi}(k,l) := k - l \tag{2.7}$$

is surjective, where B_r is defined by (2.6), $d \ge 2$; see [1]. In particular, $\tilde{\Phi}$ is bijective if Γ_E is defined as in [35]:

$$\begin{aligned} &\Gamma_E = \left\{k = k_E(p),\, l = l_E(p) \ : p \in B_{2\sqrt{E}}\right\}, \\ &k_E(p) = p/2 + (E - p^2/4)^{1/2}\gamma(p),\ l_E(p) = -p/2 + (E - p^2/4)^{1/2}\gamma(p), \end{aligned} \tag{2.8}$$

where γ is a piecewise continuous vector–function on $\mathbb{R}^d$, $d \ge 2$, such that

$$|\gamma(p)| = 1,\ \gamma(p)p = 0,\ \ p \in \mathbb{R}^d. \tag{2.9}$$

In general we assume that for each $p \in B_{2\sqrt{E}}$ the set $\tilde{\Phi}^{-1}(p)$ is a piecewise smooth manifold of size $|\tilde{\Phi}^{-1}(p)|$ and define the averaging operator

$$(\Phi f)(p) := \frac{1}{|\tilde{\Phi}^{-1}(p)|} \int_{\tilde{\Phi}^{-1}(p)} f(k,l)d(k,l),\ \ p \in B_{2\sqrt{E}}. \tag{2.10}$$

Note that if Γ_E is defined by (2.8), then

$$(\Phi f)(p) = f(k_E(p), l_E(p)),\ \ p \in B_{2\sqrt{E}}. \tag{2.11}$$

To deal with equation (2.1) at large E, it is convenient to use the following Agmon estimate

$$\|\langle x\rangle^{-s}\mathcal{G}_0^+(E)\langle x\rangle^{-s}\|_{L^2(\mathbb{R}^d)\to L^2(\mathbb{R}^d)} \le a_0(d,s)E^{-1/2},\ E \ge 1,\ s > 1/2, \tag{2.12}$$

where $\langle x\rangle$ denotes the multiplication operator by the function $(1+|x|^2)^{1/2}$, and $\mathcal{G}_0^+(E) : L^2(\mathbb{R}^d) \to L^2(\mathbb{R}^d)$ denotes the integral operator

$$\mathcal{G}_0^+(E)u(x) := \int_{\mathbb{R}^d} G_0^+(|x-y|, \sqrt{E}, d)u(y)dy, \tag{2.13}$$

with kernel $G_0^+(|x|, \sqrt{E}, d)$ defined in (2.1); see, for example, [13], [35].

2.2 Some known results on inverse scattering problems with phase information

We recall that in the Born approximation for small v, for $d \ge 2$, the scattering amplitude f on Γ_E (and on $\mathcal{M}_E$) reduces to the Fourier transform $\widehat{v}$ on $B_{2\sqrt{E}}$ via the formula

$$f(k,l) \approx \widehat{v}(p),\ (k,l) \in \mathcal{M}_E,\ p = k - l, \tag{2.14}$$

where f is defined by (2.2), $\widehat{v}$ is defined by (1.1).

Moreover, for u_E defined by

$$u_E(x) := \int_{B_{2\sqrt{E}}} e^{-ipx}\widehat{v}(p)dp, \tag{2.15}$$

we have that

$$\|v - u_E\|_{L^\infty(\mathbb{R}^d)} = \mathcal{O}(E^{-\alpha}) \text{ as } E \to +\infty \text{ with } \alpha := \frac{1}{2}(m-d), \tag{2.16}$$

where v is m-times smooth in $L^1(\mathbb{R}^d)$. For more details on the linearised monochromatic reconstruction u_E, see, for example, [39].

Besides, in general (i.e., without assumption that v is small), for finding $\widehat{v}$ from f on Γ_E at large E, for $d \geq 2$, one can use the following formulas:

$$\widehat{v}(p) = f(k,l) + \mathcal{O}(E^{-1/2}) \quad \text{as} \quad E \to +\infty, \quad (k,l) \in \mathcal{M}_E, \quad k - l = p \in \mathbb{R}^d, \tag{2.17}$$

$$\begin{aligned} &|f(k,l) - \widehat{v}(k-l)| \leq (2\pi)^{-d} a_0(d, s/2)(c_1(d,s)\|v\|_s)^2 E^{-1/2}, \\ &E^{1/2} \geq \rho_1(d, s, \|v\|_s),\ (k,l) \in \mathcal{M}_E,\ s > d. \end{aligned} \tag{2.18}$$

Here $a_0(d, s/2)$ is defined in (2.12) and

$$c_1(d,s) := \left(\int_{\mathbb{R}^d} \frac{dx}{(1+|x|^2)^{s/2}} \right)^{1/2}, \tag{2.19}$$

$$\rho_1(d,s,N) := \max\left(2a_0(d,s/2)N, 1\right). \tag{2.20}$$

Formula (2.17) goes back to [14] and can be considered as Born approximation for f at higher energies. In connection with estimate (2.18), see, for example, [35].

In turn, estimate (2.18) can be considered as particular case of the following important lemma.

Lemma 2.1. *([35]). Let v satisfy (2.3), D be bounded domain in $\mathbb{R}^d$, f be the scattering amplitude for v, and $v_{\text{appr}}(\cdot, E)$ be an approximation to v such that:*

$$|v_{\text{appr}}(x,E) - v(x)| \leq bE^{-\alpha}, \qquad x \in D,\ \sqrt{E} \geq \rho_1(d,s,N), \tag{2.21}$$

$$v_{\text{appr}}(x,E) = v(x), \qquad x \in \mathbb{R}^d \setminus D, \tag{2.22}$$

for some α, $b > 0$, and some N such that

$$\|v\|_s \leq N, \quad \|v_{\text{appr}}(\cdot, E)\|_s \leq N, \quad \sqrt{E} \geq \rho_1(d,s,N). \tag{2.23}$$

Then the following estimate holds:

$$\begin{aligned} |f(k,l) - f_{\text{appr}}(k,l) + \widehat{v}_{\text{appr}}(k-l,E) - \widehat{v}(k-l)| \leq \frac{Nb}{(2\pi)^d} a_0(d, \tfrac{s}{2}) c_1(d,s) c_2(D,s) E^{-\alpha - \frac{1}{2}}, \\ (k,l) \in \mathcal{M}_E,\ E^{1/2} \geq \rho_1(d,s,N), \end{aligned} \tag{2.24}$$

where f_{appr} is the scattering amplitude for $v_{\text{appr}}(\cdot, E)$, $\widehat{v}$ is the Fourier transform of v, $\widehat{v}_{\text{appr}}(\cdot, E)$ is the Fourier transform of $v_{\text{appr}}(\cdot, E)$,

$$c_2(D,s) = 2\|\Lambda^{s/2}\|_{L^2(D)} + 4\|\Lambda^{-s/2}\|_{L^2(\mathbb{R}^d)} \|\Lambda^s\|_{L^\infty(D)}, \tag{2.25}$$

$$\Lambda = (1+|x|^2)^{1/2}. \tag{2.26}$$

Suppose that

$$v - v_0 \in W^{m,1}(\mathbb{R}^d),\ \text{supp}(v - v_0) \subset D,\ v_0 \text{ satisfies (2.3)}, \tag{2.27}$$

with the Sobolev space

$$\begin{aligned} &W^{m,1}(\mathbb{R}^d) := \{u : \partial^J u \in L^1(\mathbb{R}^d),\ |J| \leq m\}, \\ &\|u\|_{m,1} := \max_{|J| \leq m} \|\partial^J u\|_{L^1(\mathbb{R}^d)},\ m \in \mathbb{N} \cup 0. \end{aligned} \tag{2.28}$$

Using estimate (2.18) and Lemma 2.1, under conditions (2.27), work [35] constructs the iterates u_E^j from f on Γ_E such that

$$\|v - u_E^j\|_{L^\infty(D)} = \mathcal{O}(E^{-\alpha_j}) \quad \text{as } E \to +\infty \text{ with} \tag{2.29}$$

$$\alpha_1 := \frac{m-d}{2m}, \quad \alpha_j := \left(1 - \left(\frac{m-d}{m}\right)^j\right) \frac{m-d}{2d},\ j \geq 1. \tag{2.30}$$

More precisely, this construction of u_E^j is based on formula (2.18), if $j = 1$, and uses iteratively Lemma 2.1, if $j > 1$. In addition, one can see that

$$\begin{aligned} &\alpha_j \to \alpha_\infty := \frac{m-d}{2d} && \text{as } j \to +\infty, \\ &\alpha_j \to \frac{j}{2} && \text{as } m \to +\infty, \\ &\alpha_\infty \to +\infty && \text{as } m \to +\infty. \end{aligned} \tag{2.31}$$

Therefore, the convergence in (2.29), as $E \to +\infty$, is drastically better for $j > 1$ than for $j = 1$, at least, for large m and j.

The iterative monochromatic reconstruction of [35] is implemented numerically in [6], [48] for $d = 2$. For other monochromatic phased inverse scattering reconstructions for equations (1.2) and (1.4), see, for example, [4], [10], [18], [39].

2.3 Some known results on Problems 7 and 8

In addition to v satisfying (1.3), we consider a priori known background scatterers $w_1, ..., w_n$ such that

$$\begin{aligned} &w_j \in L^\infty(\mathbb{R}^d), \ \ w_j \neq 0 \text{ in } L^\infty(\mathbb{R}^d), \quad \operatorname{supp} w_j \subset \Omega_j, \\ &\Omega_j \ \text{ is an open bounded domain in } \ \mathbb{R}^d, \ \Omega_j \cap D = \varnothing, \\ &w_{j_1} \neq w_{j_2} \ \text{ for } \ j_1 \neq j_2 \ \text{ in } \ L^\infty(\mathbb{R}^d), \\ &j, \ j_1, \ j_2 \in \{1, \dots, n\}. \end{aligned} \tag{2.32}$$

Under assumptions (1.3), (2.32), $d \geq 2$, we have that

$$|\widehat{v}_j(p)|^2 = |f_j(k,l)|^2 + \mathcal{O}(E^{-1/2}) \text{ as } E \to +\infty, \ (k,l) \in \mathcal{M}_E, \ k - l = p \in \mathbb{R}^d, \ j = 0, 1, ..., \tag{2.33}$$

where $v_0 = v$, $v_j = v + w_j$, $j \geq 1$, f_j is related to A_j according to (2.2a) and is the scattering amplitude for v_j.

In addition, for small v and w_j, we have that

$$|\widehat{v}_j(p)|^2 \approx |f_j(k,l)|^2, \ p = k - l, \ k - l \in \mathcal{M}_E. \tag{2.34}$$

Formulas (2.33), (2.34) are phaseless versions of (2.17), (2.14); for phaseless version of (2.18), see, for example, [37]. These formulas reduce Problems 8 to Problem 7.

For open bounded domains D, Ω_1, $\mathcal{U} \subset \mathbb{R}^d$ and $\varepsilon > 0$ we introduce the following notation:

$$D - \Omega_1 := \{x - y : \ x \in D, \ y \in \Omega_1\}, \tag{2.35a}$$

$$\operatorname{dist}(D, \Omega_1) := \inf_{x \in D, \, y \in \Omega_1} |x - y|, \quad \operatorname{diam} D := \sup_{x, \, y \in D} |x - y|, \tag{2.35b}$$

$$\chi_{\mathcal{U},\varepsilon} \in C^\infty(\mathbb{R}^d), \ 0 \leq \chi_{\mathcal{U},\varepsilon} \leq 1, \tag{2.35c}$$

$$\chi_{\mathcal{U},\varepsilon}(x) := \begin{cases} 1, \ x \in \mathcal{U}, \\ 0, \ \operatorname{dist}(x, \mathcal{U}) > \varepsilon \end{cases} \tag{2.35d}$$

The recent work [41] defines an approximate reconstruction v_E of the unknown potential v for Problems 8(A) and 8(B, $n = 1$) with $d \geq 2$, convex D and Ω_1, and $\mathcal{M}' = \Gamma_E$. In case of Problem 8(A) with scattering data $\sigma_1 = \sigma[v + w_1]$ on Γ_E, it is assumed that $\operatorname{dist}(D, \Omega_1) > \operatorname{diam} D$, whereas for Problem 8(B, $n = 1$) with scattering data $\{\sigma, \sigma_1\} = \{\sigma[v], \sigma[v + w_1]\}$ on Γ_E only $\operatorname{dist}(D, \Omega_1) > 0$ is required. The reconstruction v_E is defined by Algorithm 1 with $\nu = 1$ in [41] and Q_E given by

$$Q_E(p) := \tfrac{1}{|c(d,\sqrt{E})|^2}(\Phi\sigma_1)(p), \qquad p \in B_{2\sqrt{E}}, \quad \text{for Problem 8(A)}, \tag{2.36a}$$

$$Q_E(p) := \tfrac{1}{|c(d,\sqrt{E})|^2}((\Phi\sigma_1)(p) - (\Phi\sigma)(p)), \qquad p \in B_{2\sqrt{E}}, \quad \text{for Problem 8(B, } n = 1), \tag{2.36b}$$

where $c(d, \sqrt{E})$ is given by (2.2a).

Algorithm 1:

function $v_E = \texttt{reco}(Q_E, w, E, D, \nu, \tau)$

// basic reconstruction procedure proposed in [41]; see also Alg. 3 for a discrete version

Input:

Q_E: is computed from data by (2.39) for Problem 7 and by (2.36) for Problem 8

$w \in L^\infty(\mathbb{R}^d)$: background potential

$E > 0$: energy

convex $D \subset \mathbb{R}^d$ contains $\operatorname{supp} v$ for unknown function v

$\nu, \tau \in (0, 1]$: cut-off parameters

Output:

v_E: approximation of unknown function v

1 $h_E(p) := \begin{cases} Q_E(p), & p \in B_{2\nu\sqrt{E}} \\ |\mathcal{F}w_1(p)|^2, & p \in \mathbb{R}^d \setminus B_{2\nu\sqrt{E}} \end{cases}$

2 Set $\Omega \subset \mathbb{R}^d$ as convex hull of $\operatorname{supp} w$

3 $W(x) := (2\pi)^{-d} \int_\Omega w(x+y)\overline{w(y)}\, dy$

4 $q_E(x) := \chi_{D-\Omega,\varepsilon}(x)((\mathcal{F}^{-1}h_E)(x) - W(x))$

// cut-off function $\chi_{D-\Omega,\varepsilon}$ defined in (2.35c), Fourier transform $\mathcal{F}$ in (1.1)

5 $\widehat{v}_E(p) := \begin{cases} (\overline{\mathcal{F}w(p)})^{-1}(\mathcal{F}q_E)(p), & p \in B_{2\tau\sqrt{E}} \\ 0, & p \in \mathbb{R}^d \setminus B_{2\tau\sqrt{E}} \end{cases}$

6 $v_E(x) := \begin{cases} (\mathcal{F}^{-1}\widehat{v}_E)(x), & x \in D \\ 0, & x \in \mathbb{R}^d \setminus D \end{cases}$

Results of [41] include estimates on $\widehat{v} - \widehat{v}_E$ and $v - v_E$. In particular, suppose also that in Algorithm 1, where Q_E is given by (2.36) and $\nu = 1$, the potentials v, $w = w_1$ and the parameter τ are such that

$$v \in W^{m,1}(\mathbb{R}^d), \quad m > d, \tag{2.37a}$$

$$\max(\|v\|_{L^\infty(D)}, \|w_1\|_{L^\infty(\Omega_1)}) \le \eta, \tag{2.37b}$$

$$\|v + w_1\|_s \le N, \quad s > d, \tag{2.37c}$$

$$|(\mathcal{F}w_1)(p)| \ge c_3(1 + |p|)^{-\beta}, \ \forall p \in \mathbb{R}^d, \ \beta > d, \ c_3 > 0, \tag{2.37d}$$

$$\tau_1 = \tau_1(E) = \tau E^{\gamma - 1/2}, \quad 0 < \tau < 1, \quad \gamma = \frac{1}{2}\frac{1}{m+\beta}; \tag{2.37e}$$

see [41] (and also [2] in connection with condition (2.37d)). Then we have that ([41]):

$$|v(x) - v_E(x)| \le \left(C_1(m, d, \tau)\|v\|_{m,1} + C_2(\beta, \tau, d, D, \Omega_1)\frac{\eta^2}{c_3} + C_3(\beta, d, \tau, D, \Omega_1, \varepsilon)\frac{\eta^3}{c_3} \right) E^{-\alpha_1},$$
$$x \in D, \quad \sqrt{E} \ge \rho_1(d, s, N), \quad \alpha_1 = \frac{1}{2}\frac{m-d}{m+\beta}. \tag{2.38}$$

Explicit expressions for C_1, C_2, C_3 are given in [41] (with misprint c_3 in place of correct c_3^{-1}).

For small v and w_1, the function v_E given by (2.36) and lines 1–6 of Alg. 1 reduces to an approximate reconstruction for the case of Problems 7(A) and 7(B, $n = 1$) with $d \ge 2$, convex D and Ω_1, $B = B_{2\sqrt{E}}$.

In addition, for Problem 7, we use Algorithm 1, where

$$Q_E(p) := |\mathcal{F}(v + w_1)(p)|^2, \qquad p \in B_{2\sqrt{E}}, \quad \text{for Problem 8(A)}, \tag{2.39a}$$

$$Q_E(p) := |\mathcal{F}(v + w_1)(p)|^2 - |\mathcal{F}(v)(p)|^2, \qquad p \in B_{2\sqrt{E}}, \quad \text{for Problem 8(B, } n = 1), \tag{2.39b}$$

$\operatorname{dist}(D, \Omega_1) > \operatorname{diam} D$ for the case (A), and $\operatorname{dist}(D, \Omega_1) > 0$ for the case (B, $n = 1$).

In addition,

$$v_E \to v \text{ on } D \text{ as } E \to +\infty. \tag{2.40}$$

For example, under the additional assumptions (2.37a), (2.37d), (2.37e), we have that:

$$\|v - v_E\|_{L^\infty(D)} = \mathcal{O}(E^{-\alpha_1}) \text{ as } E \to +\infty \text{ with } \alpha_1 := \frac{1}{2}\frac{m-d}{m+\beta}. \tag{2.41}$$

3 Main new theoretical results

3.1 The case of Problem 7

For Problems 7(A) and 7(B, $n = 1$) with $d \geq 2$, convex D and Ω_1, and $B = B_{2\sqrt{E}}$, we consider the approximate reconstruction v_E defined by Algorithm 1 with Q_E given by (2.39).

We will use that

$$|\mathcal{F}\chi_{D-\Omega_1,\varepsilon}(p)| \leq \frac{C_4(t)}{(1+|p|)^t}, \quad p \in \mathbb{R}^d,\ t \geq 0, \tag{3.1}$$

where $\chi_{D-\Omega_1,\varepsilon}$ is the function in line 4 of Alg. 1, $C_4(t) = C_4(t, \chi_{D-\Omega_1,\varepsilon})$ is a positive constant.

Let

$$C_5(t) := \int_{\mathbb{R}^d} \frac{dp}{(1+|p|)^t}, \quad t > d. \tag{3.2}$$

Let $\mu(\mathcal{U})$ denote the Lebesgue measure of a bounded domain $\mathcal{U} \subset \mathbb{R}^d$.

We give the following new estimate on $\widehat{v}_E = \mathcal{F}v_E$ on $B_{2\sqrt{E}}$.

Proposition 3.1. *Let v, w_1 satisfy (1.3), (2.32), (2.37b), where D, Ω_1 are convex, and* $\operatorname{dist}(D, \Omega_1) > \operatorname{diam} D$. *Let $\widehat{v}_E$ be defined via (2.39a)) and lines 1–5 of Alg. 1, where $\nu = 1$. Then:*

$$|\widehat{v}(p) - \widehat{v}_E(p)| \leq \frac{C_6\eta^2}{|\mathcal{F}w_1(p)|(1+2(1-\tau)E^{1/2})^{t-d-\alpha}}, \quad p \in B_{2\tau\sqrt{E}},\ E^{1/2} \geq \rho_1(d, s, \|v + w_1\|_s), \tag{3.3}$$

$$C_6 := (2\pi)^{-2d}(\mu(D)^2 + 2\mu(D)\mu(\Omega_1))C_4(t)C_5(d+\delta), \quad \delta > 0,\ t - d - \delta > 0, \tag{3.4}$$

where ρ_1 is defined by (2.20), C_4, C_5 are the constants of (3.1), (3.2), $\tau \in (0,1)$ is the parameter in line 5 of Alg. 1 and is fixed.

The proof of Proposition 3.1 repeats the proof of Theorem 5.1 (for Problem 8(A)) in [41]. The main difference is that now formulas (114), (122) in [41] reduce to

$$\Delta h(p, E) = 0 \quad \text{for } p \in B_{2\sqrt{E}}, \tag{3.5}$$

$$I_1(p, E) = 0. \tag{3.6}$$

Actually, this completes the proof of Proposition 3.1.

Recall that if $v \in W^{m,1}(\mathbb{R}^d)$, $m \geq 0$, then the following estimate holds:

$$|\widehat{v}(p)| \leq \frac{C_7(m)}{(1+|p|)^m}, \quad p \in \mathbb{R}^d, \tag{3.7}$$

where $C_7(m) = C_7(m, d, \|v\|_{m,1})$ is positive constant.

Let $|\mathbb{S}^{d-1}|$ denote the $(d-1)$–dimensional Lebesgue measure of the unit sphere.

Proposition 3.1 and estimate (3.7) yield the following new estimate on v_E on D.

Theorem 3.2. *Let v, w_1 satisfy the assumptions of Proposition 3.1, and also satisfy (2.37a) and (2.37d). Let v_E be defined by Algorithm 1 with Q_E given by (2.39a) and $\nu = 1$. Let $\delta > 0$, $t - \beta - \delta > 2d$. Then:*

$$|v(x) - v_E(x)| \le A_1 E^{-\alpha_1} + A_2 E^{-\alpha_2},\ x \in D, \tag{3.8a}$$

$$\alpha_1 := \frac{1}{2}(m-d), \quad \alpha_2 := \frac{t-\beta-\delta}{2} - d, \tag{3.8b}$$

$$A_1 := \frac{|\mathbb{S}^{d-1}| C_7(m)}{(2\tau)^{m-d}(m-d)}, \tag{3.8c}$$

$$A_2 := \frac{(1+2\tau)^\beta (2\tau)^\beta}{(2-2\tau)^{t-d-\delta}} \mu(B_1) c_3^{-1} C_6(t) \eta^2, \tag{3.8d}$$

where C_6, C_7 are given by (3.4), (3.7), and $\tau \in (0,1)$, the parameter in line 5 of Alg. 1 is fixed.

The proof of Theorem 3.2 repeats the proof of Theorem 6.1 (for Problem 8(A)) in [41]. The main modifications consist in the following:

- In formula (136) of [41]: $\gamma = 1/2$, i.e., $\tau_1 = \tau$ is independent of E;
- In formula (139) of [41]: $I_1 = 0$.

Remark 3.3. *For Problem 7(B, $n = 1$), where $\operatorname{dist}(D, \Omega_1) > 0$, Proposition 3.1 and Theorem 3.2 are valid with Q_E given by (2.39b) and C_6 given by*

$$C_6 = 2(2\pi)^{-2d} \mu(D) \mu(\Omega_1) C_4(t) C_5(d+\delta).$$

Remark 3.4. *Estimate (3.8a) (with t such that $\alpha_2 = \alpha_1$) implies estimate (1.11) mentioned in Introduction. The point is that estimate (1.11) is completely similar to estimate (2.16) for the phased case and is principally better than estimate (2.41) for the phaseless case. Note that v_E in (2.41) is constructed with different τ than v_E in (3.8a), (1.11).*

Remark 3.5. *If the assumption that $v \in W^{m,1}(\mathbb{R}^d)$, $m > d$, is not fulfilled, then the result of Theorem 3.1 can be modified for apodized (smoothed) v in a similar way with considerations of Section 6.1 of [24] and Theorem 3.2, Remark 3.3 of [25].*

3.2 The case of Problem 8

For Problems 8(A) and 8(B, $n = 1$) with $d \ge 2$, convex D and Ω_1, and $\mathcal{M}' = \Gamma_E$, the approximate reconstruction v_E given by Algorithm 1 can be essentially improved iteratively, where $u_E^1 = v_E$ is the first approximation.

The iterative step is based on the following lemma.

Lemma 3.6. *Under the assumptions of Lemma 2.1, the following estimate holds:*

$$\left| |f(k,l)|^2 - |f_{\text{appr}}(k,l)|^2 + |\widehat{v}_{\text{appr}}(k-l,E)|^2 - |\widehat{v}(k-l)|^2 \right| \le C(s,D) \left(N + \tfrac{b}{E^\alpha}\left(1 + \tfrac{N}{E^{1/2}}\right)\right) \frac{Nb}{E^{\alpha+1/2}},$$
$$(k,l) \in \mathcal{M}_E, \quad E^{1/2} \ge \rho_1(d,s,N), \tag{3.9}$$

for some $C = C(s,D) > 0$.

The proof of Lemma 3.6 is given in Section 7.

Our iterative reconstruction is summarized in Algorithms 2(A) and 2(B).

Algorithm 2(A):

function $u_E^J = \texttt{reco2A}(\sigma_1, w, E, \{\nu_1..\nu_J\}, \{\tau_1..\tau_J\}, D)$
// iterative reconstruction algorithm for Problem 8(A)

Input:

$\sigma_1 \approx \sigma[v+w]$: measured scattering cross section for $v+w$ on $\mathcal{M}'$
$w \in L^\infty(\mathbb{R}^d)$: background potential
$E > 0$: energy
$0 < \nu_1 \le \cdots \le \nu_J \le 1$: cut-off parameters
$0 < \tau_1 \le \cdots \le \tau_J \le 1$: cut-off parameters
convex $D \subset \mathbb{R}^d$ contains $\operatorname{supp} v$

Output:

u_E^J: approximate reconstruction of v

$Q_E^1(p) := \frac{1}{|c(d,\sqrt{E})|^2}(\Phi\sigma_1)(p), p \in B_{2\sqrt{E}}$
// $c(d,\sqrt{E})$ def. in (2.2a), Fourier transform $\mathcal{F}$ in (1.1) and $\Phi : \mathcal{M}' \to B_{2\sqrt{E}}$ in (2.10)
$u_E^1 := \texttt{reco}(Q_E^1, w, E, D, \nu_1, \tau_1)$
for *j = 1..J-1* **do**
  Compute scattering amplitude $f_{1,E}^j$ for potential $u_E^j + w$
  $Q_E^{j+1}(p) := \frac{1}{|c(d,\sqrt{E}|^2}(\Phi\sigma_1)(p) + |(\mathcal{F}(u_E^j + w))(p)|^2 - (\Phi|f_{1,E}^j|^2)(p), \quad p \in B_{2\sqrt{E}}$
  $u_E^{j+1} = \texttt{reco}(Q_E^{j+1}, w, E, D, \nu_{j+1}, \tau_{j+1})$
end

Algorithm 2(B):

function $u_E^J = \texttt{reco2B}(\sigma, \sigma_1, w, E, \{\nu_1..\nu_J\}, \{\tau_1..\tau_J\}, D)$ *// iterative reconstruction algorithm for Problem 8(B) with $n = 1$*

Input:

$\sigma \approx \sigma[v]$: measured scattering cross section for v on $\mathcal{M}'$
$\sigma_1 \approx \sigma[v+w]$: measured scattering cross section for $v+w$ on $\mathcal{M}'$
w, E, ν_j, τ_j, and D as in Algorithm 2(A)

Output:

u_E^J: approximate reconstruction of v

$Q_E^1(p) := \frac{1}{|c(d,\sqrt{E})|^2}((\Phi\sigma_1)(p) - (\Phi\sigma)(p)), \quad p \in B_{2\nu_1\sqrt{E}}$
// $c(d,\sqrt{E})$ def. in (2.2a), Fourier transform $\mathcal{F}$ in (1.1) and $\Phi : \mathcal{M}' \to B_{2\sqrt{E}}$ in (2.10)
$u_E^1 := \texttt{reco}(Q_E^1, w, E, D, \nu_1, \tau_1)$
for *j = 1..J-1* **do**
  Compute scattering amplitudes f_E^j and $f_{1,E}^j$ for potentials u_E^j and $u_E^j + w$
  $\Sigma^j := \frac{1}{|c(d,\sqrt{E}|^2}\Phi\sigma + |\mathcal{F}u_E^j|^2 - \Phi|f_E^j|^2$
  $\Sigma_1^j := \frac{1}{|c(d,\sqrt{E}|^2}\Phi\sigma_1 + |\mathcal{F}(u_E^j + w)|^2 - \Phi|f_{1,E}^j|^2$
  $Q_E^{j+1}(p) := \Sigma_1^j(p) - \Sigma^j(p), \quad p \in B_{2\sqrt{E}}$
  $u_E^{j+1} = \texttt{reco}(Q_E^{j+1}, w, E, D, \nu_{j+1}, \tau_{j+1})$
end

In the iterative step in Algorithm 2(A) we use Lemma 3.6 with $v + w_1$ in place of v, and in Algorithm 2(B) twice with v itself and with $v + w_1$ in place of v.

We set

$$\tau_j = \tau E^{\gamma_j - 1/2} \quad \text{with} \tag{3.10a}$$

$$\alpha_j := \frac{1}{2}\frac{m-d}{\beta+d}\left(1 - \left(\frac{m-d}{m+\beta}\right)^j\right), \quad \gamma_1 := \frac{1}{2}\frac{1}{m+\beta}, \quad \gamma_{j+1} := \frac{\alpha_j + 1/2}{m+\beta}, \tag{3.10b}$$

where m, $j \in \mathbb{N}$, $m > d$, $\beta \in \mathbb{R}$, $\beta > d$. Here, m and β are the numbers in (2.37a) and (2.37d).

Theorem 3.7. *Let v, w_1 satisfy assumptions (1.3), (2.32), (2.37b), where D, Ω_1 are convex, and also satisfy assumptions (2.37a) and (2.37d). Let u_E^j be defined either by Algorithm 2(A) with exact data $\sigma_1 = \sigma[v + w_1]$ and $\operatorname{dist}(\Omega_1, D) > \operatorname{diam}(D)$ or by Algorithm 2(B) for exact data $\sigma = \sigma[v]$, $\sigma_1 = \sigma[v + w_1]$ and $\operatorname{dist}(\Omega_1, D) > 0$, where $\nu_j \equiv 1$ for all j, and τ_j are as in (3.10a). Then*

$$\|v - u_E^j\|_{L^\infty(D)} = \mathcal{O}(E^{-\alpha_j}) \quad \text{as } E \to +\infty, \tag{3.11}$$

where α_j are defined in (3.10b), $j \in \mathbb{N}$.

Theorem 3.7 is proved in Section 8 of Appendix.

For α_j and γ_j in Theorem 3.7, we have that

$$\begin{aligned} &\alpha_j \to \alpha_\infty := \frac{1}{2}\frac{m-d}{\beta+d} && \text{as } j \to +\infty, \\ &\alpha_j \to \frac{j}{2} && \text{as } m \to +\infty, \\ &\alpha_\infty \to +\infty && \text{as } m \to +\infty, \end{aligned} \tag{3.12}$$

$$\gamma_j < \gamma_{j+1},\ \gamma_j \to \gamma_\infty := \frac{1}{2}\frac{1}{\beta+d} \quad \text{as } j \to \infty. \tag{3.13}$$

Therefore, the convergence in (3.11), as $E \to +\infty$, is drastically better than in (2.38), at least, for large m and j. Besides, the convergence in (3.11), as $E \to +\infty$, is similar to the somewhat more rapid convergence in (2.29) for the phased case.

Note that the iterates u_E^j of Theorem 3.7 are simpler and more rapidly convergent theoretically than the iterates constructed in [1] for finding v from $\{\sigma[v], \sigma[v + w_1], \sigma[v + w_2]\}$ and w_1, w_2 (i.e., for Problem 8(B), $d \geq 2$, $n = 2$). However, the most essential point is that the iterates u_E^j, $j \geq 1$, of Theorem 3.7 use only the differential scattering cross section $\sigma[v + w_1]$ on Γ_E and the background scatterer w_1, when $\operatorname{dist}(D, \Omega_1) > \operatorname{diam} D$.

Remark 3.8. *Apparently, it is not difficult to show that iterates u_E^j in Theorem 3.7 depend in a Lipschitz way on errors in the phaseless data. Related analysis will be developped elsewhere. This issue is also related with approximate Lipschitz stability considered in [34] for the phased case.*

4 Numerical implementation

In the following we present numerical tests for our new theoretical results presented in Section 3.2 as well as results of [41]. We proceed from the numerical implementation developed in [1] for the case of Problem 8(B) with $d \geq 2$. For simplicity, we carry out these numerical studies for the two-dimensional case $d = 2$.

4.1 Discrete grids

We assume that v and w_1 are supported in the unit disk B_1. Let

$$\mathbb{Z}_N := \left\{-\frac{N}{2}, -\frac{N}{2} + 1, ..., \frac{N}{2} - 1\right\}, \quad N \in 2\mathbb{N}. \tag{4.1}$$

We represent v and w_1 by $\underline{v}$, $\underline{w}_1$ defined on the space-variable grids

$$\mathcal{X}_N := \{x = \frac{4}{N}(n_1, n_2) : n_1, n_2 \in \mathbb{Z}_N\}, \tag{4.2}$$

where $N \in 2\mathbb{N}$, $N \geq 2\sqrt{E}/\pi$.

We consider $|f(k,l)|^2$, $|f_1(k,l)|^2$ on the grid

$$\mathcal{M}_{E,M_1,M_2} := \{(k(s), l(s,t)) : s \in \mathbb{Z}_{M_1},\, t \in \mathbb{Z}_{M_2}\}, \quad M_1,\, M_2 \in 2\mathbb{N}, \tag{4.3}$$

where

$$\begin{aligned} k(s) &:= \sqrt{E}\left[\cos\left(2\pi\tfrac{s}{M_1}\right), \sin\left(2\pi\tfrac{s}{M_1}\right)\right]^\top, \\ l(s,t) &= \sqrt{E}\left[\cos\left(\tfrac{2\pi s}{M_1} + \tfrac{2\pi t}{M_2}\right), \sin\left(\tfrac{2\pi s}{M_1} + \tfrac{2\pi t}{M_2}\right)\right]^\top. \end{aligned} \tag{4.4}$$

In view of formulas (2.17), (2.33), (2.34), (3.9) for $\widehat{v}$, $\widehat{w}_1$, this leads to the following grid in Fourier space:

$$\mathcal{P}_{E,M_1,M_2} = \{p = k - l :\ (k,l) \in \mathcal{M}_{E,M_1,M_2}\},\ M_1,\, M_2 \in 2\mathbb{N}. \tag{4.5}$$

Note that the points of $\mathcal{P}_{E,M_1,M_2}$ are located on circles (Ewald circles) of raduis $\sqrt{E}$, that intersect at the origin; see Fig. II.1.

In the Fourier domain we also consider the uniform grid:

$$\mathcal{P}_N = \{p = \frac{\pi}{2}(n_1, n_2) :\ n_1, n_2 \in \mathbb{Z}_N\}. \tag{4.6}$$

In addition to $\mathcal{P}_{E,M_1,M_2}$ and $\mathcal{P}_N$, we also consider

$$\mathcal{P}_{E,M_1,M_2,N} = \mathcal{P}_{E,M_1,M_2} \cup P_N^{\text{ext}}, \tag{4.7}$$

$$\mathcal{P}_N^{\text{ext}} = \{p \in \mathcal{P}_N : p^2 > 4E\}. \tag{4.8}$$

The number N in (4.2) and (4.6)–(4.8) is the same.

In our numerical examples we use $\mathcal{P}_{E,M_1,M_2}$, $\mathcal{P}_N$ for $M_1 = 32$, $M_2 = 256$, $N = 572$, $E = 100^2$. For this choice, we have that $|\mathcal{P}_N \cap B_{2\sqrt{E}}| = 50949$, $|\mathcal{P}_{E,M_1,M_2}| = 8192$ (where $|\cdot|$ denotes the number of elements in a set), i.e. Fourier space in $B_{2\sqrt{E}}$ is severely undersampled, in particular in the neighborhood of the circle with radius $\sqrt{E}$. The resulting numerical problems and their solution will be discussed in Subsection 4.3.

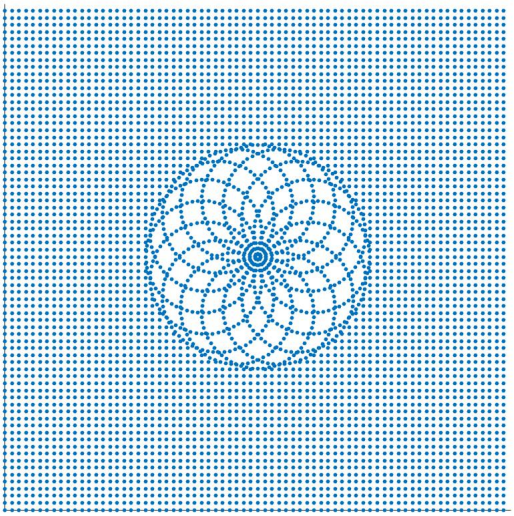

Figure II.1: The grid $\mathcal{P}_{E,M_1,M_2,N}$ in Fourier space for $M_1 = 16$, $M_2 = 64$, $N = 72$, and $E = (100/8)^2$. In our numerical computations we use $M_1 = 32$, $M_2 = 256$, $N = 572$, $E = 100^2$, i.e. the same proportions. But for the later numerical parameters we have too many points to visualize.

4.2 Discrete Fourier transforms

We consider the discrete Fourier transforms F and T :

$$\widehat{\underline{u}} = F\underline{u},\ F = [4(N\pi)^{-2}\exp(ix\cdot p)],\ x\in\mathcal{X}_N,\ p\in\mathcal{P}_N, \tag{4.9}$$

$$\widehat{\underline{u}} = T\underline{u},\ T = [4(N\pi)^{-2}\exp(ix\cdot p)],\ x\in\mathcal{X}_N,\ p\in\mathcal{P}_{E,M_1,M_2,N}, \tag{4.10}$$

where $\underline{u}$ is a test function on $\mathcal{X}_N$ considered as a vector, and F and T are considered as matrices.

Matrix-vector products with F, its adjoint F^* as well as its inverse $F^{-1} = (\frac{\pi}{2})^4 N^2 F^*$ can be computed efficiently by the Fast Fourier Transform (FFT).

Matrix-vector products with T and T^* can also be computed efficiently by non-uniform FFT methods. We use the code NFFT 3 (see [28]) for this purpose. Computations of a left inverse of T is more difficult. One can use the conjugate gradient method applied to the normal system

$$T^*\Lambda^{1/2}T\underline{u} = T^*\Lambda^{1/2}\widehat{\underline{u}} \tag{4.11}$$

for this purpose, where Λ is a diagonal weight matrix such that $\|\Lambda^{1/2}\underline{u}\|_2^2 \approx \int |u(p)|^2 dp$; see [3, §4.1.3].

4.3 Phase retrieval with background information

In this subsection we describe our numerical implementation of Algorithm 1 for finding v from Q_E approximately given by formulas (2.39) in terms of phaseless Fourier transforms on $B_{2\sqrt{E}}$, i.e. for solving Problem 7(A) and Problem 7(B, $n=1$). In addition, by line 1 of Alg. 1 we also define h_E which extends Q_E from $B_{2\sqrt{E}}$ to $\mathbb{R}^d$, $d=2$. The basic point of our implementation of Algorithm 1 consists in inversion of the discrete Fourier transforms F and T. In addition, inversion of F is standard, whereas proper inversion of T includes an essential new result. Proper implementation of $(\mathcal{F}w_1(p))^{-1}\mathcal{F}q_E(p)$ in line 5 of Algorithm 1 is also essential in view of possible zeros of $\mathcal{F}w_1(p)$ (if Assumption (2.37d) is violated). Note that, for Problem 7(A) and Problem 7(B, $n=1$) we use Algorithm 1 for cut-off parameters $\nu=\tau=1$.

The case of data on $\mathcal{P}_N\cap B_{2\sqrt{E}}$. If in formulas (2.39) the data $Q_E(p)$ are given on $\mathcal{P}_N\cap B_{2\sqrt{E}}$, then in lines 4, 6 of Algorithm 1 we implement $\mathcal{F}^{-1}$ as F^{-1} via FFT as mentioned in Subsection 4.2.

The case of data on $\mathcal{P}_{E,M_1,M_2}$. This case is especially important for Problem 8. If in formulas (2.39) the data $Q_E(p)$ are given on $\mathcal{P}_{E,M_1,M_2}$, then line 4 of Alg. 1 we implement a left inverse of the discrete Fourier transform T using the conjugate gradient method mentioned in Subsection 4.2. However, because of the geometric constraints of our setting, in particular the condition $\operatorname{dist}(\Omega_1, D) > \operatorname{diam}(D)$, the system (4.11) is much more ill-conditioned than in [1] due to the severe undersampling of Fourier space discussed at the end of Subsection 4.1; see also Fig. II.1. Therefore, the conjugate gradient method for system (4.11) does not converge properly to an approximation of $\mathcal{F}^{-1}h_E$ in line 4 of Alg. 1. To cope with this difficulty, we use a very specific property of h_E described by the formulas

$$\mathcal{F}^{-1}h(x) - W_1(x) = 0, \quad x\in\mathcal{U}^c := \mathbb{R}^d\setminus\mathcal{U}, \tag{4.12}$$

$$h(p) := \lim_{E\to+\infty} h_E(p),\ p\in\mathbb{R}^d, \tag{4.13}$$

$$\mathcal{U} := \begin{cases} (D-\Omega_1)\cup(\Omega_1-D)\cup B_{\operatorname{diam} D}, & \text{if } Q_E(p) \text{ is defined as in (2.39a)},\\ (D-\Omega_1)\cup(\Omega_1-D), & \text{if } Q_E(p) \text{ is defined as in (2.39b)}, \end{cases} \tag{4.14}$$

see formulas (47), (49), (51), (53) of [41].

It is convenient to rewrite (4.12) as

$$\mathcal{F}^{-1}\tilde{h}(x) = 0, \quad x\in\mathcal{U}^c \quad \text{with} \tag{4.15}$$

$$\tilde{h}(p) := \lim_{E\to+\infty}\tilde{h}_E(p), \quad \tilde{h}_E(p) := h_E(p) - (\mathcal{F}W_1)(p), \quad p\in\mathbb{R}^d. \tag{4.16}$$

The property (4.12), (4.15) means that $\mathcal{F}^{-1}\tilde{h}$ is identically zero on $\mathcal{U}^{\rm c}$, and $\mathcal{F}^{-1}\tilde{h}_E$ is approximately zero on $\mathcal{U}^{\rm c}$. Moreover, we have that:

$$\mathcal{F}^{-1}\tilde{h}_E(x) = \int_{|p|\geq 2\sqrt{E}} e^{-ipx}(|\hat{w}_1(p)|^2 - |\hat{v}(p)+\hat{w}_1(p)|^2)dp, \quad x\in\mathcal{U}^{\rm c}, \tag{4.17a}$$

$$\mathcal{F}^{-1}\tilde{h}_E(x) = \int_{|p|\geq 2\sqrt{E}} e^{-ipx}(|\hat{w}_1(p)|^2 + |\hat{v}(p)|^2 - |\hat{v}(p)+\hat{w}_1(p)|^2)dp, \quad x\in\mathcal{U}^{\rm c}, \tag{4.17b}$$

for the cases (A) and (B), respectively. That is, in particular, $\mathcal{F}^{-1}\tilde{h}_E$ on $\mathcal{U}^{\rm c}$ depends only on a higher frequency parts of v and w_1. Formulas (4.17) follow from (4.12)–(4.16), and from the formulas

$$h_E = h - (1-\chi_{B_{2\sqrt{E}}})|\mathcal{F}(v+w_1)|^2 + (1-\chi_{B_{2\sqrt{E}}})|\mathcal{F}w_1|^2, \tag{4.18a}$$

$$h_E = h - (1-\chi_{B_{2\sqrt{E}}})(|\mathcal{F}(v+w_1)|^2 - \mathcal{F}v|^2) + (1-\chi_{B_{2\sqrt{E}}})|\mathcal{F}w_1|^2, \tag{4.18b}$$

for the cases (A) and (B), respectively, where $\chi_{B_{2\sqrt{E}}}$ is the characteristic function of $B_{2\sqrt{E}}$.

Therefore, for finding $\mathcal{F}^{-1}\tilde{h}_E$ arising in (2.39) and line 1 of Alg. 1 in place of system (4.11) we use the conjugate gradient method for the following system for $\underline{u}$ on $\mathcal{X}_N$,

$$\Pi T^*\Lambda^{1/2}T\Pi\underline{u} = \Pi T^*\Lambda^{1/2}\underline{\tilde{h}_E}, \tag{4.19}$$

where Π is the projector defined by the characteristic function $\mathcal{U}$ in (4.14), i.e.

$$\Pi\underline{u} := \chi_{\mathcal{U}}\cdot\underline{u}. \tag{4.20}$$

Note that if $\operatorname{diam}\Omega_1 \leq \operatorname{diam} D$, then $\operatorname{supp} W_1 \subseteq B_{\operatorname{diam} D}$, and, therefore, (4.12), (4.15) also hold without W_1, and for finding $\mathcal{F}^{-1}h_E$ one can use (4.19) with $\underline{h_E}$ in place of $\underline{\tilde{h}_E}$.

Note also that if in Algorithm 1 the cut-off parameter $\nu\in(0,1)$, then h_E also depends on ν, and in formulas (4.17), (4.18) the radius $2\sqrt{E}$ should be replaced by $2\nu\sqrt{E}$. The point is that such cut-off parameters ν arise in Section 4.4.

The use of initial system (4.11) without a priori information (4.12)–(4.16) results in considerable reconstruction errors of v_E in Algorithm 1 with Q_E given by (2.39), see Figs. II.4, II.5.

In the present work, we use 40 conjugate gradient steps for system (4.19). In contrast, even 100 conjugate gradient steps for solving system (4.11) does not lead to a proper result.

Moreover, because of accumulation of such errors, our numerical iterative reconstruction presented in Sections 3.2, 4.4 does not converge properly.

Finally, in the present work, we implement line 5 of Alg. 1 (i.e. $\widehat{v}_E \equiv (\mathcal{F}w_1)^{-1}\mathcal{F}q_E$) as

$$\frac{a}{b} \approx (1+\varepsilon)\frac{ab^*}{bb^* + \varepsilon\max_p|b|^2} \quad \text{with} \quad a=\mathcal{F}q_E(p),\ b=\mathcal{F}w_1(p), \tag{4.21}$$

where ε is an appropriately small positive number. In our numerical examples we choose $\varepsilon = 5\cdot 10^{-3}$. Formula (4.21) is essentially Tikhonov regularization for solving the linear equation $b\,\hat{v}_E = a$ for $\hat{v}_E\in L_2(B_r)$ where $\varepsilon\cdot\max_p|b|^2$ is the regularisation parameter. In addition, we included the factor $(1+\varepsilon)$ in the right-hand side of (4.21) in order to have the identity $\hat{v}_{E,\varepsilon}(p) = \hat{v}_E(p)$ for $p\in\operatorname{argmax}_p|b(p)|^2$.

Note that, for example, $|\mathcal{F}w_1|^2$ has many zeros (in violation of assumption 2.37d of our theoretical analysis!) if w_1 is a multiple of the characteristic function of a box as in Fig. II.2. For such cases, formulas (4.21) are very essential.

For the phase retrieval problem our numerical realisation of Algorithm 1 is summarized as Algorithm 3.

Algorithm 3:

function $v = \texttt{reco\_discr}(N, M_1, M_2, Q, w, E, \nu, \tau, D, \Omega)$

Input:

$N \in 2\mathbb{N}$: The spatial grid $\mathcal{X}_N \subset [-2,2]^2$ and the Fourier grid $\mathcal{P}_N \subset [-\frac{\pi N}{4}, \frac{\pi N}{4}]^2$ have size $N \times N$; see (4.2), (4.6)

$M_1, M_2 \in \mathbb{N}$: number of incident fields and measurement points. This defines the Fourier grids $\mathcal{P}_{E,M_1,M_2}$, $\mathcal{P}_{E,M_1,M_2,N}$; see (4.5), (4.7) and Fig. II.1

$Q : \mathcal{P}_{E,M_1,M_2} \to \mathbb{R}$: phaseless data given by (2.39) or (2.36) for Problems 7 and 8, rsp.

$w : \mathcal{X}_N \to \mathbb{C}$ background potential

convex $D, \Omega \subset \mathcal{X}_N$ contains support of v and w, rsp.

Output:

$v : \mathcal{X}_N \to \mathbb{C}$ approximation of unknown potential such that $\operatorname{supp} v \subseteq D$

Compute vector $\lambda : \mathcal{P}_{E,M_1,M_2,N} \to \mathbb{R}$ of areas of Voronoi cells of these points and set $\Lambda := \operatorname{diag}(\lambda)$ *// see, e.g. Fig 2 in [1]*

$\chi_D(x) := \begin{cases} 1, & x \in \mathcal{X}_N \cap D \\ 0, & x \in \mathcal{X}_N \setminus D \end{cases}$ and $\chi_{D-\Omega}(x) := \begin{cases} 1, & x \in \mathcal{X}_N \cap (D-\Omega) \\ 0, & x \in \mathcal{X}_N \setminus (D-\Omega) \end{cases}$

$\chi_{\mathcal{U}}(x) := \begin{cases} 1, & x \in \mathcal{X}_N \cap ((D-\Omega) \cup (\Omega - D) \cup B_{\operatorname{diam} D}) \\ 0, & x \in \mathcal{X}_N \setminus ((D-\Omega) \cup (\Omega - D) \cup B_{\operatorname{diam} D}) \end{cases}$

$\chi_{B_{2\tau\sqrt{E}}}(p) := \begin{cases} 1, & p \in \mathcal{P}_N \cap B_{2\tau\sqrt{E}} \\ 0, & p \in \mathcal{P}_N \setminus B_{2\tau\sqrt{E}} \end{cases}$ and $\chi_{B_{2\nu\sqrt{E}}}(p) := \begin{cases} 1, & p \in \mathcal{P}_{E,M_1,M_2} \cap B_{2\nu\sqrt{E}} \\ 0, & p \in \mathcal{P}_{E,M_1,M_2} \setminus B_{2\nu\sqrt{E}} \end{cases}$

$F := [4(N\pi)^{-2} \exp(ix \cdot p)]_{x,p}$ with $x \in \mathcal{X}_N$, $p \in \mathcal{P}_N$
// matrix-vector products with F, F^*, and F^{-1} implemented by FFT

$T := [4(N\pi)^{-2} \exp(ix \cdot p)]_{x,p}$ with $x \in \mathcal{X}_N$, $p \in \mathcal{P}_{E,M_1,M_2}$
// matrix-vector products with T and T^* implemented by non-uniform FFT

$\widehat{w} := Fw$ *// defined on $\mathcal{P}_N$*

$h = \chi_{B_{2\nu\sqrt{E}}} Q$

if $(\operatorname{diam}\Omega < \operatorname{diam} D < \operatorname{dist}(D, \Omega))$ **then**

  $rhs := \chi_{\mathcal{U}} \cdot (T^* \Lambda^{1/2} h)$

else

  $W := F^{-1}(|\widehat{w}|^2)$

  $rhs := \chi_{\mathcal{U}} \cdot T^* \Lambda^{1/2} (h - TW)$

end

Solve $\chi_{\mathcal{U}} \cdot T^* \Lambda^{1/2} T (\chi_{\mathcal{U}} \cdot q_{\text{in}}) = rhs$ for $q_{\text{in}} : \mathcal{X}_N \to \mathbb{C}$ by CG method

$q := \chi_{D-\Omega} \cdot (q_{\text{in}} + F^{-1}((1 - \chi_{B_{2\nu\sqrt{E}}}) \cdot |\widehat{w}|^2))$

$\widehat{v} := (1+\varepsilon) \chi_{B_{2\tau\sqrt{E}}} \frac{Fq \cdot \overline{\widehat{w}}}{\widehat{w} \cdot \overline{\widehat{w}} + \varepsilon \max |\widehat{w}|^2}$ with $\varepsilon := 0.005$

$v := \chi_D \cdot F^{-1}(\widehat{v})$

4.4 Phaseless inverse scattering with background information

Our numerical reconstructions are based on Algorithms 1, 2(A) and 2(B), more precisely, on discrete versions of these algorithms. Recall that in the case of Problem 8, Algorithm 1 is used to provide the first approximation and its iterative improvements in Algorithms 2(A) and 2(B). A discrete version of Algorithm 1 is given as Algorithm 3. Algorithms 2(A) and 2(B) have straightforward analogues in the discrete setting, replacing Algorithm 1 by its discrete analog, Algorithm 3.

In addition, there are the following essential points:

(i) In the numerical implementations of the present work, we fix in advance the total number J of the iterates u_E^j, $j = 1, ..., J$, where $J = 1$, $J = 6$, $J = 10$ in our examples. In addition,

our choice of the cut-off parameters ν_j, τ_j in Algorithms 2(A), 2(B) is as follows:

$$\nu_j = 0.5 + 0.5\,\frac{j-1}{J}, \quad \tau_j = 1, \quad j = 1, ..., J. \tag{4.22}$$

Note that this choice of cut-off parameters ν, τ differs from the choice of these cut-off parameters in Theorem 3.7. The reason is that the cut-off parameters given by (4.22) yield better numerical results.

(ii) For normalized measured data $\sigma[v_1]^{\rm meas}(k,l)$, where $k \in \{k_1, ..., k_{M_1}\}$, $l \in \{l_1, ..., l_{M_2}\}$, we use the Poisson noise model in a similar way as in [1]. In this framework the noise level is characterized by the number N_p of measured particles. As mentioned in introduction, $\sigma[v_1](k,l)$ describes the probability density of scattering of particles with initial impulse k into direction $l/|l| \neq k/|k|$. We assume that for each incident impulse k_i the exposure time $t(k_i)$ is chosen such that the same expected number of particles N_p/M_1 is recorded in the sum over all l_j. Thus, our simulated normalized measured noisy data $\sigma[v_1]^{\rm meas}(k,l)$ were generated from exact data $\sigma[v_1](k,l)$ via the formulas

$$\sigma[v_1]^{\rm meas}(k_i,l_j) \sim \frac{1}{t(k_i)}\,{\rm Pois}(t(k_i)\sigma[v_1](k_i,l_j)),\ t(k_i) = \frac{N_p}{M_1\sigma[v_1](k_i)},\ \sigma[v_1](k_i) = \sum_{j=1}^{M_2}\sigma[v_1](k_i,l_j), \tag{4.23}$$

where $i = 1, ..., M_1$, $j = 1, ..., M_2$.

(iii) The approximation u_E^J mentioned above does not converge to v at fixed E even when J increases; see, in particular, Theorem 3.7. Therefore, we improve u_E^J using the Newton-CG method (see [19]) in a similar way with [1].
In the present work we use Newton-CG for minimizing the following quadratic approximation of the negative Poisson log-likelihood (Kullback-Leibler divergence):

$$\Delta(\sigma[v_1]^{\rm comp}, \sigma[v_1]^{\rm meas}) = \sum_{(k,l)\in\mathcal{M}_{E,M_1,M_2}} \frac{|\sigma[v_1]^{\rm comp}(k,l) - \sigma[v_1]^{\rm meas}(k,l)|^2}{\max(\varepsilon, \sigma[v_1]^{\rm meas}(k,l))}, \tag{4.24}$$

$$\varepsilon = \frac{1}{1000}\max_{(k,l)}\sigma[v_1]^{\rm meas}(k,l),$$

among all $v \in H^1$ supported in D, where $\sigma[v_1]^{\rm meas}$ is our normalized measured monochromatic phaseless scattering data defined according to (4.23), $\sigma[v_1]^{\rm comp}$ denotes the monochromatic phaseless scattering data (differential scattering cross section) computed for $v_1 = v+w$, and D is chosen as small as possible using a priori information. As initial approximation for v, one can use u_E^J mentioned above.

5 Numerical examples

5.1 Test potentials

Throughout this section we use the values of energy E and discretization parameters M_1, M_2, and N given is Subsection 4.1; see also Fig. II.1. The forward problems are solved using a periodized version of the Lippmann-Schwinger equation (2.1) as proposed in [50]. Noisy Poisson distributed synthetic data $\sigma[v_1]^{\rm meas}$ on $\mathcal{M}_{E,M_1,M_2}$ are generated with an expected total number of $N_p = 3\cdot 10^7$ counts.

We consider reconstructions of two potentials v shown in Fig. II.2, where v is smooth for case (a), and v is non-smooth for case (b). For Problem 8(B) with $n = 2$ or $n = 3$, similar potentials v with different scaling were used in [1]. Fig. II.2 shows $v_1 = v+w$ on $\mathcal{X}_N \cap [-1,1]^2$, where $N = 572$. This w is a multiple of the characteristic function of a square and will be also denoted as $w_{\rm box}$.

We also define

$$v_E^{\rm filt} = F^{-1}(\chi_{B_{2\sqrt{E}}} \cdot F\underline{v}), \tag{5.1}$$

where $\underline{v}$ is our potential v on $\mathcal{X}_N$, F is the discrete Fourier transform defined in (4.9), $\chi_{B_{2\sqrt{E}}}$ is the characteristic function of $B_{2\sqrt{E}}$. For the potentials v shown in Fig. II.2(a, b) their filtered versions $v_E^{\rm filt}$ are shown in Fig. II.3(a, b). The point is that in the present work we do not try to reconstruct v much better than $v_E^{\rm filt}$ proceeding from the scattering data $\sigma[v_1]^{\rm meas}$ at fixed energy E.

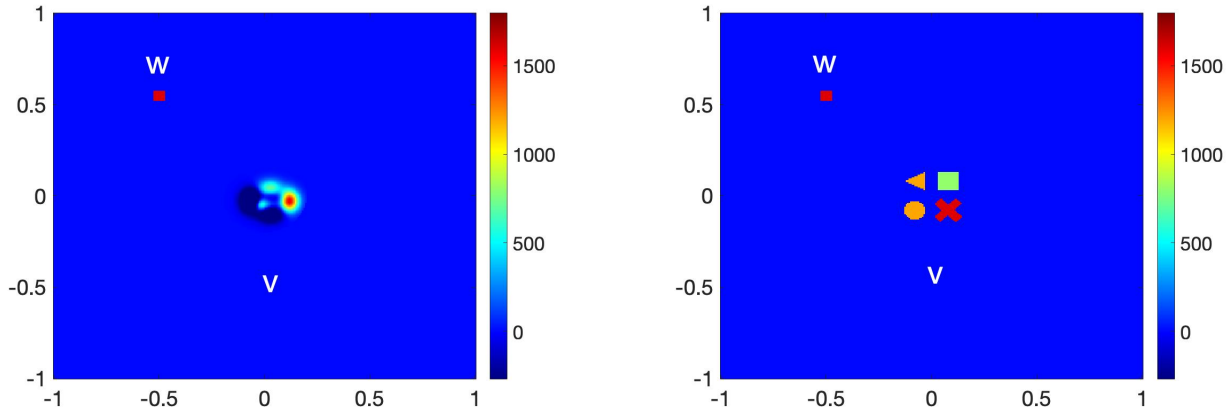

(a) (b)

Figure II.2: Test examples for the unknown potential v and the known background potential w. (a) Smooth v. (b) Non-smooth v.

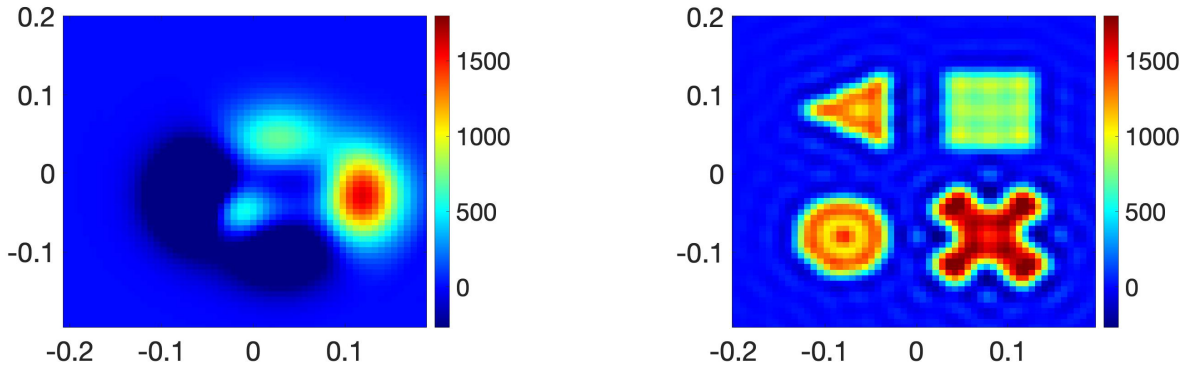

(a) (b)

Figure II.3: Filtered versions $v_E^{\rm filt}$ of the test potentials v in Fig. II.2 corresponding to ideal reconstructions within the classical diffraction limit for the chosen energy $E = 100$ (see (5.1)). (a) Smooth v : $\mathfrak{E}(v_E^{\rm filt}, v) = 0.0077$. (b) Non-smooth v : $\mathfrak{E}(v_E^{\rm filt}, v) = 0.2808$.

To measure the quality of numerical reconstructions, we use the relative error

$$\mathfrak{E}(u, u_0) = \frac{\|u - u_0\|_{\ell^2(G)}}{\|u_0\|_{\ell^2(G)}}, \tag{5.2}$$

where u, u_0 are functions on some grid G.

5.2 Reconstruction results for Problem 7(A)

As approximate solutions of Problem 7(A) or Problem 8(A), we consider the result v_E of Algorithm 1 with input data Q_E defined by formula (2.39a) or (2.36a), respectively. First, Fig. II.4 (a, b)

illustrate our reconstructions v_E from $|\mathcal{F}(v+w)|^2$ given on the uniform grid $\mathcal{P}_N \cap B_{2\sqrt{E}}$ as described in Subsection 4.3. Then, Fig. II.5 (a0, b0) illustrate our reconstructions v_E of v from $|\mathcal{F}(v+w)|^2$ on $\mathcal{P}_{E,M_1,M_2}$, where we use system (4.11) (with 40 conjugate gradient steps) for inverting the discrete Fourier transform T. Finally, Fig. II.5 (a, b) illustrate our reconstructions v_E of v from $|\mathcal{F}(v+w)|^2$ on $\mathcal{P}_{E,M_1,M_2}$, where we use modified system (4.19) (with 40 conjugate gradient steps) in place of (4.11). The point is that system (4.19) leads to much better result. More precisely, these figures show our reconstructions v_E of smooth and non-smooth v shown on Fig. II.2(a, b) from discrete phaseless Fourier data without Poisson noise.

One can see that reconstructions v_E shown at Fig. II.4 and Fig. II.5(a, b) are rather good, especially for the case of smooth v, when $\mathcal{F}v$ is rather small on $\mathbb{R}^2 \setminus B_{2\sqrt{E}}$, and also for the case of non-smooth v, in comparison with v_E^{filt}.

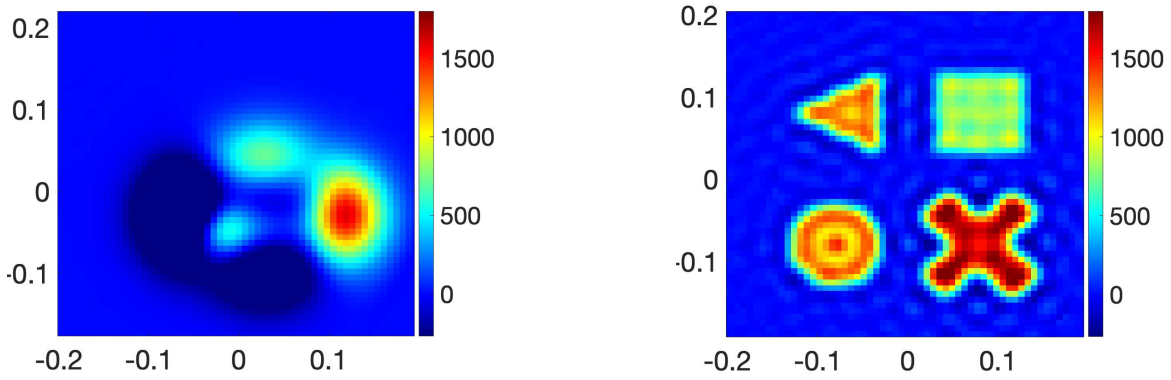

Figure II.4: Reconstructions v_E from $|\mathcal{F}(v+w)|^2$ on $\mathcal{P}_N \cap B_{2\sqrt{E}}$.
(a) Smooth v : $\mathfrak{E}(v_E, \underline{v}) = 0.005$, $\mathfrak{E}(v_E, v_E^{\text{filt}}) = 0.001$. (b) Non-smooth v : $\mathfrak{E}(v_E, \underline{v}) = 0.2816$, $\mathfrak{E}(v_E, v_E^{\text{filt}}) = 0.0292$.

5.3 Basic reconstruction results for Problem 8(A)

In this subsection we present our reconstructions for Problem 8(A) with the test potentials v and w described in Subsection 5.1 and shown in Fig. II.2. In particular, Fig. II.6 and Fig. II.7 illustrate our reconstructions of v from $\sigma[v_1]^{\text{meas}}$ on $\mathcal{M}_{E,M_1,M_2}$ with known background w. More precisely, these figures show our reconstructions u_E^J, u_E^{J+K} of smooth and non-smooth potentials v shown on Fig. II.2(a, b). Here, u_E^J are as described in Section 4.4, and u_E^{J+K} denotes u_E^J improved by K iterations of Newton-CG method. In addition: $J = 1$ for Fig. II.6 (a, d), Fig. II.7 (a, d), $J = 6$ for Fig. II.6 (b, e), $J = 10$ for Fig. II.7 (b, e), $J = 6$, $K = 5$ for Fig. II.6 (c, f), $J = 10$, $K = 5$ for Fig. II.7 (c, f). In addition, Fig. II.6 and Fig. II.7 also show the relative reconstruction errors with respect to both v and v_E^{filt}.

One can see that already reconstruction u_E^1 going back to [41] and illustrated in Fig. II.6 (a, d) with $\mathfrak{E}(u_E^1, \underline{v}) = 0.4112$ and in Fig. II.7 (a, d) with $\mathfrak{E}(u_E^1, \underline{v}) = 0.5140$ is of interest in spite of considerable errors in real and imaginary parts $\operatorname{Re} u_E^1$ and $\operatorname{Im} u_E^1$ of u_E^1. These considerable errors in u_E^1 arise as a consequence of large strength of v, yielding the Born approximation unsatisfactory. Next, one can see that reconstruction u_E^J developed in the present work for $J > 1$ (for the case beyond the Born approximation) and illustrated in Fig. II.6 (b, e) and in Fig. II.7 (b, e) is considerably more precise than u_E^1 for reasonably large E and J. Finally, similar to [1], one can see that u_E^{J+K} improves u_E^J, under the condition that u_E^J is close to v.

The visual quality of our phaseless inverse scattering reconstructions u_E^J, u_E^{J+K} shown at Fig. II.6 and Fig. II.7 (for $J > 1$) turns out to be more or less comparable with our phaseless Fourier reconstructions v_E shown at Fig. II.5(a, b) and even at Fig. II.4. In addition, the errors $\mathfrak{E}(v_E, \underline{v})$ shown at Fig. II.7, for $v_E = u_E^{10}$, u_E^{10+5}, are also comparable with the error $\mathfrak{E}(v_E, \underline{v})$ shown at Fig. II.5(b). Besides, the errors $\mathfrak{E}(v_E, \underline{v})$ shown at Fig. II.6, for $v_E = u_E^6$, u_E^{6+5}, reduce

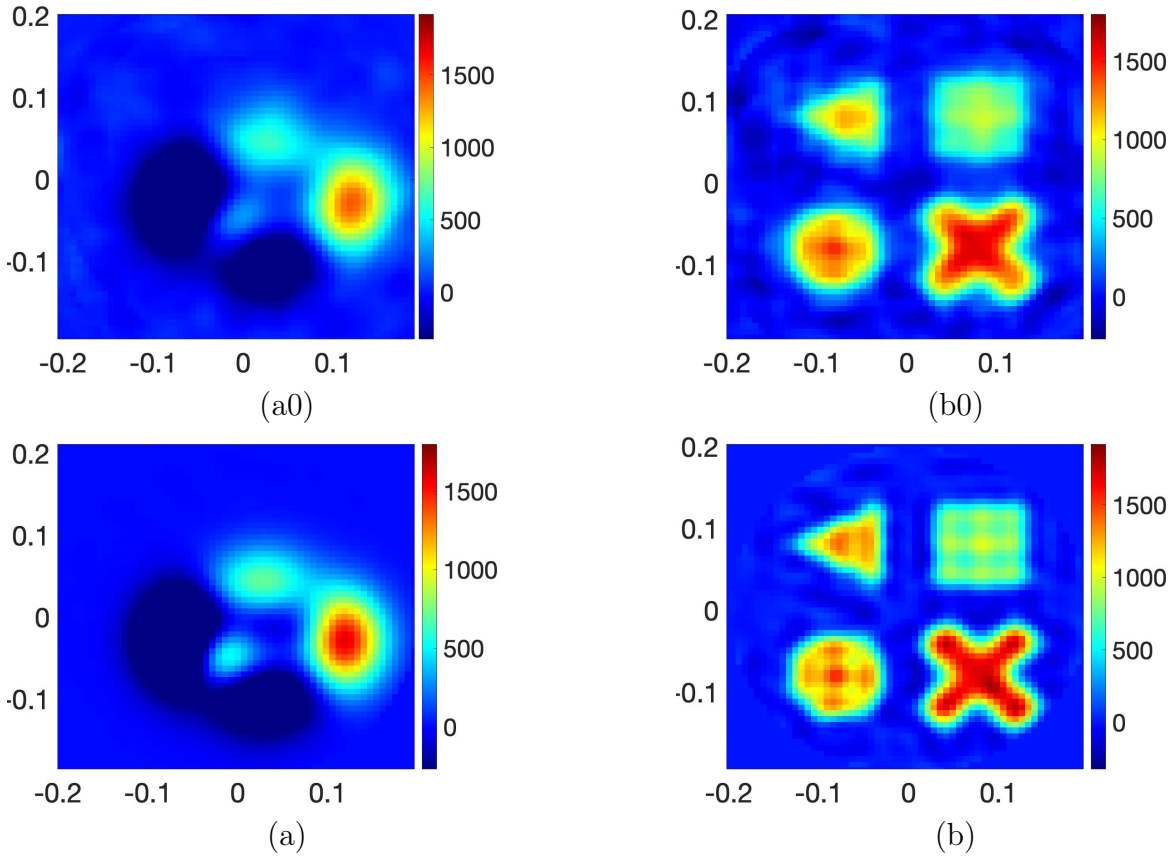

Figure II.5: Reconstructions v_E from $|\mathcal{F}(v+w)|^2$ on $\mathcal{P}_{E,M_1,M_2}$.
(a0, b0): inverting T via (4.11) (old method). (a, b): inverting T using (4.19) (new method).
(a0) Smooth v : $\mathfrak{E}(v_E, \underline{v}) = 0.1417$, $\mathfrak{E}(v_E, v_E^{\text{filt}}) = 0.1416$. (b0) Non-smooth v : $\mathfrak{E}(v_E, \underline{v}) = 0.4017$, $\mathfrak{E}(v_E, v_E^{\text{filt}}) = 0.3002$. (a) Smooth v : $\mathfrak{E}(v_E, \underline{v}) = 0.01434$, $\mathfrak{E}(v_E, v_E^{\text{filt}}) = 0.01376$. (b) Non-smooth v : $\mathfrak{E}(v_E, \underline{v}) = 0.3223$, $\mathfrak{E}(v_E, v_E^{\text{filt}}) = 0.1632$.

considerably for $v_E = u_E^{6+K}$ for large K, see Fig. II.8(c). For proper comparisons, recall also that the phaseless scattering data $\sigma[v_1]^{meas}$ used for the reconstructions of Fig. II.6 and Fig. II.7 are with Poisson noise, whereas there is no Poisson noise in the phaseless Fourier transforms used for the reconstructions of Fig. II.4 and II.5. In addition, the reconstructions of Fig. II.4 do not have non-uniform grid difficulties.

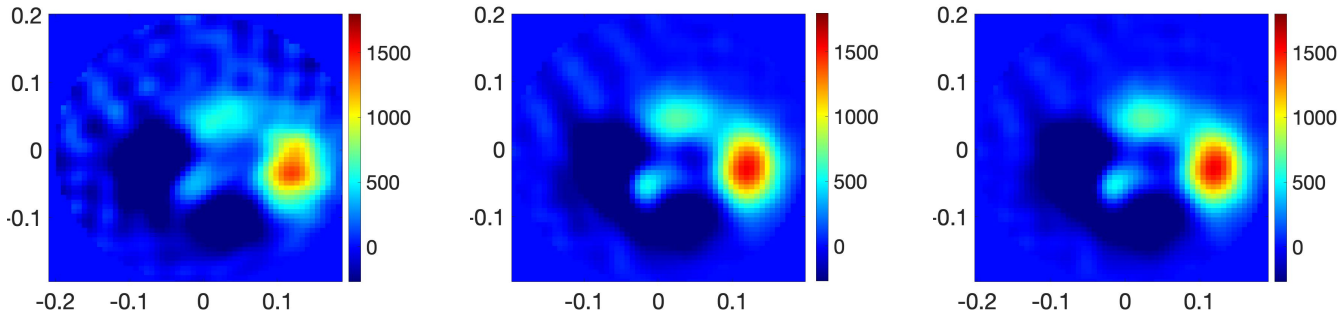

(a) Re u_E^1 (b) Re u_E^6 (c) Re u_E^{6+5}

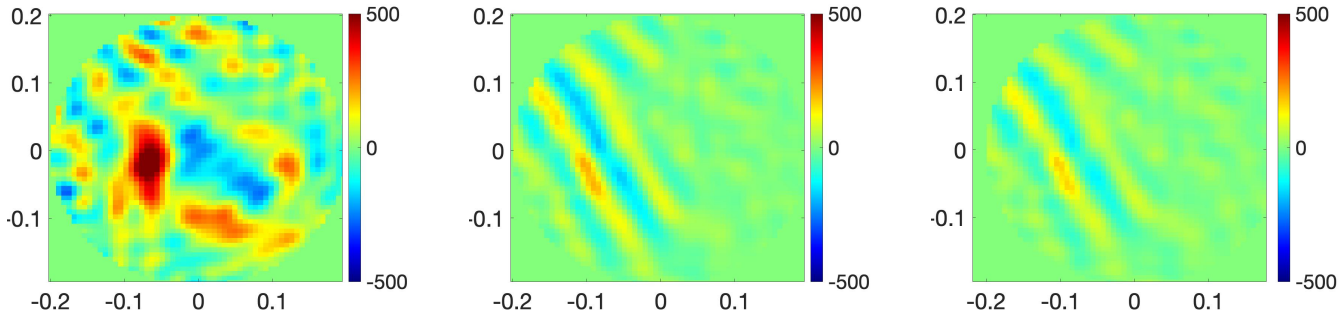

(d) Im u_E^1 (e) Im u_E^6 (f) Im u_E^{6+5}

Figure II.6: Reconstructions u_E^J, u_E^{J+K} of smooth v (see Fig. II.2) in Problem 8(A). Top row: Real parts. Bottom row: Imaginary parts. Relative errors on $\mathcal{X}_N \cap D$: $\mathfrak{E}(u_E^1, \underline{v}) = 0.4096$, $\mathfrak{E}(u_E^1, v_E^{\text{filt}}) = 0.4096$; $\mathfrak{E}(u_E^6, \underline{v}) = 0.1722$, $\mathfrak{E}(u_E^6, v_E^{\text{filt}}) = 0.1722$; $\mathfrak{E}(u_E^{6+5}, \underline{v}) = 0.1257$, $\mathfrak{E}(u_E^{6+5}, v_E^{\text{filt}}) = 0.1256$.

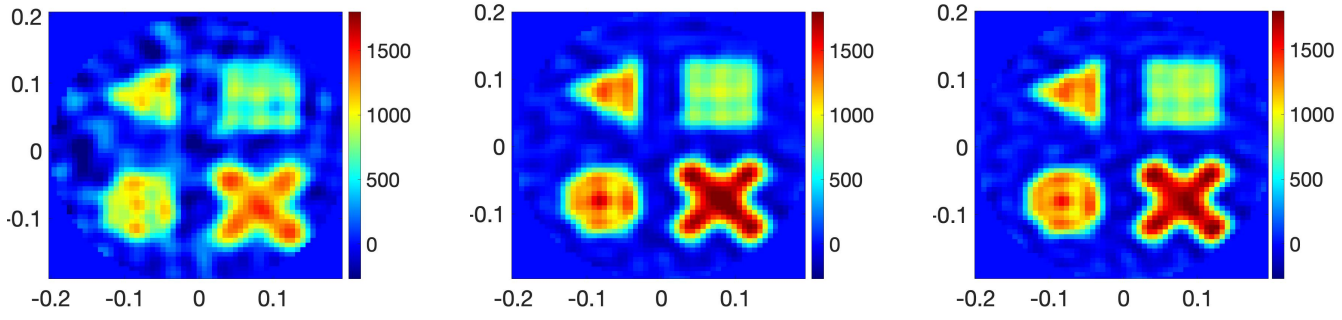

(a)Re u_E^1 (b) Re u_E^{10} (c) Re u_E^{10+5}

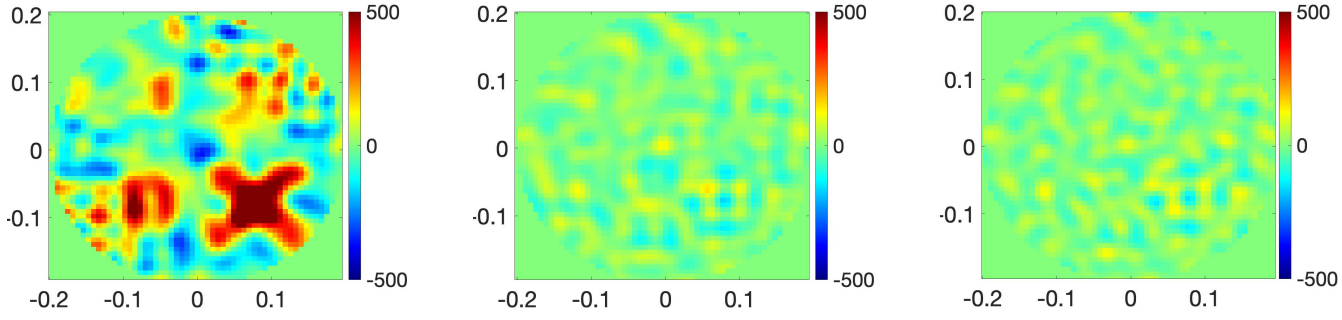

(d) Im u_E^1 (e) Im u_E^{10} (f) Im u_E^{10+5}

Figure II.7: Reconstructions u_E^J, u_E^{J+K} of non-smooth v (see Fig. II.2) in Problem 8(B) with $n = 1$. Top row: Real parts. Bottom row: Imaginary parts. Relative errors on $\mathcal{X}_N \cap D$: $\mathfrak{E}(u_E^1, \underline{v}) = 0.5140$, $\mathfrak{E}(u_E^1, v_E^{\text{filt}}) = 0.4466$; $\mathfrak{E}(u_E^{10}, \underline{v}) = 0.3396$, $\mathfrak{E}(u_E^{10}, v_E^{\text{filt}}) = 0.1873$; $\mathfrak{E}(u_E^{10+5}, \underline{v}) = 0.3196$, $\mathfrak{E}(u_E^{10+5}, v_E^{\text{filt}}) = 0.1486$.

Next, for our smooth and non-smooth v, Fig. II.8 shows L_2 discrepancies $\mathfrak{E}(j) = \mathfrak{E}(\sigma[u_E^j + w_1]^{\text{comp}}, \sigma[v_1]^{\text{meas}})$ Poisson discrepancies $\Delta(j) = \Delta(\sigma[u_E^j + w_1]^{\text{comp}}, \sigma[v_1]^{\text{meas}})$ on $\mathcal{M}_{E,M_1,M_2}$, and

relative errors $\mathfrak{E}(u_E^j, v)$ on $\mathcal{X}_N \cap D$ for the iterates u_E^j, where

$$u_E^0 \equiv 0, \tag{5.3a}$$

$$u_E^j,\ j = 1, ..., J, \text{are defined as described in item (i) of Subsection 4.4,} \tag{5.3b}$$

$$u_E^{J+k} \text{ denotes } u_E^J \text{ improved by } k \text{ iterations of Newton-CG method.} \tag{5.3c}$$

Note that $J > 0$ for the plots 'Our + NCG', and $J = 0$ for the plots 'NCG method'.

These figures also show L_2 discrepancy $\mathfrak{E}_{\text{noise}}$ and Poisson discrepancy Δ_{noise} defined by

$$\mathfrak{E}_{\text{noise}} = \mathfrak{E}(\sigma[v_1], \sigma[v_1]^{\text{meas}}), \tag{5.4}$$

$$\Delta_{\text{noise}} = \Delta(\sigma[v_1], \sigma[v_1]^{\text{meas}}), \tag{5.5}$$

or, in other words, the noise level in $\sigma[v_1]^{\text{meas}}$ in different senses. For the plots 'Our + NCG', one can see that $\mathfrak{E}(J)$ and $\Delta(J)$ are much smaller than $\mathfrak{E}(1)$ and $\Delta(1)$, respectively. However, $\mathfrak{E}(j)$ and $\Delta(j)$ are not monotonically decreasing in $j = 1, ..., J$. The reason is that the proposed iterative algorithm does not minimize the aforementioned discrepancies directly; this algorithm is based on a different principle. In addition, one can see that $\mathfrak{E}(j)$ and $\Delta(j)$ are monotonically decreasing for $j \geq J$. The reason is that the additional Newton-CG method directly minimizes $\Delta(j)$.

One can see that:

- $\mathfrak{E}(j)$ and $\Delta(j)$, for large j, are very close to the noise levels $\mathfrak{E}_{\text{noise}}$ and Δ_{noise} for smooth v;
- $\mathfrak{E}(j)$ and $\Delta(j)$, for large j, are not yet very close to the noise levels $\mathfrak{E}_{\text{noise}}$ and Δ_{noise} for non-smooth v.

The reason is that our monochromatic iterative algorithm (including additional NCG iterations) reconstruct $\hat{v}(p)$ for $|p| \leq 2\sqrt{E}$ much better than for $|p| \geq 2\sqrt{E}$.

For our examples we have that our reconstructions u_E^J give good results in configuration space (i.e., on $\mathcal{X}_N \cap D$) much faster than the Newton-CG iterates u_E^{0+k}, which start from the zero approximation, and even than u_E^{1+k}, which start from our reconstruction in the Born approximation, i.e., from u_E^J, $J = 1$. In particular, in our examples much faster means that our reconstruction u_E^J, $J = 1$, is similar to u_E^{0+18}, in the configuration space for non-smooth v, and u_E^J, $J = 1$, is similar to u_E^{0+8}, in the configuration space for smooth v. For more comparisons, see also Fig. II.8.

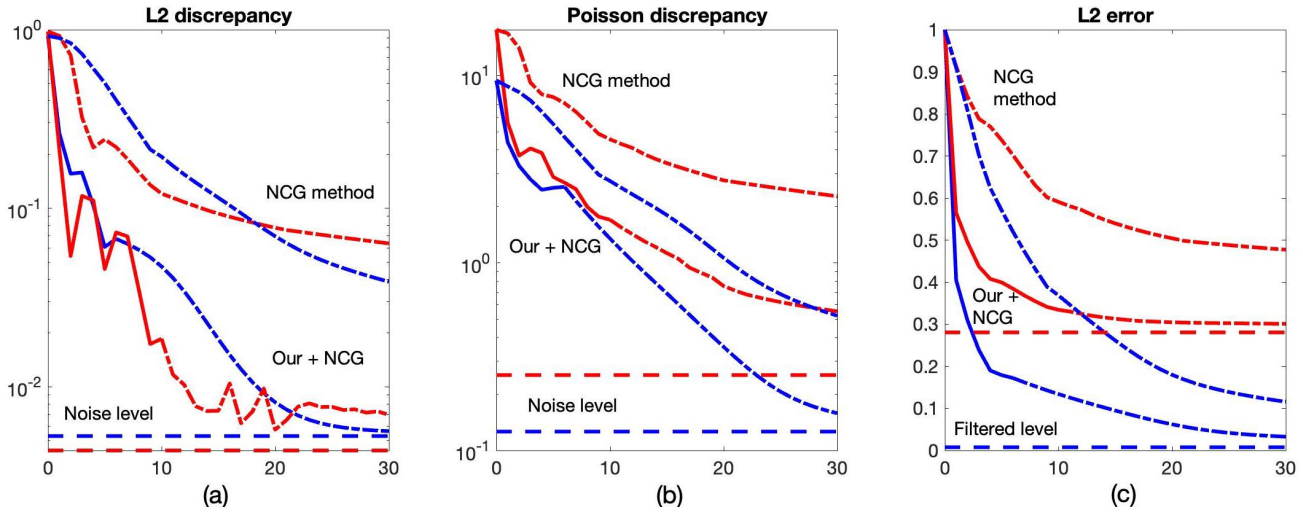

Figure II.8: L_2 discrepancy $\mathfrak{E}(\sigma[u_E^j + w_1]^{\text{comp}}, \sigma[v_1]^{\text{meas}})$, Poisson discrepancy $\Delta(\sigma[u_E^j + w_1]^{\text{comp}}, \sigma[v_1]^{\text{meas}})$ and relative errors $\mathfrak{E}(u_E^j, \underline{v}, D)$ as a function of j, in comparison with $\mathfrak{E}_{\text{noise}}$ and Δ_{noise} (horizontal lines). Solid lines indicate our iterations for $j = 1, ..., J$, dashed line indicate Newton-CG (NCG) iterations. Blue: smooth v. Red: non-smooth v. For the plots 'Our + NCG', the NCG iterations start with $j = J + 1 = 7$ for smooth v and $j = J + 1 = 11$ for non-smooth v. See notations (5.3).

5.4 Further reconstruction results for Problem 8(A)

Reconstruction examples presented in this subsection are as follows: reconstruction of complex v; reconstruction with background w satisfying the additional theoretical assumption (2.37d); reconstruction of real v taking into account a priori knowledge of real-valuedness; examples of v and w for which our method converges, whereas NCG method diverges. The expected number of particles $N_p = 3 \cdot 10^7$ characterizing Poisson noise is as in Subsection 5.3.

Fig. II.9 illustrates our reconstructions u_E^J, for $J = 1$, $J = 6$, and u_E^{J+K}, for $J = 6$, $K = 5$, of complex-valued potential. Here, $\operatorname{Re} v$ is two times smaller than in v in Fig. II.2(a), $\operatorname{Im} v \le 0$, and $|\operatorname{Im} v|$ is four times smaller than v in Fig. II.2(b), and background w is the same as in Fig. II.2.

It is remarkable that our method reconstructs two real-valued functions $\operatorname{Re} v$ and $\operatorname{Im} v$ on $\mathcal{X}_N$ from one real-valued function $\sigma[v_1]^{meas}$ on $\mathcal{M}_{E,M_1,M_2}$ for known background w.

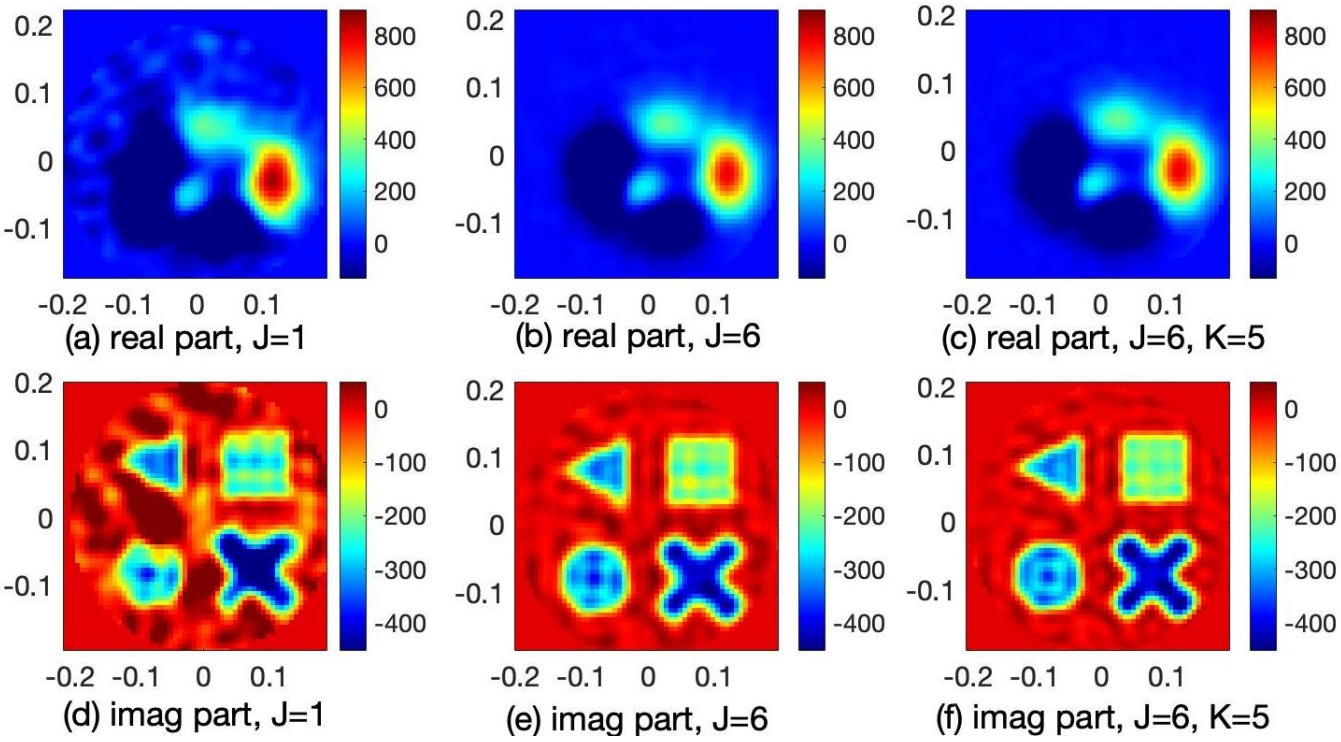

Figure II.9: Reconstructions u_E^J and u_E^{J+K} of complex-valued v with smooth $\operatorname{Re} v$ and non-smooth $\operatorname{Im} v \le 0$. $\mathfrak{E}(u_E^1, v, D) = 0.3927$, $\mathfrak{E}(u_E^6, v, D) = 0.2080$, $\mathfrak{E}(u_E^{6+5}, v, D) = 0.1911$.

Next, we study our numerical reconstructions u_E^J and u_E^{J+K} for the case when w satisfies the additional theoretical assumption (2.37d). We consider w of the form

$$w = w_\Phi(x) = \lambda_1 \Phi_1(|x - x_0|/\lambda_2), \quad \lambda_1,\ \lambda_2 > 0,\ x,\ x_0 \in \mathbb{R}^2, \tag{5.6a}$$

$$\Phi_1(r) = \max(1 - r, 0)^4 (4r + 1). \tag{5.6b}$$

Here, Φ_1 is one of Wendland's radial functions. In particular, w_Φ given by (5.6) satisfies (2.37d) with $\beta = 5$, $d = 2$, and $w_\Phi \in C^2(\mathbb{R}^d)$, see [1], [51]. We chose λ_1, λ_2, x_0 in a such way that x_0 is the center of w_{box}, $2\lambda_2$ is the length of the side of $\operatorname{supp}(w_{\text{box}})$, and λ_1 is such that $\|w_\Phi\|_{L_2} = \|w_{\text{box}}\|_{L_2}$, where w_{box} is w shown in Fig. II.2.

Our numerical reconstructions with background w_Φ were implemented with $\varepsilon = 0$ in (4.21), taking into account that $\widehat{w}_\Phi(p)$ is not too small on $B_{2\sqrt{E}}$. These reconstructions are more or less similar in quality to our reconstructions with background w_{box} presented in Subsection 5.3; see Table II.1.

Table II.1 shows relative L_2 errors $\mathfrak{E}(u, v)$ and $\mathfrak{E}(u, v_E^{\text{filt}})$ on $\mathcal{X}_N \cap D$ for different reconstructions u for smooth and non-smooth real v shown on Fig. II.2, where $w = w_{\text{box}}$ shown in Fig. II.2, or

$w = w_\Phi$ mentioned above, and $u = u_E^J$ or $u = u_E^{J+K}$. In addition, these reconstructions u are implemented either without or with the a priori assumption that $\operatorname{Im} v \equiv 0$. These reconstructions u for $w = w_{\text{box}}$ without a priori assumption that $\operatorname{Im} v \equiv 0$ are also shown in Fig. II.6, II.7.

Smooth v	w_{box}	w_Φ	w_{box} + $\operatorname{Im} v = 0$	w_Φ + $\operatorname{Im} v = 0$
$J = 1$	0.4096	0.3787	0.2165	0.1851
$J = 6$	0.1722	0.2222	0.0299	0.0284
$J = 6,\ K = 5$	0.1257	0.1672	0.0153	0.0159

(a) v shown in Fig. II.2(a).

Non-smooth v	w_{box}	w_Φ	w_{box} + $\operatorname{Im} v = 0$	w_Φ + $\operatorname{Im} v = 0$
$J = 1$	0.5140	0.4730	0.4249	0.3803
$J = 10$	0.3396	0.3214	0.3325	0.2849
$J = 10,\ K = 5$	0.3196	0.3009	0.3048	0.2788

(b1) v shown in Fig. II.2(b).

Non-smooth v vs v_E^{filt}	w_{box}	w_Φ	w_{box} + $\operatorname{Im} v = 0$	w_Φ + $\operatorname{Im} v = 0$
$J = 1$	0.4466	0.3964	0.3299	0.2667
$J = 10$	0.1873	0.1643	0.1825	0.0527
$J = 10,\ K = 5$	0.1486	0.1196	0.1329	0.0453

(b2) v_E^{filt} shown in Fig. II.3(b).

Table II.1: Relative L_2 errors $\mathfrak{E}(u, v)$ and $\mathfrak{E}(u, v_E^{\text{filt}})$ on $\mathcal{X}_N \cap D$ for different reconstructions u for smooth and non-smooth real v without and with the a priori assumption that $\operatorname{Im} v \equiv 0$, where $w = w_{\text{box}}$ or $w = w_\Phi$, and $u = u_E^J$ or $u = u_E^{J+K}$. (a) $\mathfrak{E}(u, v)$; (b1) $\mathfrak{E}(u, v)$; (b2) $\mathfrak{E}(u, v_E^{\text{filt}})$.

One can see that, in our examples, the use of the a priori assumption $\operatorname{Im} v \equiv 0$ strongly reduces $\mathfrak{E}(u, v)$ for smooth v and $\mathfrak{E}(u, v_E^{\text{filt}})$ for non-smooth v with $w = w_\Phi$.

Next, it is important to note that in some cases the reconstruction based completely on the NCG iterations with the zero initialization does not converges to the correct solution, whereas our method does. In particular, we obtained such examples as follows:

(a) We take v which is 5 times smaller and w which is 100 times smaller than v, w shown in Fig. II.2(a);

(b) We take v which is 10 times smaller and w which is 50 times smaller than v, w shown in Fig. II.2(b).

Fig. II.10 shows the L_2 discrepancy $\mathfrak{E}(\sigma[u_E^j + w_1]^{\text{comp}}, \sigma[v_1]^{\text{meas}})$ on $\mathcal{M}_{E,M_1,M_2}$ and relative error $\mathfrak{E}(u_E^j, v)$ on $\mathcal{X}_N \cap D$ as functions of j, where u_E^j are constructed via our method (solid lines) and NCG method (dash lines). Note that Fig. II.10(a) shows that the L_2 discrepancy asymptotically decreases even for the pure NCG method (i.e., with zero initialization), i.e., the pure NCG method converges to some local minimum. In contrast, Fig. II.10(b) shows that the pure NCG method fails to converge to the global minimum, whereas our iterations do converge properly.

Note that in this example the background potential is very small in comparison to unknown potential. Recall that for zero background Problem 7 does not have unique solution. Therefore, for relatively small potentials one can expect instability of convergence of iterative NCG method. In contrast, lines 3–6 of Alg. 3 are exact, and they are more stable for relatively small w.

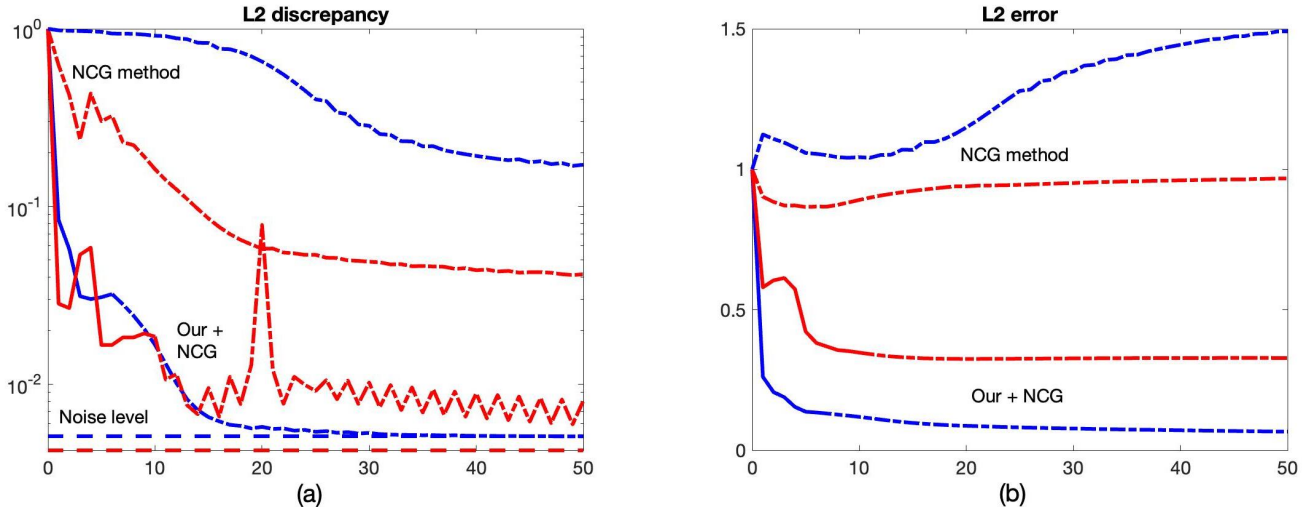

Figure II.10: L_2 discrepancy $\mathfrak{E}(\sigma[u_E^j + w_1]^{\text{comp}}, \sigma[v_1]^{\text{meas}})$ and relative error $\mathfrak{E}(u_E^j, v)$ as functions of j, in comparison with $\mathfrak{E}_{\text{noise}}$ in (5.4) (horizontal lines). Solid lines indicate our iterations for $j = 1, ..., J$, dashed line indicate Newton-CG iterations. Blue: smooth v. Red: non-smooth v. For the plots 'Our + NCG', the NCG iterations start with $j = J + 1 = 7$ for smooth v and $j = J + 1 = 11$ for non-smooth v. See notations (5.3).

6 Conclusions

In the present work we present new results on phaseless monochromatic inverse scattering with only one known background scatterer.

In comparison with [1], we reduce the required amount of data by a factor three: Theoretically, [1] deals with Problem 8(B) for $d \geq 2$ and $n = 2$, that is approximately reconstructs v from the three differential scattering cross sections $\{\sigma[v], \sigma[v + w_1], \sigma[v + w_2]\}$ with known background scatterers w_1, w_2, developing methods of [2], [35], [37]. In addition, numerically, [1] deals with Problems 7(B) and 8(B) for $d = 2$ and $n = 2$ or $n = 3$. In turn, the present work deals with Problems 7(B) and 8(B) for $d = 2$ and $n = 1$ or even Problems 7(A) and 8(A) developing theoretical and numerical methods of [1], [35], [41]. In the latter case only one differential scattering cross section $\sigma[v + w_1]$ is needed.

In comparison with [41], in particular, we take into account multiple scattering in the framework of monochromatic iterative reconstruction algorithm and develop numerical implementations, using approaches of [1], [35]. Theoretically, [41] deals only with the reconstructions given by Algorithm 1 with Q_E given by (2.39) for phaseless Fourier inversion, and by formulas (2.36), (2.10) for phaseless inverse Born scattering, without numerical implementation yet. The present work strongly develops these theoretical results already by Theorem 3.2 for phaseless Fourier inversion and mainly by Theorem 3.7 for phaseless inverse non-linearised scattering. In particular, we establish rapid convergence of approximate monochromatic reconstructions v_E and u_E^j to v, as $E \to +\infty$. Moreover, in the present work we implement numerically theoretical results of [41] and of our new theoretical results in Theorem 3.2 and Theorem 3.7.

In some respects the properties of the numerical implementations of the present work are similar to those in [1]: inversion of the discrete non-uniform Fourier transform T mentioned in Section 4.2 is realised using the conjugate gradient method; iterative reconstructions use the same solver for direct scattering problems; mathematical justification of these iterations goes back to [35]; at the end the reconstruction results are improved using the Newton-CG method; the same Poisson model for noisy data is used.

The main differences are as follows: theoretical reconstruction formulas are essentially different already in the Born approximation and then for iterations; required grid sizes are significantly larger in view of conditions like $\text{dist}(D, \Omega_1) > \text{diam}\, D$ required in [41] and the present work (see

Section 2.3); the initial CG approach for inversion of T was not working properly for reconstructions of the present work and we modified it taking into account a priori information given by theoretical formulas (4.12)–(4.14) recalled in Section 4.3; less measurements and a lower total number of 'Poisson count's, and less direct problem solutions are needed by the numerical methods of the present work.

Natural further research includes study of applicability limits of numerical implementations with respect to different parameters of the algorithm, extension of the numerical implementations to the three-dimensional case, and reconstructions from real data. The experimental scheme could be similar to that in [43].

7 Proof of Lemma 3.6.

To prove Lemma 3.6 we use, in particular, Lemma 2.1 and the following additional lemma.

Lemma 7.1. *Under the assumptions of Lemma 2.1, the following estimates hold:*

$$|f(k,l)| \le \frac{3}{2}(2\pi)^{-d} N c_1^2(d,s), \tag{7.1}$$

$$|f(k,l) - f_{\text{appr}}(k,l)| \le (2\pi)^{-d} c_4(s,D) b E^{-\alpha}, \tag{7.2}$$

$$c_4(s,D) = \left(3c_1^2(d,s)c_5(D,s) + \mu(D)\right)$$

where $(k,l) \in \mathcal{M}_E$, $E^{1/2} \ge \rho_1(d,s,N)$, c_1 *is given by (2.19),* $c_5(D,s) = \max_D (1+|x|^2)^{s/2}$.

Proof. We have that

$$|f(k,l)| \le |f(k,l) - \widehat{v}(k-l)| + |\widehat{v}(k-l)|. \tag{7.3}$$

Using (1.1), (2.5), (2.18)–(2.20), (7.3) we obtain that

$$\begin{aligned} &|f(k,l)| \le 2^{-1}(2\pi)^{-d} c_1^2(d,s)\|v\|_s + (2\pi)^{-d} c_1^2(d,s)\|v\|_s = \frac{3}{2}(2\pi)^{-d} c_1^2(d,s)\|v\|_s, \\ &(k,l) \in \mathcal{M}_E,\ E^{1/2} \ge \rho_1(d,s,N). \end{aligned} \tag{7.4}$$

Thus, estimate (7.1) is proved.

Next, we have that

$$|f(k,l) - f_{\text{appr}}(k,l)| \le |\delta f(k,l) - \delta f_{\text{appr}}(k,l)| + |\widehat{v}(k-l) - \widehat{v}_{\text{appr}}(k-l,E)|, \tag{7.5}$$

where

$$f(k,l) = \widehat{v}(k-l) + \delta f(k,l), \tag{7.6}$$

$$f_{\text{appr}}(k,l) = \widehat{v}_{\text{appr}}(k-l,E) + \delta f_{\text{appr}}(k,l). \tag{7.7}$$

Due to formula (4.11) of [35], we have that

$$\begin{aligned} &|\delta f(k,l) - \delta f_{\text{appr}}(k,l)| \le 6(2\pi)^{-d} a_0(d,s/2) c_1^2(d,s) c_5(D,s)\|v\|_s b E^{-\alpha-1/2}, \\ &(k,l) \in \mathcal{M}_E,\ E^{1/2} \ge \rho_1(d,s,N). \end{aligned} \tag{7.8}$$

Using (1.1), (2.5), (2.19)–(2.22), (7.5), (7.8), we obtain that

$$\begin{aligned} |f(k,l) - f_{\text{appr}}(k,l)| &\le 3(2\pi)^{-d} c_1^2(d,s) c_5(D,s) b E^{-\alpha} + (2\pi)^{-d}\mu(D) b E^{-\alpha} \\ &= (2\pi)^{-d}\left(3c_1^2(d,s)c_5(D,s) + \mu(D)\right) b E^{-\alpha}, \\ &\text{for } (k,l) \in \mathcal{M}_E, \quad E^{1/2} \ge \rho_1(d,s,N). \end{aligned} \tag{7.9}$$

Thus, estimate (7.2) is proved. □

We set:

$$\Delta_1 = f - \widehat{v} - f_{\text{appr}} + \widehat{v}_{\text{appr}}, \tag{7.10}$$

$$\Delta_2 = f - f_{\text{appr}}. \tag{7.11}$$

We have that:

$$|\widehat{v}|^2 = (f - \delta f)(\overline{f} - \overline{\delta f}) = |f|^2 - \overline{f}\delta f - f\overline{\delta f} + \delta f\overline{\delta f}; \tag{7.12}$$

$$\begin{aligned} &- \overline{f}\delta f - f\overline{\delta f} + \delta f\overline{\delta f} = -\overline{f}(f_{\text{appr}} - \widehat{v}_{\text{appr}} + \Delta_1) - f\overline{(f_{\text{appr}} - \widehat{v}_{\text{appr}} + \Delta_1)} + \\ &+ (f_{\text{appr}} - \widehat{v}_{\text{appr}} + \Delta_1)\overline{(f_{\text{appr}} - \widehat{v}_{\text{appr}} + \Delta_1)} = \\ &= -\overline{(f_{\text{appr}} + \Delta_2)}(f_{\text{appr}} - \widehat{v}_{\text{appr}} + \Delta_1) - (f_{\text{appr}} + \Delta_2)\overline{(f_{\text{appr}} - \widehat{v}_{\text{appr}} + \Delta_1)} + \\ &+ (f_{\text{appr}} - \widehat{v}_{\text{appr}} + \Delta_1)\overline{(f_{\text{appr}} - \widehat{v}_{\text{appr}} + \Delta_1)} = -|f_{\text{appr}}|^2 + |\widehat{v}_{\text{appr}}|^2 + \Delta_3, \end{aligned} \tag{7.13}$$

where δf is defined by (7.6), and

$$\begin{aligned} \Delta_3 := &-\overline{\Delta_2}(f_{\text{appr}} - \widehat{v}_{\text{appr}} + \Delta_1) - \Delta_2\overline{(f_{\text{appr}} - \widehat{v}_{\text{appr}} + \Delta_1)} + \Delta_1\overline{\Delta_1} - \overline{f_{\text{appr}}}(-\widehat{v}_{\text{appr}} + \Delta_1) \\ &- f_{\text{appr}}\overline{(-\widehat{v}_{\text{appr}} + \Delta_1)} + f_{\text{appr}}\overline{(-\widehat{v}_{\text{appr}} + \Delta_1)} + (-\widehat{v}_{\text{appr}} + \Delta_1)\overline{f_{\text{appr}}} - \widehat{v}_{\text{appr}}\overline{\Delta_1} - \Delta_1\overline{\widehat{v}_{\text{appr}}} = \\ = &-\overline{\Delta_2}(f_{\text{appr}} - \widehat{v}_{\text{appr}} + \Delta_1) - \Delta_2\overline{(f_{\text{appr}} - \widehat{v}_{\text{appr}} + \Delta_1)} + \Delta_1\overline{\Delta_1} - \widehat{v}_{\text{appr}}\overline{\Delta_1} - \Delta_1\overline{\widehat{v}_{\text{appr}}}. \end{aligned} \tag{7.14}$$

From (7.14) it follows that:

$$|\Delta_3| \leq 2|\Delta_2||f_{\text{appr}} - \widehat{v}_{\text{appr}}| + 2|\Delta_1||\Delta_2| + |\Delta_1|^2 + 2|\widehat{v}_{\text{appr}}||\Delta_1|. \tag{7.15}$$

From (2.24), (7.2), (7.15) it follows that

$$|\Delta_3| \leq c_6(s, D)\left(N + bE^{-\alpha} + NbE^{-\alpha-1/2}\right) bNE^{-\alpha-1/2}, \quad E^{1/2} \geq \rho_1(d, s, N). \tag{7.16}$$

Lemma 3.6 is proved.

8 Proof of Theorem 3.7

Reconstruction in Born approximation. Due to the definition of u_E^1 and estimate (2.38), we have that

$$\|v - u_E^1\|_{L^\infty(D)} = \mathcal{O}(E^{-\alpha_1}), \text{ as } E \to +\infty, \ \alpha_1 = \frac{1}{2}\frac{m-d}{m+\beta}. \tag{8.1}$$

Induction step. Let

$$\|v - u_E^j\|_{L^\infty(D)} = \mathcal{O}(E^{-\alpha_j}), \text{ as } E \to +\infty, \ j \in \mathbb{N}. \tag{8.2}$$

We consider u_E^{j+1} defined in either Algorithm 2(A) or 2(B) with $\nu_j = 1$ and τ_j given by (3.10). To estimate $v - u_E^{j+1}$, we use Lemma 3.6 with $v + w_1$, $u_E^j + w_1$ in place of v, v_{appr} in case of Algorithm 2(A) and also with v itself and with u_E^j in place of v_{appr} in case of Algorithm 2(B). From this lemma we obtain that

$$|\widehat{v}(p) + \widehat{w}_1(p)|^2 = \Sigma_1^j(p, E) + \mathcal{O}(E^{-\alpha_j - 1/2}) \quad \text{as } E \to +\infty, \ p \in B_{2\sqrt{E}}, \tag{8.3}$$

$$|\widehat{v}(p)|^2 = \Sigma^j(p, E) + \mathcal{O}(E^{-\alpha_j - 1/2}) \quad \text{as } E \to +\infty, \ p \in B_{2\sqrt{E}}, \tag{8.4}$$

where Σ_1^j, Σ^j are defined by formulas 4 and 5 of Algorithm 2(B).

We set:

$$\begin{aligned} &\Delta h^{j+1}(p, E) := |\widehat{v}(p) + \widehat{w}_1(p)|^2 - \Sigma_1^j(p, E), \ p \in B_{2\sqrt{E}}, \\ &\text{for Algorithm 2(A);} \end{aligned} \tag{8.5}$$

$$\begin{aligned} &\Delta h^{j+1}(p, E) := |\widehat{v}(p) + \widehat{w}_1(p)|^2 - |\widehat{v}(p)|^2 - \Sigma_1^j(p, E) + \Sigma^j(p, E), \ p \in B_{2\sqrt{E}}, \\ &\text{for Algorithm 2(B).} \end{aligned} \tag{8.6}$$

In order to estimate $\widehat{v} - \widehat{u}_E^{j+1}$ we repeat the proofs of Theorems 5.1 and 5.2 of [41] up to the following detail:

- We replace formulas (114), (127), (116), (129) for $\Delta h(p,E)$ in [41] by formulas (8.5), (8.6), (8.3), (8.4) of the present work.

We obtain that

$$|\widehat{v}(p)-\widehat{u}_E^{j+1}(p)|=|(\overline{\mathcal{F}w_1}(p))^{-1}|\mathcal{O}(E^{-\alpha_j-1/2}),\ p\in B_{2\tau E^{\gamma_{j+1}}},\ \gamma_{j+1}=\frac{\alpha_j+1/2}{m+\beta}. \tag{8.7}$$

In order to estimate $v-u_E^{j+1}$ we proceed from (8.7), and repeat the proofs of Theorems 6.1 and 6.2 of [41] up to the following details:

- Formula (136) of [41] should be replaced by

$$(2-\delta(E))\sqrt{E}=2\tau E^{\gamma_{j+1}},\ \gamma_{j+1}=\frac{\alpha_j+1/2}{m+\beta}, \tag{8.8}$$

- v_{appr} should be replaced by u_E^{j+1},
- formula (138) for $\widehat{v}-\widehat{u}_E^{j+1}$ in [41] should be replaced by (8.7).

This way provides us the following estimates:

$$|v(x)-u_E^{j+1}(x)|=\mathcal{O}(E^{-\gamma_{j+1}(m-d)})+\mathcal{O}(E^{-\alpha_j-1/2+\gamma_{j+1}(d+\beta)}),\ x\in D. \tag{8.9}$$

In addition, taking into account the value of γ_{j+1} we have that, for $E\to+\infty$:

$$|v(x)-u_E^{j+1}(x)|=\mathcal{O}(E^{-\alpha_{j+1}}),\ \alpha_{j+1}=\left(\alpha_j+\frac{1}{2}\right)\frac{m-d}{m+\beta}. \tag{8.10}$$

Therefore, from the properties of arithmetico-geometric sequence for $\{\alpha_j\}$ we obtain:

$$\alpha_j=\frac{1}{2}\frac{m-d}{\beta+d}\left(1-\left(\frac{m-d}{m+\beta}\right)^j\right),\ \forall\, j\in\mathbb{N}. \tag{8.11}$$

This completes the proof of Theorem 3.7.

Bibliography

[1] A.D. Agaltsov, T. Hohage, R.G. Novikov, *An iterative approach to monochromatic phaseless inverse scattering*, Inverse Problems 35, 24001 (24 pp.) (2019)

[2] A. D. Agaltsov, R.G. Novikov, *Error estimates for phaseless inverse scattering in the Born approximation at high energies*, J. Geom. Anal. (2017), https://doi.org/10.1007/s12220-017-9872-6, e-print: https://hal.archives-ouvertes.fr/hal-01303885v2

[3] T. Aktosun, P. E. Sacks, *Inverse problem on the line without phase information*, Inverse Problems 14, 211–224 (1998)

[4] N.V. Alexeenko, V.A. Burov, O.D. Rumyantseva, *Solution of the three-dimensional acoustical inverse scattering problem. The modified Novikov algorithm,* Acoust. Phys. 54(3), 407–419 (2008)

[5] H. Ammari, Y.T. Chow, J. Zou, *Phased and phaseless domain reconstructions in the inverse scattering problem via scattering coefficients,* SIAM J. Appl. Math. 76, no. 3, 1000–1030 (2016)

[6] J. A. Barceló, C. Castro, and J. M. Reyes, *Numerical approximation of the potential in the two-dimesional inverse scattering problem,* Inverse Problems, 32(1), 015006 (19pp) (2016)

[7] A.H. Barnett, Ch.L. Epstein, L.F. Greengard, J.F. Magland, *Geometry of the phase retrieval problem—graveyard of algorithms*, Cambridge University Press, Cambridge (2022)

[8] F.A. Berezin, M.A. Shubin, *The Schrödinger Equation*, Mathematics and Its Applications, Vol. 66, Kluwer Academic, Dordrecht, 1991

[9] M. Born, *Quantenmechanik der Stossvorgange*, Zeitschrift fur Physik 38 (11-12), 803-827 (1926)

[10] V.A. Burov, N.V. Alekseenko, O.D. Rumyantseva, *Multifrequency generalization of the Novikov algorithm for the two-dimensional inverse scattering problem,* Acoust. Phys. 55(6), 843–856 (2009)

[11] K. Chadan, P.C. Sabatier, *Inverse Problems in Quantum Scattering Theory*, 2nd edn. Springer, Berlin, 1989

[12] K. Engel, B. Laasch, *The modulus of the Fourier transform on a sphere determines 3-dimensional convex polytopes*, J. Inverse Ill-Posed Probl., https://doi.org/10.1515/jiip-2020-0103

[13] G. Eskin, *Lectures on Linear Partial Differential Equations*, Graduate Studies in Mathematics, Vol. 123, American Mathematical Society, 2011

[14] L.D. Faddeev, *Uniqueness of the solution of the inverse scattering problem,* Vestn. Leningrad Univ. 7, 126–130 (1956) (in Russian)

[15] D. Fanelli, O. Öktem, *Electron tomography: a short overview with an emphasis on the absorption potential model for the forward problem,* Inverse Problems, 24(1), 013001 (51 pp.) (2008)

[16] L.D. Faddeev, S.P. Merkuriev, *Quantum Scattering Theory for Multi-particle Systems*, Mathematical Physics and Applied Mathematics, 11. Kluwer Academic Publishers Group, Dordrecht, 1993

[17] A.A. Govyadinov, G.Y. Panasyuk, J.C. Schotland, *Phaseless three-dimensional optical nanoimaging*, Phys. Rev. Lett. 103, 213901 (2009)

[18] P. Hähner, T. Hohage, *New stability estimates for the inverse acoustic inhomogeneous medium problem and applications,* SIAM J. Math. Anal., 33(3):670–685, (2001)

[19] M. Hanke, *Regularizing properties of a truncated Newton-CG algorithm for nonlinear inverse problems*, Numer. Funct. Anal. Optim., 18:971-993, 1997.

[20] T. Hohage, R.G. Novikov, *Inverse wave propagation problems without phase information*, Inverse Problems 35, 070301 (4 pp.)(2019)

[21] N.E. Hurt, *Phase retrieval and zero crossings*, Kluwer Academic Publishers Group, Dordrecht (1989)

[22] T. Hohage, F. Werner, *Inverse problems with Poisson data: statistical regularization theory, applications and algorithms*, Inverse Problems, 32:093001, 56 (2016)

[23] O. Ivanyshyn, R. Kress, *Inverse scattering for surface impedance from phase-less far field data*, J. Comput. Phys. 230(9), 3443-3452 (2011)

[24] M. Isaev, R.G. Novikov, *Hölder-logarithmic stability in Fourier synthesis*, Inverse Problems 36, 125003 (2020)

[25] M. Isaev, R.G. Novikov, *Stability estimates for reconstruction from the Fourier transform on the ball*, Journal of Inverse and Ill-posed Problems, 29(3), 421-433 (2021)

[26] M. Isaev, R.G. Novikov , G. V. Sabinin, *Numerical reconstruction from the Fourier transform on the ball using prolate spheroidal wave functions*, Inverse Problems, 38(10), 105002 (2022)

[27] A. Jesacher, W. Harm, S. Bernet, M. Ritsch-Marte, *Quantitative single-shot imaging of complex objects using phase retrieval with a designed periphery*, Opt. Express 20, 5470–5480 (2012)

[28] J. Keiner, S. Kunis, D. Potts, *Using NFFT 3—a software library for various nonequispaced fast Fourier transforms*, ACM Trans. Math. Software, 36(4), (2009)

[29] M.V. Klibanov, *Phaseless inverse scattering problems in three dimensions*, SIAM J.Appl. Math. 74(2), 392-410 (2014)

[30] M.V. Klibanov, N.A. Koshev, D.-L. Nguyen, L.H. Nguyen, A. Brettin, V.N. Astratov, *A numerical method to solve a phaseless coefficient inverse problem from a single measurement of experimental data*, SIAM J. Imaging Sci. 11(4), 2339-2367 (2018)

[31] M.V. Klibanov, V.G. Romanov, *Reconstruction procedures for two inverse scattering problems without the phase information*, SIAM J. Appl. Math. 76(1), 178-196 (2016)

[32] M.V. Klibanov, P.E. Sacks, A.V. Tikhonravov, *The phase retrieval problem*, Inverse Problems 11, 1–28 (1995)

[33] B. Leshem, R. Xu, Y. Dallal, J. Miao, B. Nadler, D. Oron, N. Dudovich, O. Raz, *Direct single-shot phase retrieval from the diffraction pattern of separated objects,* Nature Communications 7(1), 1-6 (2016)

[34] R. G. Novikov, *Approximate Lipschitz stability for non-overdetermined inverse scattering at fixed energy*, J. Inverse Ill-Posed Probl., 21:6, 813–823 (2013)

[35] R. G. Novikov, *An iterative approach to non-overdetermined inverse scattering at fixed energy*, Sbornik: Mathematics 206(1), 120-134 (2015)

[36] R. G. Novikov, *Inverse scattering without phase information*, Seminaire Laurent Schwartz - EDP et applications (2014-2015), Exp. No16, 13p

[37] R. G. Novikov, *Explicit formulas and global uniqueness for phaseless inverse scattering in multidimensions*, J. Geom. Anal. 26(1), 346-359 (2016), e-print: https://hal.archives-ouvertes.fr/hal-01095750v1

[38] R. G. Novikov, *Multipoint formulas for phase recovering from phaseless scattering data*, The Journal of Geometric Analysis, 31(2), 1965-1991 (2021)

[39] R.G. Novikov, *Multidimensional inverse scattering for the Schrödinger equation*, In: Cerejeiras, P., Reissig, M. (eds) Mathematical Analysis, its Applications and Computation. ISAAC 2019. Springer Proceedings in Mathematics & Statistics, vol 385, pp 75-98 (2022).Springer, Cham.

[40] R. G. Novikov, V. N. Sivkin, *Error estimates for phase recovering from phaseless scattering data*, Eurasian Journal of Mathematical and Computer Applications, vol. 8(1), 44–61, (2020)

[41] R. G. Novikov, V. N. Sivkin, *Phaseless inverse scattering with background information*, Inverse Problems, 37(5), 055011 (2021)

[42] R. G. Novikov, V. N. Sivkin, *Fixed-distance multipoint formulas for the scattering amplitude from phaseless measurements*, Inverse Problems, 38(2), 025012 (2022)

[43] M.F. Perutz, *X-ray Analysis of Hemoglobin: The results suggest that a marked structural change accompanies the reaction of hemoglobin with oxygen,* Science, 140(3569), 863-869 (1963)

[44] S.G. Podorov, K.M. Pavlov, D.M. Paganin, *A non-iterative reconstruction method for direct and unambiguous coherent diffractive imaging*, Optics Express, 15(16), 9954-9962 (2007)

[45] V. G. Romanov, *Inverse problems without phase information that use wave interference*, Sib. Math. J. 59(3), 494-504 (2018)

[46] V.G. Romanov, *Phaseless problem of determination of anisotropic conductivity in electrodynamic equations*, Dokl. Math., 104(3), 385-389 (2021)

[47] Y. Shechtman, Y.C. Eldar, O. Cohen, H.N. Chapman, J. Miao, J. M. Segev, *Phase retrieval with application to optical imaging: a contemporary overview,* IEEE signal processing 32, 87–109 (2015)

[48] A.S. Shurup, *Numerical comparison of iterative and functional-analytic algorithms for inverse acoustic scattering,* Eurasian Journal of Mathematical and Computer Applications **10**(1), 79-99 (2022)

[49] T. Salditt, A.-L. Robisch, *Coherent X-ray Imaging,* Nanoscale Photonic Imaging (eds. T. Salditt, A. Egner, R. Luke), pp. 35–70, Springer Int'l Publishing, https://doi.org/10.1007/978-3-030-34413-9_2 (2020)

[50] G. Vainikko, *Fast Solvers of the Lippmann-Schwinger equation* Direct and Inverse Problems of Mathematical Physics (eds R.P. Gilbert, J. Kajiwara, Y.S. Xu) Kluwer, Dordrecht (2000).

[51] H. Wendland, *Error estimates for interpolation by compactly supported radial basis functions of minimal degree,* J. Approx. Theory 93, 258–72 (1998)

[52] X. Xu, B. Zhang, H. Zhang, *Uniqueness in inverse electromagnetic scattering problem with phaseless far–field data at a fixed frequency*, IMA Journal of Applied Mathematics 85(6), 823-839 (2020)

[53] Y. Ziyang, H. Wang, *Phase retrieval with background information*, Inverse Problems 35, 054003 (20pp.) (2019)

Article III

Approximate Lipschitz stability for phaseless inverse scattering with background information

V.N. Sivkin

We prove approximate Lipschitz stability for monochromatic phaseless inverse scattering with background information in dimension $d \geq 2$. Moreover, these stability estimates are given in terms of non-overdetermined and incomplete data. Related results for reconstruction from phaseless Fourier transforms are also given. Prototypes of these estimates for the phased case were given in Novikov (2013 J. Inverse Ill-Posed Problems, 21, 813-823).

Keywords: Schrödinger equation, phaseless inverse scattering, phaseless Fourier transform, approximate Lipschitz stability, monochromatic and non-overdetermined data.

1 Introduction

In this work we continue studies on phaseless inverse scattering for the stationary Schrödinger equation:

$$-\Delta\psi + V(x)\psi = E\psi, \quad x \in \mathbb{R}^d, \quad d \geq 2, \quad E > 0, \tag{1.1}$$

where

$$V \in L^\infty(\mathbb{R}^d), \text{ and is compactly supported.} \tag{1.2}$$

For equation (1.1), under conditions (1.2), we consider the scattering solutions $\psi^+ = \psi^+(x,k)$, $k \in \mathbb{R}^d$, $k^2 = E$, such that

$$\psi^+(x,k) = e^{ik\cdot x} + \psi^{\text{sc}}(x,k), \tag{1.3}$$

$$|x|^{(d-1)/2}\left(\frac{\partial}{\partial|x|} - i|k|\right)\psi^{\text{sc}}(x,k) \to 0 \quad \text{as } |x| \to +\infty, \tag{1.4}$$

uniformly in $x/|x|$. In particular, we have that

$$\psi^{\text{sc}}(x,k) = \frac{e^{i|k||x|}}{|x|^{(d-1)/2}} c(d,|k|) f\left(k, |k|\frac{x}{|x|}\right) + \mathcal{O}\left(\frac{1}{|x|^{(d+1)/2}}\right) \quad \text{as } |x| \to +\infty, \tag{1.5}$$

$$c(d,|k|) := -\pi i(-2\pi i)^{(d-1)/2}|k|^{(d-3)/2}, \text{ for } \sqrt{-2\pi i} = \sqrt{2\pi}e^{-i\pi/4}. \tag{1.6}$$

The coefficient $f = f[V]$ arising in (1.5) is known as the scattering amplitude for equation (1.1). In turn, $|f|^2$ is known as the differential scattering cross section for equation (1.1).

Note that f is defined on

$$\mathcal{M}_E = \{k, l \in \mathbb{R}^d : \quad k^2 = l^2 = E\} = \mathbb{S}^{d-1}_{\sqrt{E}} \times \mathbb{S}^{d-1}_{\sqrt{E}}. \tag{1.7}$$

We recall that in quantum mechanics complex values of ψ^+ and f have no direct physical sense, whereas $|\psi^+|^2$ and $|f|^2$ admit probabilistic intepritations and can be measured (Born principle going back to [6]). In particular, $|f(k,l)|^2$ describes the probability density of scattering of the quantum mechanical particle with initial impulse k into direction $l/|l| \neq k/|k|$.

We consider the following monochromatic phaseless inverse scattering problem for equation (1.1) under assumptions (1.2):

Problem 9. *(A) Reconstruct a compactly supported potential v from the differential scattering cross section $|f[v+w]|^2$ given on some appropriate $\mathcal{M}' \subseteq \mathcal{M}_E$ for some known compactly supported background potential w sufficiently separated from v.*

(B) Reconstruct a compactly supported potential v from the differential scattering cross sections $|f[v]|^2$, $|f[v+w_1]|^2$, ..., $|f[v+w_n]|^2$ given on some appropriate $\mathcal{M}' \subseteq \mathcal{M}_E$ for some known compactly supported background potentials $w_1, ..., w_n$ sufficiently separated from v.

Actually, in Problem 9(A) we consinder the Schrödinger equation (1.1) with $V = v + w$, while in Problem 9(B) we consider $n+1$ Schrödinger equations (1.1) for $V = v + w_j$, $j = 1, ..., n$, and $V = v$.

Approximate reconstruction for Problem 9(A) in dimension $d \geq 2$ was developed in [24], [12].

Approximate reconstruction for Problem 9(B) in dimension $d \geq 2$ was developed, in particular, in [1], [2], [12], [22], [23], [24].

We also consider Problems 9(A), 9(B) in the Born approximation, when the phaseless scattering data are reduced to the phaseless Fourier transforms. In this respect, we continue, in particular, studies of [12], [24].

In the present work, we give the **first** approximate stability results for Problem 9(A) and Problem 9(B) for $n = 1$. Related results for reconstruction from phaseless Fourier transforms are also given. Prototypes of these estimates for the phased case were given in [20].

In addition to Problem 9, there are also other phaseless inverse problems for equation (1.1) and for related equations; see, for example, [3], [5], [8], [9], [13], [14], [15], [16], [17], [18], [25], [26], [27], [28], and references therein.

In particular, in connection with phaseless inverse scattering with background information for equation (1.1) at positive energies E for $d = 1$, we refer to [3] and references therein.

The main results of the present work are formulated in Section 2; see Theorems 2.1 and 2.2, Propositions 2.6 and 2.7. Preliminary results required for the proof of these theorems are given in Section 3. Theorems 2.1 and 2.2 are proved in Section 4. Propositions 2.6 and 2.7 are proved in Section 5.

2 Main results

We assume that:

$$v_1,\, v_2 \in L^\infty(\mathbb{R}^d), \quad d \geq 2, \tag{2.1a}$$

$$supp\, v_1,\, supp\, v_2 \subseteq D,\, supp\, w \subseteq \Omega, \tag{2.1b}$$

$$D,\, \Omega \text{ are open convex bounded domains, } D \cap \Omega = \varnothing. \tag{2.1c}$$

We also assume that:

$$v_1 - v_2 \in W^{m,1}(\mathbb{R}^d) \text{ for some } m > d, \tag{2.2}$$

$$\|v_j\|_\infty \leq N_1,\, j = 1, 2;\, \|v_1 - v_2\|_{m,1} \leq N_2, \tag{2.3}$$

where

$$W^{m,1}(\mathbb{R}^d) = \{u : \partial^J u \in L^1(\mathbb{R}^d),\, |J| \leq m\},$$
$$\|u\|_{m,1} = \max_{|J| \leq m} \|\partial^J u\|_{L^1(\mathbb{R}^d)}, \tag{2.4}$$

$$\|u\|_\infty = \|u\|_{L^\infty(\mathbb{R}^d)}. \tag{2.5}$$

Finally, we assume that:

$$\|w\|_\infty \le N_1, \quad |\widehat{w}(p)| \ge c_1(1+|p|)^{-\beta}, \quad p \in \mathbb{R}^d, \tag{2.6}$$

for some $c_1 > 0$ and $\beta > d$. Here $\widehat{w}$ is Fourier transform of w, defined by

$$\widehat{u}(p) = \mathcal{F}u(p) = \frac{1}{(2\pi)^d}\int_{\mathbb{R}^d} e^{ip\cdot x}u(x)dx. \tag{2.7}$$

For examples of w satisfying (2.6), see [2], [30].

In addition to $\mathcal{M}_E$ defined by (1.7), we also consider its subsets $\Gamma_E^\tau \subset \mathcal{M}_E$, for $\tau \in (0,1)$:

$$\begin{aligned} &\Gamma_E^\tau = \left\{k = k_E(p),\, l = l_E(p)\ : p \in B_{2\tau\sqrt{E}}\right\}, \\ &k_E(p) = p/2 + (E - p^2/4)^{1/2}\gamma(p),\ l_E(p) = -p/2 + (E-p^2/4)^{1/2}\gamma(p), \end{aligned} \tag{2.8}$$

where γ is a piecewise continuous vector–function on $\mathbb{R}^d$, $d \ge 2$, such that

$$|\gamma(p)| = 1,\ \gamma(p)\cdot p = 0,\ \ p \in \mathbb{R}^d. \tag{2.9}$$

Let $C(\mathcal{M}_E)$ denote continuous functions on $\mathcal{M}_E$, and $C(\Gamma_E^\tau)$ denotes their restrictions on Γ_E^τ.

Theorem 2.1. *Let functions v_1, v_2 satisfy assumptions (2.1)–(2.6), and* $\operatorname{dist}(D,\Omega) > \operatorname{diam} D$. *Then, for any $\varepsilon \in (0,1/2)$,*

$$\|v_1 - v_2\|_{L^\infty(D)} \le C_1 E^{\frac12-\varepsilon}\||f[v_1+w]|^2 - |f[v_2+w]|^2\|_{C(\Gamma_E^\tau)} + C_2 E^{-(\frac12-\varepsilon)\frac{m-d}{\beta+d}}, \tag{2.10}$$

for $E \ge E_1 = E_1(D, N_1, \Omega, \beta, c_1, \tau, \varepsilon)$, where $\tau \in (0,1)$, E_1 is defined in (4.29), $C_1 = 2K_2K_3$, $C_2 = 2K_1$, and constants $K_1 = \widetilde{K}_1(d,m)N_2$, $K_2 = c_1^{-1}\widetilde{K}_2(d,\beta,\varepsilon)$, $K_3 = K_3(d,\beta)$ are defined in (4.25), (4.26).

Theorem 2.2. *Let functions v_1, v_2 satisfy assumptions (2.1)–(2.6). Then, for any $\varepsilon \in (0,1/2)$,*

$$\|v_1 - v_2\|_{L^\infty(D)} \le C_1 E^{\frac12-\varepsilon}\|(|f[v_1+w]|^2 - |f[v_2+w]|^2) - (|f[v_1]|^2 - |f[v_2]|^2)\|_{C(\Gamma_E^\tau)} + C_2 E^{-(\frac12-\varepsilon)\frac{m-d}{\beta+d}}, \tag{2.11}$$

for $E \ge E_2 = E_2(D, N_1, \Omega, \beta, c_1, \tau, \varepsilon)$, where $\tau \in (0,1)$, E_2 is defined in (4.39), $C_1 = 2K_2K_3$, $C_2 = 2K_1$, and constants $K_1 = \widetilde{K}_1(d,m)N_2$, $K_2 = c_1^{-1}\widetilde{K}_2(d,\beta,\varepsilon)$, $K_3 = (d,\beta,\alpha)$ are defined in (4.25), (4.26).

Theorems 2.1 and 2.2 are proved in Section 4.

One can see that Theorem 2.1 is a stability result to Problem 9(A), while Theorem 2.2 is a stability result to Problem 9(B) for $n = 1$.

Remark 2.3. *For the phased case, the prototype of (2.10), (2.11) is as follows:*

$$\|v_1 - v_2\|_{L^\infty(D)} \le A_1 E^{\frac12}\|f_1 - f_2\|_{C(\Gamma_E^\tau)} + A_2 E^{-\frac12\frac{m-d}{d}}, \tag{2.12}$$

where $\tau\sqrt{E} = \tau(E)\sqrt{E} = E^{1/(2d)}$, $A_1 = A_1(N_1, D)$, $A_2 = A_2(N_1, N_2, D, m)$, $E \ge 1$; see [20].

Following [20], we say that (2.10), (2.11), (2.12) are approximate Lipschitz stability esimates.

One can see that the right hand sides of (2.10), (2.11), (2.12) are sums of two terms. The first one is Lipschitz term with respect to data difference, and the second one is approximate but decaying for high energies. In addition, its decay is very fast for large m, that is for smooth $v_1 - v_2$. One can see that, at fixed energy E, the right-hand sides in estimates (2.10), (2.11), (2.12) tend to positive constants if data differences tend to zero. However, these constants become very small for large E. This is completely sufficient from the point of view of numerical analysis: numerical

reconstructions are never absolutely precise. Therefore, it is very natural to study reconstructions (including stability) up to some small constants (that is, approximate reconstructions). In particular, the inverse scattering algorithm related with the stability estimate (2.12) was given in [21] and implemented numerically in [4], [29], whereas the inverse scattering algorithm related with the stability estimates (2.10), (2.11) was given and implemented numerically in [12]. Note also that, under the assumptions of Theorem 2.1, Theorem 2.2 and Remark 2.3, exact Lipschitz and Hölder stability estimates at fixed energy E are impossible; see [19], [10], [11], for such instability results for more or less similar non-linear and linear inverse problems.

Remark 2.4. *Estimates* (2.10), (2.11), (2.12) *also imply Hölder stability estimates for the case when data are given for arbitrary large energies. For example, if* v_1, v_2, w *satisfy the assumptions of Theorem 2.1, and*

$$\begin{aligned} &\| |f[v_1+w]|^2 - |f[v_2+w]|^2 \|_{C(\Gamma^\tau_{E(\delta)})} \le \delta, \\ &E = E(\delta) = \max(E_1, \delta^{-\zeta}), \\ &\zeta = \frac{\beta + d}{(1/2-\varepsilon)(m+\beta)}, \end{aligned} \tag{2.13}$$

then the following estimate holds:

$$\|v_1 - v_2\|_{L^\infty(D)} \le (C_1 + C_2)\delta^{\frac{m-d}{m+\beta}}, \tag{2.14}$$

where E_1, C_1, C_2, β, ε, m, τ *are as in Theorem 2.1. Similar Hölder stability estimates can be given proceeding from Theorem 2.2 and Remark 2.3.*

Remark 2.5. *The second (approximate) terms in estimates* (2.10), (2.11) *are similar to the error estimates in formula (3.12) in [12] for iterative reconstructions* u^j_E, *when* $j \to \infty$.

Note that in formulas (2.10), (2.11) the norm of difference is taken on Γ^τ_E, where τ could be very small. In fact, τ can even decrease as $E \to +\infty$, but not very fast, that is $\tau(E)E^{1/2} \ge E^\gamma$, for $\gamma = \left(\frac{1}{2} - \varepsilon\right)\frac{1}{\beta+d}$. Therefore, Theorems 2.1, 2.2 can be considered as stability results for non-overdetermined and non-complete data.

We recall that, for the case of Born approximation for small V, scattering amplitude reduces to the Fourier transform:

$$f[V](k,l) \approx \widehat{V}(k-l), \quad (k,l) \in \mathcal{M}_E. \tag{2.15}$$

Therefore, Fourier analogs of Theorems 2.1, 2.2 can be summarized as the following result:

Proposition 2.6. *Let functions* v_1, v_2, w *satisfy assumptions* (2.1)–(2.6), *and* $\operatorname{dist}(D, \Omega) > \operatorname{diam} D$. *Then, for any* $\varepsilon \in (0, 1/2)$,

$$\|v_1 - v_2\|_{L^\infty(D)} \le C_1 E^{\frac{1}{2}-\varepsilon} \| |\mathcal{F}(v_1+w)|^2 - |\mathcal{F}(v_2+w)|^2 \|_{C(B_{2\tau\sqrt{E}})} + C_2 E^{-(\frac{1}{2}-\varepsilon)\frac{m-d}{\beta+d}}, \tag{2.16}$$

for $E \ge E_3 = E_3(D, N_1, \Omega, \beta, c_1, \tau, \varepsilon)$. *In addition, if the condition on supports is relaxed to* $\operatorname{dist}(D, \Omega) > 0$, *then*

$$\|v_1 - v_2\|_{L^\infty(D)} \le C_1 E^{\frac{1}{2}-\varepsilon} \| (|\mathcal{F}(v_1+w)|^2 - |\mathcal{F}(v_2+w)|^2) - (|\mathcal{F}v_1|^2 - |\mathcal{F}v_2|^2) \|_{C(B_{2\tau\sqrt{E}})} + C_2 E^{-(\frac{1}{2}-\varepsilon)\frac{m-d}{\beta+d}} \tag{2.17}$$

for $E \ge E_4 = E_4(D, N_1, \Omega, \beta, c_1, \tau, \varepsilon)$. *Here* C_1, C_2 *are the same as in* (2.10), (2.11), *and* E_3, E_4 *are defined in* (5.3).

The estimates (2.16), (2.17) follow from (2.10), (2.11) up to values of E_3 and E_4.

Note that estimates (2.16), (2.17) have considerable similarity with some of results of [12] and, in particular, with estimate (1.11). These results of [12] can be specified also as the following approximate Lipschitz stability estimates:

Proposition 2.7. *Let functions v_1, v_2, w satisfy assumptions (2.1)–(2.6), and* $\operatorname{dist}(D, \Omega) > \operatorname{diam} D$. *Then*

$$\|v_1 - v_2\|_{L^\infty(D)} \le C_1 \tau^{\beta+d} E^{\frac{\beta+d}{2}} \| |\mathcal{F}(v_1 + w)|^2 - |\mathcal{F}(v_2 + w)|^2 \|_{C(B_{2\tau\sqrt{E}})} + C_2 \tau^{-(m-d)} E^{-\frac{m-d}{2}}, \quad (2.18)$$

for $E \ge E_5$. In addition, if the condition on supports is relaxed to $\operatorname{dist}(D, \Omega) > 0$, *then*

$$\|v_1 - v_2\|_{L^\infty(D)} \le C_1 \tau^{\beta+d} E^{\frac{\beta+d}{2}} \| (|\mathcal{F}(v_1 + w)|^2 - |\mathcal{F}(v_2 + w)|^2) - (|\mathcal{F}v_1|^2 - |\mathcal{F}v_2|^2) \|_{C(B_{2\tau\sqrt{E}})} + C_2 \tau^{-(m-d)} E^- \quad (2.19)$$

for $E \ge E_5$, where $E_5 = E_5(\tau)$ is defined in (5.10); $C_1 = C_1(d, \beta, c_1)$ is defined in (5.8), $C_2 = C_2(d, m, N_1, N_2, D, \Omega, \beta, c_1)$ is defined by (5.9) for (2.18), and by (5.11) for (2.19).

Propositions 2.6 and 2.7 are proved in Section 5. These proofs are based on the explicit reconstruction formulas of [24]. The proof of Proposition 2.6 follows the scheme of proofs of Theorems 2.1, 2.2. The proof of Proposition 2.7 is more straightforward. This straightforward scheme can be also used for the case of Proposition 2.6. This approach leads to somewhat different constants C_1, C_2, E_4, E_5 in formulas (2.16), (2.17).

3 Preliminaries

3.1 Direct scattering

Starting from v, in order to find ψ^+ and f, one can use, in particular, the Lippmann-Schwinger integral equation

$$\psi^+(x, k) = e^{ik\cdot x} + \int_{\mathbb{R}^d} G^+(x - y, k) V(y) \psi^+(y, k) dy, \quad (3.1)$$

$$G^+(x, k) = -\frac{1}{(2\pi)^d} \int_{\mathbb{R}^d} \frac{e^{i\xi\cdot x} d\xi}{\xi^2 - k^2 - i0}, \quad (3.2)$$

and the relation

$$f[V](k, l) = \frac{1}{(2\pi)^d} \int_{\mathbb{R}^d} e^{-il\cdot y} V(y) \psi^+(y, k) dy, \quad (3.3)$$

where $x, k, l \in \mathbb{R}^d$, $k^2 = l^2 = E$; see, for example, [7].

To deal with equation (3.1) and formula (3.3), it is convenient to use the following Agmon estimate:

$$\|\Lambda^{-s} G^+(k) \Lambda^{-s}\|_{L^2(\mathbb{R}^d) \to L^2(\mathbb{R}^d)} \le a_0(d, s) |k|^{-1}, \quad |k| \to \infty, \quad s > 1/2, \quad (3.4)$$

where Λ is the multiplication operator by the function $(1+|x|^2)^{1/2}$, $G^+(k)$ denotes integral operator with Schwartz kernel $G^+(x - y, k)$.

In particular, it follows from (3.4) that (3.1) is uniquely solvable in $L^\infty(\mathbb{R}^d)$ for fixed k, for $|k| = E^{1/2} \ge \rho_1(d, s, \|V\|_{\infty,s})$, where

$$\rho_1(d, s, N) = \max(2a_0(d, s/2)N, 1), \quad (3.5)$$

and the following estimate holds:

$$\|\Lambda^{-s/2} \psi^+(x, k) - \Lambda^{-s/2} e^{ik\cdot x}\|_{L^2(\mathbb{R}^d)} \le b_1(d, s) \|V\|_{\infty,s} |k|^{-1}, \quad (3.6)$$

for $|k| \ge \rho_1(d, s, \|V\|_{\infty,s})$, $k \in \mathbb{R}^d$. Here

$$\|u\|_{\infty,s} = \operatorname*{ess\,sup}_{x\in\mathbb{R}^d} (1 + |x|)^s |u(x)|, \ s > 0. \quad (3.7)$$

We also have that

$$f[V](k,l) = \widehat{V}(k-l) + \delta f[V](k,l),$$
$$|\delta f[V](k,l)| \le b_2(d,s)(\|V\|_{\infty,s})^2 E^{-1/2}, \tag{3.8}$$

for $k, l \in \mathbb{R}^d$, $|k| = |l| \ge \rho_1(d, s, \|V\|_{\infty,s})$.

In connection with (3.4), (3.6), (3.8), see [21].

3.2 Estimates for direct scattering

We consider scattering potentials V_j of the form

$$V_j = v_j + w, \quad j = 1, 2, \tag{3.9}$$

where v_1, v_2, w satisfy the assumptions of Section 2. Note that the following properties hold:

$$\|V_j\|_\infty = \|v_j + w\|_\infty \le N_1, \quad \|V_2 - V_1\|_\infty = \|v_2 - v_1\|_\infty,$$
$$supp\, V_j \subseteq (D \cup \Omega), \quad supp(V_1 - V_2) \subseteq D, \tag{3.10}$$

for $j = 1, 2$; see (2.1)-(2.6). Note also that:

$$|V_2 - V_1| = |v_2 - v_1| \text{ are bounded on } D,$$
$$V_2 = V_1 = w \qquad \text{on } \mathbb{R}^d \setminus D. \tag{3.11}$$

We also consider

$$f_j := f[V_j] = f[v_j + w], \quad j = 1, 2. \tag{3.12}$$

In view of (2.1), (2.3), (2.6), (3.8), (3.9), we have that

$$f_j(k,l) = f[V_j](k,l) = \widehat{V}_j(k-l) + \delta f_j(k,l),$$
$$|\delta f_j| \le a_1(D \cup \Omega) N_1^2 E^{-1/2}, \quad j = 1, 2, \tag{3.13}$$

for $(k,l) \in \mathcal{M}_E$, $E \ge (\rho_1(d, s, \lambda_s(D \cup \Omega)N_1))^2$, where ρ_1 is defined in (3.5), $a_1(D \cup \Omega) = b_2(d,s)\lambda_s^2(D \cup \Omega)$, $s > d$, and

$$\lambda_s(\mathcal{U}) := (1 + \max_{x \in \mathcal{U}} |x|)^s. \tag{3.14}$$

We also have the following Lemma (see [20]):

Lemma 3.1. *Let v_j, V_j, and $f_j = f[V_j]$, $j = 1, 2$, be as in (2.1), (3.9), (3.12). Then the following estimate holds:*

$$f_2(k,l) - f_1(k,l) = \widehat{v}_2(k-l) - \widehat{v}_1(k-l) + \Delta(k,l),$$
$$|\Delta(k,l)| \le a_2(D \cup \Omega) N_1 \|v_2 - v_1\|_\infty E^{-1/2}, \tag{3.15}$$

for $k, l \in \mathbb{R}^d$, $\sqrt{E} = |k| = |l| \ge \rho_1(d, s, \lambda_s(D \cup \Omega)N_1)$ and some positive $a_2(D \cup \Omega)$. Here N_1, D, Ω are as in (3.10), (3.11).

Let $\mu(\mathcal{U})$ be Lebesgue measure of a domain $\mathcal{U} \subset \mathbb{R}^d$.

We also have the following Lemma, which will be used in Section 4.

Lemma 3.2. *Let $V_j = v_j + w$, $j = 1, 2$, be as in Lemma 3.1. Then*

$$\begin{aligned} &\left| |f[v_2 + w](k,l)|^2 - |f[v_1 + w](k,l)|^2 + |(\widehat{v}_1 + \widehat{w})(k-l)|^2 - |(\widehat{v}_2 + \widehat{w})(k-l)|^2 \right| \leq \\ &\leq 2\left((2\pi)^{-d}(a_1\mu(D) + a_2\mu(D \cup \Omega)) + a_1 a_2 N_1 E^{-1/2}\right) N_1^2 E^{-1/2} \|v_2 - v_1\|_\infty, \end{aligned} \tag{3.16}$$

$$(k,l) \in \mathcal{M}_E, \quad E^{1/2} \geq \rho_1(d, s, \lambda_s(D \cup \Omega) N_1), \tag{3.17}$$

and

$$\left| |\widehat{v}_2 + \widehat{w}|^2 - |\widehat{v}_1 + \widehat{w}|^2 \right|(p) \leq 2(2\pi)^{-2d} \mu(D \cup \Omega)\mu(D) N_1 \|v_2 - v_1\|_\infty, \quad \forall p \in \mathbb{R}^d, \tag{3.18}$$

$$\left| |\widehat{v}_2 + \widehat{w}|^2 - |\widehat{v}_1 + \widehat{w}|^2 \right|(p) \leq 2(2\pi)^{-d} \mu(D \cup \Omega) N_1 |\widehat{v}_2 - \widehat{v}_1|(p), \quad \forall p \in \mathbb{R}^d, \tag{3.19}$$

$$\left| |\widehat{v}_2 + \widehat{w}|^2 - |\widehat{v}_2|^2 - |\widehat{v}_1 + \widehat{w}|^2 + |\widehat{v}_1|^2 \right|(p) \leq 2(2\pi)^{-2d} \mu(D)\mu(\Omega) N_1 \|v_2 - v_1\|_\infty, \quad \forall p \in \mathbb{R}^d, \tag{3.20}$$

$$\left| |\widehat{v}_2 + \widehat{w}|^2 - |\widehat{v}_2|^2 - |\widehat{v}_1 + \widehat{w}|^2 + |\widehat{v}_1|^2 \right|(p) \leq 2(2\pi)^{-d} \mu(\Omega) N_1 |\widehat{v}_2 - \widehat{v}_1|(p), \quad \forall p \in \mathbb{R}^d, \tag{3.21}$$

where a_1, a_2 are as in (3.13), (3.15), D, Ω, N_1 are as in (3.10), ρ_1 is as in (3.5), λ_s is as in (3.14), $s > d$.

This Lemma is a variation of Lemma 3.6 in [12].

Proof of Lemma 3.2. Note that, for z_1, $z_2 \in \mathbb{C}$,

$$|z_2|^2 - |z_1|^2 = \overline{z}_2(z_2 - z_1) + z_1(\overline{z_2 - z_1}). \tag{3.22}$$

Using (3.22) for f_j in place of z_j, and (3.13), (3.15), we obtain

$$\begin{aligned} &|f_2|^2 - |f_1|^2 = \overline{f}_2(f_2 - f_1) + f_1(\overline{f_2 - f_1}) = (\overline{\widehat{V}_2} + \overline{\delta f_2})(\widehat{V}_2 - \widehat{V}_1 + \Delta) + (\widehat{V}_1 + \delta f_1)(\overline{\widehat{V}_2 - \widehat{V}_1 + \Delta}) = \\ &= |\widehat{V}_2|^2 - |\widehat{V}_1|^2 + \delta f_1(\overline{\widehat{V}_2 - \widehat{V}_1}) + \overline{\delta f_2}(\widehat{V}_2 - \widehat{V}_1) + \delta f_1 \overline{\Delta} + \overline{\delta f_2}\Delta + \widehat{V}_1\overline{\Delta} + \overline{\widehat{V}_2}\Delta. \end{aligned} \tag{3.23}$$

From (3.23), using (3.10), (3.13), (3.15), (3.11), we conclude

$$\begin{aligned} &||f_2|^2 - |f_1|^2 - (|\widehat{V}_2|^2 - |\widehat{V}_1|^2)| \leq 2a_1 N_1^2 E^{-1/2} |\widehat{V}_2 - \widehat{V}_1| + (|\widehat{V}_1| + |\widehat{V}_2|) a_2 N_1 \|V_2 - V_1\|_\infty E^{-1/2} + \\ &+ 2a_1 N_1^2 E^{-1/2} a_2 N_1 \|V_2 - V_2\|_\infty E^{-1/2} \leq 2\left((2\pi)^{-d}(a_1\mu(D) + a_2\mu(D \cup \Omega)) + a_1 a_2 N_1 E^{-1/2}\right) N_1^2 E^{-1/2} \|V_2 - \end{aligned} \tag{3.24}$$

Formula (3.16) follows from (3.9), (3.24).

Using (2.1), (2.7), (3.11), (3.22), we obtain

$$\begin{aligned} &\left| |\widehat{v}_2 + \widehat{w}|^2 - |\widehat{v}_1 + \widehat{w}|^2 \right| = \left| (\overline{\widehat{v}_2 + \widehat{w}})(\widehat{v}_2 - \widehat{v}_1) + (\widehat{v}_1 + \widehat{w})(\overline{\widehat{v}_2 - \widehat{v}_1}) \right| \leq \\ &\leq 2(2\pi)^{-d} \mu(D \cup \Omega) N_1 |\widehat{v}_2 - \widehat{v}_1|(p) \leq 2(2\pi)^{-2d} \mu(D \cup \Omega) N_1 \mu(D) \|v_2 - v_1\|_\infty. \end{aligned} \tag{3.25}$$

Analogously to (3.25), we obtain

$$\begin{aligned} &\left| |\widehat{v}_2 + \widehat{w}|^2 - |\widehat{v}_2|^2 - |\widehat{v}_1 + \widehat{w}|^2 + |\widehat{v}_1|^2 \right| \leq \left| \overline{(\widehat{v}_2 + \widehat{w})}\widehat{w} + \widehat{v}_2\overline{\widehat{w}} - \overline{(\widehat{v}_1 + \widehat{w})}\widehat{w} - \widehat{v}_1\overline{\widehat{w}} \right| \leq \\ &\leq \left| \overline{(\widehat{v}_2 - \widehat{v}_1)}\widehat{w} + (\widehat{v}_2 - \widehat{v}_1)\overline{\widehat{w}} \right| \leq 2(2\pi)^{-d} \mu(\Omega) N_1 |\widehat{v}_2 - \widehat{v}_1| \leq 2(2\pi)^{-2d} \mu(D)\mu(\Omega) N_1 \|v_2 - v_1\|_\infty. \end{aligned} \tag{3.26}$$

Thus, (3.18)–(3.21) are also proved.

3.3 Phase retrieval formulas

In this section we give phase retrieval formulas of [24].

Let $v = v_1$ and w be as in (2.1). Then

$$\widehat{v}(p) = (\widehat{w}(p))^{-1}\mathcal{F}\left(\chi_{D-\Omega}\cdot\left(\mathcal{F}^{-1}(|\mathcal{F}(v+w)|^2 - |\mathcal{F}(v)|^2) - W\right)\right), \quad p\in\mathbb{R}^d, \tag{3.27}$$

and if $\operatorname{dist}(D,\Omega) > \operatorname{diam} D$, then

$$\widehat{v}(p) = (\widehat{w}(p))^{-1}\mathcal{F}\left(\chi_{D-\Omega}\cdot\left(\mathcal{F}^{-1}(|\mathcal{F}(v+w)|^2) - W\right)\right), \quad p\in\mathbb{R}^d, \tag{3.28}$$

where

$$W(x) := (2\pi)^{-d}\int_{\mathbb{R}^d} w(x+y)\overline{w(y)}dy. \tag{3.29}$$

Formulas (3.27), (3.28) were given in Section 3 of [24].

In formulas (3.27), (3.28), $D-\Omega$ is defined by

$$D-\Omega = \{x-y,\, x\in D,\, y\in\Omega\}\subset\mathbb{R}^d, \tag{3.30}$$

and $\chi_{D-\Omega}$ is a function such that

$$\begin{cases} \chi_{D-\Omega}(x) = 1, & x\in D-\Omega,\\ \chi_{D-\Omega}(x) = 0, & \operatorname{dist}(x, D-\Omega) > \varepsilon,\\ \chi_{D-\Omega}(x)\in[0,1], & 0 < \operatorname{dist}(x, D-\Omega) < \varepsilon,\\ \chi_{D-\Omega}(x)\in C^\infty(\mathbb{R}^d), \end{cases} \tag{3.31}$$

for some

$$\varepsilon \in \begin{cases} (0, \operatorname{dist}(D-\Omega, B_{\operatorname{diam} D})), & \text{for Theorem 2.1},\\ (0, \operatorname{dist}(D-\Omega, \Omega-D)), & \text{for Theorem 2.2}. \end{cases} \tag{3.32}$$

In particular, we have that

$$|\widehat{\chi}_{D-\Omega}(p)| \le \frac{C(\sigma)}{(1+|p|)^\sigma}, \quad \forall p\in\mathbb{R}^d, \tag{3.33}$$

for any $\sigma\ge 0$, and some $C(\sigma) = C(\chi_{D-\Omega},\sigma) > 0$; see formula (82) of [24].

4 Proof of Theorems 2.1 and 2.2

4.1 Proof of Theorem 2.1

We start with the following inequalities:

$$|v_1 - v_2|(x) \le \left|\int_{\mathbb{R}^d} e^{-ip\cdot x}(\widehat{v}_1(p) - \widehat{v}_2(p))dp\right| \le I_1(\kappa) + I_2(\kappa), \tag{4.1}$$

$$I_1(\kappa) := \int_{|p|\ge\kappa} |\widehat{v}_1(p) - \widehat{v}_2(p)|dp, \quad I_2(\kappa) := \int_{|p|\le\kappa} |\widehat{v}_1(p) - \widehat{v}_2(p)|dp, \tag{4.2}$$

where $x\in D$, $\kappa\in(0,\tau\sqrt{E})$, $\tau\in(0,1)$. Here and below τ is the parameter of Theorem 2.1.

Estimating I_1 is as in [20]. Due to (2.2), (2.3), we have that

$$|\widehat{v}_1(p) - \widehat{v}_2(p)| \le a_3(m,d)N_2(1+|p|)^{-m}, \tag{4.3}$$

and, therefore,

$$I_1(\kappa) \le \frac{c(d)a_3(m,d)N_2}{m-d}\frac{1}{\kappa^{m-d}}, \tag{4.4}$$

where $c(d) = |\mathbb{S}^d|$.

Estimating I_2 is as follows. Due to (3.28), we have that

$$\begin{aligned} &|\widehat{v}_1(p) - \widehat{v}_2(p)| = |(\widehat{w}(p))^{-1}\mathcal{F}\left(\chi_{D-\Omega}(x)\cdot\mathcal{F}^{-1}(|\mathcal{F}(v_1+w)|^2 - |\mathcal{F}(v_2+w)|^2)\right)| \le \\ &\le |(\widehat{w}(p))^{-1}|\left(|\mathcal{F}\chi_{D-\Omega}| * ||\mathcal{F}(v_1+w)|^2 - |\mathcal{F}(v_2+w)|^2|\right), \end{aligned} \tag{4.5}$$

where $*$ denotes the convolution

$$\nu_1 * \nu_2(x) := \int_{\mathbb{R}^d} \nu_1(x-y)\nu_2(y)dy, \tag{4.6}$$

for test-functions ν_1, ν_2. In (4.5) we also used the following property of the Fourier transform:

$$\mathcal{F}(\varphi_1\varphi_2) = (\mathcal{F}\varphi_1) * (\mathcal{F}\varphi_2), \tag{4.7}$$

for test-functions φ_1, φ_2.

Using formulas (2.6), (3.33), (4.5), we obtain that:

$$I_2(\kappa) \le \int_{|p|\le\kappa} c_1^{-1}(1+|p|)^\beta\left(|\mathcal{F}\chi_{D-\Omega}| * ||\mathcal{F}(v_1+w)|^2 - |\mathcal{F}(v_2+w)|^2|\right)dp \le c_1^{-1}C(\sigma)(I_3(\kappa,\delta) + I_4(\kappa,\delta)); \tag{4.8}$$

$$I_3(\kappa,\delta) = \int_{|p|\le\kappa}(1+|p|)^\beta dp \int_{|p'|\le\delta\sqrt{E}+\kappa}\frac{g(p')}{(1+|p-p'|)^\sigma}dp', \tag{4.9}$$

$$I_4(\kappa,\delta) = \int_{|p|\le\kappa}(1+|p|)^\beta dp \int_{|p'|\ge\delta\sqrt{E}+\kappa}\frac{g(p')}{(1+|p-p'|)^\sigma}dp', \tag{4.10}$$

where

$$g(p') := ||\mathcal{F}(v_1+w)(p')|^2 - |\mathcal{F}(v_2+w)(p')|^2|, \tag{4.11}$$

and $\delta\sqrt{E} \in (\kappa, 2\tau\sqrt{E} - \kappa)$.

Applying formula (3.16) for $|p'| \le B_{\delta\sqrt{E}+\kappa}$ and formula (3.18) for $|p'| \ge B_{\delta\sqrt{E}+\kappa}$, we obtain that

$$g(p') \le \begin{cases} G_1, & \text{for } |p'| \le \delta E^{1/2} + \kappa, \\ G_2, & \text{for } |p'| \ge \delta E^{1/2} + \kappa, \end{cases} \tag{4.12}$$

where

$$\begin{aligned} G_1 &:= \||f[v_1+w]|^2 - |f[v_2+w]|^2\|_C + \\ &+ 2\left((2\pi)^{-d}(a_1\mu(D) + a_2\mu(D\cup\Omega)) + a_1a_2N_1E^{-1/2}\right)N_1^2E^{-1/2}\|v_1-v_2\|_\infty, \end{aligned} \tag{4.13}$$

$$G_2 := 2(2\pi)^{-2d}\mu(D)\mu(D\cup\Omega)N_1\|v_1-v_2\|_\infty. \tag{4.14}$$

Here and further $\|\cdot\|_C$ denotes the uniform norm for functions on $C(\Gamma_E^{(\delta+\kappa E^{-1/2})/2})$, and $\|\cdot\|_\infty$ is defined by (2.5).

Estimating I_3 *and* I_4. To estimate I_3 defined by (4.9), we use that

$$I_3 \le G_1(A_1 + A_2), \tag{4.15}$$

where

$$A_1 := \int_{|p|\le\kappa} (1+|p|)^\beta dp \int_{|p-p'|\le\kappa} \frac{dp'}{(1+|p-p'|)^\sigma}, \tag{4.16}$$

$$A_2 := \int_{|p|\le\kappa} (1+|p|)^\beta dp \int_{|p-p'|\ge\kappa,\, |p'|\le\delta E^{1/2}+\kappa} \frac{dp'}{(1+|p-p'|)^\sigma}. \tag{4.17}$$

Note that in (4.16) the condition $|p'| \le \delta E^{1/2} + \kappa$ is fulfilled automatically, due to the choice of κ and δ.

We have that

$$\int_{|p-p'|\le\kappa} \frac{dp'}{(1+|p-p'|)^\sigma} \le \int_{0<r\le\infty} \frac{c(d) r^{d-1} dr}{(1+r)^\sigma} = c(d) B(d, \sigma-d), \tag{4.18}$$

where $c(d) = |\mathbb{S}^d|$, B is the beta-function.

Therefore,

$$A_1 \le \int_{0<r_1\le\kappa} c(d) r_1^{d-1} (1+r_1)^\beta dr_1 \int_{0<r\le\infty} \frac{c(d) r^{d-1} dr}{(1+r)^\sigma} \le \frac{c^2(d) B(d, \sigma-d)}{\beta+d} (1+\kappa)^{\beta+d}. \tag{4.19}$$

In addition, for arbitrary $\alpha > 0$, such that $\sigma - d - \alpha \ge 1$, we have that,

$$\begin{aligned}
A_2 &\le \int_{|p|\le\kappa} (1+|p|)^\beta dp \int_{|p-p'|\ge\kappa} \frac{dp'}{(1+|p-p'|)^\sigma} \le \\
&\le \int_{|p|\le\kappa} (1+|p|)^\beta dp \int_{|p-p'|\ge\kappa} \frac{dp'}{(1+\kappa)^{\sigma-d-\alpha}(1+|p-p'|)^{d+\alpha}} \le \\
&\le \frac{1}{(1+\kappa)^{\sigma-d-\alpha}} \int_{|p|\le\kappa} (1+|p|)^\beta dp \int_{\mathbb{R}^d} \frac{dp'}{(1+|p-p'|)^{d+\alpha}} \le \\
&\le \frac{1}{(1+\kappa)^{\sigma-d-\alpha}} \int_{|p|\le\kappa} (1+|p|)^\beta dp \int_{r\in(0,\infty)} \frac{c(d) r^{d-1} dr}{(1+r)^{d+\alpha}} \le \\
&\le \frac{1}{(1+\kappa)^{\sigma-d-\alpha}} \int_{0<r\le\kappa} c(d) r^{d-1} (1+r)^\beta dr\, c(d) B(d,\alpha) \le \frac{c^2(d) B(d,\alpha)}{\beta+d} \frac{(1+\kappa)^{\beta+d}}{(1+\kappa)^{\sigma-d-\alpha}}.
\end{aligned} \tag{4.20}$$

Therefore, we estimate $A_1 + A_2$ of (4.15) as

$$A_1 + A_2 \le \frac{c^2(d)(1+\kappa)^{\beta+d}}{\beta+d} \left(B(d, \sigma-d) + \frac{B(d,\alpha)}{(1+\kappa)^{\sigma-d-\alpha}} \right). \tag{4.21}$$

In order to estimate I_4 defined by (4.10), we use (4.14) and obtain

$$\begin{aligned}
&I_4 \le G_2 \int_{|p|\le\kappa} (1+|p|)^\beta dp \int_{|p'|\ge\delta E^{1/2}+\kappa} \frac{dp'}{(1+|p-p'|)^\sigma} \le G_2 \int_{|p|\le\kappa} (1+|p|)^\beta dp \int_{r\in(0,\infty)} \frac{c(d) r^{d-1} dr}{(1+r)^\sigma} \le \\
&\le G_2 \int_{|p|\le\kappa} (1+|p|)^\beta dp \frac{c(d) B(d,\alpha)}{(1+\delta E^{1/2})^{\sigma-d-\alpha}} \le G_2 \frac{c^2(d) B(d,\alpha)}{\beta+d} \frac{(1+\kappa)^{\beta+d}}{(1+\delta E^{1/2})^{\sigma-d-\alpha}}.
\end{aligned} \tag{4.22}$$

Final part of the proof. Let

$$\kappa = E^\gamma, \quad \gamma = \left(\frac{1}{2} - \varepsilon\right) \frac{1}{\beta+d}, \quad \sigma = \left(\frac{1}{2} - \varepsilon\right)^{-1} (\beta+d)(d+1), \quad \alpha = d, \quad s = s(d) = d + 1/2, \quad \delta = \tau. \tag{4.23}$$

Then, for $E \ge \tau^{-\frac{1}{1/2-\gamma}}$, we have that $\kappa \in (0, \tau\sqrt{E})$ and $\delta\sqrt{E} \in (\kappa, 2\tau\sqrt{E} - \kappa)$.

Using formulas (4.1), (4.4), (4.8)–(4.10), (4.13), (4.14), (4.21), (4.22), and (4.23), we obtain that

$$\|v_1 - v_2\|_\infty \le K_1 E^{-\left(\frac12-\varepsilon\right)\frac{m-d}{\beta+d}} + \\ + K_2\left(K_3 E^{\frac12-\varepsilon}\left(\||f[v_1+w]|^2 - |f[v_2+w]|^2\|_C + K_4 E^{-1/2}\|v_1-v_2\|_\infty\right) + \frac{K_5 E^{\frac12-\varepsilon}\|v_1-v_2\|_\infty}{(1+\tau E^{1/2})^{\sigma-d-\alpha}}\right), \tag{4.24}$$

$$K_1 := K_1(d,m,N_2) = \frac{c(d)a_3(m,d)N_2}{m-d}, \quad K_2 := K_2(w,\sigma) = c_1^{-1}C(\sigma), \tag{4.25}$$

$$K_3 := K_3(d,\beta) \le 2\frac{c^2(d)}{\beta+d}\left(B(d,\sigma-d)+B(d,d)\right), \tag{4.26}$$

$$K_4 := K_4(D,\Omega,d,N_1) \le \\ \le 2\left((2\pi)^{-d}(a_1(d,D\cup\Omega)\mu(D)+a_2(D\cup\Omega)\mu(D\cup\Omega)) + \frac{a_1(d,D\cup\Omega)a_2(D\cup\Omega)}{2a_0(d,s(d)\lambda_{s(d)}(D\cup\Omega))}\right)N_1^2, \tag{4.27}$$

$$K_5 := K_5(D,\Omega,N_1,d,\beta) = 2(2\pi)^{-2d}\mu(D)\mu(D\cup\Omega)N_1\frac{c^2(d)B(d,d)}{\beta+d}. \tag{4.28}$$

Let

$$E_1 = \max(E_{root},\, \tau^{-\frac{1}{1/2-\gamma}},\, \rho_1^2(d,s,\lambda_s(D\cup\Omega)N_1)), \tag{4.29}$$

where E_{root} is the maximal root of equation for E

$$K_2K_3K_4E^{-\varepsilon} + K_2K_5E^{\frac12-\varepsilon}(1+\tau E^{1/2})^{-\sigma+d+\alpha} = 1/2, \tag{4.30}$$

ρ_1 is defined in (3.5), λ_s is defined in (3.14). Note that E_{root} exists, since

$$\frac12 - \varepsilon - (\sigma-d-\alpha)/2 < 0. \tag{4.31}$$

Therefore, for $E \ge E_1$,

$$K_2K_3K_4E^{-\varepsilon} + K_2K_5E^{\frac12-\varepsilon}(1+\tau E^{1/2})^{-\sigma+d+\alpha} \le 1/2. \tag{4.32}$$

In view of (4.32), the coefficient with $\|v_2-v_1\|_\infty$ in the right-hand side of (4.24) is less than $1/2$. Therefore,

$$\|v_2 - v_1\|_\infty \le 2K_1E^{-\left(\frac12-\varepsilon\right)\frac{m-d}{\beta+d}} + 2K_2K_3E^{\frac12-\varepsilon}\||f_2|^2-|f_1|^2\|_C, \tag{4.33}$$

for $E \ge E_1$.

Note that $\tau\sqrt{E} \ge \kappa$, for $E \ge E_1$, see (4.23), (4.29). Therefore, $\Gamma_E^{(\tau+\kappa E^{-1/2})/2} \subseteq \Gamma_E^\tau$, and $\|\cdot\|_C = \|\cdot\|_{C(\Gamma_E^{(\tau+\kappa E^{-1/2})/2))}} \le \|\cdot\|_{C(\Gamma_E^\tau)}$. This completes the proof.

4.2 Proof of Theorem 2.2

Proof of Theorem 2.2 is similar to the Proof of Theorem 2.1 up to the following changes:

- For estimate of I_2 we use formula (3.27) in place of (3.28).
- Formulas (4.5) and (4.11) are replaced by

$$|\widehat{v}_1(p) - \widehat{v}_2(p)| \le \\ \le |(\widehat{w}(p))^{-1}|\left(|\mathcal{F}\chi_{D-\Omega}| * \left(|(|\mathcal{F}(v_1+w)|^2 - |\mathcal{F}(v_2+w)|^2) - (|\mathcal{F}v_1|^2 - |\mathcal{F}v_2|^2)|\right)\right), \tag{4.34}$$

$$g(p') := |(|\mathcal{F}(v_1+w)(p')|^2 - |\mathcal{F}(v_2+w)(p')|^2) - (|\mathcal{F}v_1(p')|^2 - |\mathcal{F}v_2(p')|^2)|. \tag{4.35}$$

- Taking into account (3.20), formulas (4.13), (4.14) are replaced by

$$\begin{aligned} &G_1 := \|(|f[v_1+w]|^2 - |f[v_2+w]|^2) - (|f[v_1]|^2 - |f[v_2]|^2)\|_C + \\ &+ 4\left((2\pi)^{-d}(a_1\mu(D) + a_2\mu(D\cup\Omega)) + a_1a_2N_1E^{-1/2}\right) N_1^2E^{-1/2}\|v_1-v_2\|_\infty, \end{aligned} \tag{4.36}$$

$$G_2 := 2(2\pi)^{-2d}\mu(D)\mu(\Omega)N_1\|v_1-v_2\|_\infty. \tag{4.37}$$

- In formula (4.24), the term $\||f[v_1+w]|^2 - |f[v_2+w]|^2\|_C$ should be replaced by $\|(|f[v_1+w]|^2 - |f[v_2+w]|^2) - (|f[v_1]|^2 - |f[v_2]|^2)\|_C$.

- In formula (4.27) constant K_4 should be replaced by $2K_4$.

- Due to (4.37), in formula (4.28) constant K_5 should be replaced by

$$K_5 = 2(2\pi)^{-2d}\mu(D)\mu(\Omega)N_1\frac{c^2(d)B(d,d)}{\beta+d}. \tag{4.38}$$

- We define

$$E_2 := \max(E_{root},\, \tau^{-\frac{1}{1/2-\gamma}},\, \rho_1^2(d,s,\lambda_s(D\cup\Omega)N_1)), \tag{4.39}$$

where E_{root} is the maximal root of equation for E

$$2K_2K_3K_4E^{-\varepsilon} + K_2K_5E^{\frac12-\varepsilon}(1+\delta E^{1/2})^{-\sigma+d+\alpha} = 1/2, \tag{4.40}$$

for K_2, K_3, K_4 defined by (4.25)-(4.27), and K_5 defined by (4.38).

- For $E \ge E_2$ we have the following formula in place of (4.32)

$$2K_2K_3K_4E^{-\varepsilon} + K_2K_5E^{\frac12-\varepsilon}(1+\tau E^{1/2})^{-\sigma+d+\alpha} \le 1/2, \tag{4.41}$$

for K_2, K_3, K_4 defined by (4.25)-(4.27), and K_5 defined by (4.38).

5 Proof of Propositions 2.6 and 2.7

5.1 Proof of Proposition 2.6

We repeat the proofs of Theorems 2.1, 2.2 up to the following changes:

- In formulas (4.13), (4.36), G_1 should be replaced by

$$G_1 := \||\mathcal{F}(v_1+w)|^2 - |\mathcal{F}(v_2+w)|^2\|_{C(B_{\tau\sqrt{E}+E^\gamma})}, \tag{5.1}$$

$$G_1 := \|(|\mathcal{F}(v_1+w)|^2 - |\mathcal{F}(v_2+w)|^2) - (|\mathcal{F}v_1|^2 - |\mathcal{F}v_2|^2)\|_{C(B_{\tau\sqrt{E}+E^\gamma})}, \tag{5.2}$$

respectively.

- Consequently, formula (4.27) should be replaced by $K_4 = 0$.

- We define E_3, E_4 as

$$\begin{aligned} E_3 &= \max(E_{root,3}, \tau^{-\frac{1}{1/2-\gamma}}, 1), \\ E_4 &= \max(E_{root,4}, \tau^{-\frac{1}{1/2-\gamma}}, 1), \end{aligned} \tag{5.3}$$

where $E_{root,3}$, $E_{root,4}$, are the maximal roots of the equations for E :

$$\begin{aligned} K_2K_6E^{\frac12-\varepsilon}(1+\tau E^{1/2})^{-\sigma+d+\alpha} &= 1/2, \\ K_2K_7E^{\frac12-\varepsilon}(1+\tau E^{1/2})^{-\sigma+d+\alpha} &= 1/2, \end{aligned} \tag{5.4}$$

respectively; if there are no roots, we take $E_{root,j} = 0$, for $j = 3$ or 4. Here, K_2 is as in (4.25), $K_6 = K_5$ defined in (4.28), and $K_7 = K_5$ defined in (4.38).

5.2 Proof of Proposition 2.7

We repeat the proof of Section 4.1, till to formula (4.21), where we use change (5.1). We estimate I_4 of (4.10) via formula (3.19) and formula (4.3) as follows:

$$\begin{aligned} I_4(\kappa,\delta) &\le \int_{|p|\le\kappa}(1+|p|)^{\beta}dp\int_{|p'|\ge\delta\sqrt{E}+\kappa}\frac{2(2\pi)^{-d}\mu(D\cup\Omega)N_1|\widehat{v}_2(p)-\widehat{v}_1(p)|}{(1+|p-p'|)^{\sigma}}dp' \le \\ &\le 2(2\pi)^{-d}\mu(D\cup\Omega)N_1\int_{|p|\le\kappa}(1+|p|)^{\beta}dp\int_{|p'|\ge\delta\sqrt{E}+\kappa}\frac{a_3(m,d)N_2}{(1+|p-p'|)^{\sigma}(1+|p'|)^{m}}dp' \le \\ &\le \frac{2(2\pi)^{-d}\mu(D\cup\Omega)N_1}{(1+\tau\sqrt{E})^{\sigma}}\int_{|p|\le\kappa}(1+|p|)^{\beta}dp\int_{|p'|\ge\delta\sqrt{E}+\kappa}\frac{a_3(m,d)N_2}{(1+|p'|)^{m}}dp' \le \\ &\le \frac{2(2\pi)^{-d}\mu(D\cup\Omega)a_3(m,d)N_1N_2c^2(d)}{(1+\tau\sqrt{E})^{\sigma-\beta-d}(\beta+d)}\frac{1}{(1+\frac{3}{2}\tau\sqrt{E})^{m-d}(m-d)}. \end{aligned} \tag{5.5}$$

We fix our parameters as follows:

$$\kappa=(\tau/2)E^{1/2},\quad \sigma=\beta+d+1,\quad \alpha=d,\quad \delta=\tau. \tag{5.6}$$

Using formulas (4.1), (4.4), (4.8)–(4.10), (4.21), (5.1), (5.5) and (5.6), we obtain that

$$\|v_1-v_2\|_{\infty}\le C_1\tau^{\beta+d}E^{\frac{\beta+d}{2}}\||\mathcal{F}(v_1+w)|^2-\mathcal{F}(v_2+w)|^2\|_{C(B_{2\tau\sqrt{E}})}+C_2\tau^{-(m-d)}E^{-\frac{m-d}{2}}, \tag{5.7}$$

$$C_1:=C_1(d,\beta,c_1)\le c_1^{-1}C(\beta+d+1)\frac{c^2(d)}{\beta+d}\left(B(d,\beta+1)+\frac{B(d,d)}{2^{\beta-d+1}}\right), \tag{5.8}$$

$$C_2:=C_2(d,m,N_1,N_2,D,\Omega,\beta,c_1)\le\frac{2^{m-d}c(d)a_3(m,d)N_2}{m-d}\left(1+\frac{2(2\pi)^{-d}c_1^{-1}c(d)C(\beta+d+1)\mu(D\cup\Omega)N_1}{3^{m-d+1}(\beta+d)}\right) \tag{5.9}$$

for

$$E\ge E_5:=E_5(\tau)=4/\tau^2. \tag{5.10}$$

Formula (2.18) is proved.

Note that, increasing E_5, we can down constant C_2.

In order to prove formula (2.19), it is sufficient to replace (3.19) by (3.21) in (5.5), and (5.1) by (5.2) in (5.7). In this case C_2 should be defined as

$$C_2:=C_2(d,m,N_1,N_2,\Omega,\beta,c_1)\le\frac{2^{m-d}c(d)a_3(m,d)N_2}{m-d}\left(1+\frac{2(2\pi)^{-d}c_1^{-1}c(d)C(\beta+d+1)\mu(\Omega)N_1}{3^{m-d+1}(\beta+d)}\right). \tag{5.11}$$

Bibliography

[1] A.D. Agaltsov, T. Hohage, R.G. Novikov, *An iterative approach to monochromatic phaseless inverse scattering*, Inverse Problems 35, 24001 (24 pp.) (2019)

[2] A. D. Agaltsov, R.G. Novikov, *Error estimates for phaseless inverse scattering in the Born approximation at high energies*, J. Geom. Anal. (2017), https://doi.org/10.1007/s12220-017-9872-6, e-print: https://hal.archives-ouvertes.fr/hal-01303885v2

[3] T. Aktosun, P. E. Sacks, *Inverse problem on the line without phase information*, Inverse Problems 14, 211–224 (1998)

[4] J. A. Barceló, C. Castro, and J. M. Reyes, *Numerical approximation of the potential in the two-dimesional inverse scattering problem,* Inverse Problems, 32(1), 015006 (19pp) (2016)

[5] A.H. Barnett, Ch.L. Epstein, L.F. Greengard, J.F. Magland, *Geometry of the phase retrieval problem—graveyard of algorithms*, Cambridge University Press, Cambridge (2022)

[6] M. Born, *Quantenmechanik der Stossvorgange*, Zeitschrift fur Physik 38 (11-12), 803-827 (1926)

[7] F.A. Berezin, M.A. Shubin, *The Schrödinger Equation*, Mathematics and Its Applications, Vol. 66, Kluwer Academic, Dordrecht, (1991)

[8] V.A. Dedok, A.L. Karchevsky, V.G. Romanov, *A Numerical Method of Determining Permittivity from the Modulus of the Electric Intensity Vector of an Electromagnetic Field*, J. Appl. Ind. Math. 13, 436–446 (2019) https://doi.org/10.1134/S1990478919030050

[9] T. Hohage, R.G. Novikov, *Inverse wave propagation problems without phase information*, Inverse Problems 35, 070301 (4 pp.)(2019)

[10] M. I. Isaev, *Exponential instability in the inverse scattering problem on the energy interval*, Functional Analysis and Its Applications, vol. 47, 187–194 (2013)

[11] M. I. Isaev, R. G. Novikov, *Hölder-logarithmic stability in Fourier synthesis*, Inverse Problems, 36 (12), 125003 (2020)

[12] T. Hohage, R. G. Novikov, V. N. Sivkin, *Reconstruction from differential scattering cross section with background information*, hal-03806616 (2022)

[13] M.V. Klibanov, *Phaseless inverse scattering problems in three dimensions*, SIAM J.Appl. Math. 74(2), 392-410 (2014)

[14] M.V. Klibanov, N.A. Koshev, D.-L. Nguyen, L.H. Nguyen, A. Brettin, V.N. Astratov, *A numerical method to solve a phaseless coefficient inverse problem from a single measurement of experimental data*, SIAM J. Imaging Sci. 11(4), 2339-2367 (2018)

[15] M.V. Klibanov, P.E. Sacks, A.V. Tikhonravov, *The phase retrieval problem*, Inverse Problems 11, 1–28 (1995)

[16] M.V. Klibanov, V. G. Romanov, *Two reconstruction procedures for a 3D phaseless inverse scattering problem for the generalized Helmholtz equation*, Inverse Problems, 32(1), 015005 (2015)

[17] M.V. Klibanov, V.G. Romanov, *Reconstruction procedures for two inverse scattering problems without the phase information*, SIAM J. Appl. Math. 76(1), 178-196 (2016)

[18] B. Leshem, R. Xu, Y. Dallal, J. Miao, B. Nadler, D. Oron, N. Dudovich, O. Raz, *Direct single-shot phase retrieval from the diffraction pattern of separated objects,* Nature Communications 7(1), 1-6 (2016)

[19] N. Mandache, *Exponential instability in an inverse problem for the Schrödinger equation*, Inverse Problems, 17:5, 1435–1444 (2001)

[20] R. G. Novikov, *Approximate Lipschitz stability for non-overdetermined inverse scattering at fixed energy*, Journal of Inverse and Ill-posed Problems. 21(6), 813–823 (2013)

[21] R. G. Novikov, *An iterative approach to non-overdetermined inverse scattering at fixed energy*, Sbornik: Mathematics 206(1), 120-134 (2015)

[22] R. G. Novikov, *Inverse scattering without phase information*, Seminaire Laurent Schwartz - EDP et applications (2014-2015), Exp. No16, 13p

[23] R. G. Novikov, *Explicit formulas and global uniqueness for phaseless inverse scattering in multidimensions*, J. Geom. Anal. 26(1), 346-359 (2016), e-print: https://hal.archives-ouvertes.fr/hal-01095750v1

[24] R. G. Novikov, V. N. Sivkin, *Phaseless inverse scattering with background information*, Inverse Problems, 37(5), 055011 (2021)

[25] R. G. Novikov, V. N. Sivkin, *Fixed-distance multipoint formulas for the scattering amplitude from phaseless measurements*, Inverse Problems, 38(2), 025012 (2022)

[26] V. G. Romanov, *The problem of recovering the permittivity coefficient from the modulus of the scattered electromagnetic field*, Siberian Math. J., 58:4, 711–717 (2017)

[27] V. G. Romanov, *Phaseless inverse problems for Schrödinger, Helmholtz, and Maxwell equations*, Computational Mathematics and Mathematical Physics, 60 (6), 1045-1062 (2020)

[28] Y. Shechtman et al., *Phase retrieval with application to optical imaging: a contemporary overview* IEEE signal processing magazine, 32(3), 87-109 (2015)

[29] A.S. Shurup, *Numerical comparison of iterative and functional-analytic algorithms for inverse acoustic scattering,* Eurasian Journal of Mathematical and Computer Applications **10**(1), 79-99 (2022)

[30] H. Wendland, *Error estimates for interpolation by compactly supported radial basis functions of minimal degree,* J. Approx. Theory 93, 258–72 (1998)

Article IV

Error estimates for phase recovering from phaseless scattering data

R.G. Novikov, V.N. Sivkin

We study the simplest explicit formulas for approximate finding the complex scattering amplitude from modulus of the scattering wave function. We obtain detailed error estimates for these formulas in dimensions $d = 3$ and $d = 2$.

Keywords: Schrödinger equation, monochromatic scattering data, phase recovering, phaseless inverse scattering.

1 Introduction

We consider the Schrödinger equation

$$-\Delta\psi + v(x)\psi = E\psi, \quad x \in R^d, \ d \geq 1, \ E > 0, \tag{1.1}$$

$$v \in L_\infty(R^d), \ supp\ v \subset D, \tag{1.2}$$
$$D \text{ is an open bounded domain in } R^d.$$

Here Δ is the standart Laplacian in x, v is a scalar potential.

For equation (1.1) we consider the classical scattering solutions ψ^+ specified by the following asymptotics as $|x| \to \infty$:

$$\psi^+(x,k) = e^{ikx} + c(d,|k|)\frac{e^{i|k||x|}}{|x|^{(d-1)/2}} f(k, |k|\frac{x}{|x|}) + O\left(\frac{1}{|x|^{(d+1)/2}}\right), \tag{1.3}$$

$$c(d,|k|) = -\pi i(-2\pi i)^{(d-1)/2}|k|^{(d-3)/2}, \text{ for } \sqrt{-2\pi i} = \sqrt{2\pi}e^{-i\pi/4}, x, k \in R^d, \ k^2 = E,$$

where a priori unknown function $f = f(k,l), \ k,l \in R^d, k^2 = l^2 = E$, arising in (1.3) is the classical scattering amplitude for (1.1).

In order to study ψ^+ and f one can use the Lippmann-Schwinger integral equation (1.4) and formula (1.6):

$$\psi^+(x,k) = e^{ikx} + \int_{R^d} G^+(x-y,k)v(y)\psi^+(y,k)dy, \tag{1.4}$$

$$G^+(x,k) := -\frac{1}{(2\pi)^d}\int_{R^d}\frac{e^{i\xi x}d\xi}{\xi^2 - k^2 - i0} = G_0^+(|x|,|k|), \tag{1.5}$$

$$f(k,l)=\frac{1}{(2\pi)^d}\int_{R^d} e^{-ilx}v(x)\psi^+(x,k)dx, \tag{1.6}$$

where $x,k,l\in R^d, k^2=l^2=E$, and G_0^+ also depends on d. Note that:

$$G^+(x,k)=-\frac{i}{4}H_0^1(|x||k|) \text{ for } d=2,\ G^+(x,k)=-\frac{e^{i|k||x|}}{4\pi|x|} \text{ for } d=3, \tag{1.7}$$

where H_0^1 is the Hankel function of the first type.

In the present work we also assume that

$$\text{equation (1.4) is uniquely solvable for } \psi^+(\cdot,k)\in L^\infty(R^d) \text{ for fixed } E>0, \tag{1.8}$$

where $k\in R^d, k^2=E$. For example, for real-valued v satisfying (1.2) it holds true.

We recall that ψ^+ describes scattering of the incident plane waves described by e^{ikx} on the scatterer described by v. In addition, the second term on the right-hand side of (1.3) describes the leading scattered spherical waves.

We also recall that in quantum mechanics the values of scatttering functions $\psi^+(x,k)$ and $f(k,l)$ have no direct physical sense, whereas the phaseless values $|\psi^+(x,k)|^2$ and $|f|^2$ have probabilistic interpretation (the Born's principle) and can be obtained in experiments; see [3], [6].

We consider the following problems:

Problem 1. Find v on R^d from $f=f(k,l)$ given for appropriate pairs (k,l).

Problem 2. Find $f(k,l)$ from $|\psi^+(x,k)|^2$ at appropriate points x such that $x\in R^d\setminus D$ and $x/|x|=l/|l|$.

Problem 3. Find v on R^d from $|\psi^+|^2$ appropriately given outside of D.

Problem 1 is the classical inverse scattering problem. This problem was studied in many works; see, for example, [4], [5], [13], [14] and references therein.

Problem 2 is a problem of phase recovering. Note that finding f considered in this problem and formula (1.3) also yield approximate finding ψ^+ for large $|x|$. In connection with known results on Problem 2, see [15]-[18].

Problem 3 is a problem of inverse scattering without phase information. In connection with known results on this problem, see [8], [15]-[18], [11].

Actually, in the present work we continue studies on Problem 2 in dimentions $d=3$ and $d=2$. Problem 2 for $d=1$ was solved in [16]. In addition, results on Problem 1 and Problem 2 admit direct applications to Problem 3.

Note that Problem 2 is one of possible problems of phase recovering and Problem 3 is one of possible problems of inverse scattering without phase information. In connection with results given on other inverse wave propagation problems without phase information, see [4], [7], [10], [15], [17], [12], [21], [2], [1], [9], [19] and references therein.

We recall that Problem 2 can be solved approximately by the following explicit formulas of [15], [17]:

$$\begin{pmatrix} Re\ c(d,|k|)f(k,l)\\ Im\ c(d,|k|)f(k,l)\end{pmatrix}=M\left(\begin{pmatrix}a(x_1,k)\\ a(x_2,k)\end{pmatrix}-\begin{pmatrix}\delta a(x_1,k)\\ \delta a(x_2,k)\end{pmatrix}\right), \tag{1.9}$$

where

$$a(x,k)=|x|^{(d-1)/2}(|\psi^+(x,k)|^2-1), \tag{1.10}$$

$$M = \frac{1}{2\sin(\varphi_2-\varphi_1)}\begin{pmatrix}\sin(\varphi_2) & -\sin(\varphi_1)\\ -\cos(\varphi_1) & \cos(\varphi_2)\end{pmatrix}, \tag{1.11}$$

$$x_1 = s\hat{l},\ x_2 = (s+\tau)\hat{l},\ \hat{l} = l/|l|, \tag{1.12}$$

$$\varphi_j = |k||x_j| - kx_j,\ j = 1,2, \tag{1.13}$$

$$\varphi_2 - \varphi_1 = \tau(|k| - k\hat{l}), \tag{1.14}$$

$$\delta a(x_1,k) = O(s^{-\sigma}),\ \delta a(x_2,k) = O(s^{-\sigma}) \ \text{ as } \ s\to+\infty, \tag{1.15}$$

uniformly in $\hat{k} = k/|k|,\ \hat{l} = l/|l|$ and τ at fixed $E > 0$,

$$\sigma = 1/2 \text{ for } d = 2,\ \sigma = 1 \text{ for } d \geq 3, \tag{1.16}$$

where $k, l \in R^d, k^2 = l^2 = E, s > 0, \tau > 0$, $\sin(\varphi_1 - \varphi_2) \neq 0, c(d,|k|)$ is the constant of (1.3) .

In order to control error in finding $f(k,l)$ from $|\psi^+(x,k)|^2$ at $x = x_1, x_2$ via formulas (1.9)-(1.15) it is necessary to estimate $\delta a(x,k) = O(s^{-\sigma})$ in detail. However, detailed estimates for $\delta a(x,k)$ were not yet given in the literature. For the first time such estimates are given in the present work, see Theorem 2.1 and Lemmas 2.1 and 2.2 of Section 2. These estimates are proved in Sections 3-5.

Finally, we recall that $2n$-point version of formulas (1.9)-(1.16) with error term estimated as $O(s^{-n})$, $s\to+\infty$, is given in [18]. Detailed estimates of this $O(s^{-n})$ generalizing the estimates (2.2)-(2.5) (see Section 2) of the present work will be given elsewhere.

2 Main results

Let

$$D \subset B_r = \{x \in R^d : |x| \leq r\} \tag{2.1}$$

for some fixed $r > 0$.

Theorem 2.1. ***(A)*** *Under assumptions (1.2),(1.8),(2.1) for $d = 3$, the following estimate holds, for $|x| \geq 3r$:*

$$|\delta a(x,k)| \leq \rho_3 \frac{\|\psi^+\|_\infty \|v\|_{L_1}}{2\pi|x|} + \left(1 + \frac{2\rho_3}{|x|} + \frac{\rho_3^2}{|x|^2}\right)\frac{\|\psi^+\|_\infty^2\|v\|_{L_1}^2}{16\pi^2|x|}, \tag{2.2}$$

$$\rho_3 := r(4.5 + 7.65|k|r + 3.91|k|^2r^2), \tag{2.3}$$

where $k, x \in R^3, k^2 = E > 0$.

(B) *Under assumptions (1.2),(1.8),(2.1) for $d = 2$, the following estimate holds:*

$$|\delta a(x,k)| \leq \left(1 + \frac{\rho_2\sqrt{2}}{|x|} + \frac{\rho_2^2}{2|x|^2}\right)\frac{\|\psi^+\|_\infty^2\|v\|_{L_1}^2}{8\pi|x|^{1/2}|k|} + \rho_2\frac{\|\psi^+\|_\infty\|v\|_{L_1}}{2\sqrt{\pi}|k|^{1/2}|x|}, \tag{2.4}$$

$$\rho_2 := r\left(\frac{0.33}{|k|r} + 2.51 + 5.36|k|r + 2.14|k|^2r^2\right), \tag{2.5}$$

where $k, x \in R^2, k^2 = E > 0$.

In Theorem 2.1 we use the notation $\|\psi^+\|_\infty := \|\psi^+(\cdot,k)\|_{L_\infty(D)}$.

Theorem 2.1 is proved in Sections 3, 4.

In addition, $\|\psi^+\|_\infty$ is estimated in Lemmas 2.2 and 2.3 given below.

Let

$$Q = C_0(d,s)\sup_{x\in D}|(1+|x|^2)^s v(x)||k|^{-1}, \tag{2.6}$$

where C_0 is the constant of the Agmon estimate (5.3) (see Section 5).

Lemma 2.2. ***(A)*** *Under assumptions (1.2), (2.1), for $Q < 1$ and $d = 3$, the following estimate holds:*

$$\|\psi^+(\cdot,k)\|_{L_\infty(R^3)} \leq 1 + \sqrt{\frac{5}{6}}\frac{\|v\|_{L_\infty(D)}(1+r^2)^{s/2}r^{1/2}}{(1-Q)}, \tag{2.7}$$

where $s = (d+\varepsilon)/2, \varepsilon > 0, |k| \geq 1$.

(B) *Under assumptions (1.2), (2.1), for $Q < 1$ and $d = 2$, the following estimate holds:*

$$\|\psi^+(\cdot,k)\|_{L_\infty(R^2)} \leq 1 + \frac{\sqrt{\pi}\|v\|_{L_\infty(D)}(1+r^2)^{s/2}r^{1/2}}{\sqrt{2\varepsilon|k|}(1-Q)}, \tag{2.8}$$

where $s = (d+\varepsilon)/2, \varepsilon > 0, |k| \geq 1$.

Lemma 2.3. ***(A)*** *Under assumptions (1.2), (2.1), for $\|v\|_{L_\infty(D)}r^2 \leq 2, d = 3$, the following estimate holds:*

$$\|\psi^+\|_{L_\infty(R^3)} \leq \frac{1}{1 - \|v\|_{L_\infty(D)}r^2/2}. \tag{2.9}$$

(B) *Under assumptions (1.2), (2.1), for $\sqrt{\frac{2\pi}{|k|}}\frac{\|v\|_{L_\infty(D)}r^{5/2}}{5} < 1, d = 2$, the following estimate holds:*

$$\|\psi^+\|_{L_\infty(R^2)} \leq \frac{1}{1 - \sqrt{\frac{2\pi}{|k|}}\frac{\|v\|_{L_\infty(D)}r^{3/2}}{3}}. \tag{2.10}$$

Lemmas 2.2 and 2.3 are proved in Section 5.

3 Proof of Theorem 2.1(A)

We have that (see [15]):

$$|\delta a(x,k)| = |x|^{-\frac{d-1}{2}}|c|^2|f|^2 + 2|x|^{\frac{d-1}{2}}Re(\delta\psi^+(x,k)\overline{\psi_1^+(x,k)}) + |x|^{\frac{d-1}{2}}|\delta\psi^+(x,k)|^2, \tag{3.1}$$

where $f = f(k, \frac{|k|x}{|x|})$,

$$\psi_1^+(x,k) := e^{ikx} + c(d,|k|)\frac{e^{i|k||x|}}{|x|^{(d-1)/2}}f(k,|k|\frac{x}{|x|}), \tag{3.2}$$

$$\delta\psi^+(x,k) := \psi^+(x,k) - \psi_1^+(x,k). \tag{3.3}$$

Note that

$$|f| = \frac{1}{(2\pi)^d}|\int_{R^d} e^{-ilx}v(x)\psi^+(x,k)dx| \leq \frac{1}{(2\pi)^d}\|\psi^+\|_\infty\|v\|_{L_1}. \tag{3.4}$$

Further in this section we always assume that $d = 3$.

The following estimate holds:

$$|\delta a(x,k)| \leq |x|^{-1}(2\pi^2)^2|f|^2 + 2|x||\delta\psi^+(x,k)||1 + \frac{2\pi^2|f|}{|x|}| + |x||\delta\psi^+(x,k)|^2. \tag{3.5}$$

In addition, $|\delta\psi^+(x,k)|$ is estimated in the following lemma:

Lemma 3.1. *Under the assumptions of Theorem 2.1(A), the following estimate holds, for* $|x| \geq 3r$:

$$|\delta\psi^+(x,k)| \leq \frac{\|\psi^+\|_\infty \|v\|_{L_1}}{4\pi|x|^2}\rho_3(r,k). \tag{3.6}$$

Using estimates (3.1), (3.4), (3.6) we have that:

$$|\delta a(x,k)| \leq |x|^{-1}(2\pi^2)^2\frac{1}{((2\pi)^3)^2}\|\psi^+\|_\infty^2\|v\|_{L_1}^2+$$

$$+2|x|\frac{1}{4\pi}\|\psi^+\|_\infty\|v\|_{L_1}\frac{\rho_3}{|x|^2}(1+\frac{2\pi^2\frac{1}{(2\pi)^3}\|\psi^+\|_\infty\|v\|_{L_1}}{|x|})+|x|(\frac{1}{4\pi}\|\psi^+\|_\infty\|v\|_{L_1}\frac{\rho_3}{|x|^2})^2 \leq$$

$$\leq \frac{\|\psi^+\|_\infty^2\|v\|_{L_1}^2}{16\pi^2|x|}+\|\psi^+\|_\infty\|v\|_{L_1}\frac{\rho_3}{2\pi|x|}(1+\frac{\|\psi^+\|_\infty\|v\|_{L_1}}{4\pi|x|})+$$

$$+\|\psi^+\|_\infty^2\|v\|_{L_1}^2\frac{\rho_3^2}{16\pi^2|x|^3}, |x| \geq 3r. \tag{3.7}$$

Estimate (2.2) of Theorem 2.1(A) follows from (3.7). Therefore, in order to prove Theorem 2.1(A) it remains to prove Lemma 3.1.

Proof of Lemma 3.1. Using the Lippmann-Schwinger integral equation (1.4) and formulas (1.6), (3.3) we obtain

$$\delta\psi^+(x,k) = -\int_{R^3}\frac{e^{i|k||x-y|}}{4\pi|x-y|}v(y)\psi^+(y,k)dy+$$

$$+2\pi^2\frac{e^{i|k||x|}}{|x|}\frac{1}{(2\pi)^3}\int_{R^3}e^{-i|k|\frac{xy}{|x|}}v(y)\psi^+(y,k)dy =$$

$$=\frac{1}{4\pi}\int_{R^3}\left(\frac{e^{i|k||x|-i|k|\frac{xy}{|x|}}}{|x|}-\frac{e^{i|k||x-y|}}{|x-y|}\right)v(y)\psi^+(y,k)dy. \tag{3.8}$$

From (3.8) we obtain :

$$|\delta\psi^+(x,k)| \leq \frac{1}{4\pi}\|\psi^+(\cdot,k)\|_\infty\int_{R^3}\left|\frac{e^{i|k||x|-i|k|\frac{xy}{|x|}}}{|x|}-\frac{e^{i|k||x-y|}}{|x-y|}\right||v(y)|dy. \tag{3.9}$$

Lemma 3.2. *Let* $x, y \in R^3, |y| \leq r, |x| \geq 3r$. *Then:*

$$\left|\frac{e^{i|k||x|-i|k|\frac{xy}{|x|}}}{|x|}-\frac{e^{i|k||x-y|}}{|x-y|}\right| \leq \frac{r}{|x|^2}(4.5+7.65|k|r+3.91|k|^2r^2). \tag{3.10}$$

Estimate (3.6) of Lemma 3.1 follows from estimates (3.9), (3.10). Thus, in order to prove Lemma 3.1, it remains to prove Lemma 3.2.

Proof of Lemma 3.2. To prove Lemma 3.2 we use in particular Lemma 3.3.

Lemma 3.3. *Let* $x, y \in R^3, |y| \leq r, |x| \geq 3r$. *Then the following estimates hold:*

$$|x-y| = |x|\left(1-\frac{xy}{|x|^2}+\frac{|y|^2}{2|x|^2}-\frac{(xy)^2}{2|x|^4}+L_3(x,y)\right), |L_3(x,y)| \leq \frac{4.13r^3}{|x|^3}; \tag{3.11}$$

$$|x-y| = |x|\left(1-\frac{xy}{|x|^2}+L_2(x,y)\right), |L_2(x,y)| \leq \frac{2.38r^2}{|x|^2}. \tag{3.12}$$

Proof of Lemma 3.3. Recall that

$$(1+\varepsilon)^{1/2} = \sum_{n=0}^{\infty} \frac{(-1)^n (2n)!}{(1-2n)n!^2 4^n} \varepsilon^n = \sum_{n=0}^{\infty} a_n \varepsilon^n, \forall |\varepsilon| < 1. \tag{3.13}$$

Note that

$$k_{n+1} := \frac{a_{n+1}}{a_n} = \frac{(-1)(2n+1)(2n+2)(1-2n)}{(n+1)(n+1)4(1-2n-2)} = -\frac{2(2n+1)(2n-1)}{4(2n+1)(n+1)} = -\left(1 - \frac{3}{2n+2}\right), \tag{3.14}$$

$|k_{n+1}| < 1$, for $n \in N \cup \{0\}$.
Therefore,

$$|\sum_{n=3}^{\infty} a_n \varepsilon^n| \le |a_3| \sum_{n=3}^{\infty} |\varepsilon^n| \le |a_3| \frac{|\varepsilon|^3}{1-|\varepsilon|}, |\varepsilon| < 1, \tag{3.15}$$
$$|a_3| = \frac{6!}{5 * 3!3!4^3} = \frac{6 * 5 * 4 * 6}{5 * 6 * 6 * 4^3} = \frac{1}{16}.$$

In the present work we use formulas (3.13), (3.15) for

$$\varepsilon = -\frac{2xy}{|x|^2} + \frac{|y|^2}{|x|^2}, \ x, y \in R^d, |y| \le r, |x| \ge 3r. \tag{3.16}$$

From (3.16) it follows that:

$$|\varepsilon| \le \frac{7}{9}, |\varepsilon| \le \frac{7}{3}\frac{r}{|x|}. \tag{3.17}$$

Using (3.13),(3.16) we have that

$$|x-y| = |x| \left| \frac{x}{|x|} - \frac{y}{|x|} \right| = |x| \left(1 - \frac{2xy}{|x|^2} + \frac{|y|^2}{|x|^2}\right)^{\frac{1}{2}} = \tag{3.18}$$
$$= |x| \left(1 - \frac{xy}{|x|^2} + \frac{|y|^2}{2|x|^2} - \frac{1}{8}\left(\frac{|y|^2}{|x|^2} - \frac{2xy}{|x|^2}\right)^2 + R_3(x,y)\right),$$

where

$$|R_3(x,y)| = |\sum_{n=3}^{\infty} a_n \varepsilon^n| \le |a_3| \frac{|\varepsilon|^3}{1-|\varepsilon|} \le \frac{1}{16} \frac{7^3 r^3}{3^3 |x|^3} \frac{1}{2/9} \le 3.58 \frac{r^3}{|x|^3}. \tag{3.19}$$

Using (3.18), (3.19) and gathering the terms with equal degrees in $|x|$, we obtain:

$$|x-y| = |x| \left(1 - \frac{xy}{|x|^2} + \frac{|y|^2}{2|x|^2} - \frac{(xy)^2}{2|x|^4} + L_3(x,y)\right), \tag{3.20}$$

$$|L_3(x,y)| \le \frac{1}{8}\frac{|y|^4}{|x|^4} + \frac{1}{2}\frac{xy|y|^2}{|x|^4} + R_3(x,y) \le \frac{r^3}{24|x|^3} + \frac{r^3}{2|x|^3} + 3.58\frac{r^3}{|x|^3} \le \frac{4.13 r^3}{|x|^3}. \tag{3.21}$$

Thus, estimate (3.11) is proved.

In addition to (3.18), (3.19), we also need the following formulas:

$$|x-y| = |x|\left(1 - \frac{xy}{|x|^2} + \frac{|y|^2}{2|x|^2} + R_2(x,y)\right), \tag{3.22}$$

$$|R_2(x,y)| = |\sum_{n=2}^{\infty} a_n \varepsilon^n| \le |a_2\varepsilon^2| + R_3(x,y) \le \frac{7^2/3^2}{8}\frac{r^2}{|x|^2} + 3.58\frac{r^3}{|x|^3} \le 1.88\frac{r^2}{|x|^2}. \tag{3.23}$$

In a similar way with (3.20), (3.21) we have

$$|x-y| = |x|\left(1 - \frac{xy}{|x|^2} + L_2(x,y)\right), \tag{3.24}$$

$$|L_2(x,y)| \le \frac{r^2}{2|x|^2} + 1.88\frac{r^2}{|x|^2} \le \frac{2.38r^2}{|x|^2}. \tag{3.25}$$

Thus, estimate (3.12) is proved. This completes the prove of Lemma 3.3. □
Now we are ready to prove estimate (3.10). We have

$$\begin{aligned}
&\left|\frac{e^{i|k||x|-i|k|\frac{xy}{|x|}}}{|x|} - \frac{e^{i|k||x-y|}}{|x-y|}\right| = \\
&= \left|\frac{e^{i|k||x|-i|k|\frac{xy}{|x|}}}{|x|} - \frac{e^{i|k||x|\left(1-\frac{xy}{|x|^2}+\frac{|y|^2}{2|x|^2}-\frac{(xy)^2}{2|x|^4}+L_3(x,y)\right)}}{|x|\left(1-\frac{xy}{|x|^2}+L_2(x,y)\right)}\right| = \\
&= \frac{1}{|x|}\left|1 - \frac{e^{i|k||x|\left(\frac{|y|^2}{2|x|^2}-\frac{(xy)^2}{2|x|^4}+L_3(x,y)\right)}}{1-\frac{xy}{|x|^2}+L_2(x,y)}\right| =: \frac{1}{|x|}\left|1 - \frac{e^{iL}}{1-t}\right|.
\end{aligned} \tag{3.26}$$

Note that

$$|e^{iL} - 1 - iL| \le \frac{L^2}{2}, \text{ for } L \in R, \text{ and } |\frac{1}{1-t} - 1 - t| \le t^2\frac{1}{1-|t|}, |t| < 1, \tag{3.27}$$

and further

$$\begin{aligned}
&|1 - \frac{e^{iL}}{1-t}| \le |1 - (1 + L + L^2/2)(1 + t + t^2/(1-|t|))| \le \\
&\le L + L^2/2 + t + \frac{t^2}{1-|t|} + (L + L^2/2)(t + t^2/(1-|t|)).
\end{aligned} \tag{3.28}$$

In our case:

$$|L| = |k||x|\left|\frac{|y|^2}{2|x|^2} - \frac{(xy)^2}{2|x|^4} + L_3(x,y)\right| \le \frac{|k|}{|x|}\left(\frac{r^2}{2} + \frac{r^2}{2} + \frac{4.13r^3}{|x|}\right) \le \frac{2.38|k|r^2}{|x|}; \tag{3.29}$$

$$L^2/2 \le \frac{2.38^2|k|^2r^4}{2|x|^2};$$

$$|t| = |\frac{xy}{|x|^2} - L_2(x,y)| \le \frac{r}{|x|} + \frac{2.38r^2}{|x|^2} \le \frac{r}{|x|} + \frac{0.8r}{|x|} \le \frac{1.8r}{|x|};$$

$$\frac{t^2}{1-t} \le \frac{\frac{1.8^2r^2}{|x|^2}}{1-1.8/3} = \frac{1.8^2r^2}{|x|^2}\frac{1}{0.4} = 8.1\frac{r^2}{|x|^2}.$$

Finally,

$$|1 - \frac{e^{iL}}{1-t}| \le \frac{2.38|k|r^2}{|x|} + \frac{2.38^2|k|^2r^4}{2|x|^2} + \frac{1.8r}{|x|} + \frac{8.1r^2}{|x|^2} +$$
$$+(\frac{2.38|k|r^2}{|x|} + \frac{2.38^2|k|^2r^4}{2|x|^2})(\frac{1.8r}{|x|} + \frac{8.1r^2}{|x|^2}) \le$$
$$\le \frac{3.06|k|r^2}{|x|} + \frac{3.06^2|k|^2r^4}{2|x|^2} + \frac{1.8r}{|x|} + \frac{8.1r^2}{|x|^2} + 1.5(\frac{3.06|k|r^2}{|x|} + \frac{3.06^2|k|^2r^4}{2|x|^2}) \le$$
$$\le \frac{r}{|x|}(4.5 + 7.65|k|r + 3.91|k|^2r^2). \tag{3.30}$$

Estimate (3.10) follows from (3.26), (3.30), that proves Lemma 3.2. □.
This also completes the proof of Theorem 2.1(A). □.

4 Proof of Theorem 2.1(B)

Proceeding from (3.1)-(3.3), for $d = 2$, we have:

$$|\delta a(x,k)| \le |x|^{-1/2}|c|^2|f|^2 + 2|x|^{1/2}|\delta\psi^+(x,k)|\left(1 + \frac{|c||f|}{|x|^{1/2}}\right) + |x|^{1/2}|\delta\psi^+(x,k)|^2, \tag{4.1}$$

where

$$c = c(2,|k|) = -\pi i(-2\pi i)^{\frac{2-1}{2}}|k|^{\frac{2-3}{2}} = -(1+i)\pi^{3/2}|k|^{-1/2}. \tag{4.2}$$

Now $|f|$ is estimated in (3.4) for $d = 2$ and $|\delta\psi^+(x,k)|$ is estimated in the following lemma:

Lemma 4.1. *Under the assumptions of Theorem 2.1(B), the following estimate holds for $|x| \ge 3r$:*

$$|\delta\psi^+(x,k)| \le \frac{\|v\|_{L_1}\|\psi^+\|_\infty\rho_2(|k|,r)}{4(\pi|k|)^{1/2}|x|^{3/2}}. \tag{4.3}$$

Using estimates (4.1), (3.4), (4.3) we have that

$$|\delta a(x,k)| \le |x|^{-1/2}|k|^{-1}\frac{\|\psi^+\|_\infty^2\|v\|_{L_1}^2}{8\pi} + \tag{4.4}$$
$$+ |x|^{1/2}\frac{\|v\|_{L_1}\|\psi^+\|_\infty\rho_2}{2\sqrt{\pi}|k|^{1/2}|x|^{3/2}}\left(1 + \frac{\|\psi^+\|_\infty\|v\|_{L_1}}{2|x|^{1/2}(2\pi)^{1/2}|k|^{1/2}}\right) + |x|^{1/2}\frac{\|v\|_{L_1}^2\|\psi^+\|_\infty^2\rho_2^2}{16\pi|k||x|^3} \tag{4.5}$$

Estimate (2.4) of Theorem 2.1(B) follows from (4.4). Therefore, in order to prove Theorem 2.1(B) it remains to prove Lemma 4.1.

Proof of Lemma 4.1. Using the Lippmann-Schwinger integral equation (1.4) and formulas (1.6), (3.3), (1.7) we obtain

$$\delta\psi^+(x,k)=\int_{R^2}-\frac{iH_0^{(1)}(|k||x-y|)}{4}v(y)\psi^+(y,k)dy+$$
$$+(1+i)\frac{\pi^{3/2}}{|k|^{1/2}}\frac{e^{i|k||x|}}{|x|^{1/2}}\frac{1}{(2\pi)^2}\int_{R^2}e^{-i|k|\frac{xy}{|x|}}v(y)\psi^+(y,k)dy=$$

$$=\int_{R^2}\left(-\frac{iH_0^{(1)}(|k||x-y|)}{4}+\frac{(1+i)e^{i|k||x|-i|k|\frac{xy}{|x|}}}{4(\pi|k||x|)^{1/2}}\right)v(y)\psi^+(y,k)dy. \tag{4.6}$$

From (4.6) we obtain:

$$|\delta\psi^+(x,k)|\le\|\psi^+(\cdot,k)\|_\infty\int_{R^2}\left|-\frac{iH_0^{(1)}(|k||x-y|)}{4}+\frac{(1+i)e^{i|k||x|-i|k|\frac{xy}{|x|}}}{4(\pi|k||x|)^{1/2}}\right||v(y)|dy. \tag{4.7}$$

Lemma 4.2. *Let $x,y\in R^2, |y|\le r, |x|\ge 3r$. Then*

$$\left|-\frac{iH_0^{(1)}(|k||x-y|)}{4}+\frac{(1+i)e^{i|k||x|-i|k|\frac{xy}{|x|}}}{4(\pi|k||x|)^{1/2}}\right|=M_1+M_2,\ \textit{where} \tag{4.8}$$

$$M_1\le\frac{\sqrt{2}}{4(\pi k)^{1/2}|x|^{3/2}}\left(1.77+3.79|k|r+1.51|k|^2r^2\right); \tag{4.9}$$

$$M_2\le\frac{3\sqrt{3}}{64(\pi|k||x|)^{1/2}|k||x|}. \tag{4.10}$$

Note that

$$M_1+M_2\le\frac{\sqrt{2}r}{4(\pi|k|)^{1/2}|x|^{3/2}}\left(\frac{3\sqrt{3}}{16\sqrt{2}|k|r}+1.77+3.79|k|r+1.51|k|^2r^2\right). \tag{4.11}$$

Estimate (4.3) of Lemma 4.1 follows from (4.7)-(4.11). Thus, in order to prove Lemma 4.1 it remains to prove Lemma 4.2.

Proof of Lemma 4.2. To prove Lemma 4.2 we use, in particular, estimate (3.11) of Lemma 3.3, which remains the same for $d=2$. Besides, we use, in particular, Lemma 4.3.

Lemma 4.3. *For Hankel funtion the following representation holds:*

$$H_0^{(1)}(|k||x|)=\left(\frac{2}{\pi|k||x|}\right)^{1/2}e^{i|k||x|-i\pi/4}(1+h(|k||x|)),\ |h(|k||x|)|\le\frac{1}{8|k||x|}. \tag{4.12}$$

Lemma 4.3 is proved at the end of this Section.

Using formula (4.12) we have

$$\left|-\frac{iH_0^{(1)}(|k||x-y|)}{4}+\frac{(1+i)e^{i|k||x|-i|k|\frac{xy}{|x|}}}{4(\pi|k||x|)^{1/2}}\right|\le$$
$$\left|-\frac{i}{4}\left(\frac{2}{\pi|k||x-y|}\right)^{1/2}e^{i|k||x-y|-i\pi/4}(1+h(|k|(x-y)))+\frac{(1+i)e^{i|k||x|-i|k|\frac{xy}{|x|}}}{4(\pi|k||x|)^{1/2}}\right|\le$$
$$\le\frac{1}{4(\pi|k|)^{1/2}}\left|-i\sqrt{2}(\frac{\sqrt{2}}{2}-i\frac{\sqrt{2}}{2})\frac{e^{i|k||x-y|}}{|x-y|^{1/2}}+(1+i)\frac{e^{i|k||x|-i|k|\frac{xy}{|x|}}}{|x|^{1/2}}\right|+$$
$$+\frac{1}{4}\left(\frac{2}{\pi|k||x-y|}\right)^{1/2}\frac{1}{8|k||x-y|}=:M_1+M_2. \tag{4.13}$$

The term M_2 can be estimated easily:

$$M_2 \le \frac{3\sqrt{3}}{64(\pi|k||x|)^{1/2}|k||x|}, |y| \le r, |x| \ge 3r. \tag{4.14}$$

Lemma 4.4. *The term M_1 can be estimated as follows:*

$$M_1 \le \frac{\sqrt{2}}{4(\pi|k|)^{1/2}|x|^{3/2}} \left(1.77 + 3.79|k|r + 1.51|k|^2r^2\right), |y| \le r, |x| \ge 3r. \tag{4.15}$$

Proof of Lemma 4.4. One can see that

$$M_1 = \frac{\sqrt{2}}{4(\pi|k|)^{1/2}} \left| \frac{e^{i|k||x| - i|k|\frac{xy}{|x|}}}{|x|^{1/2}} - \frac{e^{i|k||x-y|}}{|x-y|^{1/2}} \right|. \tag{4.16}$$

Further, we obtain

$$M_1 \le \frac{\sqrt{2}}{4(\pi|k|)^{1/2}} \left| \frac{e^{i|k||x| - i|k|\frac{xy}{|x|}}}{|x|^{1/2}} - \frac{e^{i|k||x|(1 - \frac{xy}{|x|^2} + \frac{|y|^2}{2|x|^2} - \frac{(xy)^2}{2|x|^4} + L_3(x,y))}}{|x|^{1/2}(1 - \frac{xy}{2|x|^2} + \widetilde{L_2}(x,y))} \right| =$$

$$= \frac{\sqrt{2}}{4(\pi|k||x|)^{1/2}} \left| 1 - \frac{e^{i|k||x|(\frac{|y|^2}{2|x|^2} - \frac{(xy)^2}{2|x|^4} + L_3(x,y))}}{(1 - \frac{xy}{2|x|^2} + \widetilde{L_2}(x,y))} \right|. \tag{4.17}$$

Here we use the same expantion as in (3.11) and the following additional expantion:

$$|x-y|^{1/2} = |x|^{1/2} \left(1 - \frac{2xy}{|x|^2} + \frac{|y|^2}{|x|^2}\right)^{1/4} = |x|^{1/2} \left(1 - \frac{xy}{2|x|^2} + \widetilde{L_2}(x,y)\right). \tag{4.18}$$

To complete the proof of Lemma 4.4 we use, in particular, the estimate for L_3 in (3.11) and the estimate for $\widetilde{L_2}$ given in the following Lemma.

Lemma 4.5. *Let $x, y \in R^2, |y| \le r, |x| \ge 3r$. Then:*

$$|\widetilde{L_2}(x,y)| \le 1.81 \frac{r^2}{|x|^2}. \tag{4.19}$$

Proof of Lemma 4.5. Recall that

$$(1+\varepsilon)^{1/4} = \sum_{n=0}^{\infty} b_n \varepsilon^n, |\varepsilon| < 1, \text{ where } b_n = \prod_{k=1}^{n} \frac{1/4 - k + 1}{k}. \tag{4.20}$$

Note that

$$l_{n+1} := \frac{b_{n+1}}{b_n} = \frac{1/4 - n - 1 + 1}{n+1} = (-1)(1 - \frac{5}{4(n+1)}),$$

$|l_{n+1}| < 1$, for $n \in N \cup \{0\}$.
Therefore,

$$|\sum_{n=2}^{\infty} b_n \varepsilon^n| \le |b_2|\varepsilon^2 + |b_3| \frac{|\varepsilon|^3}{1 - |\varepsilon|}, \tag{4.21}$$

$$|b_2| = 3/32, |b_3| = 7/128.$$

In the present work we use formulas (4.20), (4.21) for

$$\varepsilon = -\frac{2xy}{|x|^2} + \frac{|y|^2}{|x|^2}, x, y \in R^2, |y| \le r, |x| \ge 3r, \tag{4.22}$$

$$|\varepsilon| \le \frac{7}{9}, |\varepsilon| \le \frac{7}{3}\frac{r}{|x|}. \tag{4.23}$$

Using (4.20), (4.22) we have that

$$|x-y|^{1/2} = |x|^{1/2}\left(1 - \frac{2xy}{|x|^2} + \frac{|y|^2}{|x|^2}\right)^{1/4} = |x|^{1/2}(1 - \frac{xy}{2|x|^2} + \frac{|y|^2}{4|x|^2} + \widetilde{R_2}(x,y)), \tag{4.24}$$

where

$$|\widetilde{R_2}(x,y)| = |\sum_{n=2}^{\infty} b_n \varepsilon^n| \le |b_2|\varepsilon^2 + |b_3|\frac{\varepsilon^3}{1-|\varepsilon|} \le \frac{3}{32}\frac{7^2}{3^2}\frac{r^2}{|x|^2} + \frac{7}{128}\frac{7^3}{3^3}\frac{r^3}{|x|^3}\frac{9}{2} \le$$
$$\le \left(\frac{7^2}{32*3} + \frac{7*7^3*9}{128*3^3*3*2}\right)\frac{r^2}{|x|^2} \le 1.56\frac{r^2}{|x|^2} \tag{4.25}$$

Using (4.24), (4.25) and gathering the terms with equal degrees in $|x|$, we obtain:

$$|\widetilde{L_2}(x,y)| = \left|\frac{|y|^2}{4|x|^2} + \widetilde{R_2}(x,y)\right| \le \frac{r^2}{4|x|^2} + 1.56\frac{r^2}{|x|^2} \le 1.81\frac{r^2}{|x|^2}. \tag{4.26}$$

Lemma 4.5 is proved.

Returning to the proof of Lemma 4.4, we rewrite (4.17) as:

$$M_1 \le \frac{\sqrt{2}}{4(\pi|k|x)^{1/2}}|1 - \frac{e^{iL}}{1-t}|. \tag{4.27}$$

We have

$$|1 - \frac{e^{iL}}{1-t}| \le |1 - (1 + L + L^2/2)(1 + t + t^2/(1-t))| \le$$
$$\le L + L^2/2 + t + \frac{t^2}{1-t} + (L + L^2/2)(t + t^2/(1-t)). \tag{4.28}$$

In addition:

$$L \le |k||x|(\frac{r^2}{2|x|^2} + \frac{r^2}{2|x|^2} + \frac{4.13r^3}{|x|^3}) \le \frac{|k|r^2}{|x|}(1 + \frac{4.13}{3}) \le \frac{2.38|k|r^2}{|x|}; \tag{4.29}$$

$$L^2/2 \le 2.84\frac{|k|^2 r^4}{|x|^2}; \tag{4.30}$$

$$t \le \frac{r}{2|x|} + 1.81\frac{r^2}{|x|^2} \le 1.11\frac{r}{|x|}; \tag{4.31}$$

$$\frac{t^2}{1-t} \le \frac{(1.11\frac{r}{|x|})^2}{1 - 1.11/3} \le 1.9558\frac{r^2}{|x|^2}; \tag{4.32}$$

$$(L+L^2/2)(t+t^2/(1-t)) \le (\frac{2.38|k|r^2}{|x|}+\frac{2.84|k|^2r^4}{|x|^2})(1.11\frac{r}{|x|}+1.9558\frac{r^2}{|x|^2}) \le$$
$$\le 0.59(\frac{2.38|k|r^2}{|x|}+\frac{2.84|k|^2r^4}{|x|^2}). \tag{4.33}$$

Using (4.28)-(4.33), we obtain:

$$\left|1-\frac{e^{iL}}{1-t}\right| \le \frac{2.38*1.59|k|r^2}{|x|}+\frac{2.84*1.59|k|^2r^4}{|x|^2}+1.77\frac{r}{|x|} \le$$
$$\le \frac{r}{|x|}\left(1.77+3.79|k|r+1.51|k|^2r^2\right). \tag{4.34}$$

The estimate (4.15) follows from (4.27) and (4.34). This completes the proof of Lemma 4.4. □

Proof of Lemma 4.3. For H_0^1 the following equality holds, for $s>0$, see in [20] formula (43) for $\nu=0,\beta=0$:

$$H_0^{(1)}(s)=\left(\frac{2}{\pi s}\right)^{1/2}\frac{e^{is-i\pi/4}}{\Gamma(1/2)}\int_0^{+\infty}e^{-u}u^{-1/2}\left(1+\frac{iu}{2s}\right)^{-1/2}du. \tag{4.35}$$

Then we apply the Teylor's expantion with one term and the integral reminder to the function $g(t)=(1+\frac{iut}{2s})^{1/2}, t\in[0,1], u,s\in R^+$. We obtain:

$$g(1)=\left(1+\frac{iu}{2s}\right)^{-1/2}=g(0)+\frac{1/2}{0!}\frac{u}{2is}\int_0^1\left(1-\frac{ut}{2is}\right)^{-3/2}dt. \tag{4.36}$$

So,

$$\left|\left(1+\frac{iu}{2s}\right)^{-1/2}\right| \le 1+\frac{u}{4s}\int_0^1\left|1-\frac{ut}{2is}\right|^{-3/2}dt \le 1+\frac{u}{4s}. \tag{4.37}$$

Using (4.35), (4.37), we obtain:

$$\left|\frac{H_0^{(1)}(s)-\left(\frac{2}{\pi s}\right)^{1/2}e^{is-i\pi/4}}{\left(\frac{2}{\pi s}\right)^{1/2}e^{is-i\pi/4}}\right| \le \frac{1}{4s\Gamma(1/2)}\int_0^{\infty}e^{-u}u^{-1/2}udu \le \frac{\Gamma(3/2)}{4s\Gamma(1/2)}=\frac{1}{8s}. \tag{4.38}$$

Estimate (4.38) implies (4.12). □

5 Estimates for $\|\psi^+\|_\infty$

The Lippmann-Schwinger integral equation (1.4) can also be rewritten as:

$$(I-A^+(|k|))\varphi^+(\cdot,k)=\varphi_0^+(\cdot,k), \tag{5.1}$$

where

$$\varphi^+(x,k)=\Lambda^{-s}\psi^+(x,k), \varphi_0^+(x,k)=\Lambda^{-s}e^{ikx}, \tag{5.2}$$
$$A^+(|k|)=\Lambda^{-s}G^+(|k|)\Lambda^{-s}(\Lambda^{2s}v),$$

where I is the identity operator, Λ denotes the multiplication operator by the functions $(1+|x|^2)^{1/2}$, $G^+(|k|)$ denotes the integral operator with the Schwartz kernel $G^+(x-y,k)$ of (1.4), (1.5), v is the multiplication operator by the function $v(x)$, $s=(d+\varepsilon)/2, \varepsilon>0$, $k\in R^d\setminus\{0\}, x\in R^d$.

We recall that the following Agmon estimate holds:

$$\|\Lambda^{-s}G^+(|k|)\Lambda^{-s}\|_{L_2(R^d)\to L_2(R^d)}\le C_0(d,s)|k|^{-1}, s>1/2, |k|\ge 1, \tag{5.3}$$

see, for example, [5], [14] and references therein.

Using (5.3) one can see that

$$\|A^+(|k|)\|_{L_2(R^d)\to L_2(R^d)}\le Q, s>1/2, |k|\ge 1, \tag{5.4}$$

$$Q:=C_0(d,s)\|\Lambda^{2s}v\|_\infty|k|^{-1}. \tag{5.5}$$

As a corollary of (5.1), (5.2), (5.4), we have that if $Q<1, s>d/2, |k|\ge 1$, then:

$$\|\varphi^+\|_{L_2(R^d)}\le\frac{\|\varphi_0^+\|_{L_2(R^d)}}{1-Q}, \tag{5.6}$$

where

$$\|\varphi_0^+\|_{L_2(R^d)}=\left(\int_{R^d}\frac{dx}{(1+|x|^2)^s}\right)^{1/2}=:I_d(s). \tag{5.7}$$

Proof of Lemma 2.2. Using (5.1), (5.2), (5.6) we obtain that

$$|\psi^+(x,k)-e^{ikx}|\le\left|\int_{B_r}G^+(x-y,k)v(y)<y>^s\varphi^+(y,k))dy\right|\le \tag{5.8}$$
$$\le\|\varphi^+(\cdot,k)\|_{L_2(R^d)}J(x)\le\frac{\|\varphi_0^+(\cdot,k)\|_{L_2}}{1-Q}J(x),\quad x\in R^d,$$

$$J(x)=\left(\int_{B_r}|G^+(x-y,k)v(y)<y>^s|^2dy\right)^{1/2}. \tag{5.9}$$

For $d=3$ we have:

$$\|\varphi_0^+\|^2_{L_2(R^3)}\le\int_{R^3}\frac{dy}{(1+|y|^2)^s}\le 4\pi\int_0^\infty\frac{r^2dr}{(1+r^2)^s}\le$$
$$\le 4\pi\left(\int_0^1\frac{r^2dr}{(1+r^2)^s}+\int_1^\infty\frac{r^2dr}{(1+r^2)^s}\right)\le$$
$$\le 4\pi\left(\frac13+\int_1^\infty\frac{r^2dr}{(r^2)^s}\right)=4\pi\left(\frac13+\frac{1}{(2s-1)}\right)\le\frac{10}{3}\pi; \tag{5.10}$$

$$J(x)=\left(\int_{B_r}\frac{v^2(y)(1+y^2)^s}{16\pi^2|x-y|^2}dy\right)^{1/2}\le\frac{\|v\|_{L_\infty(D)}(1+r^2)^{s/2}}{4\pi}\left(\int_{B_r}\frac{1}{|y|^2}dy\right)^{1/2}$$
$$\le\frac{1}{4\pi}\|v\|_{L_\infty(D)}(1+r^2)^{s/2}\|(4\pi\int_0^r d\rho)^{1/2}\|=\frac{\|v\|_{L_\infty(D)}(1+r^2)^{s/2}r^{1/2}}{2\sqrt{\pi}}, x\in R^3. \tag{5.11}$$

For $d=2$ we have:

$$\|\varphi_0^+\|_{L_2}^2=\int_{R^d}|\varphi_0^+(y,k)|^2dy=\int_{R^2}\frac{dy}{(1+|y|^2)^s}=$$
$$=\pi\int_0^\infty\frac{dr^2}{(1+r^2)^s}\le\pi\int_0^\infty\frac{dz}{(1+z)^s}=\frac{2\pi}{\varepsilon};\tag{5.12}$$

$$J(x)=\left(\int_{B_r}\frac{|H_0^{(1)}(|k||x-y|)|^2}{16}|v(y)|^2(1+|y|^2)^sdy\right)^{1/2}\le$$
$$\le\|v\|_{L_\infty(D)}(1+r^2)^{s/2}\frac14(\int_{B_r}|H_0^{(1)}(|k||x-y|)|^2dy)^{1/2}.\tag{5.13}$$

From (4.35) we obtain:

$$|H_0^{(1)}(s)|\le\left(\frac{2}{\pi s}\right)^{1/2}\frac{1}{\Gamma(1/2)}\int_0^\infty e^{-u}u^{-1/2}\left|1+\frac{iu}{2s}\right|^{-1/2}du\le\left(\frac{2}{\pi s}\right)^{1/2}.\tag{5.14}$$

Hence, we have:

$$\left(\int_{B_r}|H_0^{(1)}(|k||x-y|)|^2dy\right)^{1/2}\le\left(\int_{B_r}\frac{2}{\pi|k||x-y|}dy\right)^{1/2}\le$$
$$\le\left(\int_0^r2\pi r\frac{2}{\pi|k|r}dr\right)^{1/2}=2\sqrt{\frac{r}{|k|}}.\tag{5.15}$$

Estimate (2.7) follows from (5.8), (5.10), (5.11).
Estimate (2.8) follows from (5.8), (5.12), (5.13), (5.15).
Lemma 2.2 is proved.

Proof of Lemma 2.3 **(A).** Using the Lippmann-Schwinger equation (1.4) for $d=3$, we obtain that

$$\|\psi^+\|_\infty\le1+\|\psi^+\|_\infty\|v\|_\infty\int_{B_r}\frac{dx}{4\pi|x|}\le1+\|\psi^+\|_\infty\|v\|_\infty\int_0^r\frac{r^2}{r}dr\le$$
$$\le1+\|\psi^+\|_\infty\|v\|_\infty\frac{r^2}{2}dr.\tag{5.16}$$

Estimates (2.9) follows from (5.16).

(B). Using the Lippmann-Schwinger equation (1.4) for $d=2$, we obtain that

$$\|\psi^+\|_\infty\le1+\|\psi^+\|_\infty\|v\|_\infty\int_{B_r}\frac{|H_0^1(|x||k|)|dx}{4}\le1+\frac{\|\psi^+\|_\infty\|v\|_\infty}{4}\int_0^r\left(\frac{2}{\pi|k|r}\right)^{1/2}2\pi rdr\le$$
$$\le1+\|\psi^+\|_\infty\|v\|_\infty\sqrt{\frac{\pi}{2|k|}}\int_0^r r^{1/2}dr\le1+\sqrt{\frac{2\pi}{|k|}}\frac{\|\psi^+\|_\infty\|v\|_\infty r^{3/2}}{3}.\tag{5.17}$$

Estimates (2.10) follows from (5.17).
Lemma 2.3 is proved.□

Bibliography

[1] A.D. Agaltsov, T. Hohage, R.G. Novikov, *An iterative approach to monochromatic phaseless inverse scattering*, Inverse Problems 35(2), 24001 (24 pp.) (2019).

[2] A. D. Agaltsov, R.G. Novikov, *Error Estimates for Phaseless Inverse Scattering in the Born Approximation at High Energies*, Journal of Geometric Analysis (2017), https://doi.org/10.1007/s12220-017-9872-6.

[3] M. Born, *Quantenmechanik der Stossvorgange*, Zeitschrift fur Physik 38 (11-12)(1926), 803-827.

[4] K. Chadan, P.C. Sabatier, *Inverse Problems in Quantum Scattering Theory*, 2nd edn. Springer, Berlin, 1989.

[5] G. Eskin, *Lectures on Linear Partial Differential Equations*, Graduate Studies in Mathematics, Vol. 123, American Mathematical Society, 2011.

[6] L.D. Faddeev, S.P. Merkuriev, *Quantum Scattering Theory for Multi-particle Systems*, Mathematical Physics and Applied Mathematics, 11. Kluwer Academic Publishers Group, Dordrecht, 1993.

[7] O. Ivanyshyn, R. Kress, *Identification of sound-soft 3D obstacles from phaseless data*, Inverse Probl. Imaging 4(2010), 131-149.

[8] P. Jonas, A.K. Louis, *Phase contrast tomography using holographic measurements*, Inverse Problems 20(1)(2004), 75-102.

[9] T. Hohage, R.G. Novikov, *Inverse wave propagation problems without phase information*, Inverse Problems 35(7), 070301 (4 pp.)(2019).

[10] M.V. Klibanov, *Phaseless inverse scattering problems in three dimensions*, SIAM J.Appl. Math. 74(2)(2014), 392-410 .

[11] M.V. Klibanov, N.A. Koshev, D.-L. Nguyen, L.H. Nguyen, A. Brettin, V.N. Astratov, *A numerical method to solve a phaseless coefficient inverse problem from a single measurement of experimental data*, SIAM J. Imaging Sci. 11(4) (2018), 2339-2367.

[12] M.V. Klibanov, V.G. Romanov, *Reconstruction procedures for two inverse scattering problems without the phase information*, SIAM J. Appl. Math. 76(1)(2016), 178-196.

[13] R.B. Melrose, *Geometric scattering theory*, Stanford Lectures. Cambridge University Press, 1995.

[14] R. G. Novikov, *An iterative approach to non-overdetermined inverse scattering at fixed energy*, Sbornik: Mathematics 206(1)(2015), 120-134 .

[15] R. G. Novikov, *Formulas for phase recovering from phaseless scattering data at fixed frequency*, Bulletin des Sciences Mathematiques 139(8)(2015), 923-936 .

[16] R. G. Novikov, *Phaseless inverse scattering in the one-dimensional case*, Eurasian Journal of Mathematical and Computer Applications 3(1)(2015), 63-69 .

[17] R. G. Novikov, *Inverse scattering without phase information*, Seminaire Laurent Schwartz - EDP et applications (2014-2015), Exp. No16, 13p.

[18] R. G. Novikov, *Multipoint formulas for phase recovering from phaseless scattering data*, Journal of Geometric Analysis, https://doi.org/10.1007/s12220-019-00329-6.

[19] V. Palamodov, *A fast method of reconstruction for X-ray phase contrast imaging with arbitrary Fresnel number*, arXiv:1803.08938v1 (2018) .

[20] N. J. Sekeljic, *Asymptotic Expansion of Bessel Functions; Applications to Esectromagnetics*, Dynamics at the Horsetooth, Vol. 2A, Focussed Issue: Asymptotics and Perturbations, 2010.

[21] V. G. Romanov, *Inverse problems without phase information that use wave interference*, Sib. Math. J. 59(3)(2018), 494-504 .

Article V

Fixed-distance multipoint formulas for the scattering amplitude from phaseless measurements

R.G. Novikov, V.N. Sivkin

Abstract. We give new formulas for finding the complex (phased) scattering amplitude at fixed frequency and angles from absolute values of the scattering wave function at several points $x_1, ..., x_m$. In dimension $d \geq 2$, for $m > 2$, we significantly improve previous results in the following two respects. First, geometrical constraints on the points needed in previous results are significantly simplified. Essentially, the measurement points x_j are assumed to be on a ray from the origin with fixed distance $\tau = |x_{j+1} - x_j|$, and high order convergence (linearly related to m) is achieved as the points move to infinity with fixed τ. Second, our new asymptotic reconstruction formulas are significantly simpler than previous ones. In particular, we continue studies going back to [Novikov, Bull. Sci. Math. 139(8), 923-936, 2015].

Keywords: Schrödinger equation, Helmholtz equation, monochromatic scattering data, phase retrieval, phaseless inverse scattering

1 Introduction

We consider monochromatic scattering modelled using the equation

$$-\Delta\psi + v(x)\psi = E\psi,\ x \in \mathbb{R}^d,\ d \geq 1,\ E > 0, \tag{1.1}$$

where

$$\begin{aligned} &v \in L^\infty(D),\ \ v \equiv 0 \text{ on } \mathbb{R}^d \setminus D, \\ &D \text{ is an open bounded domain in } \mathbb{R}^d. \end{aligned} \tag{1.2}$$

We assume that v is complex-valued. The regularity assumption that $v \in L^\infty(D)$ is just for simplicity and can be relaxed; see Remark 2.1. The main point is that for equation (1.1), under such an assumption, we can consider the scattering solutions ψ^+ specified via Sommerfeld type radiation condition like (1.3).

Equation (1.1) arises in quantum mechanics as the Schrödinger equation at fixed energy and in acoustics and electrodynamics as the Helmholtz equation at fixed frequency. Under assumption (1.2), the coefficient v describes a scatterer contained in D. The number E is related to the time-harmonic frequency and corresponds to the energy in the framework of the Schrödinger equation. In addition, v may depend on E, at least, in acoustics and electrodynamics. See, for example, [5], [7], [9], [13].

For equation (1.1) we consider the solutions $\psi^+(x,k)$, $k\in\mathbb{R}^d$, $k^2=E$, specified by the following asymptotic as $|x|\to\infty$:

$$\psi^+(x,k)=e^{ikx}+\frac{e^{i|k||x|}}{|x|^{(d-1)/2}}f_1(k,|k|\frac{x}{|x|})+\mathcal{O}\left(\frac{1}{|x|^{(d+1)/2}}\right), \tag{1.3}$$

for some a priori unknown f_1. The solutions $\psi^+=\psi^+(x,k)$ are the scattering solutions, or scattering wave functions, for equation (1.1). These solutions describe scattering of the incident plan waves described by e^{ikx} on the scatterer described by v. In particular, the second term on the right-hand side of (1.3) describes the leading scattered spherical waves. The coefficient f_1 arising in (1.3) is a function defined on

$$\mathcal{M}_E=\{k,l\in\mathbb{R}^d : k^2=l^2=E\}=\mathbb{S}^{d-1}_{\sqrt{E}}\times\mathbb{S}^{d-1}_{\sqrt{E}}, \tag{1.4}$$

where $l=|k|\frac{x}{|x|}$, $\mathbb{S}^{d-1}_r$ is the sphere of radius r centered at the origin in $\mathbb{R}^d$.

The function f_1 is the scattering amplitude, or far field pattern, for equation (1.1).

In order to study ψ^+ and f_1 one can use, in particular, the Lippmann–Schwinger integral equation (2.1) for ψ^+ and formulas (2.5)–(2.7) for f_1; see Subsection 2.1.

We recall that in quantum mechanics the complex values of the functions ψ^+ and f_1 have no direct physical sense, whereas the phaseless values of $|\psi^+|^2$ and $|f_1|^2$ have probabilistic interpretation (according to the Born's rule) and can be directly measured. See [6] and, for example, [12], for details. In turn, in acoustics or electrodynamics the complex values of ψ^+ and f_1 can be directly measured, at least, in principle. However, in electro–magnetic wave propagation at very high frequencies (as for X–rays and lasers) only phaseless values of $|\psi^+|^2$ and $|f_1|^2$ can be measured in practice by modern technical devices; see, e.g., [17] and references therein.

For equation (1.1) under assumptions (1.2), we consider, in particular, the following problems:

Problem 1.1. Reconstruct potential v from its scattering amplitude f_1.

Problem 1.2. Reconstruct potential v from its phaseless scattering data $|\psi^+|^2$ appropriately given outside of D.

Problem 1.3. Find f_1 from $|\psi^+|^2$ appropriately given outside of D.

A recent survey on these problems is given in [30]. Actually, in the present work we continue studies of [11], [26]–[31], [33] on Problem 1.3. These studies on Problem 1.3 and results on Problem 1.1 admit straightforward applications to Problem 1.2. For other possible approaches to Problem 1.2, see, for example, [40], [41], [22], [10], [16], [23], [24], [19], [35].

In particular, in the present work we give, for fixed $(k,l)\in\mathcal{M}_E$, $l\neq k$, for $d\geq 2$,

$$\begin{aligned}&\text{formulas for finding } f_1(k,l) \text{ up to } \mathcal{O}(s^{-n}) \text{ as } s\to+\infty,\\ &\text{from } |\psi^+(x,k)|^2 \text{ given at } m \text{ points } x=x_1(s),...,x_m(s),\end{aligned} \tag{1.5}$$

where m depends linearly on n,

$$\begin{aligned}&x_j(s)=(s+\tau_j)\hat{l},\ j=1,...,m,\ \hat{l}=l/|l|,\\ &s>0,\ \tau_1=0,\ \tau_{j_1}<\tau_{j_2},\ j_1<j_2.\end{aligned} \tag{1.6}$$

These formulas are explicit and are presented in detail below in Introduction and in Section 3, where our precise assumptions on $m=m(n)$ and on τ_1, ..., τ_m are specified.

One can see that in formulas (1.5), (1.6) the measurement points $x_j=x_j(s)$ are on the ray starting at the origin in direction $\hat{l}$, where s is the distance between the origin and the set of these points, and the distances $\tau_{j+1}-\tau_j=|x_{j+1}-x_j|$ are fixed. In addition, the reconstruction formulas mentioned in (1.5) are asymptotic, where n can be considered as their convergence rate in terms of $\mathcal{O}(s^{-n})$ as $s\to+\infty$, that is when the points $x_j=x_j(s)$ move to infinity.

Note that, to our knowledge, for the first time formulas (1.5), (1.6) were realized in [26], [28] for $n=1$, $m=2$, $d\geq 3$ and for $n=1/2$, $m=2$, $d=2$, and in [29] for $n=1$, $m=2$, $d=2$.

In addition, for $m = 3$, $d = 1$, an exact (not asymptotic !) analog of formulas (5), (6) was given in [27]. In the present work, for the first time we realize formulas (5), (6) for $n > 1$, $d \geq 2$. In this respect we proceed from studies recently developed in [29] and [31]; more comments are given below in Introduction and in Section 2.

Let

$$a(x,k) = |x|^{(d-1)/2}(|\psi^+(x,k)|^2 - 1), \tag{1.7}$$

where $x, k \in \mathbb{R}^d \setminus \{0\}$.

Assume in (1.5), (1.6) that $d = 3$, $m = 2n$, $n \in \mathbb{N} = \{1, 2, 3, ...\}$, and that

$$\tau_j = \begin{cases} (j-1)\tau,\ j = 1, ..., n, \\ \sigma + (j-1-n)\tau,\ j = n+1, ..., 2n, \end{cases} \tag{1.8}$$

$$\tau = \tau(k,l) = \frac{2\pi}{\kappa},\ 0 < \sigma \neq 0\,(mod\,\frac{\pi}{\kappa}),\ \kappa = \kappa(k,l) = |k| - k\hat{l}. \tag{1.9}$$

Then our formulas (1.5), (1.6) are as follows:

$$f_1(k,l) = \frac{e^{-i(s+\sigma)\kappa}a_1(s) - e^{-is\kappa}a_2(s) + \mathcal{O}(s^{-n})}{-2i\sin(\sigma\kappa)},\ s \to +\infty, \tag{1.10}$$

$$a_1(s) = a_1(k,l,s) = \sum_{j=1}^{n} \frac{(-1)^{n-j}(s+\tau_j)^{n-1}a(x_j(s),k)}{(j-1)!(n-j)!\tau^{n-1}}, \tag{1.11}$$

$$a_2(s) = a_2(k,l,s) = \sum_{j=n+1}^{2n} \frac{(-1)^{j}(s+\tau_j)^{n-1}a(x_j(s),k)}{(j-1-n)!(2n-j)!\tau^{n-1}}, \tag{1.12}$$

where $(k,l) \in \mathcal{M}_E$, $l \neq k$, $d = 3$, $a(x,k)$ is defined by (1.7), $x_j(s)$ are defined in (1.6), (1.8), (1.9), τ, τ_j, σ, κ are the numbers of (1.8), (1.9).

Formulas (1.10)–(1.12) are new for $n \geq 2$; for $n = 1$ these formulas were given in [26], [28].

Somewhat more general version of formulas (1.10)–(1.12) is given as Theorem 3.1; see Subsection 3.1.

One can see that formulas (1.10)–(1.12) and formulas of Theorem 3.1 are completely explicit ! However, a possible practical inconvenience of these formulas is that the differences between the measurement points $x_j(s)$, $j = 1, ..., n$, or $x_j(s)$, $j = n+1, ..., 2n$, in (1.10)–(1.12) (and between the related points in Theorem 3.1) are multiple to $\tau = \tau(k,l) = 2\pi/\kappa$, where $\kappa = \kappa(k,l)$ is defined in (1.9). The inconvenience is that this τ depend on k, l. Besides, these formulas are valid for $d = 3$ but are not valid for $d = 2$ (because of slightly different structure of the asymptotic expansions (3), (19) for ψ^+ for $d = 3$ and for $d = 2$). Therefore, in the present work we also give the following further results without the aforementioned multiplicity condition for the differences between $x_j(s)$, for $d \geq 2$.

We give an explicit version of formulas (1.5), (1.6) for the case of the linearised Problem 1.3 (near $v = 0$) for $d \geq 2$, $m = 2n$, $n \in \mathbb{N}$, where

$$\tau_j = (j-1)\tau,\ j = 1, ..., 2n,\ \tau > 0,\ \tau \neq 0\,(mod\,\frac{\pi}{\kappa}), \tag{1.13}$$

$\kappa = \kappa(k,l)$ in defined in (1.9); see Theorem 3.2 of Subsection 3.2.

We give explicit versions of formulas (1.5), (1.6) for the general non–linearised case for $d = 3$, $m = 3n - 1$, and for $d = 2$, $m = 3n$, where

$$\tau_j = (j-1)\tau,\ j = 1, ..., m,\ \tau > 0, \tau \neq 0\,(mod\,\frac{\pi}{\kappa}), \tag{1.14}$$

$\kappa = \kappa(k,l)$ in defined in (1.9); see Proposition 3.1 of Subsection 3.3 and Proposition 3.2 of Subsection 3.4. For the general non-linearized case, finding such formulas for $m = 2n$ is an open

question for $n > 1$, for $d = 3$ or $d = 2$, under assumption (1.14). We recall that for $n = 1$, $d = 3$, this question was solved in [26], [28]; whereas for $n = 1$, $d = 2$, this question was solved in Section 9 of [29].

Note that τ in (1.13), (1.14) is fixed and independent of k, l (except the property that $\tau \neq 0\,(mod\,\pi/\kappa)$) in contrast with τ in (1.9).

The results of the present work are obtained proceeding from methods developed in [26], [29], [31]. In particular, for fixed $(k,l) \in \mathcal{M}_E$, $l \neq k$, for $d = 3$ or $d = 2$, the work [29] gives a version of formulas (1.5), where

$$\begin{aligned} &x_j(s) = r_j(s)\hat{l},\ j = 1, ..., 2n,\ \hat{l} = l/|l|, \\ &r_{2i-1}(s) = \lambda_i s,\ r_{2i}(s) = \lambda_i s + \tau,\ i = 1, ..., n, \\ &\lambda_1 = 1,\ \lambda_{i_1} < \lambda_{i_2} \text{ for } i_1 < i_2,\ \tau > 0. \end{aligned} \tag{1.15}$$

Formulas (5), (15) realized in [29] are recurrent in n. For $n = 1$, $d = 3$, these formulas were given in [26].

Advantages of formulas (1.5), (1.6) (realized in the present work) in comparison with formulas (5), (15) (realized in [29]) can be summarized as follows:

(a) The geometry of $x_j(s)$ in (1.5), (1.6) is essentially simpler in the sense that the distances between all these points are fixed and are independent of $s \to +\infty$.

(b) Formulas (1.5), (1.6) (realized as formulas (1.10)–(1.12), (3.9)–(3.11), (3.20)–(3.22), (3.28)–(3.31), (3.39)–(3.41)) are drastically more explicit for large n.

Note that the results of the present work essentially use the technique of the recent work [31], where [31] gives explicit asymptotic multipoint formulas for finding f from ψ^+.

Note also that explicit estimates on the reminder $\mathcal{O}(s^{-n})$ in our formulas (1.5), (1.6) can be given proceeding from methods developed in [31], [33].

Numerical aspects of formulas of [26], [28], [29], [33] and of the present article with their applications to Problem 1.2 will be addressed in further works.

In addition to Problem 1.3 and Problem 1.2, there are also other possible formulations of phase retrieval and phaseless inverse scattering problems for equation (1.1) and for other equations of wave propagations. In connection with such other formulations and related results, see, for example, [8], [13], [15], [17], [18], [20], [28], [30], [34], [36], [37], [38], [42] and references therein. Note that formulas of [26], [28], [29] and the present work can be also used for Problems 1.3 and 1.2 when coefficient v in equation (1.1) is replaced, e.g., by an impenetrable obstacle (see, e.g., [9] for definition of impenetrable obstacles).

The further structure of the present article is as follows. In Section 2 we recall, in particular, some results on direct scattering for equation (1.1) under assumptions (1.2) and some formulas of [29] and [31]. The results of the present work on Problem 1.2, consisting in realizations of formulas (1.5), (1.6), are given in Section 3. These results are proved in Sections 4, 5, and 6. In Section 7, for completeness of presentation, we give a sketch of proof of formulas (2.8)–(2.10) for the higher scattering amplitudes f_j, $j \geq 2$.

2 Preliminaries

2.1 Asymptotics of the scattering solutions

We recall that the scattering solutions ψ^+ satisfy the following Lippmann-Schwinger integral equation:

$$\begin{aligned} &\psi^+(x,k) = e^{ikx} + \int_D G^+(x-y,k)v(y)\psi^+(y,k)dy, \\ &G^+(x,k) := -(2\pi)^{-d}\int_{\mathbb{R}^d} \frac{e^{i\xi x}d\xi}{\xi^2 - k^2 - i\cdot 0} = G_0^+(|x|,|k|), \end{aligned} \tag{2.1}$$

where $x, k \in \mathbb{R}^d$, $k^2 = E$; see, for example, [5], [9], [30].

Note also that

$$G^+(x,k) = \frac{e^{i|k||x|}}{2i|k|},\ d=1,$$
$$G^+(x,k) = -\frac{i}{4}H_0^1(|x||k|),\ d=2,\ G^+(x,k) = -\frac{e^{i|k||x|}}{4\pi|x|},\ d=3, \tag{2.2}$$

where H_0^1 is the Hankel function of the first type.

Actually, in the present work, in addition to (1.2), we assume that, for fixed $E > 0$,

$$\text{equation (2.1) is uniquely solvable for } \psi^+(\cdot,k) \in L^\infty(D). \tag{2.3}$$

In addition, if v satisfies (1.2) and is real-valued, then (2.3) is fulfilled automatically.

Remark 2.1. The regularity assumption that $v \in L^\infty(D)$ can be essentially relaxed in (2) (although this assumption is used often in the literature). In the results of Section 3 on Problem 1.3 in place of (2), (18), it is sufficient to assume that v supported in D is such that:

equation (1) for fixed $E > 0$ has an unique solution $\psi^+(\cdot,k)$ specified via Sommerfeld type radiation condition like (3) for each $k \in \mathbb{R}^d$, $k^2 = E$, in Subsections 3.1, 3.3, 3.4;

and in addition $\psi^+(x,k) - e^{ikx}$ is small on ∂D if v is small, where ∂D is regular, in Subsection 3.2.

Proceeding, for example, from (2.1) one can show that the scattering solutions ψ^+ have the following Atkinson-type expansion:

$$\psi^+(x,k) = e^{ikx} + \frac{e^{i|k||x|}}{|x|^{(d-1)/2}}\left(\sum_{j=1}^{N}\frac{f_j(k,|k|\frac{x}{|x|})}{|x|^{j-1}} + \mathcal{O}\left(\frac{1}{|x|^N}\right)\right),\ |x| \to +\infty,\ N \in \mathbb{N}, \tag{2.4}$$

where the coefficients f_j arising in (2.4) are functions defined on $\mathcal{M}_E$; see [3], [39], [25], [29], [31].

Formula (2.4) for $N = 1$ reduces to (1.3). We say that the functions f_j for $j \geq 2$ are the higher scattering amplitudes for equation (1.1).

It is well-known that

$$f_1(k,l) = c(d,|k|)f(k,l), \tag{2.5}$$
$$c(d,|k|) = -\pi i(-2\pi i)^{(d-1)/2}|k|^{(d-3)/2},\ \text{for } \sqrt{-2\pi i} = \sqrt{2\pi}e^{-i\pi/4}, \tag{2.6}$$
$$f(k,l) = (2\pi)^{-d}\int_D e^{-ily}v(y)\psi^+(y,k)dy, \tag{2.7}$$

where $(k,l) \in \mathcal{M}_E$; see, for example, [30].

It is also well-known that $f_j \equiv 0$ for $j \geq 2$, $d = 1$, under assumptions (1.2), (2.3).

Besides, in the present work we also use the following formulas, for $d \geq 2$:

$$f_j(k,l) = (2\pi)^{-d}c(d,|k|)\int_D \varphi_j(y,l)v(y)\psi^+(y,k)dy,\ j \geq 1, \tag{2.8}$$
$$\varphi_1(y,l) = e^{-ily}, \tag{2.9}$$
$$\varphi_j(y,l) = \frac{(d - 3/4 - d^2/4 + (j-1)(j-2))\varphi_{j-1}(y,l) + \Delta_S\varphi_{j-1}(y,l)}{2i|l|(j-1)},\ j \geq 2, \tag{2.10}$$

where Δ_S is the Beltrami-Laplace operator on the unit sphere $\mathbb{S}^{d-1}$, acting with respect to $\hat{l} = l/|l|$. Formulas (23)-(24) follow from (20)-(22) and the following Barrar-Kay-Wilcox type recursion formulas:

$$f_j(y,l) = \frac{(d - 3/4 - d^2/4 + (j-1)(j-2))f_{j-1}(y,l) + \Delta_S f_{j-1}(y,l)}{2i|l|(j-1)},\ j \geq 2, \tag{2.11}$$

see [39] in connection with (2.11) for $d = 3$.

For completeness of the presentation, a sketch of proof of formulas (2.8)–(2.10), for $j \geq 2$, is given in Section 7. Note that the precise form of the recurrent relations (2.10) is not essential for the main results of the present work.

2.2 Asymptotic formulas for $a(x,k)$

Consider the function $a=a(x,k)$ defined by (1.7). Let $\kappa=\kappa(k,|k|\frac{x}{|x|})$ be defined as in (1.9). Let

$$f_j=f_j(k,|k|\frac{x}{|x|}), \tag{2.12}$$

where f_j are the functions arising in (2.4), $j\in\mathbb{N}$, $x,k\in\mathbb{R}^d\setminus\{0\}$. Then $a(x,k)$ can be presented as follows (see [29] for $d=3$ or $d=2$):

$$a(x,k)=a_N(x,k)+\delta_N a(x,k), \tag{2.13}$$

$$a_N(x,k)=a_N^1(x,k)+a_N^2(x,k), \tag{2.14}$$

$$a_N^1(x,k)=\sum_{j=1}^{N}\frac{e^{i|x|\kappa}f_j}{|x|^{j-1}}+\sum_{j=1}^{N}\frac{e^{-i|x|\kappa}\overline{f}_j}{|x|^{j-1}}, \tag{2.15}$$

$$a_N^2=\sum_{j=1}^{N-[(d-1)/2]}\frac{h_j}{|x|^{j-1+(d-1)/2}},\quad h_j=\sum_{\alpha=1}^{j}f_\alpha\overline{f}_{j-\alpha+1}, \tag{2.16}$$

$$\delta_N a(x,k)=\mathcal{O}(|x|^{-N}),\ \text{as}\ |x|\to+\infty, \tag{2.17}$$

where $x\in\mathbb{R}^d\setminus\{0\}$, $k\in\mathbb{R}^d$, $k^2=E>0$, $d\geq 2$, $[\cdot]$ stands for the integer part.

Note that formulas (1.7), (2.4) imply formulas (2.13)–(2.17) as follows:

$$a(x,k)=a_N^1(x,k)+\mathcal{O}(|x|^{-N})+\frac{1}{|x|^{(d-1)/2}}\left(\sum_{j_1=1}^{N}\frac{f_{j_1}}{|x|^{j_1-1}}+\mathcal{O}(|x|^{-N})\right)\left(\sum_{j_2=1}^{N}\frac{\overline{f}_{j_2}}{|x|^{j_2-1}}+\mathcal{O}(|x|^{-N})\right)=$$

$$=a_N^1(x,k)+\mathcal{O}(|x|^{-N})+\frac{1}{|x|^{(d-1)/2}}\left(\sum_{j_1,j_2=1}^{N}\frac{f_{j_1}\overline{f}_{j_2}}{|x|^{j_1-1}|x|^{j_2-1}}+\mathcal{O}(|x|^{-N})\right)\overset{j=j_1+j_2-1}{=}$$

$$=a_N^1(x,k)+\mathcal{O}(|x|^{-N})+\frac{1}{|x|^{(d-1)/2}}\left(\sum_{j=1}^{N}\sum_{j_1=1}^{j}\frac{f_{j_1}\overline{f}_{j-j_1+1}}{|x|^{j-1}}+\mathcal{O}(|x|^{-N})\right)=$$

$$=a_N^1(x,k)+\sum_{j=1}^{N-[(d-1)/2]}\frac{h_j}{|x|^{j-1+(d-1)/2}}+\mathcal{O}(|x|^{-N}), \tag{2.18}$$

where we used the change of variables $(j_1,j_2)\to(j_1,j)$, $j=j_1+j_2-1$.

Consider also the case of the Born approximation for small potentials. Suppose that potential v is small, for example, in the sense of the norm $\|\cdot\|_{L^\infty(D)}$, for fixed D. Then in formulas (2.13)–(2.17) the quadratic term a_N^2 is negligible in comparison with the linear term a_N^1. Such a situation arises in many applications (see, for example, [6], [13], [16], [23], [24], [40], [41]). Thus, in the Born approximation for small potentials formula (2.14) reduces to the formula

$$a_N(x,k)\approx a_N^1(x,k). \tag{2.19}$$

The aforementioned smallness assumption on v can be specified as

$$\|v\|_{L^\infty(D)}=\mathcal{O}(\varepsilon),\ \text{where}\ \varepsilon\to 0. \tag{2.20}$$

Then using (2.1), (2.5)–(2.10), (2.20) one can show that

$$\|f_j\|_{C(\mathcal{M}_E)}=\mathcal{O}(\varepsilon),\ \text{for each}\ j\in\mathbb{N}. \tag{2.21}$$

In turn, formulas (2.14), (2.16) imply that

$$a_N(x,k)-a_N^1(x,k)=|x|^{-(d-1)/2}\mathcal{O}(\varepsilon^2), \tag{2.22}$$

where $N\in\mathbb{N}$.

Formula (2.22) specifies (2.19) under assumption (2.20).

2.3 Some results of [31]

We recall that the work [31] gives, in particular, explicit asymptotic multipoint formulas for finding f_1 from ψ^+ for $d \geq 2$. This work proceeds from formula (2.4) and considers, in particular, the functions $z = z(s)$, $s \in [r, +\infty)$, $r > 0$, of the form

$$z(s) = \sum_{j=1}^{N} \frac{f_j}{s^{j-1}} + \mathcal{O}(s^{-N}), \text{ as } s \to +\infty, \tag{2.23}$$

where f_j, $j = 1, ..., n$, are the complex numbers.

Functions of the form (2.23) arise in the second term on the right-hand side of (2.4), where $s = |x|$. Functions of the form (2.23) also arise in the framework of direct and inverse scattering at high energies for equation (1.1) with smooth v; see [25] and [32].

For functions z satisfying (2.23) the work [31] considers, in particular, the problem of finding f_1 from $z(s)$ given at n points $s_j \in [r, +\infty)$, $j = 1, ..., n$, of the form

$$\begin{aligned} &s_j = s_j(s) = s + \tau_j,\ j = 1, ..., n, \\ &s > r,\ \tau_1 = 0,\ \tau_{j+1} > \tau_j,\ j = 1, ..., n-1, \\ &\vec{\tau} = (\tau_1, ..., \tau_n). \end{aligned} \tag{2.24}$$

Suppose that $N \geq 2n - 1$. Then the following formulas of [31] hold:

$$f_1 = \sum_{j=1}^{n} y_j(s, \vec{\tau}) z(s + \tau_j) + \mathcal{O}(s^{-n}), \text{ as } s \to +\infty, \tag{2.25}$$

where $y_j(s, \vec{\tau})$ are defined by

$$\sum_{j=1}^{n} \frac{y_j(s, \vec{\tau})}{(s + \tau_j)^{i-1}} = \begin{cases} 1, & \text{for } i = 1, \\ 0, & \text{for } i = 2, ..., n; \end{cases} \tag{2.26}$$

in addition:

$$y_j(s, \vec{\tau}) = \frac{(-1)^{n-j}(s + \tau_j)^{n-1}}{\alpha_j(\vec{\tau})\beta_{n,j}(\vec{\tau})},\ 1 \leq j \leq n, \tag{2.27}$$

$$\alpha_j(\vec{\tau}) = \Pi_{k=1}^{j-1}(\tau_j - \tau_k),\ \beta_{n,j}(\vec{\tau}) = \Pi_{k=j+1}^{n}(\tau_k - \tau_j), \tag{2.28}$$

$$\sum_{j=1}^{n} \frac{y_j(s, \vec{\tau})}{(s + \tau_j)^{i-1}} = \mathcal{O}(s^{-n}) \text{ as } s \to +\infty, \text{ for } n < i < 2n. \tag{2.29}$$

3 Main results

3.1 Formulas for finding f_1 from a at $2n$ points for $d = 3$

For $d = 3$, the function $a(x, k)$ of formulas (1.7), (2.13)–(2.17) at fixed k and $\hat{x} = x/|x|$ can be written as

$$a(s) = a(s, \hat{x}, k) := a(s\hat{x}, k), \tag{3.1}$$

$$a(s) = \sum_{j=1}^{N} \frac{e^{is\kappa} f_j + e^{-is\kappa} \overline{f}_j + h_j}{s^{j-1}} + \mathcal{O}(s^{-N}),\ s \to +\infty,\ h_1 = 0, \tag{3.2}$$

$$h_j = \sum_{k=1}^{j-1} f_k \overline{f}_{j-k},\ j = 1, ..., N, \tag{3.3}$$

where $s = |x|$, $\kappa = |k| - k\hat{x}$, and $\kappa > 0$ if $\hat{x} = x/|x| \neq \hat{k} = k/|k|$.

Proceeding from this motivation we consider arbitrary functions $a = a(s)$, $s \in [r, +\infty), r > 0$, such that formula (3.2) holds for some fixed $\kappa > 0$ and some complex numbers f_j, $j = 1, ..., N$, and h_j, $j = 2, ..., N$.

We consider $2n$ points $s_{1,j}$, $s_{2,j} \in [r, +\infty)$, $j = 1, ..., n$, of the form

$$s_{1,j} = s_{1,j}(s) = s + \tau_{1,j}, \ j = 1, ..., n, \tag{3.4}$$

$$s_{2,j} = s_{2,j}(s) = s + \sigma + \tau_{2,j}, \ j = 1, ..., n, \tag{3.5}$$

$$\tau_{1,j} = \nu_{1,j}\tau, \ j = 1, ..., n, \ \tau = \frac{2\pi}{\kappa}, \ 0 = \nu_{1,1} < \nu_{1,2} < ... < \nu_{1,n}, \ \{\nu_{1,j}\} \in \mathbb{N}, \tag{3.6}$$

$$\tau_{2,j} = \nu_{2,j}\tau, \ j = 1, ..., n, \ \tau = \frac{2\pi}{\kappa}, \ 0 = \nu_{2,1} < \nu_{2,2} < ... < \nu_{2,n}, \{\nu_{2,j}\} \in \mathbb{N}, \tag{3.7}$$

$$s > r, \ \sigma > 0, \ \sigma \neq 0 \ (mod \ \frac{\pi}{\kappa}). \tag{3.8}$$

Theorem 3.1. *Let $a = a(s)$ satisfy (3.2) for some $N \geq 2n - 1$, $n \in \mathbb{N}$. Then $a(s)$ at $2n$ points $s_{1,j}$, $s_{2,j}$ of (3.4)–(3.8) approximately determines f_1 as follows:*

$$f_1 = \frac{e^{-i(s+\sigma)\kappa}a_1(s) - e^{-is\kappa}a_2(s) + \mathcal{O}(s^{-n})}{-2i\sin(\sigma\kappa)}, \ s \to +\infty, \tag{3.9}$$

$$a_1(s) := \sum_{j=1}^{n} \frac{(-1)^{n-j}(s_{1,j}(s))^{n-1}a(s_{1,j}(s))}{\tau^{n-1}\Pi_{k=1}^{j-1}(\nu_{1,j} - \nu_{1,k})\Pi_{k=j+1}^{n}(\nu_{1,k} - \nu_{1,j})}, \tag{3.10}$$

$$a_2(s) := \sum_{j=1}^{n} \frac{(-1)^{n-j}(s_{2,j}(s))^{n-1}a(s_{2,j}(s))}{\tau^{n-1}\Pi_{k=1}^{j-1}(\nu_{2,j} - \nu_{2,k})\Pi_{k=j+1}^{n}(\nu_{2,k} - \nu_{2,j})}. \tag{3.11}$$

Remark 3.1. *Suppose that $\nu_{1,j} = \nu_{2,j} = j - 1$, $j = 1, ..., n$. Then formulas (3.10), (3.11) reduce to the formulas*

$$a_1(s) = \sum_{j=1}^{n} \frac{(-1)^{n-j}(s_{1,j}(s))^{n-1}a(s_{1,j}(s))}{(j-1)!(n-j)!\tau^{n-1}}, \tag{3.12}$$

$$a_2(s) = \sum_{j=1}^{n} \frac{(-1)^{n-j}(s_{2,j}(s))^{n-1}a(s_{2,j}(s))}{(j-1)!(n-j)!\tau^{n-1}}. \tag{3.13}$$

Theorem 3.1 is proved in Section 4.

Formulas (3.9)–(3.13) of Theorem 3.1 and Remark 3.1 are completely explicit ! But a possible inconvenience of these formulas is that the differences between the points $s_{1,j}$, $j = 1, ..., n$, or $s_{2,j}, j = 1, ..., n$, are multiple to $2\pi/\kappa$. Below in Subsections 3.2, 3.3, we give approaches for relaxing this multiplicity condition.

Formulas (1.7), (3.1), (3.4)–(3.13) realize (1.5), (1.6) for $d = 3$. In addition, due to formulas (1.7), (2.18), function $a(s)$ defined in (3.1) satisfies (3.2) for any odd $d \geq 3$ for some h_j, where $h_1 = h_2 = ... = h_{(d-1)/2} = 0$ (and further h_j are given by analogs of (2.18) for odd $d > 3$). Therefore, formulas (3.4)–(3.13) remain valid for any odd $d \geq 3$; in fact, these formulas follow just from (3.2).

3.2 Formulas for finding f_1 from a at $2n$ points for small potentials

In the Born approximation for small potentials v formula (2.14) reduces to formula (2.19).

In these framework, the function $a(x, k)$ of (2.13)–(2.17) at fixed k and $\hat{x} = x/|x|$, for $d \geq 2$, can be written as

$$a(x, k) \approx a(s), \tag{3.14}$$

where

$$a(s)=\sum_{j=1}^{N}\frac{e^{is\kappa}f_j+e^{-is\kappa}\overline{f}_j}{s^{j-1}}+\mathcal{O}(s^{-N}),\ s\to+\infty, \tag{3.15}$$

where $s=|x|$, $\kappa=|k|-k\hat{x}$, and $\kappa>0$ if $\hat{x}=x/|x|\neq\hat{k}=k/|k|$. Formulas (3.14), (3.15) follow from (2.13), (2.15), (2.17), (2.19).

Proceeding from this motivation, we consider arbitrary functions $a=a(s)$, $s\in[r,+\infty)$, $r>0$, such that formula (3.15) holds for some fixed $\kappa>0$ and some complex numbers f_j, $j=1,...,N$.

We consider $2n$ points $s_j\in[r,+\infty)$, $j=1,...,2n$, of the form

$$s_j=s_j(s)=s+\tau_j,\ j=1,...,2n, \tag{3.16}$$

$$\tau_j=(j-1)\tau,\ j=1,...,2n, \tag{3.17}$$

$$s>r,\ \tau>0,\ \tau\neq 0\,(mod\,\frac{\pi}{\kappa}). \tag{3.18}$$

Let $\Sigma_{n,\tau}$ be the operator acting on functions u on $[r,+\infty)$ and defined by the formula

$$\Sigma_{n,\tau}u(s)=\sum_{j=1}^{n}\frac{(-1)^{n-j}(s_j(s))^{n-1}u(s_j(s))}{(j-1)!(n-j)!\tau^{n-1}},\ s\in[r,+\infty), \tag{3.19}$$

where s_j are defined according to (3.16)–(3.18), $j=1,...,n$.

Theorem 3.2. *Let $a=a(s)$ satisfy (3.15) for some $N\geq 2n-1$, $n\in\mathbb{N}$. Let $\Sigma_{n,\tau}$ be defined by (3.19). Then $a(s)$ at $2n$ points s_j of (3.16)–(3.18) approximately determines f_1 as follows:*

$$f_1=C(\kappa,\tau,n)(\tau^{n-1}(e^{-2i\tau\kappa}a_2(s)-a_2(s+\tau))+\mathcal{O}(s^{-n})),\ s\to+\infty, \tag{3.20}$$

$$a_2(s):=\Sigma_{n,\tau}a_1(s),\ a_1(s):=\frac{e^{-2is\kappa}}{s^{n-1}}\Sigma_{n,\tau}(e^{is\kappa}a)(s), \tag{3.21}$$

$$C(\kappa,\tau,n):=\frac{(n-1)!}{(e^{2i\tau\kappa}-1)^{n-1}(e^{-2i\tau\kappa}-1)}. \tag{3.22}$$

Remark 3.2. *For $\Sigma_{n,\tau}$ defined by (3.19) and $2n$ points s_j of (3.16)–(3.18), we have that*

$$\Sigma_{n,\tau}(w_2\Sigma_{n,\tau}(w_1u))(s)=$$
$$=\sum_{1\leq j_1,\,j_2\leq n}\frac{(-1)^{j_1+j_2}(s_{j_1}(s))^{n-1}(s_{j_1+j_2-1}(s))^{n-1}w_2(s_{j_1}(s))w_1(s_{j_1+j_2-1}(s))}{(j_1-1)!(n-j_1)!(j_2-1)!(n-j_2)!\tau^{2n-2}}u(s_{j_1+j_2-1}(s)), \tag{3.23}$$

where w_1, w_2 are fixed functions on $[r,+\infty)$, and u is a test function on $[r,+\infty)$. In addition,

$$s_{j_1+j_2-1}(s+\tau)=s_{j_1+j_2}(s),\ 1\leq j_1,j_2\leq n. \tag{3.24}$$

Formulas (3.23), (3.24) explain that formula (3.20) involves $a(s)$ exactly in $2n$ points s_j of (3.16)–(3.18), $j=1,...,2n$. Actually, formula (3.23) explains that computing $a_2(s)$ via (3.21) requires $a(s)$ in $2n-1$ points s_j of (3.16)–(3.18), $j=1,...,2n-1$; formulas (3.24), (3.23), (3.20) explain that computing $a_2(s+\tau)$ requires $a(s)$ in shifted $2n-1$ points s_j of (3.16)–(3.18), $j=2,...,2n$.

Theorem 3.2 is proved in Section 5.

Note that formulas (3.20)–(3.22) for finding f_1 from $a(s)$ coincide with formulas (3.9)–(3.11) for the case when $N=n=1$, $\sigma=\tau$.

Note also that Theorem 3.2 is used in the proofs of Propositions 3.1 and 3.2; see Subsections 3.3, 3.4 and Section 6.

3.3 Formulas for finding f_1 from a at $3n-1$ points for $d=3$

In this Subsection we give formulas for finding f_1 up to $\mathcal{O}(s^{-n})$, as $s\to+\infty$, from $a(s_j(s))$, $j=1,...,3n-1$, where $a(s)$ is defined by (3.1), $s_j=s_j(s)$ are the points of (3.25)–(3.27). We use that $a(s)$ satisfies (3.2). In constrast to Theorem 3.1, we do not assume that differences between some of these points are multiple to π/κ. In addition, in constrast to Theorem 3.2, we do not assume that a is reduced to the linearised a of the form (3.15). On the other hand, the disadvantage of approximate finding f_1 mentioned above, is that this finding uses a at $3n-1$ points, in contrast to $2n$ points of Theorems 3.1 and 3.2.

We consider $3n-1$ points $s_j\in[r,+\infty)$, $j=1,...,3n-1$, of the form

$$s_j=s_j(s)=s+\tau_j,\ j=1,...,3n-1, \tag{3.25}$$

$$\tau_j=(j-1)\tau,\ j=1,...,3n-1, \tag{3.26}$$

$$s>r,\ \tau>0,\ \tau\neq 0\,(mod\,\frac{\pi}{\kappa}). \tag{3.27}$$

Proposition 3.3. *Let $a=a(s)$ satisfy (3.2) for some $N\geq 2n-1$, $n\in\mathbb{N}$. Let $\Sigma_{n,\tau}$ be defined by (3.19). Then $a(s)$ at $3n-1$ points s_j of (3.25)–(3.27) approximately determines f_1 as follows:*

$$f_1=C_1(\kappa,\tau,n)(\tau^{n-1}(e^{-2i\tau\kappa}a_2(s)-a_2(s+\tau))+\mathcal{O}(s^{-n})),\ s\to+\infty, \tag{3.28}$$

$$a_2(s):=\Sigma_{n,\tau}a_1(s),\ a_1(s):=\frac{e^{-2is\kappa}}{s^{n-1}}\Sigma_{n,\tau}(e^{is\kappa}a_0)(s), \tag{3.29}$$

$$a_0(s):=\frac{1}{s^{n-1}}\Sigma_{n,\tau}a(s), \tag{3.30}$$

$$C_1(\kappa,\tau,n)=\frac{(n-1)!\tau^{n-1}}{(e^{i\tau\kappa}-1)^{n-1}}C(\kappa,\tau,n), \tag{3.31}$$

where $C(\kappa,\tau,n)$ is given by (3.22).

Remark 3.3. *For $\Sigma_{n,\tau}$ defined by (3.19) and $3n-1$ points s_j of (3.25)–(3.27), we have that*

$$\Sigma_{n,\tau}(w_3\Sigma_{n,\tau}(w_2\Sigma_{n,\tau}w_1u))(s)=$$
$$=\sum_{1\leq j_1,j_2,j_3\leq n}\frac{(-1)^{n+j_1+j_2+j_3}(s_{j_1}(s))^{n-1}(s_{j_1+j_2-1}(s))^{n-1}(s_{j_1+j_2+j_3-2}(s))^{n-1}}{(j_1-1)!(n-j_1)!(j_2-1)!(n-j_2)!(j_3-1)!(n-j_3)!\tau^{3n-3}}\times$$
$$w_3(s_{j_1}(s))w_2(s_{j_1+j_2-1}(s))w_1(s_{j_1+j_2+j_3-2}(s))u(s_{j_1+j_2+j_3-2}(s)), \tag{3.32}$$

where w_1, w_2, w_3 are fixed functions on $[r,+\infty)$, and u is a test function on $[r,+\infty)$. In addition,

$$s_{j_1+j_2+j_3-2}(s+\tau)=s_{j_1+j_2+j_3-1}(s),\ 1\leq j_1,j_2,j_3\leq n. \tag{3.33}$$

Formulas (3.32), (3.33) explain that formula (3.28) involves $a(s)$ exactly in $3n-1$ points s_j of (3.25)–(3.27), $j=1,...,3n-1$. Actually, formulas (3.29), (3.30) and (3.32) explain that computing $a_2(s)$ via (3.29), (3.30) involves $a(s)$ in $3n-2$ points s_j of (3.25)–(3.27), $j=1,...,3n-2$; formulas (3.32), (3.33) explain that computing $a_2(s+\tau)$ via formulas (3.29), (3.30) requires $a(s)$ in shifted $3n-2$ points s_j of (3.25)–(3.27), $j=2,...,3n-1$.

Proposition 3.1 is proved in Section 6.

Note that formulas (3.1), (3.25)–(3.31) for finding f_1 from a remain valid for any odd $d\geq 3$, in a similar way with formulas (3.1), (3.4)–(3.13).

Note also that formulas (3.28)–(3.31) for finding f_1 from $a(s)$ coincide with formulas (3.9)–(3.11) and with formulas (3.20)–(3.22) for the case when $N=n=1$, $\sigma=\tau$. For this case these formulas were given in [26], [28].

3.4 Formulas for finding f_1 from a at $3n$ points for $d = 2$

For $d = 2$, the function $a(x, k)$ of formulas (1.7), (2.13)–(2.17) at fixed k and $\hat{x} = x/|x|$ can be written as $a(s)$ defined according to (3.1), where

$$a(s) = \sum_{j=1}^{N} \frac{e^{is\kappa} f_j + e^{-is\kappa}\overline{f}_j}{s^{j-1}} + \sum_{j=1}^{N} \frac{h_j}{s^{j-1/2}} + \mathcal{O}\left(\frac{1}{s^N}\right), \ s \to +\infty, \tag{3.34}$$

$$h_j = \sum_{k=1}^{j} f_k \overline{f}_{j-k+1}, \ j = 1, ..., N, \tag{3.35}$$

where $s = |x|$, $\kappa = |k| - k\hat{x}$, and $\kappa > 0$ if $\hat{x} = x/|x| \neq \hat{k} = k/|k|$.

Proceeding from this motivation, we consider arbitrary functions $a = a(s)$, $s \in [r, +\infty)$, $r > 0$, such that formula (3.34) holds for some fixed $\kappa > 0$ and some complex numbers f_j, $j = 1, ..., N$, and h_j, $j = 1, ..., N$.

In this Subsection we give formulas for finding f_1 up to $\mathcal{O}(s^{-n})$, as $s \to +\infty$, from $a(s_j(s))$, $j = 1, ..., 3n$, where $a(s)$ is of the form (3.34), $s_j = s_j(s)$ are the points of (3.36)–(3.38). In constrast to Theorem 3.2, we do not assume that a is reduced to the linearised a of the form (3.15). On the other hand, the disadvantage of approximate finding f_1 mentioned above, is that this finding uses a at $3n$ points, in contrast to $2n$ points of Theorem 3.2.

We consider $3n$ points $s_j \in [r, +\infty)$, $j = 1, ..., 3n$ of the form

$$s_j(s) = s + \tau_j, \ j = 1, ..., 3n, \tag{3.36}$$

$$\tau_j = (j-1)\tau, \ j = 1, ..., 3n, \tag{3.37}$$

$$s \geq r > 0, \ \tau > 0, \tau \neq 0 \ (mod \ \frac{\pi}{\kappa}). \tag{3.38}$$

Proposition 3.4. *Let $a(s)$ satisfy (3.34) for some $N \geq 2n + 1$, $n \in \mathbb{N}$. Let $\Sigma_{n,\tau}$ be defined by (3.19). Then $a(s)$ at $3n$ points s_j of (3.36)–(3.38) approximately determines f_1 as follows:*

$$f_1 = C_2(\kappa, \tau, n)(\tau^{n-1}(e^{-2i\tau\kappa}a_3(s) - a_3(s+\tau)) + \mathcal{O}(s^{-n})), \ s \to +\infty, \tag{3.39}$$

$$a_3(s) := \Sigma_{n,\tau}a_2(s), \ a_2(s) := \frac{e^{-2is\kappa}}{s^{n-1}}\Sigma_{n,\tau}(e^{is\kappa}a_1)(s), \ a_1(s) = \frac{1}{s^{n-1/2}}\Sigma_{n+1,\tau}a_0(s), \ a_0(s) = a(s)/\sqrt{s}, \tag{3.40}$$

$$C_2(\kappa, \tau, n) = \frac{n!(n-1)!\tau^n}{(e^{i\tau\kappa} - 1)^n(e^{2i\tau\kappa} - 1)^{n-1}(e^{-2i\tau\kappa} - 1)}. \tag{3.41}$$

Remark 3.4. *For $\Sigma_{n,\tau}$ defined by (3.19) and $3n$ points s_j of (3.36)–(3.38), we have that*

$$\begin{aligned}
&\Sigma_{n,\tau}(w_3\Sigma_{n,\tau}(w_2\Sigma_{n+1,\tau}w_1u))(s) = \\
&= \sum_{1\leq j_1, j_2\leq n} \sum_{1\leq j_3\leq n+1} \frac{(-1)^{n+j_1+j_2+j_3}(s_{j_1}(s))^{n-1}(s_{j_1+j_2-1}(s))^{n-1}(s_{j_1+j_2+j_3-2}(s))^{n-1}}{(j_1-1)!(n-j_1)!(j_2-1)!(n-j_2)!(j_3-1)!(n-j_3)!\tau^{3n-3}} \times \\
&\times w_3(s_{j_1}(s))w_2(s_{j_1+j_2-1}(s))w_1(s_{j_1+j_2+j_3-2}(s))u(s_{j_1+j_2+j_3-2}(s)),
\end{aligned} \tag{3.42}$$

where w_1, w_2, w_3 are fixed functions on $[r, +\infty)$, and u is a test function on $[r, +\infty)$. In addition,

$$s_{j_1+j_2+j_3-2}(s+\tau) = s_{j_1+j_2+j_3-1}(s), \ 1 \leq j_1, j_2, j_3 \leq n. \tag{3.43}$$

Formulas (3.42), (3.43) explain that formulas (3.39) involves $a(s)$ exactly in $3n$ points s_j of (3.36)–(3.38), $j = 1, ..., 3n$. Actually, formulas (3.42) and (3.40) explain that computing $a_2(s)$ via (3.40) involves $a(s)$ in $3n - 1$ points s_j of (3.36)–(3.38), $j = 1, ..., 3n - 1$; formulas (3.42), (3.43) explain that computing $a_2(s + \tau)$ via formulas (3.40) involves $a(s)$ in $3n - 1$ shifted points s_j of (3.36)–(3.38), $j = 2, ..., 3n$.

Proposition 3.2 is proved in Section 6.

Note that formulas (3.1), (3.36)–(3.41) for finding f_1 from a remain valid for any even $d \geq 2$, in a similar way with formulas (3.1), (3.4)–(3.13), (3.25)–(3.31) for odd $d \geq 3$.

4 Proof of Theorem 3.1

Let

$$\vec{\tau}_1 = (\tau_{1,1}, ..., \tau_{1,n}),\ \vec{\tau}_2 = (\tau_{2,1}, ..., \tau_{2,n}). \tag{4.1}$$

Let $y_j(s, \vec{\tau}_1), y_j(s, \vec{\tau}_2)$, $j = 1, ..., n$, be defined according to (2.26), (2.27). We have that

$$a_1(s) = \sum_{j=1}^{n} y_j(s, \vec{\tau}_1) a(s_{1,j}(s)),\ a_2(s) = \sum_{j=1}^{n} y_j(s, \vec{\tau}_2) a(s_{2,j}(s)). \tag{4.2}$$

Note that

$$\begin{aligned} e^{is_{1,j}(s)\kappa} &= e^{is\kappa} e^{i\nu_{1,j}\tau\kappa} = e^{is\kappa},\ \ j = 1, ..., n, \\ e^{is_{2,j}(s)\kappa} &= e^{i(s+\sigma)\kappa} e^{i\nu_{2,j}\tau\kappa} = e^{i(s+\sigma)\kappa},\ \ j = 1, ..., n. \end{aligned} \tag{4.3}$$

Using formulas (2.26)–(2.29), (3.2), (4.2), (4.3) and the assumption that $N \geq 2n-1$, we obtain that:

$$\begin{aligned} a_1(s) &= \sum_{j=1}^{n} y_j(s, \vec{\tau}_1) \left(\sum_{m=1}^{N} \frac{e^{is_{1,j}(s)\kappa} f_m + e^{-is_{1,j}(s)\kappa} \overline{f}_m + h_m}{(s + \tau_{1,j})^{m-1}} + \mathcal{O}(s^{-N}) \right) = \\ &= \sum_{m=1}^{N} (e^{is\kappa} f_m + e^{-is\kappa} \overline{f}_m + h_m) \sum_{j=1}^{n} \frac{y_j(s, \vec{\tau}_1)}{(s + \tau_{1,j})^{m-1}} + \mathcal{O}(s^{-n}) = \\ &= e^{is\kappa} f_1 + e^{-is\kappa} \overline{f}_1 + \mathcal{O}(s^{-n}),\ \ \text{as } s \to +\infty; \end{aligned} \tag{4.4}$$

$$\begin{aligned} a_2(s) &= \sum_{j=1}^{n} y_j(s, \vec{\tau}_2) \left(\sum_{m=1}^{N} \frac{e^{is_{2,j}(s)\kappa} f_m + e^{-is_{2,j}(s)\kappa} \overline{f}_m + h_m}{(s + \sigma + \tau_{2,j})^{m-1}} + \mathcal{O}(s^{-N}) \right) = \\ &= \sum_{m=1}^{N} (e^{i(s+\sigma)\kappa} f_m + e^{-i(s+\sigma)\kappa} \overline{f}_m + h_m) \sum_{j=1}^{n} \frac{y_j(s, \vec{\tau}_2)}{(s + \sigma + \tau_{2,j})^{m-1}} + \mathcal{O}(s^{-n}) = \\ &= e^{i(s+\sigma)\kappa} f_1 + e^{-i(s+\sigma)\kappa} \overline{f}_1 + \mathcal{O}(s^{-n}),\ \ \text{as } s \to +\infty. \end{aligned} \tag{4.5}$$

We consider formulas (4.4), (4.5) as a linear system for approximate finding f_1, $\overline{f}_1$ from $a_1(s)$, $a_2(s)$, where s is sufficiently large.

If $\sigma > 0$, $\sigma \neq 0\,(mod\ \pi/\kappa)$, then from (4.4), (4.5) we obtain that

$$\begin{pmatrix} f_1 \\ \overline{f}_1 \end{pmatrix} = \frac{1}{e^{-i\sigma\kappa} - e^{i\sigma\kappa}} \begin{pmatrix} e^{-i(s+\sigma)\kappa} & -e^{-is\kappa} \\ -e^{i(s+\sigma)\kappa} & e^{is\kappa} \end{pmatrix} \begin{pmatrix} a_1(s) + & \mathcal{O}(s^{-n}) \\ a_2(s) + & \mathcal{O}(s^{-n}) \end{pmatrix}. \tag{4.6}$$

Formula (3.9) follows from (4.6).

Theorem 3.1 is proved.

5 Proof of Theorem 3.2

Lemma 5.1. *Let $\Sigma_{n,\tau}$ be defined via (3.19). Let*

$$u(s) = \sum_{j=1}^{N} \frac{e^{is\kappa} f_j}{s^{j-1}},\ s \in [r, +\infty), \tag{5.1}$$

for some fixed $\kappa \in \mathbb{R}$ and some complex numbers $f_j, j = 1, ..., N$, where $N \geq 2n-1$. Then:

$$\Sigma_{n,\tau} u(s) = s^{n-1} \sum_{m=1}^{2n-1} \frac{e^{is\kappa} f_{m,\kappa}}{s^{m-1}} + \mathcal{O}(s^{-n}),\ s \in [r, +\infty), \tag{5.2}$$

$$f_{m,\kappa} = f_{m,\kappa,n,\tau}(f_1, ..., f_m) = \sum_{j_2=1}^{m} \frac{f_{j_2} C_{n-j_2}^{m-j_2}}{\tau^{n-1}} \sum_{j_1=1}^{n} \frac{(-1)^{n-j_1} \tau_{j_1}^{m-j_2} e^{i\tau_{j_1}\kappa}}{(j_1-1)!(n-j_1)!},\ \forall m = 1, ..., 2n-1, \tag{5.3}$$

where C_β^α denote the binomial coefficients,

$$f_{1,\kappa} = \frac{(e^{i\tau\kappa}-1)^{n-1}}{(n-1)!\tau^{n-1}} f_1, \tag{5.4}$$

$$f_{n,\kappa} = \frac{(e^{i\tau\kappa}-1)^{n-1}}{(n-1)!\tau^{n-1}} f_n \text{ if } f_1 = ... = f_{n-1} = 0. \tag{5.5}$$

Proof of Lemma 5.1. Using (3.19), (5.1), we obtain that

$$\Sigma_{n,\tau} u(s) = \sum_{j_1=1}^{n} \sum_{j_2=1}^{N} \frac{(-1)^{n-j_1}(s+\tau_{j_1})^{n-1}}{(j_1-1)!(n-j_1)!\tau^{n-1}} \frac{e^{i(s+\tau_{j_1})\kappa} f_{j_2}}{(s+\tau_{j_1})^{j_2-1}} =$$

$$= \frac{e^{is\kappa}}{\tau^{n-1}} \sum_{j_2=1}^{N} f_{j_2} \sum_{j_1=1}^{n} \frac{(-1)^{n-j_1}(s+\tau_{j_1})^{n-j_2} e^{i\tau_{j_1}\kappa}}{(j_1-1)!(n-j_1)!},\ s \in [r, +\infty). \tag{5.6}$$

$$\tag{5.7}$$

Note that

$$(s+\tau_{j_1})^{n-j_2} = \sum_{j_3=0}^{n-j_2} C_{n-j_2}^{j_3} s^{n-j_2-j_3} \tau_{j_1}^{j_3} = \sum_{j_3=0}^{2n-j_2-1} C_{n-j_2}^{j_3} \tau_{j_1}^{j_3} s^{n-j_2-j_3},\ n-j_2 \geq 0, \tag{5.8}$$

$$(s+\tau_{j_1})^{n-j_2} = \frac{1}{s^{j_2-n}} \sum_{j_3=0}^{\infty} C_{n-j_2}^{j_3} \tau_{j_1}^{j_3} s^{-j_3} = \sum_{j_3=0}^{2n-j_2-1} C_{n-j_2}^{j_3} \tau_{j_1}^{j_3} s^{n-j_2-j_3} + \mathcal{O}(s^{-n}),\ n-j_2 < 0, \tag{5.9}$$

where C_β^α are the binomial coefficients; we used in (5.8) that $C_\beta^\alpha = 0$, for $\alpha > \beta$, if $\beta \in \mathbb{N}$. Using (5.6), (5.8), (5.9) we obtain that

$$\frac{\Sigma_{n,\tau} u(s)}{s^{n-1}} = \frac{e^{is\kappa}}{\tau^{n-1}} \sum_{j_2=1}^{N} f_{j_2} \sum_{j_1=1}^{n} \frac{(-1)^{n-j_1} \sum_{j_3=0}^{2n-j_2-1} (C_{n-j_2}^{j_3} \tau_{j_1}^{j_3} / s^{j_2+j_3-1}) e^{i\tau_{j_1}\kappa}}{(j_1-1)!(n-j_1)!} + \mathcal{O}(s^{-2n+1}) =$$

$$= \frac{e^{is\kappa}}{\tau^{n-1}} \sum_{j_2=1}^{2n-1} f_{j_2} \sum_{j_1=1}^{n} \frac{(-1)^{n-j_1} \sum_{j_3=0}^{2n-j_2-1} (C_{n-j_2}^{j_3} \tau_{j_1}^{j_3} / s^{j_2+j_3-1}) e^{i\tau_{j_1}\kappa}}{(j_1-1)!(n-j_1)!} + \mathcal{O}(s^{-2n+1}) =$$

$$= \frac{e^{is\kappa}}{\tau^{n-1}} \sum_{j_3=0}^{2n-2} \sum_{j_2=1}^{2n-j_3-1} \frac{f_{j_2} C_{n-j_2}^{j_3}}{s^{j_2+j_3-1}} \sum_{j_1=1}^{n} \frac{(-1)^{n-j_1} \tau_{j_1}^{j_3} e^{i\tau_{j_1}\kappa}}{(j_1-1)!(n-j_1)!} + \mathcal{O}(s^{-2n+1}) \overset{m=j_2+j_3}{=}$$

$$= \sum_{m=1}^{2n-1} \frac{e^{is\kappa}}{s^{m-1}} \sum_{j_2=1}^{m} \frac{f_{j_2} C_{n-j_2}^{m-j_2}}{\tau^{n-1}} \sum_{j_1=1}^{n} \frac{(-1)^{n-j_1} \tau_{j_1}^{m-j_2} e^{i\tau_{j_1}\kappa}}{(j_1-1)!(n-j_1)!} + \mathcal{O}(s^{-2n+1}) = \sum_{m=1}^{2n-1} \frac{e^{is\kappa} f_{m,\kappa}}{s^{m-1}} + \mathcal{O}(s^{-2n+1}), \tag{5.10}$$

where

$$f_{m,\kappa} = \sum_{j_2=1}^{m} \frac{f_{j_2} C_{n-j_2}^{m-j_2}}{\tau^{n-1}} \sum_{j_1=1}^{n} \frac{(-1)^{n-j_1} \tau_{j_1}^{m-j_2} e^{i\tau_{j_1}\kappa}}{(j_1-1)!(n-j_1)!}, \tag{5.11}$$

$$f_{1,\kappa} = \frac{f_1 C_{n-1}^0}{\tau^{n-1}} \sum_{j=1}^{n} \frac{(-1)^{n-j} e^{i\tau(j-1)\kappa}}{(j-1)!(n-j)!} = \frac{(e^{i\tau\kappa}-1)^{n-1}}{(n-1)!\tau^{n-1}} f_1. \tag{5.12}$$

Note that in (5.10) we used the change of variables $(j_1, j_2, j_3) \to (j_1, j_2, m)$, $m = j_2 + j_3$.

Formulas (5.2), (5.4) follows from (5.10), (5.11), (5.12).

In addition, if $f_1 = ... = f_{n-1} = 0$, then

$$f_{n,\kappa} = f_n \frac{C_0^0}{\tau^{n-1}} \sum_{j=1}^{n} \frac{(-1)^{n-j} e^{i(j-1)\tau\kappa}}{(j-1)!(n-j)!} = \frac{(e^{i\tau\kappa}-1)^{n-1}}{(n-1)!\tau^{n-1}} f_n. \tag{5.13}$$

Lemma 5.1 is proved.

The rest of the proof of Theorem 3.2 is as follows. Due to (3.15), we have that

$$\begin{aligned} &e^{is\kappa}a(s) = u(s) + z(s), \\ &u(s) = \sum_{j=1}^{N} \frac{e^{2is\kappa} f_j}{s^{j-1}}, \quad z(s) = \sum_{j=1}^{N} \frac{\overline{f}_j}{s^{j-1}} + \mathcal{O}(s^{-N}), \ \text{ as } s \to +\infty. \end{aligned} \tag{5.14}$$

Due to formulas (2.25), (2.27), (2.29), (3.19), and the formula for z in (5.14), we have that

$$\Sigma_{n,\tau} z(s) = \overline{f}_1 + \mathcal{O}(s^{-n}), \ \text{ as } s \to +\infty. \tag{5.15}$$

Due to Lemma 5.1 (with 2κ in place of κ) and the formula for u in (5.14), we have that

$$\begin{aligned} &\Sigma_{n,\tau} u(s) = s^{n-1} \sum_{m=1}^{2n-1} \frac{e^{2is\kappa} f_{m,2\kappa}}{s^{m-1}} + \mathcal{O}(s^{-n}), \ \text{ where} \\ &f_{1,2\kappa} = \frac{(e^{2i\tau\kappa}-1)^{n-1}}{(n-1)!\tau^{n-1}} f_1. \end{aligned} \tag{5.16}$$

Due to (5.14), (5.15), (5.16), we have that

$$\Sigma_{n,\tau}(e^{is\kappa}a)(s) = s^{n-1} \sum_{m=1}^{2n-1} \frac{e^{2is\kappa} f_{m,2\kappa}}{s^{m-1}} + \mathcal{O}(s^{-n}) + \overline{f}_1 + \mathcal{O}(s^{-n}), \ \text{ as } s \to +\infty. \tag{5.17}$$

The definition of a_1 in (3.21) and formula (5.17) imply that

$$\begin{aligned} &a_1(s) = u_1(s) + z_1(s), \ \text{ where} \\ &u_1(s) = \frac{e^{-2is\kappa}\overline{f}_1}{s^{n-1}}, \ z_1(s) = \sum_{m=1}^{2n-1} \frac{f_{m,2\kappa}}{s^{m-1}} + \mathcal{O}(s^{-2n+1}), \ \text{ as } s \to +\infty. \end{aligned} \tag{5.18}$$

Due to formulas (2.25), (2.27), (2.29), (3.19), and the formula for z_1 in (5.18), we have that

$$\Sigma_{n,\tau} z_1(s) = f_{1,2\kappa} + \mathcal{O}(s^{-n}), \ \text{ as } s \to +\infty. \tag{5.19}$$

Besides, the following formula holds,

$$\Sigma_{n,\tau} u_1(s) = e^{-2is\kappa}\overline{f}_{1,-2\kappa}, \quad \overline{f}_{1,-2\kappa} = \frac{(e^{-2i\tau\kappa}-1)^{n-1}}{(n-1)!\tau^{n-1}}\overline{f}_1. \tag{5.20}$$

Formula (5.20) follows from formulas (5.2), (5.3), (5.5) of Lemma 5.1, with (-2κ) in place of κ, $f_n = \overline{f}_1$, where $\overline{f}_1$ is the number in definition of u_1 in (5.18).

The definition of a_2 in (3.21) and formulas (5.16), (5.18)–(5.20) imply that

$$\begin{aligned} &a_2(s) = f_{1,2\kappa} + e^{-2is\kappa}\overline{f}_{1,-2\kappa} + \mathcal{O}(s^{-n}) = \\ &= \frac{(e^{2i\tau\kappa}-1)^{n-1} f_1 + e^{-2is\kappa}(e^{-2i\tau\kappa}-1)^{n-1}\overline{f}_1}{(n-1)!\tau^{n-1}} + \mathcal{O}(s^{-n}), \ s \to +\infty. \end{aligned} \tag{5.21}$$

From (5.21) we obtain that

$$(e^{2i\tau\kappa}-1)^{n-1}f_1+e^{-2is\kappa}(e^{-2i\tau\kappa}-1)^{n-1}\overline{f}_1=(n-1)!\tau^{n-1}a_2(s)+\mathcal{O}(s^{-n}),\ s\to+\infty, \tag{5.22}$$
$$(e^{2i\tau\kappa}-1)^{n-1}f_1+e^{-2i(s+\tau)\kappa}(e^{-2i\tau\kappa}-1)^{n-1}\overline{f}_1=(n-1)!\tau^{n-1}a_2(s+\tau)+\mathcal{O}(s^{-n}),\ s\to+\infty.$$

We consider formulas (5.22) as a linear system for approximate finding f_1, $\overline{f}_1$ from $(n-1)!\tau^{n-1}a_2(s)$, $(n-1)!\tau^{n-1}a_2(s+\tau)$, where s is sufficiently large. From this system, for $\tau>0$, $\tau\neq 0\,(mod\,\pi/\kappa)$, we obtain that

$$\begin{pmatrix}f_1\\ \overline{f}_1\end{pmatrix}=\frac{1}{(e^{2i\tau\kappa}-1)^{n-1}(e^{-2i\tau\kappa}-1)^{n-1}e^{-2is\kappa}(e^{-2i\tau\kappa}-1)}\times$$
$$\begin{pmatrix}e^{-2i(s+\tau)\kappa}(e^{-2i\tau\kappa}-1)^{n-1} & -e^{-2is\kappa}(e^{-2i\tau\kappa}-1)^{n-1}\\ -(e^{2i\tau\kappa}-1)^{n-1} & (e^{2i\tau\kappa}-1)^{n-1}\end{pmatrix}\begin{pmatrix}(n-1)!\tau^{n-1}a_2(s)+\mathcal{O}(s^{-n})\\ (n-1)!\tau^{n-1}a_2(s+\tau)+\mathcal{O}(s^{-n})\end{pmatrix},\ s\to+\infty. \tag{5.23}$$

Formula (5.23) implies that

$$f_1=\frac{(n-1)!\tau^{n-1}(e^{-2i\tau\kappa}a_2(s)-a_2(s+\tau))+\mathcal{O}(s^{-n})}{(e^{2i\tau\kappa}-1)^{n-1}(e^{-2i\tau\kappa}-1)},\ s\to+\infty. \tag{5.24}$$

This completes the proof of Theorem 3.2.

6 Proofs of Propositions 3.1 and 3.2

Proof of Proposition 3.1. The following formula holds:

$$\Sigma_{n,\tau}a(s)=s^{n-1}\sum_{m=1}^{n}\frac{e^{is\kappa}f_{m,\kappa}+e^{-is\kappa}\overline{f}_{m,-\kappa}}{s^{m-1}}+\mathcal{O}(s^{-n}),\ s\to+\infty, \tag{6.1}$$

where $f_{m,\kappa}$ and $\overline{f}_{m,-\kappa}$ are defined according to (5.3) in terms of $f_1,...,f_m$ and $\overline{f}_1,...,\overline{f}_m$, respectively. In particular, according to (5.4), we have that

$$f_{1,\kappa}=\frac{(e^{i\tau\kappa}-1)^{n-1}}{(n-1)!\tau^{n-1}}f_1,\ \overline{f}_{1,-\kappa}=\frac{(e^{-i\tau\kappa}-1)^{n-1}}{(n-1)!\tau^{n-1}}\overline{f}_1. \tag{6.2}$$

Formula (6.1) follows from formula (3.2), Lemma 5.1 and formulas (2.25), (2.27), (2.29), (3.19).

Formula (3.28), where a_2 is defined by (3.29), (3.30), follows from formulas (6.1), (6.2), and Theorem 3.2.

Proposition 3.1 is proved.

Proof of Proposition 3.2. Assume that

$$n\tau/s<1,\ \text{where } s\geq r>0. \tag{6.3}$$

From the definition of a_0 in (3.40) and formula (3.34) we have that

$$a_0(s)=\sum_{j=1}^{N}\frac{e^{is\kappa}f_j}{s^{j-1/2}}+\sum_{j=1}^{N}\frac{e^{-is\kappa}\overline{f}_j}{s^{j-1/2}}+\left(\sum_{j=2}^{N}\frac{h_{j-1}}{s^{j-1}}+\mathcal{O}\left(\frac{1}{s^N}\right)\right)=:a_{0,1}(s)+a_{0,2}(s)+a_{0,3}(s). \tag{6.4}$$

Using that $N\geq 2n+1$ and formulas (2.23), (2.25) with $n+1$ in place of n, we obtain that

$$\Sigma_{n+1,\tau}a_{0,3}(s)=\mathcal{O}(s^{-(n+1)}),\ s\to+\infty. \tag{6.5}$$

We also have that

$$\Sigma_{n+1,\tau}a_{0,1}(s)=\sum_{j=1}^{n+1}\frac{(-1)^{n+1-j}(s+\tau_j)^n\sum_{k=1}^{N}e^{i(s+\tau_j)\kappa}f_k/(s+\tau_j)^{k-1/2}}{(j-1)!(n+1-j)!\tau^n}=$$

$$=e^{is\kappa}\sum_{j=1}^{n+1}\sum_{k=1}^{N}\frac{(-1)^{n+1-j}(s+\tau_j)^{n-k+1/2}e^{i(j-1)\tau\kappa}f_k}{(j-1)!(n+1-j)!\tau^n}. \tag{6.6}$$

Note that

$$\frac{(s+\tau_j)^{n-k+1/2}}{s^{n-1/2}}=\frac{(1+\tau_j/s)^{n-k+1/2}}{s^{k-1}}, \tag{6.7}$$

$$(1+\tau_j/s)^{n-k+1/2}=\sum_{l=0}^{2n}C^l_{n-k+1/2}\left(\frac{\tau_j}{s}\right)^l+\mathcal{O}(s^{-2n-1}),\ s\to+\infty, \tag{6.8}$$

where in (6.8) we used assumption (6.3) and that $\tau_j=(j-1)\tau$, $j=1,...,n+1$. Using that $N\geq 2n+1$ and formulas (6.6), (6.7), (6.8), we obtain that

$$\begin{aligned}
&\Sigma_{n+1,\tau}a_{0,1}(s)/s^{n-1/2}=e^{is\kappa}\sum_{j=1}^{n+1}\sum_{k=1}^{N}\frac{(-1)^{n+1-j}(1+(j-1)\tau/s)^{n-k+1/2}e^{i(j-1)\tau\kappa}f_k}{(j-1)!(n+1-j)!\tau^n s^{k-1}}=\\
&=\frac{e^{is\kappa}}{\tau^n}\sum_{j=1}^{n+1}\sum_{k=1}^{N}\left(\sum_{l=0}^{2n}\frac{(-1)^{n+1-j}C^l_{n-k+1/2}\left(\frac{(j-1)\tau}{s}\right)^l e^{i(j-1)\tau\kappa}f_k}{(j-1)!(n+1-j)!s^{k-1}}+\mathcal{O}(s^{-2n-1})\right)=\\
&=\frac{e^{is\kappa}}{\tau^n}\sum_{j=0}^{n}\sum_{k=1}^{2n+1}\sum_{l=0}^{2n}\frac{(-1)^{n-j}C^l_{n-k+1/2}\left(j\tau\right)^l e^{ij\tau\kappa}f_k}{j!(n-j)!s^{k-1+l}}+\mathcal{O}(s^{-2n-1})\quad\overset{l=m-k}{=}\\
&=\frac{e^{is\kappa}}{\tau^n}\sum_{m=1}^{2n+1}\sum_{k=1}^{m}\sum_{j=0}^{n}\frac{(-1)^{n-j}C^{m-k}_{n-k+1/2}(j\tau)^{m-k}e^{ij\tau\kappa}}{j!(n-j)!s^{m-1}}f_k+\mathcal{O}(s^{-2n-1})=\\
&=\frac{1}{\tau^n}\sum_{m=1}^{2n+1}\frac{e^{is\kappa}}{s^{m-1}}\sum_{k=1}^{m}f_kC^{m-k}_{n-k+1/2}\sum_{j=0}^{n}\frac{(-1)^{n-j}(j\tau)^{m-k}e^{ij\tau\kappa}}{j!(n-j)!}+\mathcal{O}(s^{-2n-1})=\\
&=\sum_{m=1}^{2n+1}\frac{e^{is\kappa}f_{m,\kappa}}{s^{m-1}}+\mathcal{O}(s^{-2n-1}),\ s\to+\infty,
\end{aligned} \tag{6.9}$$

where

$$f_{m,\kappa}=\frac{1}{\tau^n}\sum_{k=1}^{m}f_kC^{m-k}_{n-k+1/2}\sum_{j=0}^{n}\frac{(-1)^{n-j}(j\tau)^{m-k}e^{ij\tau\kappa}}{j!(n-j)!},\ m=1,...,2n+1, \tag{6.10}$$

$$f_{1,\kappa}=\frac{f_1}{\tau^n}\sum_{j=0}^{n}\frac{(-1)^{n-j}e^{ij\tau\kappa}}{j!(n-j)!}=\frac{(e^{i\tau\kappa}-1)^n}{\tau^n n!}f_1,\quad\text{where }\frac{(e^{i\tau\kappa}-1)^n}{\tau^n n!}\neq 0. \tag{6.11}$$

Note that in (6.9) we used the change of variables $(j,k,l)\to(j,k,m)$, $l=m-k$.

In (6.11) we have that $e^{i\tau\kappa}\neq 1$ due to (3.38). In a similar way with (6.9) we also have that

$$\Sigma_{n+1,\tau}a_{0,2}(s)/s^{n-1/2}=\sum_{m=1}^{2n+1}\frac{e^{-is\kappa}\overline{f_{m,\kappa}}}{s^{m-1}}+\mathcal{O}(s^{-2n-1}),\ s\to+\infty. \tag{6.12}$$

From formulas (6.5), (6.9), (6.12) we obtain that

$$a_1(s) := \frac{\Sigma_{n+1,\tau} a_0(s)}{s^{n-1/2}} = \sum_{j=1}^{2n+1} \frac{e^{is\kappa} f_{j,\kappa} + e^{-is\kappa}\overline{f_{j,\kappa}}}{s^{j-1}} + \mathcal{O}(s^{-2n-1}) + \mathcal{O}(s^{-2n-1/2}) =$$
$$= \sum_{j=1}^{2n+1} \frac{e^{is\kappa} f_{j,\kappa} + e^{-is\kappa}\overline{f_{j,\kappa}}}{s^{j-1}} + \mathcal{O}(s^{-2n-1/2}) = \sum_{j=1}^{2n-1} \frac{e^{is\kappa} f_{j,\kappa} + e^{-is\kappa}\overline{f_{j,\kappa}}}{s^{j-1}} + \mathcal{O}(s^{-2n+1}), \ s \to +\infty. \tag{6.13}$$

From (6.13) one can see that the function $a_1(s)$ satisfies the assumptions of Theorem 3.2 for $N = 2n-1$. Therefore, applying Theorem 3.2 to the function $a_1(s)$ we reconstruct $f_{1,\kappa}$ via formulas

$$f_{1,\kappa} = C(\kappa,\tau,n)(\tau^{n-1}(e^{-2i\tau\kappa}a_3(s) - a_3(s+\tau)) + \mathcal{O}(s^{-n})), \ s \to +\infty, \tag{6.14}$$

$$a_3(s) := \Sigma_{n,\tau} a_2(s), \ a_2(s) := \frac{e^{-2is\kappa}}{s^{n-1}} \Sigma_{n,\tau}(e^{is\kappa} a_1)(s), \tag{6.15}$$

$$C(\kappa,\tau,n) := \frac{(n-1)!}{(e^{2i\tau\kappa}-1)^{n-1}(e^{-2i\tau\kappa}-1)}. \tag{6.16}$$

In addition, formula (6.11) implies that

$$f_1 = \frac{n!\tau^n f_{1,\kappa}}{(e^{i\tau\kappa}-1)^n}. \tag{6.17}$$

Formulas (3.39), (3.40), (3.41) follow from formulas (6.14)–(6.17) and the definitions of $a_1(s)$, $a_0(s)$. This completes the proof of Proposition 3.2.

7 Sketch of proof of formulas (2.8)–(2.10)

We will use that

$$\begin{aligned}
&G^+(x-y,k) = G_n^+(x-y,k) + \rho_n(y,x,|k|),\\
&G_n^+(x-y,k) = \frac{e^{i|k||x|}}{|x|^{(d-1)/2}} \left(\sum_{j=1}^{n} \frac{g_j(y,\hat{x},|k|)}{|x|^{j-1}} \right),\\
&g_1(y,\hat{x},|k|) = e^{-i|k|y\hat{x}}, \ \rho_n(y,x,|k|) := \frac{e^{i|k||x|}}{|x|^{(d-1)/2}} \varepsilon_n(y,x,|k|),\\
&\varepsilon_n(y,x,|k|) = \mathcal{O}\left(\frac{1}{|x|^n}\right), \ |x| \to +\infty, \text{ uniformly in } y \in D,
\end{aligned} \tag{7.1}$$

where G^+ is defined in (2.1), $\hat{x} = x/|x|$. The Lippman-Schwinger integral equation (2.1) and formula (7.1) imply formulas (2.4), (2.8), (2.9), where

$$(2\pi)^{-d} c(d,|k|)\varphi_j(y,l) = g_j(y,\hat{l},|k|), \ \hat{l} = l/|l|. \tag{7.2}$$

The recurrent relations (2.10) can be proved using also that:

$$(\Delta_x + k^2)G^+(x-y,k) = 0, \text{ for } x \in \mathbb{R}^d \setminus D, \ y \in D; \tag{7.3}$$

$$\Delta_x = \frac{\partial^2}{\partial r^2} + \frac{d-1}{r}\frac{\partial}{\partial r} + \frac{1}{r^2}\Delta_S, \tag{7.4}$$

where $r = |x|$, Δ_S is the Beltrami–Laplace operator with respect to $\hat{x} \in \mathbb{S}^{d-1}$, $\hat{x} = x/|x|$;

$$\Delta_x \rho_n(y,x,|k|) = \mathcal{O}\left(\frac{1}{|x|^{n+(d-1)/2}}\right), \ |x| \to +\infty. \tag{7.5}$$

We prove below the recurrent relations (2.10) proceeding from (7.1)–(7.5). Our approach consists in expanding equation (7.3) in $|x|^{-j}$, as $|x| \to +\infty$.

Note that

$$\frac{\partial}{\partial r}\frac{e^{i|k|r}}{r^{\frac{d-1}{2}+j}} = \frac{e^{i|k|r}}{r^{\frac{d-1}{2}}}\left(\frac{i|k|}{r^j} + \frac{(-\frac{d-1}{2}-j)}{r^{j+1}}\right), \tag{7.6}$$

$$\frac{\partial}{r\partial r}\frac{e^{i|k|r}}{r^{\frac{d-1}{2}+j-1}} = \frac{e^{i|k|r}}{r^{\frac{d-1}{2}}}\left(\frac{i|k|}{r^j} + \frac{(-\frac{d-1}{2}-j+1)}{r^{j+1}}\right), \tag{7.7}$$

$$\frac{1}{r^2}\Delta_S G^+(x-y,k) = \frac{e^{i|k|r}}{r^{(d-1)/2}}\left(\sum_{j=1}^{n}\frac{\Delta_S g_j(y,\hat{x},|k|)}{r^{j+1}}\right) + \mathcal{O}\left(\frac{1}{r^{n+(d+3)/2}}\right), \ r \to +\infty. \tag{7.8}$$

Using (7.1), (7.7) we obtain that

$$\begin{aligned}
&\frac{\partial G_n^+(x-y,k)}{r\partial r} = \sum_{j=1}^{n} g_j(y,\hat{x},|k|)\frac{\partial}{r\partial r}\frac{e^{i|k|r}}{r^{\frac{d-1}{2}+j-1}} = \\
&= \frac{e^{i|k|r}}{r^{(d-1)/2}}\sum_{j=1}^{n}\left(\frac{i|k|g_j(y,\hat{x},|k|)}{r^j} + (-\frac{d-1}{2}-j+1)\frac{g_j(y,\hat{x},|k|)}{r^{j+1}}\right) = \\
&= \frac{e^{i|k|r}}{r^{(d-1)/2}}\left(\sum_{j=2}^{n+1}\frac{i|k|g_{j-1}(y,\hat{x},|k|)}{r^{j-1}} + \sum_{j=3}^{n+2}(-\frac{d-1}{2}-j+3)\frac{g_{j-2}(y,\hat{x},|k|)}{r^{j-1}}\right) = \\
&= \frac{e^{i|k|r}}{r^{(d-1)/2}}(\frac{i|k|g_1(y,\hat{x},|k|)}{r} + \sum_{j=3}^{n+1}\frac{i|k|g_{j-1}(y,\hat{x},|k|) + (-\frac{d-1}{2}-j+3)g_{j-2}(y,\hat{x},|k|)}{r^{j-1}} + \\
&+ (-\frac{d-1}{2}-n+1)\frac{g_n(y,\hat{x},|k|)}{r^{n+1}}) = \frac{e^{i|k|r}}{r^{(d-1)/2}}\sum_{j=2}^{n}\frac{\theta_{j,d}}{r^{j-1}},
\end{aligned} \tag{7.9}$$

$$\theta_{j,d} = \begin{cases} i|k|g_{j-1}(y,\hat{x},|k|), \ j=2, \\ i|k|g_{j-1}(y,\hat{x},|k|) + (-\frac{d-1}{2}-j+3)g_{j-2}(y,\hat{x},|k|), \ j=3,...,n+1, \\ (-\frac{d-1}{2}-j+3)g_{j-2}(y,\hat{x},|k|), \ j=n+2. \end{cases} \tag{7.10}$$

Using (7.7) and the result of the second equality in (7.9) we obtain that:

$$\begin{aligned}
&\frac{\partial^2 G_n^+(x-y,k)}{\partial r^2} = \frac{\partial}{\partial r}\left(\frac{e^{i|k|r}}{r^{(d-1)/2}}\left(\sum_{j=1}^{n}\frac{i|k|g_j(y,\hat{x},|k|)}{r^{j-1}} + \sum_{j=2}^{n+1}(-\frac{d-1}{2}-j+2)\frac{g_{j-1}(y,\hat{x},|k|)}{r^{j-1}}\right)\right) = \\
&= \sum_{j=1}^{n} i|k|g_j(y,\hat{x},|k|)\frac{\partial}{\partial r}\frac{e^{i|k|r}}{r^{\frac{d-1}{2}+j-1}} + \sum_{j=2}^{n+1}(-\frac{d-1}{2}-j+2)g_{j-1}(y,\hat{x},|k|)\frac{\partial}{\partial r}\frac{e^{i|k|r}}{r^{\frac{d-1}{2}+j-1}} = \\
&= \sum_{j=1}^{n} i|k|g_j(y,\hat{x},|k|)\left(\frac{i|k|e^{i|k|r}}{r^{\frac{d-1}{2}+j-1}} + (-\frac{d-1}{2}-j+1)\frac{e^{i|k|r}}{r^{\frac{d-1}{2}+j}}\right) + \\
&+ \sum_{j=2}^{n+1}(-\frac{d-1}{2}-j+2)g_{j-1}(y,\hat{x},|k|)\left(\frac{i|k|e^{i|k|r}}{r^{\frac{d-1}{2}+j-1}} + (-\frac{d-1}{2}-j+1)\frac{e^{i|k|r}}{r^{\frac{d-1}{2}+j}}\right) = \frac{e^{i|k|r}}{r^{\frac{d-1}{2}}}\sum_{j=1}^{n}\frac{\omega_{j,d}}{r^{j-1}},
\end{aligned} \tag{7.11}$$

$$\omega_{j,d} = \begin{cases} -|k|^2 g_j(y,\hat{x},|k|), \ j=1, \\ -|k|^2 g_j(y,\hat{x},|k|) + i|k|(-d-2j+5)g_{j-1}(y,\hat{x},|k|), \ j=2, \\ -|k|^2 g_j(y,\hat{x},|k|) + i|k|(-d-2j+5)g_{j-1}(y,\hat{x},|k|) + \\ +(-\frac{d-1}{2}-j+3)(-\frac{d-1}{2}-j+2)g_{j-2}(y,\hat{x},|k|), \ j=3,...,n. \end{cases} \tag{7.12}$$

From (7.1), (7.3)–(7.5), (7.8), (7.9), (7.11) we have that

$$(d-1)\frac{e^{i|k|r}}{r^{\frac{d-1}{2}}}\sum_{j=1}^{n}\frac{\theta_{j,d}}{r^{j-1}}+\frac{e^{i|k|r}}{r^{(d-1)/2}}\sum_{j=2}^{n}\frac{\omega_{j,d}}{r^{j-1}}+\frac{e^{i|k|r}}{r^{(d-1)/2}}\sum_{j=3}^{n+2}\frac{\Delta_S g_{j-2}}{r^{j-1}}=$$
$$=-k^2\frac{e^{i|k|r}}{r^{(d-1)/2}}\sum_{j=1}^{n}\frac{g_j}{r^{j-1}}+\mathcal{O}\left(\frac{|k|^2}{r^{n+(d-1)/2}}\right),\ r\to+\infty, \tag{7.13}$$

where $\theta_{j,d}$, $\omega_{j,d}, g_j$ do not depend on r. Since n is arbitrary, we obtain, from (7.13), for $j\geq 3$, that

$$(d-1)\theta_{j,d}+\omega_{j,d}+\Delta_S g_{j-2}=-k^2 g_j. \tag{7.14}$$

Using definitions (7.10) for $\theta_{j,d}$, (7.12) for $\omega_{j,d}$ and equation (7.14) we obtain, for $j\geq 2$,

$$g_j(y,\hat{x},|k|)=\frac{1}{2i|k|(j-1)}\left(\left(\frac{4d-3-d^2}{4}+(j-1)(j-2)\right)g_{j-1}(y,\hat{x},|k|)+\Delta_S g_{j-1}(y,\hat{x},|k|)\right). \tag{7.15}$$

Formulas (2.10) follow from (7.2), (7.15).

Bibliography

[1] A.D. Agaltsov, T. Hohage, R.G. Novikov, *An iterative approach to monochromatic phaseless inverse scattering*, Inverse Problems 35(2), 24001 (24 pp.) (2019)

[2] T. Aktosun, P. E. Sacks, *Inverse problem on the line without phase information*, Inverse Problems 14, 211–224 (1998)

[3] F. V. Atkinson, *On Sommerfeld's "Radiation Condition"* , Philos. Mag., Vol. XI, 645-651 (1949)

[4] A.H. Barnett, Ch.L. Epstein, L.F. Greengard, J.F. Magland, *Geometry of the phase retrieval problem*, Inverse Problems 36, 094003 (2020)

[5] F.A. Berezin, M.A. Shubin, *The Schrödinger Equation*, Mathematics and Its Applications, Vol. 66, Kluwer Academic, Dordrecht, 1991

[6] M. Born, *Quantenmechanik der Stossvorgange*, Zeitschrift fur Physik 38 (11-12), 803-827 (1926)

[7] V.A. Burov, O.D. Rumyantseva, *Inverse wave problems of acoustic tomography, Part 2 : Inverse problems of acoustic scattering*, Lenand, Moscow, (in Russian) 2020

[8] K. Chadan, P.C. Sabatier, *Inverse Problems in Quantum Scattering Theory*, 2nd edn. Springer, Berlin, 1989

[9] D. Colton, R. Kress, *Inverse Acoustic and Electromagnetic Scattering Theory*, 4th. ed. Applied Mathematical Sciences, 93. Springer, Cham, 2019

[10] L. Crocco, M. D'Urso, T. Isernia, *Inverse scattering from phaseless measurements of the total field on a closed curve*, Journal of the Optical Society of America A 21(4), 622-631 (2004)

[11] A.J. Devaney, *Structure determination from intensity measurements in scattering experiments*, Physical Review Letters 62(20), 2385-2388 (1989)

[12] L.D. Faddeev, S.P. Merkuriev, *Quantum Scattering Theory for Multi-particle Systems*, Mathematical Physics and Applied Mathematics, 11. Kluwer Academic Publishers Group, Dordrecht, 1993

[13] D. Fanelli, O. Öktem, *Electron tomography: a short overview with an emphasis on the absorption potential model for the forward problem*, Inverse Problems, 24(1), 013001 (51 pp.) (2008)

[14] A. Jesacher, W. Harm, S. Bernet, M. Ritsch-Marte, *Quantitative single-shot imaging of complex objects using phase retrieval with a designed periphery*, Optics Express 20(5), 5470-5480 (2012)

[15] O. Ivanyshyn, R. Kress, *Identification of sound-soft 3D obstacles from phaseless data*, Inverse Probl. Imaging 4, 131-149 (2010)

[16] P. Jonas, A.K. Louis, *Phase contrast tomography using holographic measurements*, Inverse Problems 20(1), 75-102 (2004)

[17] T. Hohage, R.G. Novikov, *Inverse wave propagation problems without phase information*, Inverse Problems 35(7), 070301 (4 pp.)(2019)

[18] M.V. Klibanov, *Phaseless inverse scattering problems in three dimensions*, SIAM J.Appl. Math. 74(2), 392-410 (2014)

[19] M.V. Klibanov, N.A. Koshev, D.-L. Nguyen, L.H. Nguyen, A. Brettin, V.N. Astratov, *A numerical method to solve a phaseless coefficient inverse problem from a single measurement of experimental data*, SIAM J. Imaging Sci. 11(4), 2339–2367 (2018)

[20] M.V. Klibanov, V.G. Romanov, *Reconstruction procedures for two inverse scattering problems without the phase information*, SIAM J. Appl. Math. 76(1), 178-196 (2016)

[21] M.V. Klibanov, P.E. Sacks, A.V. Tikhonravov, *The phase retrieval problem*, Inverse Problems 11, 1–28 (1995)

[22] M.H. Maleki, A.J. Devaney, A. Schatzberg, *Tomographic reconstruction from optical scattered intensities*, Journal of the Optical Society of America A 9(8), 1356-1363 (1992)

[23] S. Maretzke, *A uniqueness result for propagation-based phase contrast imaging from a single measurement*, Inverse Problems 31(6), 065003 (16 pp.) (2015)

[24] S. Maretzke, T. Hohage, *Stability estimates for linearized near-field phase retrieval in X-ray phase contrast imaging*, SIAM J. Appl. Math. 77(2), 384-408 (2017)

[25] R.B. Melrose, *Geometric scattering theory*, Stanford Lectures. Cambridge University Press, 1995

[26] R. G. Novikov, *Formulas for phase recovering from phaseless scattering data at fixed frequency*, Bulletin des Sciences Mathematiques 139(8), 923-936 (2015)

[27] R. G. Novikov, *Phaseless inverse scattering in the one-dimensional case*, Eurasian Journal of Mathematical and Computer Applications 3(1), 63-69 (2015)

[28] R. G. Novikov, *Inverse scattering without phase information*, Seminaire Laurent Schwartz - EDP et applications, Exp. No16, (13pp) (2014-2015)

[29] R. G. Novikov, *Multipoint formulas for phase recovering from phaseless scattering data*, Journal of Geometric Analysis 31(2), 1965-1991 (2021)

[30] R.G. Novikov, *Multidimensional inverse scattering for the Schrödinger equation*, Book series: Springer Proceedings in Mathematics and Statistics. Title of volume: Mathematical Analysis, its Applications and Computation - ISAAC 2019, Aveiro, Portugal, July 29-August 2; Editors: P. Cerejeiras, M. Reissig (to appear), e-preprint: https://hal.archives-ouvertes.fr/hal-02465839v1

[31] R. G. Novikov, *Multipoint formulas for scattered far field in multidimensions*, Inverse Problems 36(9), 095001 (12 pp) (2020)

[32] R.G. Novikov, *Multipoint formulas for inverse scattering at high energies*, Russian Math. Surveys (to appear), https://hal.archives-ouvertes.fr/hal-02983682v1

[33] R. G. Novikov, V. N. Sivkin, *Error estimates for phase recovering from phaseless scattering data*, Eurasian Journal of Mathematical and Computer Applications, 8(1), 44–61 (2020)

[34] R. G. Novikov, V. N. Sivkin, *Phaseless inverse scattering with background information*, Inverse Problems, vol. 37(5), 055011 (20 pp) (2021)

[35] V. Palamodov, *A fast method of reconstruction for X-ray phase contrast imaging with arbitrary Fresnel number*, arXiv:1803.08938v1 (2018)

[36] V. G. Romanov, *Inverse problems without phase information that use wave interference*, Sib. Math. J. 59(3), 494-504 (2018)

[37] V. G. Romanov, *Phaseless inverse problems for Schrödinger, Helmholtz, and Maxwell equations*, Comput. Math. Math. Phys., 60 (6) 1045–1062 (2020)

[38] V.G. Romanov, *A phaseless inverse problem for electrodynamic equations in the dispersible medium*, Applicable Analysis, https://doi.org/10.1080/00036811.2020.1846721

[39] C. H. Wilcox, *A generalization of theorems of Rellich and Atkinson*, Proceedings of the American Mathematical Society, 7(2), 271-276 (1956)

[40] E. Wolf, *Three-dimensional structure determination of semi-transparent objects from holographic data*, Optics Communications 1(4), 153-156 (1969)

[41] E. Wolf, *Determination of the amplitude and the phase of scattered fields by holography*, Journal of the Optical Society of America 60(1), 18-20 (1970)

[42] X. Xu, B. Zhang, H. Zhang, *Uniqueness in inverse electromagnetic scattering problem with phaseless far–field data at a fixed frequency*, IMA Journal of Applied Mathematics 85(6), 823-839 (2020)

Article VI

Multipoint formulas in inverse problems and their numerical implementation

R.G. Novikov, V.N. Sivkin, G.V. Sabinin

We present the first numerical study of multipoint formulas for finding leading coefficients in asymptotic expansions arising in potential and scattering theories. In particular, we implement different formulas for finding the Fourier transform of potential from the scattering amplitude at several high energies. We show that the aforementioned approach can be used for essential numerical improvements of classical results including the slowly convergent Born-Faddeev formula for inverse scattering at high energies. The approach of multipoint formulas can be also used for recovering the X-ray transform of potential from boundary values of the scattering wave functions at several high energies. Determination of total charge (electric or gravitational) from several exterior measurements is also considered. In addition, we show that the aforementioned multipoint formulas admit an efficient regularization for the case of random noise. In particular, we proceed from theoretical works [Novikov, 2020, 2021].

Keywords: inverse scattering, charge recovery, multipoint formulas, numerical implementation

1 Introduction

Many functions of potential theory, scattering theory, and other fields admit asymptotic expansions of the form

$$z(s) = \sum_{j=1}^{N} \frac{a_j}{s^{j-1}} + \mathcal{O}(s^{-N}), \text{ as } s \to +\infty, \tag{1.1}$$

where $s \in (\sigma, +\infty)$, for some $\sigma > 0$, and a_j are complex numbers; see, for example, [1], [21], [22], [27], [28], [32], [41], [42]. In addition, in some cases, the most important information is contained in a_1 (and/or some next leading coefficients), whereas $z(s)$ is measured in several points $s \in (\sigma, +\infty)$. In the present work we continue studies of [27], [28] on finding a_1 from $z(s)$, given at several sufficiently large s, with applications to inverse scattering at high energies. We also consider determination of total charge (electrical or gravitational) from measurements at several remote points. For other applications of such studies to phased and phaseless inverse scattering, see [27], [32].

One of the most essential results of the present work consists in an efficient regularization of the formulas of [27] for finding a_1 from z at several points in the presence of random noise; see Sections 2, 5, 6, 7. This regularization opens perspectives for practical applications where data are always noisy.

In particular, we consider the stationary Schrödinger equation

$$-\Delta\psi + v(x)\psi = E\psi, \quad x \in \mathbb{R}^d, \quad E > 0, \tag{1.2}$$

where

$$v \text{ is compactly supported and sufficiently regular on } \mathbb{R}^d. \tag{1.3}$$

For equation (1.2), we consider the scattering solutions $\psi^+ = \psi^+(x,k)$, $k \in \mathbb{R}^d$, $k^2 = E$, specified by

$$\psi^+(x,k) = e^{ikx} + \frac{e^{i|k||x|}}{|x|^{(d-1)/2}} f_1\left(k, |k|\frac{x}{|x|}\right) + \mathcal{O}\left(\frac{1}{|x|^{(d+1)/2}}\right) \quad \text{as } |x| \to +\infty, \tag{1.4}$$

uniformly on $x/|x|$. The coefficient f_1 arising in (1.4) is the scattering amplitude for equation (1.2). The function f_1 at a fixed energy E is defined on

$$\mathcal{M}_E = \{k,\, l \in \mathbb{R}^d : \quad k^2 = l^2 = E\} = \mathbb{S}^{d-1}_{\sqrt{E}} \times \mathbb{S}^{d-1}_{\sqrt{E}}. \tag{1.5}$$

For more information on direct scattering for equation (1.2), see, for example, [5].

We consider, in particular, polychromatic inverse scattering at high energies for equation (1.2), formulated as follows:

Problem 10. *Find v (or some information about v) from f_1 at several sufficiently large energies E.*

Let

$$\widehat{v}(p) = \mathcal{F}v(p) = (2\pi)^{-d} \int_{\mathbb{R}^d} e^{ipx} v(x)dx, \quad p \in \mathbb{R}^d. \tag{1.6}$$

For some formulas, it is convenient to write f_1 as

$$\begin{aligned} &f_1(k,l) = c(d,|k|)f(k,l), \\ &c(d,|k|) := -\pi i(-2\pi i)^{(d-1)/2}|k|^{(d-3)/2}, \text{ for } \sqrt{-2\pi i} = \sqrt{2\pi}e^{-i\pi/4}. \end{aligned} \tag{1.7}$$

In particular, we have that

$$f(k,l) = \widehat{v}(p) + \mathcal{O}(E^{-1/2}), \quad p = k - l, \quad (k,l) \in \mathcal{M}_E, \quad E \to +\infty. \tag{1.8}$$

Formula (1.8) goes back to [4], [9] and is known as the Born-Faddeev formula at high energies; see also, for example, [26]. This formula gives the simplest method for inverse scattering at high energies for $d \geq 2$. In addition, formula (1.8) admits much more detailed versions, at least, for smooth v.

Let, for example, $v \in \mathcal{C}_c^\infty(\mathbb{R}^d)$, where $\mathcal{C}_c^\infty$ denotes compactly supported infinitely smooth functions. Then (see Proposition 3.4 of [22]):

$$f(k(s), l(s)) = \sum_{j=1}^{N} \frac{a_j(p,\omega)}{s^{j-1}} + \mathcal{O}(s^{-N}) \text{ as } s \to +\infty, \tag{1.9}$$

where

$$\begin{aligned} &k(s) = p + (E - p^2)^{1/2}\omega, \quad l(s) = E^{1/2}\omega, \quad E = E(s) = s^2, \\ &p \in \mathbb{R}^d, \quad p \cdot \omega = 0, \quad \omega \in \mathbb{S}^{d-1}, \end{aligned} \tag{1.10}$$

and

$$a_1(p,\omega) = \widehat{v}(p), \tag{1.11}$$

where $\widehat{v}$ is defined by (1.6). One can see that expansion (1.9) is of the form (1.1), and the most important information (in the framework of inverse scattering) is contained in a_1.

In particular, due to (1.9), (1.11), we have that

$$\widehat{v}(p) = f(k(s), l(s)) + \mathcal{O}(s^{-1}), \text{ as } s \to +\infty. \tag{1.12}$$

Formula (1.12) is a variation of formula (1.8). In a similar way with (1.8), formulas (1.12), (1.10) give a method for inverse scattering at high energies for $d \geq 2$ (for $d = 1$ these formulas can be used only for $p = 0$).

In inverse scattering, the main disadvantage of Born-Faddeev formulas like (1.8), (1.12) consists in their slow convergence for large energies. This convergence corresponds to $\mathcal{O}(s^{-1})$ in (1.12). In this connection, recently, the article [28] suggested

$$\begin{aligned} &\text{formulas for finding } \widehat{v}(p) \text{ up to } \mathcal{O}(s^{-n}) \text{ as } s \to +\infty \\ &\text{from } f(k,l) \text{ given at } n \text{ points } (k,l) = (k_1(s), l_1(s)), ..., (k_n(s), l_n(s)), \end{aligned} \tag{1.13}$$

where, for example,

$$\begin{aligned} &k_j(s) = k(s_j) = k(s + \tau_j), \quad l_j(s) = l(s_j) = l(s + \tau_j), \\ &s > 0, \quad 0 = \tau_1 < \tau_2 < ... < \tau_n, \end{aligned} \tag{1.14}$$

where $(k(s), l(s))$ are defined as in (1.10) and (1.12). Formulas (1.13) are recalled in details in Subsection 3.1.

The results of the present work include the first numerical implementation of the multipoint formulas of [27], [28] for finding a_1 in (1.1) from $z(s)$ given at several points s, with applications to inverse scattering at high energies via formulas (1.13). The results of the present work also include extension of formulas (1.13) to phaseless inverse scattering at high energies.

The results of the present work also include a variation of formulas (1.9)–(1.11) which is considerably more convenient for applications to inverse scattering at high energies. And we implement these more convenient formulas on inverse scattering numerically. See Subsections 4.1 and 7.2.

Note that the asymptotic of the scattering functions ψ^+ at high energies also reduces to an asymptotic of the form (1.1). In the present work we also explain in which way the multipoint approach can be applied to recovering the X-ray transform of the potential v from boundary values ψ^+ at several high energies. See Subsection 4.2.

For other important results given in the literature on inverse scattering problems, see, for example, [2], [6], [8], [10], [11], [12], [13], [16], [19], [20], [28], [30], [31], [34], [35], [36], [37], [38], [39] and references therein. In particular, we expect that the multipoint approach can be also applied to inverse scattering for the Newton equation; see [18], [25] for known results on this inverse scattering. We also expect that the multipoint approach can be applied to finding the Fourier transform of potential from the Faddeev scattering data h in complex domain at a fixed energy with applications to inverse boundary value problems; see [13], [24].

Natural directions for further research also include possible generalizations of asymptotics like (1.9), (4.1) for potentials v with discontinuities. Our preliminary numerical tests of reconstruction formulas of Subsection 4.1 and Section 5 give encouraging results in this connection.

We also consider an electrical or gravitational field with potential

$$U(x) = \int_D \frac{\rho(x')dx'}{|x - x'|}, \quad x \in \mathbb{R}^3, \tag{1.15}$$

where D is a bounded domain in $\mathbb{R}^3$. It is well-known that $sU(s\theta)$ admits multipole expansion of the form (1.1) with

$$a_1 = \int_D \rho(x)dx; \tag{1.16}$$

see, for example, [21].

We consider, in particular, the question of finding a_1 from measurements of $sU(s\theta)$ at several sufficiently large s. This question is of independent interest, but we consider this issue also for numerical testing multipoint formulas of [27] with their regularizations developed in the present work. In these numerical tests we assume for simplicity that

$$\rho(x) = \sum_{j=1}^{J} q_j \delta(x - x_j), \quad q_j \in \mathbb{R}, \quad x_j \in D. \tag{1.17}$$

The further structure of the present article is as follows. In Section 2 we recall the formulas of [27] for finding a_1 in (1.1) from z at several points, and describe related numerical algorithms. In Section 3 we recall the multipoint formulas of [28] for inverse scattering at several high energies, and give analogs of these formulas for phaseless inverse scattering. In Section 4 we give further theoretical results on inverse scattering at several high energies. This includes new formulas for the reconstruction from the scattering amplitude and from boundary values of the wave functions. In Section 5, for data with random noise, we give an efficient regularization of multipoint formulas recalled in Section 2, and describe related numerical algorithm. In Section 6 we present numerical tests of the aforementioned multipoint formulas for the case of finding a_1 in (1.16)–(1.17) from $z(s) = sU(s\theta)$ given at several points s. In Section 7 we present numerical tests of the aforementioned multipoint formulas in their application to inverse scattering at several high energies. Some conclusions are summarized in Section 8.

Numerical simulations of the present work were fulfilled using Matlab.

2 Reconstruction of the leading coefficient in z-expansion

In this section we recall multipoint formulas of [27] for finding a_1 in (1.1) from z given at several sufficiently large s; see formulas (2.4)–(2.7). In addition, we also describe algorithms for their numerical implementation; see Algorithms 4 and 5.

Let $z = z(s)$ be an abstract function of the form (1.1). We consider points $s_j \in (r, +\infty)$ such that

$$\begin{aligned} &s_j = s + \tau_j, \quad j = 1, ..., n, \\ &0 = \tau_1 < \tau_2 < ... < \tau_n \text{ are fixed}, \\ &\vec{\tau} := (\tau_1, ..., \tau_n), \quad 2n + 1 < N, \end{aligned} \tag{2.1}$$

or

$$\begin{aligned} &s_j = s\lambda_j, \quad j = 1, ..., n, \\ &1 = \lambda_1 < \lambda_2 < ... < \lambda_n \text{ are fixed}, \\ &\vec{\lambda} := (\lambda_1, ..., \lambda_n), \quad n = N. \end{aligned} \tag{2.2}$$

Let

$$\begin{aligned} &\alpha_j(\vec{\xi}) := \prod_{i=1}^{j-1} (\xi_j - \xi_i) \quad \text{for} \quad 1 < j \leq n, \quad \alpha_1(\vec{\xi}) = 1, \\ &\beta_{n,j}(\vec{\xi}) := \prod_{i=j+1}^{n} (\xi_i - \xi_j) \quad \text{for} \quad 1 \leq j < n, \quad \beta_{n,n}(\vec{\xi}) = 1, \end{aligned} \tag{2.3}$$

where $\vec{\xi} = (\xi_1, \ldots, \xi_n)$.

Then the following formulas for finding a_1 from $z(s)$ at the points s_j hold (see [27]):

$$a_1 = a_{1,n}(s, \vec{\tau}) + \mathcal{O}(s^{-n}), \text{ as } s \to +\infty, \tag{2.4}$$

$$\begin{aligned} a_{1,n}(s, \vec{\tau}) &= \sum_{j=1}^{n} y_j(s, \vec{\tau}) z(s + \tau_j), \\ y_j(s, \vec{\tau}) &= \frac{(-1)^{n-j}(s + \tau_j)^{n-1}}{\alpha_j(\vec{\tau})\beta_{n,j}(\vec{\tau})}, \quad 1 \le j \le n, \end{aligned} \tag{2.5}$$

where s_j are defined by (2.1);

$$a_1 = a_{1,n}(s, \vec{\lambda}) + \mathcal{O}(s^{-n}), \text{ as } s \to +\infty, \tag{2.6}$$

$$\begin{aligned} a_{1,n}(s, \vec{\lambda}) &= \sum_{j=1}^{n} y_j(s, \vec{\lambda}) z(\lambda_j s), \\ y_j(s, \vec{\lambda}) &= \frac{(-1)^{n-j}\lambda_j^{n-1}}{\alpha_j(\vec{\lambda})\beta_{n,j}(\vec{\lambda})}, \quad 1 \le j \le n, \end{aligned} \tag{2.7}$$

where s_j are defined by (2.2).

Algorithm 4:

function $a_1 =$ `z_reco`(s, n, τ, z)
// reconstruction procedure proposed in [27]
Input:
s: minimal point
n: number of points
τ : vector of point steps $(\tau_1, ..., \tau_n)$
z: function of the form (1.1) defined in points $\{s + \tau_1, ..., s + \tau_n\}$
Output:
a_1: approximation of the first term of function z

```
a_1 := 0
for j = 1..n do
    c = (-1)^(n-j)/(alpha(j, τ) × beta(n, j, τ))
    // alpha, beta are defined in (2.3)
    a_1 = a_1 + c × z(j) × (s + τ(j))^(n-1)
end
```

Algorithm 5:

function $a_1 =$ `z_reco_multi`(s, n, λ, z)
// reconstruction procedure proposed in [27]
Input:
s: minimal point
n: number of points
λ : vector of point factors $(\lambda_1, ..., \lambda_n)$
z: function of the form (1.1) defined in points $\{s\lambda_1, ..., s\lambda_n\}$
Output:
a_1: approximation of the first term of function z

```
a_1 := 0
for j = 1..n do
    c = (-1)^(n-j)/(alpha(j, λ) × beta(n, j, λ))
    // alpha, beta are defined in (2.3)
    a_1 = a_1 + c × z(j) × λ_j^(n-1)
end
```

In connection with formulas (2.5), (2.7), note that if $\xi_{j+1}-\xi_j=\delta$, $j=1,...,n-1$, then

$$\alpha_j(\vec{\xi})\beta_{n,j}(\vec{\xi})=\delta^{n-1}(j-1)!(n-j)!,\quad j=1,...,n. \tag{2.8}$$

Numerical examples of implementation of formula (2.4) are given in Section 6.

Remark 2.1. *For fixed s, we have that*

$$a_{1,n}(s,\vec{\tau})=a_{1,n}(s,\vec{\lambda}),\ \textit{if}\ \tau_j=(\lambda_j-1)s,\quad j=1,...,n. \tag{2.9}$$

We recall also that:
$y=(y_1,...,y_n)$ in (2.5) arises as the solution of the system

$$(\gamma_i,y)=\sum_{j=1}^{n}\frac{y_j}{(s+\tau_j)^{i-1}}=\begin{cases}1 \text{ for } i=1,\\ 0 \text{ for } 1<i\le n;\end{cases} \tag{2.10}$$

$y=(y_1,...,y_n)$ in (2.7) arises as the solution of the system

$$(\gamma_i,y)=\sum_{j=1}^{n}\frac{y_j}{(\lambda_j s)^{i-1}}=\begin{cases}1 \text{ for } i=1,\\ 0 \text{ for } 1<i\le n.\end{cases} \tag{2.11}$$

Here, (γ_i,y) are the scalar products of y with vectors $\{\gamma_i\}_{i=1}^n$.

3 Application to inverse scattering at high energies

In this section we recall the result of [28] consisting in application of asymptotic formulas (1.9)-(1.11) and multipoint formulas (2.4)–(2.7) to finding the Fourier transform $\widehat{v}$ from the scattering amplitude f at several sufficiently large energies; see Subsection 3.1. In addition, we also extend this result to finding $|\widehat{v}|^2$ from the differential scattering cross section $|f|^2$ at several sufficiently large energies; see Subsection 3.2.

3.1 Reconstruction of the Fourier transform in z-expansion

In this section we present formulas reconstruction of the Fourier transform in expansion (1.9)-(1.11)

Applying the abstract formulas (2.4), (2.6) to the scattering expansion (1.9)-(1.11), we have (see [28]):

$$\begin{aligned}
&\widehat{v}(p)=\widehat{v}_n(p,s,\vec{\tau})+\mathcal{O}(s^{-n}),\quad \text{as}\ \ s\to+\infty,\\
&\widehat{v}_n(p,s,\vec{\tau})=\sum_{j=1}^{n}\frac{(-1)^{n-j}(s+\tau_j)^{n-1}f(k_j(s),l_j(s))}{\alpha_j(\vec{\tau})\beta_{n,j}(\vec{\tau})},\\
&|k_j(s)|^2=|l_j(s)|^2=E_j(s)=(s+\tau_j)^2,\quad s>0,\\
&\vec{\tau}=(\tau_1,\dots,\tau_n),\ \tau_1=0,\ \tau_{j_1}<\tau_{j_2}\ \text{ for }\ j_1<j_2,
\end{aligned} \tag{3.1}$$

and

$$\begin{aligned}
&\widehat{v}(p)=\widehat{v}_n(p,s,\vec{\lambda})+\mathcal{O}(s^{-n})\ \ \text{as}\ \ s\to+\infty,\\
&\widehat{v}_n(p,s,\vec{\lambda})=\sum_{j=1}^{n}\frac{(-1)^{n-j}\lambda_j^{n-1}f(k_j(s),l_j(s))}{\alpha_j(\vec{\lambda})\beta_{n,j}(\vec{\lambda})},\\
&|k_j(s)|^2=|l_j(s)|^2=E_j(s)=(\lambda_j s)^2,\quad s>0,\\
&\vec{\lambda}=(\lambda_1,\dots,\lambda_n),\ \lambda_1=1,\ \lambda_{j_1}<\lambda_{j_2}\ \text{ for }\ j_1<j_2,
\end{aligned} \tag{3.2}$$

where

$$k_j(s) = p + (E_j(s) - p^2)^{1/2}\omega, \quad l_j(s) = (E_j(s))^{1/2}\omega, \tag{3.3}$$

$p \in \mathbb{R}^d$, $p \cdot \omega = 0$, $\omega \in \mathbb{S}^{d-1}$ (and ω, p are fixed), and $\alpha_j(\vec{\tau})$, $\beta_{n,j}(\vec{\tau})$ are defined in (2.3).

For $n = 1$, formulas (3.1), (3.2) reduce to (1.12). In formulas (1.12), (3.1)–(3.3) we have that

$$\begin{aligned} &k_j(s) - l_j(s) \neq p, \text{ if } p \neq 0, \\ &k_j(s) - l_j(s) = p + \left((E_j(s) - p^2)^{1/2} - E_j^{1/2}(s)\right)\omega, \\ &k_j(s) - l_j(s) = p - \frac{p^2}{2\sqrt{E_j(s)}}\omega + \mathcal{O}(s^{-2}), \text{ as } s \to +\infty. \end{aligned} \tag{3.4}$$

The property that $k - l = p$ is an advantage of the Born-Faddeev formulas (1.8) with respect to (1.12), (3.1), (3.2).

The Born-Faddeev formula (1.8) for fixed $E = s^2$ is considered for $|p| \leq 2s$. Formula (1.12) for fixed $s = \sqrt{E}$ is considered for $|p| \leq s$. For arbitrary n, formulas (3.1), (3.2) for fixed $s = \sqrt{E}$ are also considered for $|p| \leq s$. A larger domain for p is an advantage of (1.8) in comparison with (1.12) and (3.1), (3.2) for fixed $s > 0$.

However, a rapid convergence described by $\mathcal{O}(s^{-n})$, is the principle advantage of (3.1), (3.2), for $n \geq 2$, in comparison with (1.8), when $s \to +\infty$.

A version of formulas (3.1), (3.2) without the aforementioned disadvantage is given in Subsection 4.1.

3.2 Applications to phaseless inverse scattering

Formulas (3.1), (3.2) also have their phaseless analogs. The results can be summarized as follows:

Theorem 3.1. *Let $v \in \mathcal{C}_c^\infty(\mathbb{R}^d)$. Then*

$$\begin{aligned} &|\widehat{v}(p)|^2 = |\widehat{v}|^{2,n}(p, s, \vec{\tau}) + \mathcal{O}(s^{-n}), \quad \text{as} \quad s \to +\infty, \\ &|\widehat{v}|^{2,n}(p, s, \vec{\tau}) = \sum_{j=1}^{n} \frac{(-1)^{n-j}(s + \tau_j)^{n-1}|f(k_j(s), l_j(s))|^2}{\alpha_j(\vec{\tau})\beta_{n,j}(\vec{\tau})}, \\ &|k_j(s)|^2 = |l_j(s)|^2 = E_j(s) = (s + \tau_j)^2, \quad s > 0, \\ &\vec{\tau} = (\tau_1, \ldots, \tau_n), \ \tau_1 = 0, \ \tau_{j_1} < \tau_{j_2} \ \text{ for } \ j_1 < j_2, \end{aligned} \tag{3.5}$$

and

$$\begin{aligned} &|\widehat{v}(p)|^{2,n} = |\widehat{v}|^{2,n}(p, s, \vec{\lambda}) + \mathcal{O}(s^{-n}) \ \text{ as } \ s \to +\infty, \\ &|\widehat{v}|^{2,n}(p, s, \vec{\lambda}) = \sum_{j=1}^{n} \frac{(-1)^{n-j}\lambda_j^{n-1}|f(k_j(s), l_j(s))|^2}{\alpha_j(\vec{\lambda})\beta_{n,j}(\vec{\lambda})}, \\ &|k_j(s)|^2 = |l_j(s)|^2 = E_j(s) = (\lambda_j s)^2, \quad s > 0, \\ &\vec{\lambda} = (\lambda_1, \ldots, \lambda_n), \ \lambda_1 = 1, \ \lambda_{j_1} < \lambda_{j_2} \ \text{ for } \ j_1 < j_2, \end{aligned} \tag{3.6}$$

where $k_j(s)$, $l_j(s)$ are defined by (3.3), and $p \in \mathbb{R}^d$, $p \cdot \omega = 0$, $\omega \in \mathbb{S}^{d-1}$ (and ω, p are fixed), and $\alpha_j(\vec{\tau})$, $\beta_{n,j}(\vec{\tau})$ are defined in (2.3).

Proof. Using (1.9) we obtain that

$$|f(k(s), l(s))|^2 = f(k(s), l(s))\overline{f(k(s), l(s))} = \left(\sum_{j=1}^{N} \frac{a_j(p, \omega)}{s^{j-1}} + \mathcal{O}(s^{-N})\right)\overline{\left(\sum_{j=1}^{N} \frac{a_j(p, \omega)}{s^{j-1}} + \mathcal{O}(s^{-N})\right)} =$$

$$= \sum_{j=1}^{N} \frac{b_j(p, \omega)}{s^{j-1}} + \mathcal{O}(s^{-N}), \text{ as } s \to +\infty, \tag{3.7}$$

where

$$b_1(p,\omega) = |a_1(p,\omega)|^2, \tag{3.8}$$

and

$$b_j(p,\omega) = \sum_{k=1}^{j} a_k(p,\omega)\overline{a_{j-k+1}(p,\omega)}. \tag{3.9}$$

Formulas (3.5), (3.6) follow from (3.7) and (2.4)–(2.7).

□

4 Further theoretical results on inverse scattering at high energies

The results of this section include a variation of formulas (3.1), (3.2), (3.5), (3.6) which is considerably more convenient for numerical applications to inverse scattering at high energies. The results of this section also include formulas for inverse scattering from boundary values of the scattering wave functions ψ^+ at several large energies.

4.1 Further formulas for inverse scattering from the scattering amplitude f

Note that formulas (1.12), (3.1), (3.2), (3.5), (3.6) are not very convenient for numerical inverse scattering. The reason is that the parametrisation of k and l given by (1.10) is not very convenient. This point was already explained at the end of Subsection 3.1. However, for $v \in \mathcal{C}_c^\infty(\mathbb{R}^d)$, the following formula also holds:

$$f(k(s), l(s)) = \sum_{j=1}^{N} \frac{a_j(p,\omega)}{s^{j-1}} + \mathcal{O}(s^{-N}) \text{ as } s \to +\infty, \tag{4.1}$$

where

$$\begin{aligned} &k(s) = p/2 + (E - p^2/4)^{1/2}\omega, \quad l(s) = -p/2 + (E - p^2/4)^{1/2}\omega, \quad E = E(s) = s^2, \\ &p \in \mathbb{R}^d, \quad p \cdot \omega = 0, \quad \omega \in \mathbb{S}^{d-1}, \end{aligned} \tag{4.2}$$

and

$$a_1(p,\omega) = \widehat{v}(p), \tag{4.3}$$

where $\widehat{v}$ is defined by (1.6). In particular, due to (4.1)-(4.3), we have that

$$\widehat{v}(p) = f(k(s), l(s)) + \mathcal{O}(s^{-1}), \text{ as } s \to +\infty, \tag{4.4}$$

which follows also from (1.8).

Formulas (4.1)-(4.4) (as well as formulas (1.9)-(1.12)) follow from formula (1.5) and Propositions 2.4, 2.7 of [42] (see also, [15], [7] and other references in [42]). Note that a_j in (4.1) are different from a_j in (1.9) (in general).

In contrast with formulas (1.9)-(1.12), formulas (4.1)-(4.4) for fixed $s = \sqrt{E}$, $d \geq 2$, are considered for $|p| \leq 2\sqrt{E}$ in place of $|p| \leq \sqrt{E}$, and $k(s) - l(s) = p$ in (4.2). This is the advantage of formulas (4.1)-(4.4) in comparison with (1.9)-(1.12).

As a corollary of formulas (2.4)–(2.7) and formulas (4.1)–(4.3), we obtain the following result.

Theorem 4.1. *Let $v \in \mathcal{C}_c^\infty(\mathbb{R}^d)$. Then formulas (3.1), (3.2), (3.5), (3.6) are valid, where*

$$k_j(s) = p/2 + (E_j - p^2/4)^{1/2}\omega, \quad l_j(s) = -p/2 + (E_j - p^2/4)^{1/2}\omega, \quad E_j = E(s_j) = s_j^2, \\ p \in \mathbb{R}^d, \quad p \cdot \omega = 0, \quad \omega \in \mathbb{S}^{d-1}, \tag{4.5}$$

in place of (3.3).

The formulas of Theorem 4.1 (as well as formulas (3.1), (3.2), (3.5), (3.6)) and inversion formulas for the Fourier transform give a method for inverse scattering from the scattering amplitude f at several large energies.

In particular, in connection with reconstruction from the Fourier transform on a ball, see [17] and references therein.

4.2 Multipoint formulas for inverse scattering from boundary values of ψ^+

Consider the scattering solutions ψ^+ satisfying (1.2), (1.3). For $v \in \mathcal{C}_c^\infty(\mathbb{R}^d)$, we have that

$$\psi^+(x,k) = e^{ikx}\left(1 + \sum_{j=1}^{N-1} \frac{b_j(x,\theta)}{s^j} + \mathcal{O}(s^{-N})\right), \text{ as } s \to +\infty, \tag{4.6}$$

$$b_1(x,\theta) = \frac{1}{2i} Dv(x,-\theta), \quad Dv(x,\theta) := \int_0^{+\infty} v(x+\tau\theta)d\tau, \tag{4.7}$$

where $x \in \mathbb{R}^d$, $s = |k|$, $\theta = k/|k|$ (x and θ are fixed). Formulas (4.6), (4.7) are well-known; see [42] and references therein. Note that Dv is known as the divergent beam transform of v; see, for example, [23].

Suppose that $supp\, v \subset \Omega$, where Ω is an open bounded convex domain in $\mathbb{R}^d$ with smooth boundary $\partial\Omega$. Let

$$\Sigma = \{(x,\theta) : x \in \partial\Omega,\ \theta \in \mathbb{S}^{d-1},\ \nu_x\theta > 0\}, \tag{4.8}$$

where ν_x denotes the outward normal to $\partial\Omega$ at point x. Then $2ib_1(x,\theta) = Dv(x,-\theta)$, $(x,\theta) \in \Sigma$, can be considered as the X-ray transform of v.

The methods for reconstructing v from its X-ray transform are developed in very details; see, for example, [23].

As a corollary of formulas (2.4)–(2.7) and (4.6), (4.7), we obtain the following result.

Theorem 4.2. *Let $v \in \mathcal{C}_c^\infty(\mathbb{R}^d)$. Let*

$$z(x,k) = 2i|k|(e^{-ikx}\psi^+(x,k) - 1). \tag{4.9}$$

Then

$$Dv(x,-\theta) = a_{1,n}(x,\theta,s,\vec{\tau}) + \mathcal{O}(s^{-n}), \text{ as } s \to +\infty, \tag{4.10}$$

$$a_{1,n}(x,\theta,s,\vec{\tau}) = \sum_{j=1}^{n} y_j(s,\vec{\tau}) z(x, s_j(s)\theta), \tag{4.11}$$

where s_j are defined by (2.1), y_j are defined by (2.5);

$$Dv(x,-\theta) = a_{1,n}(x,\theta,s,\vec{\lambda}) + \mathcal{O}(s^{-n}), \text{ as } s \to +\infty, \tag{4.12}$$

$$a_{1,n}(x,\theta,s,\vec{\lambda}) = \sum_{j=1}^{n} y_j(s,\vec{\lambda}) z(x, s_j(s)\theta), \tag{4.13}$$

where s_j are defined by (2.2), y_j are defined by (2.7).

Formulas (4.9)-(4.13) are new for $n \geq 2$.

Formulas (4.9)-(4.13) and inversion formulas for the X-ray transform (see, e.g., [23]) give a method for inverse scattering from the boundary values $\psi^+(x,s\theta)$, $(x,\theta) \in \Sigma$ at several large s (that is, at several large energies).

5 Regularisation of multipoint formulas for the noisy case

Note that formulas (2.4), (2.5) and related formulas of Sections 3 and 4 are unstable with respect to random noise in z, in f and $|f|^2$, and in ψ^+, if $n \geq 2$ and s increases; see Sections 6 and 7. Formulas (2.6), (2.7) are considerably more stable in this respect. The reasons are that the coefficients $y_j(s, \vec{\tau})$ behave as

$$y_j(s, \vec{\tau}) = \mathcal{O}(s^{n-1}), \quad s \to +\infty, \tag{5.1}$$

in formulas (2.5), and as

$$y_j(s, \vec{\lambda}) = \mathcal{O}(1), \quad s \to +\infty, \tag{5.2}$$

in formulas (2.7). Therefore, the approximation $a_{1,n}$ in formulas (2.4) lose stability for large n, and also lose stability, when $\tau_{j+1} - \tau_j$ are small.

Suppose, for example, that the data z are given as $\zeta = z_{noisy}$:

$$\zeta(s) = z_{noisy}(s) = z(s) + \varepsilon N(s), \quad N(s) \sim \mathcal{N}(0, 1), \tag{5.3}$$

where the random variables $N(s)$ are independent for different s, and $\mathcal{N}(0, 1)$ is the normal distribution.

Below we suggest an efficient regularisation of formulas (2.4), (2.5) and also (2.6), (2.7) for the noisy case, including the model given by (5.3). In this connection, in place of $a_{1,n}$ and y_j we consider their regularised versions $a^r_{1,n}$ and y^r_j, where

$$a^r_{1,n} = \sum_{j=1}^{n} y^r_j \zeta(s_j), \tag{5.4}$$

where $s_j = s_j(s)$ is defined by (2.1) for the case of formulas (2.4), (2.5), and $s_j = s_j(s)$ is defined by (2.2) for the case of formulas (2.6), (2.7). Note that if $\varepsilon = 0$ in (5.3), then $a^r_{1,n}$ reduces to regularized reconstruction from noiseless data. Our construction of y^r is as follows.

Let π_k denote the orthogonal projection of $\mathbb{R}^n$ on the $span(\gamma_1, ..., \gamma_k)$, where γ_j are the vectors arising in (2.10) or in (2.11), and $k = 1, ..., n$.

Lemma 5.1. *Let y solve (2.10) or (2.11). Then:*

$$(\gamma_i, \pi_k y) = \begin{cases} 1 \text{ for } i = 1, \\ 0 \text{ for } 1 < i \leq k; \end{cases} \tag{5.5}$$

$$\pi_1 y = \frac{\gamma_1}{n}, \quad \pi_n y = y, \tag{5.6}$$

$$\frac{1}{\sqrt{n}} = \|\pi_1 y\| \leq \|\pi_2 y\| \leq ... \leq \|\pi_n y\| = \|y\|. \tag{5.7}$$

Proof of Lemma 5.1. Let $y^\perp_k := y - \pi_k y$. From the definition of π_k, we have that $(y^\perp_k, \gamma_j) = 0$, for $j = 1, ..., k$. Therefore, from formulas (2.10) or (2.11) we have that

$$(\gamma_i, \pi_k y) = (\gamma_i, y - y^\perp_k) = (\gamma_i, y) - (\gamma_i, y^\perp_k) = \delta^1_i, \tag{5.8}$$

where δ^j_i is the Kronecker delta. Thus, (5.5) is proved.

Next, using the definition of π_1, formula (5.5) for $k = 1$, and the fact that $\gamma_1 = (1, 1, ..., 1)$, we have that $\pi_1 y = \gamma_1/n$.

In addition, π_n is an identity operator, since $\gamma_1, ..., \gamma_n$ are linearly independent in $\mathbb{R}^n$. Thus, (5.6) is proved.

Formula (5.7) follows from (5.6) and the definition of π_k.

Lemma 5.1 is proved. □

We consider a regularisation parameter $r \in [n^{-1/2}, +\infty)$, where $r = +\infty$ corresponds to no regularization, and $r = n^{-1/2}$ corresponds to the strongest regularisation. Let

$$\mathbb{S}_r^{n-1} := \{x \in \mathbb{R}^n : \|x\| = r\}. \tag{5.9}$$

Let L denote the broken line defined by

$$L := \cup_{k=1}^{n-1}[\pi_k y, \pi_{k+1} y], \tag{5.10}$$

where y solves (2.10) or (2.11).

Our regularised $y^r = (y_1^r, ..., y_n^r)$ mentioned in (5.4) is defined by

$$y^r := \begin{cases} y, \text{ if } |y| \le r, \\ L \cap \mathbb{S}_r^{n-1}, \text{ if } |y| > r, \end{cases} \tag{5.11}$$

where y solves (2.10) or (2.11). This definition takes into account formula (5.7).

Computation of y^r is described in Algorithm 6 for the case of y solving (2.10). The case of y solving (2.11) is similar.

Proposition 5.2. *Suppose that assumptions (5.3), (5.4), (5.11) are fulfilled. Let*

$$m = m(y, r) = \max\{k : \|\pi_k y\| \le r\}. \tag{5.12}$$

Then:

$$\mathbb{D}(a_{1,n}^r) \le r^2 \varepsilon^2, \tag{5.13}$$

$$\mathbb{E}a_{1,n}^r = a_1 + \sum_{j=1}^{n} y_j^r z_m(s_j), \tag{5.14}$$

where

$$z_m(s) = z(s) - \sum_{k=1}^{m} \frac{a_k}{s^{k-1}}. \tag{5.15}$$

Due to formula (5.13), using parameter r, we control the dispersion $\mathbb{D}(a_{1,n}^r)$. The point is that without regularization (i.e., for $r = +\infty$) the dispersion $\mathbb{D}(a_{1,n}(s))$ rapidly increases when $n \ge 2$ and s increases for the case (2.5), (2.10).

In addition, for the case (2.7), (2.11), the number $m = m(y, r)$ in (5.12) is independent of s. Therefore, for this case, the error

$$\mathbb{E}(a_{1,n}^r) - a_1 = \mathcal{O}(s^{-m}), \quad s \to +\infty, \tag{5.16}$$

where m may be considerably greater than 1 for large n and not too small r.

In turn, for the case (2.5), (2.10), a proper theoretical analysis of advantages of $\mathbb{E}(a_{1,n}^r)$ in comparison with $\mathbb{E}(a_{1,1}^r)$ is more complicated and will be given elsewhere. However, we clearly see these advantages in our numerical examples.

Proof of Proposition 5.2. Using (5.3), (5.4), (5.11), we obtain that

$$\mathbb{D}(a_{1,n}^r) = \mathbb{D}\left(\sum_{j=1}^{n} y_j^r \zeta(s_j(s))\right) = \left(\sum_{j=1}^{n} (y_j^r)^2\right) \varepsilon^2 \le r^2 \varepsilon^2. \tag{5.17}$$

From (5.3), (5.4), (5.5), (5.15) we have

$$\mathbb{E}a^r_{1,n} = \mathbb{E}\sum_{j=1}^{n} y_j^r \zeta(s_j(s)) = \sum_{j=1}^{n} y_j^r z(s_j(s)) = \sum_{j=1}^{n} y_j^r \left(\sum_{k=1}^{m} \frac{a_k}{s_j^{k-1}} + z_m(s_j) \right) =$$
$$= \sum_{k=1}^{m} a_k \sum_{j=1}^{n} \frac{y_j^r}{s_j^{k-1}} + \sum_{j=1}^{n} y_j^r z_m(s_j) = \sum_{k=1}^{n} a_k(\gamma_j, y^r) + \sum_{j=1}^{n} y_j^r z_m(s_j) = a_1 + \sum_{j=1}^{n} y_j^r z_m(s_j). \tag{5.18}$$

Proposition 5.2 is proved. □

The approach based on formulas (5.4), (5.11), (5.13), (5.14) for regularising formulas (2.4)-(2.7) can be also used for the case when

$$\begin{aligned} &\zeta(s) = z^{noise}(s) = z(s) + \xi(s), \\ &\mathbb{E}\xi = 0, \text{ and } \xi(s) \text{ are independent for different } s. \end{aligned} \tag{5.19}$$

In this connection, the simplest possibility consists in replacing the dispersion ε^2 in (5.13) by

$$D = \max_{j=1\ldots n} (\mathbb{D}\xi(s_j)). \tag{5.20}$$

Algorithm 6:

function $a_1 = \texttt{z\_reco\_stable}(s, n, \tau, z, r)$

// regularized reconstruction Algorithm proposed in Section 5.

Input:

$s > 0$: minimal point

n: number of points

$\tau = (\tau_1, ..., \tau_n)$: vector of point steps, s.t. $0 = \tau_1 < ... < \tau_n$

z: function of the form (1.1) given in points $\{s + \tau_1, ..., s + \tau_n\}$

$r \geq n^{-1/2}$: regularization parameter

Output:

$a^r_{1,n}$: stable approximation of the first term of function z

$a^r_{1,n} = 0$

// Compute initial vector $\vec{y}$ defined in (2.5)

for *j = 1..n* **do**

  $y(j) = (-1)^{n-j}/(\text{alpha}(j, \tau) \times \text{beta}(n, j, \tau))$

  // alpha, beta are defined in (2.3)

  $y(j) = y(j) \times (s + \tau(j))^{n-1}$

end

// Define vectors gamma{j} arising in Lemma 5.1

for *j = 1..n* **do**

  for *k = 1..n* **do**

    gamma{j}(k) $= 1/(s + \tau(k))^{j-1}$

  end

end

// Compute Gram matrix for vectors gamma{j}.

for *j = 1..n* **do**

  for *k = 1..n* **do**

    $G(j, k) = dot(gamma\{j\}, gamma\{k\})$

    // dot(·, ·) is scalar product of vectors

  end

end

// Find scalar products of y and space vectors gamma{k}

for *k = 1..n* **do**

  $Ay(k) = dot(y, gamma\{k\})$

end

// Find orthogonal projections $P\{k\}$ of vector $\vec{y}$ to subspaces
$< gamma\{1\}, .., gamma\{k\} >$

for *k = 1..n* **do**

  // Solve system of linear equations with matrix G(1:k, 1:k) and right-hand side Ay(1:k)

  $Projection = \text{Solve}(G(1{:}k, 1{:}k), Ay(1{:}k))$

  // G(1:k, 1:k) is k-submatrix of Gram matrix, Ay(1:k) is k-subvector of vector Ay

  $P\{k\} = \sum_{j=1..k} Projection(j) \cdot gamma\{j\}$

end

Find k, s.t. $|P\{k\}| \leq r < |P\{k+1\}|$.

Find $t \in [0, 1)$, s.t. $|P\{k\}(1-t) + P\{k+1\}t| = r$.

$a^r_{1,n} = dot(P\{k\}(1-t) + P\{k+1\}t, z)$

6 Numerical examples of total charge recovering

We consider

$$z(s) = s\sum_{j=1}^{J}\frac{q_j}{|s\theta - x_j|}, \quad a_1 = \sum_{j=1}^{J} q_j, \quad \theta \in \mathbb{S}^2, \quad x_j \in \mathbb{R}^3. \tag{6.1}$$

Such functions z are of the form (1.1). In addition, z in (6.1) can be written as $z(s) = sU(s\theta)$, where U is defined by (1.15), (1.17).

For such functions z we consider the n-point reconstructions $a_{1,n}$ of a_1 defined by (2.5). We also consider the regularized reconstructions $a^r_{1,n}$ defined using formulas (5.4), (5.11). In addition, we model the noisy date using (5.3) and some other special cases of (5.19).

Note that in order to compare n-point reconstructions $a_{1,n}$ properly for different n, we compare $\widetilde{a}_{1,n}(s) = a_{1,n}(s - \tau_n, \vec{\tau})$. The reason is that $\widetilde{a}_{1,n}(s)$ are constructed from $\{z(s - \tau_n), ..., z(s - \tau_1)\}$ with the same maximal point $s - \tau_1 = s$ for different n. Similarly, for the regularized case, we compare $\tilde{a}^r_{1,n}(s) = a^r_{1,n}(s - \tau_n, \vec{\tau})$ for different n.

Note also that numerical examples given below in Subsections 6.1 and 6.2 can be also considered as preliminary tests of n-points reconstructions $a_{1,n}$ and $a^r_{1,n}$ before much more complicated numerical problem studied in Section 7.

6.1 Simplest test

Let

$$z(s) = \frac{s}{s+1}, \quad s > 0. \tag{6.2}$$

Then $a_1 = 1$ in expansion (1.1).

Note that $z(s)$ in (6.2) arise as $z(s)$ in (6.1), where $J = 1$, $q_1 = 1$, $x_1 = (-1, 0, 0)$, $\theta = (1, 0, 0)$.

Fig. VI.1(a) shows the n-point reconstructions $\widetilde{a}_{1,n}(s) = a_{1,n}(s - \tau_n, \vec{\tau})$ from noiseless data $\{z(s - \tau_n), ..., z(s - \tau_1)\}$, where z is defined by (6.2), $n = 1, 2, 3$, and $\tau_j = (j - 1)$. Fig. VI.1(b) shows related reconstructions $\widetilde{a}_{1,n}(s)$ from noisy data $\{\zeta(s - \tau_n), ..., \zeta(s - \tau_1)\}$, where $n = 1, 2, 3$, and

$$\zeta(s) := z(s) + 0.01 \cdot N(s), \quad \text{where } N(s) \sim \mathcal{N}(0, 1) \text{ are i.i.d. for different } s. \tag{6.3}$$

Fig. VI.1(a) confirms that the precision of n-point reconstructions $\widetilde{a}_{1,n}$ from the exact data increases when n increases; see Section 2 for related theoretical results. Fig. VI.1(b) confirms that the reconstructions $\widetilde{a}_{1,n}(s)$ from noisy data become very unstable when $n \geq 2$, and s increases; see Section 5 for related theoretical discussion.

Fig. VI.2(a) shows the regularized n-point reconstructions $\tilde{a}^r_{1,n}(s) = a^r_{1,n}(s - \tau_n, \vec{\tau})$ from noiseless data $\{z(s - \tau_n), ..., z(s - \tau_1)\}$, where z is defined by (6.2), $n = 1, 2, 3$, and $\tau_j = (j - 1)$. Fig. VI.2(b) shows the related regularized n-point reconstructions $\tilde{a}^r_{1,n}(s)$ from noisy data $\{\zeta(s - \tau_n), ..., \zeta(s - \tau_1)\}$, where $\zeta(s)$ is defined by formula (6.3). These regularized reconstructions are defined using formulas (5.4), (5.11), with $r = \sqrt{5}$.

Fig. VI.1(a) and Fig. VI.2(a) show that $\tilde{a}^r_{1,n}(s)$ converges more slowly to a_1, than $\widetilde{a}_{1,n}(s)$, for $n = 2, 3$. However, the principle advantage of $\tilde{a}^r_{1,n}(s)$ in comparison with $\widetilde{a}_{1,n}(s)$ consists in much stronger stability with respect to noise; see Fig. VI.1(b) and Fig. VI.2(b). Note that the relationship between stability and precision of $\tilde{a}^r_{1,n}(s)$ depends on r.

Note that the reconstructions $\widetilde{a}_{1,n}$ and $\tilde{a}^r_{1,n}$ shown in Fig. VI.1(a) and Fig. VI.2(a) are the mathematical expectations of the reconstructions from noisy data shown in Fig. VI.1(b) and Fig. VI.2(b), respectively.

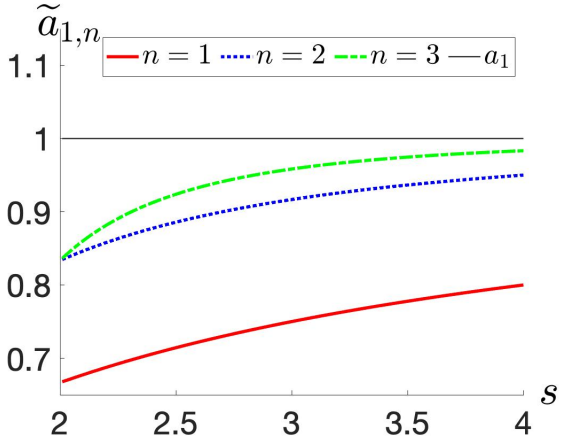

(a) Exact data. No regularization.

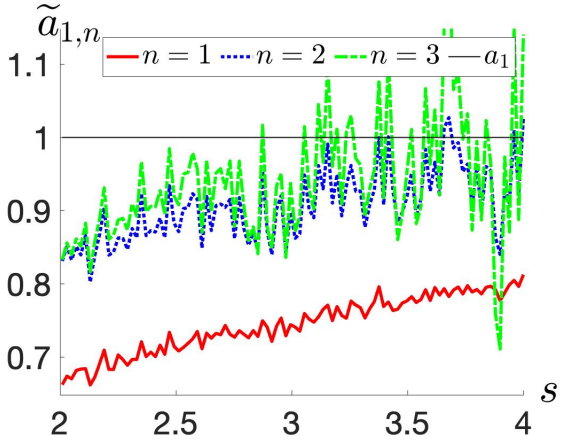

(b) Noisy data. No regularization.

Figure VI.1: n-point reconstructions $\widetilde{a}_{1,n}(s) = a_{1,n}(s-\tau_n, \vec{\tau})$ of $a_1 = 1$ for the case of z defined by (6.2) with $\tau_j = j-1$, $j = 1, ..., n$.
(a) The case of exact data.
(b) The case of noisy data simulated using formula (6.3).

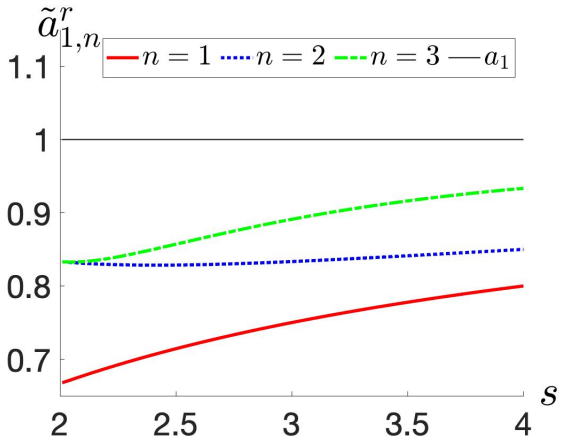

(a) Exact data. Regularization.

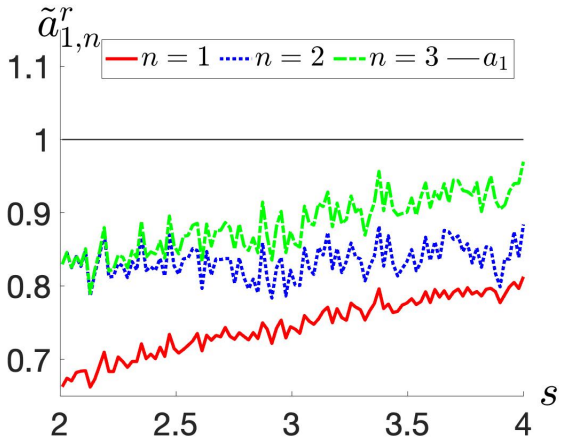

(b) Noisy data. Regularization.

Figure VI.2: n-point regularized reconstructions $\tilde{a}^r_{1,n}(s) = a^r_{1,n}(s-\tau_n, \vec{\tau})$ of $a_1 = 1$ for the case of z defined by (6.2) with $\tau_j = j-1$, $j = 1, ..., n$. Regularization parameter $r = \sqrt{5}$.
(a) The case of exact data.
(b) The case of noisy data simulated using formula (6.3).

6.2 Two point charge

Let z be of form (6.1), where

$$\begin{aligned} &J = 2, \qquad \theta = (1,0,0), \\ &q_1 = -1, \quad x_1 = (0.3669, 0.2505, -0.0518), \\ &q_2 = 2, \qquad x_2 = (0.1067, 0.2002, -0.2665). \end{aligned} \tag{6.4}$$

Then the total charge $a_1 = 1$ in expansion (1.1). This configuration can be considered as 'a dipole' with non-zero total charge.

Fig. VI.3(a) shows the n-point reconstructions $\widetilde{a}_{1,n}(s) = a_{1,n}(s-\tau_n, \vec{\tau})$ from noiseless data $\{z(s-\tau_n), ..., z(s-\tau_1)\}$, where z is defined by (6.1), (6.4), $n = 1, 2, 3$, and $\tau_j = (j-1)$. Fig. VI.3(b) shows related reconstructions $\widetilde{a}_{1,n}(s)$ from noisy data $\{\zeta(s-\tau_n), ..., \zeta(s-\tau_1)\}$, where

$n = 1, 2, 3$, and

$$\zeta(s) := z(s) + 0.01s \cdot N(s), \qquad \text{where } N(s) \sim \mathcal{N}(0,1) \text{ are i.i.d. for different } s. \tag{6.5}$$

Note that the noise model (6.5) is slightly different from the noise model (6.3), but is also a partucaler case of (5.19).

Fig. VI.3(a) confirms that the precision of n-point reconstructions $\widetilde{a}_{1,n}$ from the exact data increases when n increases (analogously to Fig. VI.1(a)). Fig. VI.3(b) confirms that the reconstructions $\widetilde{a}_{1,n}(s)$ from noisy data become very unstable when $n \geq 2$ and s increases; this instability is even stronger than for Fig. VI.1(b) because of different noise model.

Fig. VI.4(a) shows the regularized n-point reconstructions $\tilde{a}^r_{1,n}(s) = a^r_{1,n}(s - \tau_n, \vec{\tau})$ from noiseless data $\{z(s - \tau_n), ..., z(s - \tau_1)\}$, where z is defined by (6.1), (6.4), $n = 1, 2, 3$, and $\tau_j = (j - 1)$. Fig. VI.4(b) shows the related regularized n-point reconstructions $\tilde{a}^r_{1,n}(s)$ from noisy data $\{\zeta(s - \tau_n), ..., \zeta(s - \tau_1)\}$, where $\zeta(s)$ is defined by formula (6.5). These regularized reconstructions are defined using formulas (5.4), (5.11), with $r = \sqrt{2}$.

Fig. VI.3(a) and Fig. VI.4(a) show that $\tilde{a}^r_{1,n}(s)$ converges more slowly to a_1, than $\widetilde{a}_{1,n}(s)$, for $n = 2, 3$ (analogously to Fig. VI.1(a) and Fig. VI.2(a)). However, the principle advantage of $\tilde{a}^r_{1,n}(s)$ in comparison with $\widetilde{a}_{1,n}(s)$ consists in much stronger stability with respect to noise; see Fig. VI.3(b) and Fig. VI.4(b). This point is similar to the case of Fig. VI.1(b) and Fig. VI.2(b).

Note that the reconstructions $\widetilde{a}_{1,n}$ and $\tilde{a}^r_{1,n}$ shown in Fig. VI.3(a) and Fig. VI.4(a) are the mathematical expectations of the reconstructions from noisy data shown in Fig. VI.3(b) and Fig. VI.4(b), respectively.

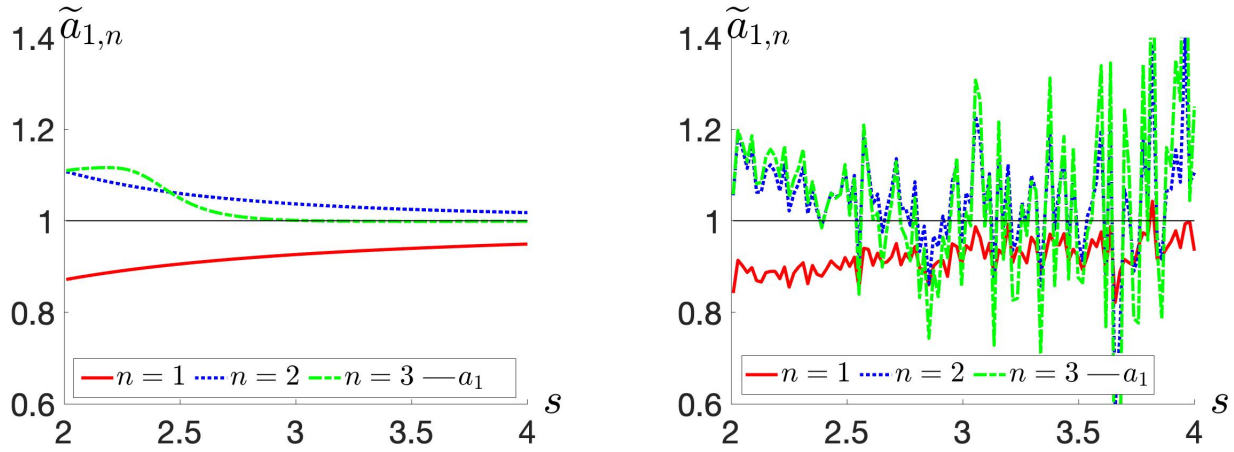

(a) Exact data. No regularization. (b) Noisy data. No regularization.

Figure VI.3: n-point reconstructions $\widetilde{a}_{1,n}(s) = a_{1,n}(s - \tau_n, \vec{\tau})$ of $a_1 = 1$ for the case of z defined by (6.1), (6.4) with $\tau_j = j - 1$, $j = 1, ..., n$.
(a) The case of exact data.
(b) The case of noisy data simulated using formula (6.5).

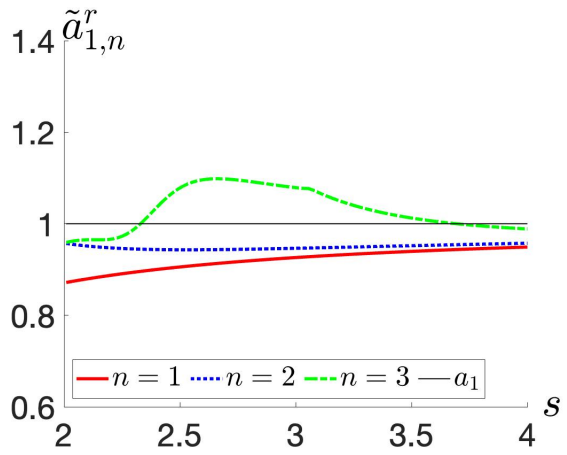

(a) Exact data. Regularization.

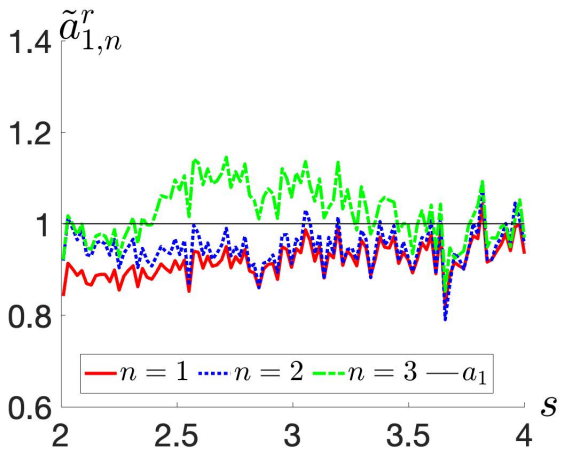

(b) Noisy data. Regularization.

Figure VI.4: n-point regularized reconstructions $\tilde{a}^r_{1,n}(s) = a^r_{1,n}(s-\tau_n, \vec{\tau})$ of $a_1 = 1$ for the case of z defined by (6.1), (6.4) with $\tau_j = j-1$, $j = 1, ..., n$. Regularization parameter $r = \sqrt{2}$.
(a) The case of exact data.
(b) The case of noisy data simulated using formula (6.5).

7 Numerical examples for inverse scattering

In this section we implement numerically formulas (1.13) and their phaseless analogues presented in Introduction, in Section 3, and with regularization of Section 5. More precisely, we illustrate numerically the n-point approximate reconstructions $\widehat{v}_n$ and $|\widehat{v}|^{2,n}$ defined in (3.1) and (3.5) and we illustrate numerically their regularized versions defined according to formulas (5.4), (5.11) and (5.19). We also present similar numerical results proceeding from Theorem 4.1.

In Subsection 7.1 we present some numerical preliminaries on direct scattering. In Subsection 7.2 we give numerical examples on finding the phased and phaseless Fourier transforms $\widehat{v}$ and $|\widehat{v}|^2$ from the phased and phaseless scattering amplitudes f and $|f|^2$ via the aforementioned $\widehat{v}_n$ and $|\widehat{v}|^{2,n}$. In particular, we show that this inverse scattering works better numerically when proceeding from its theoretical version given in Subsection 4.1.

7.1 Finding the scattering amplitude f

Given potential v, for finding the scattering amplitude $f = f(k,l)$ defined in (1.4), (1.10), we use the same codes as in [3, 24]. This numerical approach goes back to [40]. As in [3, 24], we consider the same Poisson noise model for $|f|^2$, and, for simplicity, we consider the case $d = 2$.

As in [3, 24], we represent v by $\underline{v}$ defined on the space-variable grid

$$\mathcal{X}_N := \{x = \frac{4}{N}(n_1, n_2) : n_1, n_2 \in \mathbb{Z}_N\}, \tag{7.1}$$

where

$$\mathbb{Z}_N := \left\{-\frac{N}{2}, -\frac{N}{2}+1, ..., \frac{N}{2}-1\right\}, \quad N \in 2\mathbb{N}. \tag{7.2}$$

It is also assumed that $N \geq 2\sqrt{E}/\pi$, where E is the energy in (1.2).

The main difference with [3, 24] consists in somewhat different choice of (k,l), at least, in connection with formulas (1.13), where we choose (k,l) following formula (1.10) with fixed p and ω. For the version of formulas (1.13) given in Subsection 4.1, the aforementioned difference in choice of (k,l) is considerably smaller. In any case, for simplicity, in the present work we deal with

$$\mathcal{P}^{int}_N = \{p = \frac{\pi}{2}(n_1, n_2),\ p^2 < E :\ n_1, n_2 \in \mathbb{Z}_N\}. \tag{7.3}$$

For $p \in \mathcal{P}_N^{int}$, we deal with (k,l) defined by (1.10) or (4.2), where $\omega = (-p_2,\, p_1)/|p|$, for $p \neq 0$, and $\omega = (-1,0)$, for $p = 0$. The implementation of this choice of (k,l) is described in Algorithm 7.

Our numerical implementation of $\widehat{v}_n(p,s,\vec{\tau})$ in formulas (3.1) and in their version given in Subsection 4.1 is based on Algorithms 4 and 6 in Sections 2 and 5. In this implementation, $p \in \mathcal{P}_N^{int}$. Our studies include comparisons of $\widehat{v}(p)$ and $\widehat{v}_n(p,s,\vec{\tau})$.

In particular, we show that $\widehat{v}_n$, for $n = 2$ and $n = 3$, (for the case of formulas (3.1) with exact data without regularization) improves the well-known approximation $\widehat{v}_1$, when s is not too large, $\tau_{j+1} - \tau_j$ are not too small, and p is not too far from zero.

Our studies also include similar numerical implementations of $|\widehat{v}|^{2,n}(p,s,\tau)$ via formulas (3.5).

We also show that formulas (3.1), (3.5) in their version given in Subsection 4.1 lead to better numerical results.

Algorithm 7:

function $[k\_directions, l\_directions] =$ `directions`$(s, N, type)$

// the choice of proper incident and scattered directions for formula (1.10) or (4.2)

Input:

s: current energy level $E = s^2$

N: number in $\mathcal{P}_N^{int}$

$type$: type of the grid:

$type == Melrose$ corresponds to formula (1.10), $type == Faddeev$ corresponds to formula (4.2)

Output:

$[k\_directions, l\_directions]$: set of pairs of directions $(k, l)/s$

// list of x coordinates

$p_1 = (\pi * N/2) * ((0:1:N-1)/N - 0.5)$

// list of y coordinates

$p_2 = (\pi * N/2) * ((0:1:N-1)/N - 0.5)$

// define the grid of nodes with all possible coordinates

$[P_1, P_2] = Meshgrid(p_1, p_2)$

// find small nodes indeces

$nodes\_index = find\_index(P_1^2 + P_2^2 < (s/2)^2)$

// int_nodes corresponds to $\mathcal{P}_N^{int}$ of (7.3) and p of (1.10) or (4.2)

$int\_nodes = [P_1(nodes\_index), P_2(nodes\_index)]$

// list int_nodes_ort of vectors which are orthogonal to int_nodes;

// int_nodes_ort corresponds to ω of (1.10) or (4.2)

for *k=1:length(nodes_index)* **do**

  if $P_1(nodes\_index(k))^2 + P_2(nodes\_index(k))^2 = 0$ **then**

    $int\_nodes\_ort(k) = [-1, 0]$

  else

    $int\_nodes\_ort(k) = [-P_2(nodes\_index(k)), P_1(nodes\_index(k))]/$
    $(P_1(nodes\_index(k))^2 + P_2(nodes\_index(k))^2)^{1/2}$

  end

end

// construction of k_directions and l_directions starting from int_nodes and int_nodes_ort

if $type == Melrose$ **then**

  $k\_directions = (int\_nodes + (s^2 - int\_nodes(1,:)^2 - int\_nodes(2,:)^2)^{(1/2)} * int\_nodes\_ort)/s$

  $l\_directions = int\_nodes\_ort$

else

  $k\_directions = (int\_nodes/2 + (s^2 - int\_nodes(1,:)^2/4 - int\_nodes(2,:)^2/4)^{(1/2)} * int\_nodes\_ort)/s$

  $l\_directions = (-int\_nodes/2 + (s^2 - int\_nodes(1,:)^2/4 - int\_nodes(2,:)^2/4)^{(1/2)} * int\_nodes\_ort)/s$

end

7.2 Numerical examples

We test the n-point reconstructions $\widehat{v}_n$ and $|\widehat{v}|^{2,n}$ defined in (3.1), (3.5) and their version of Subsection 4.1 for smooth potential $v = cv_0$, where v_0 is the potential shown in Figure 3(a) of [3]; and $c = 20.05/6$. The potential v is also shown in Figure 5(a) of [33]. In addition, Figure VI.5(a) below shows $|\widehat{v}|^2$, where $\widehat{v}$ is defined by (1.6).

For testing $\widehat{v}_n$ and $|\widehat{v}|^{2,n}$ defined in (3.1), (3.5) and their version of Subsection 4.1, we consider

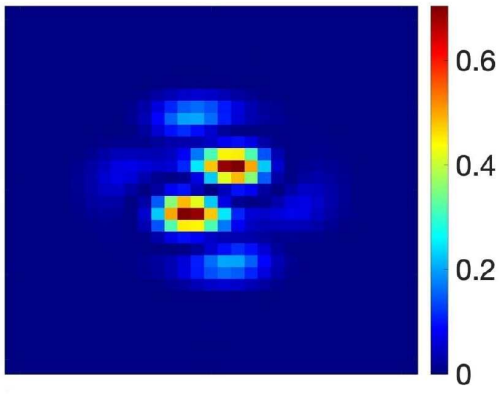

(a) Exact $|\widehat{v}|^2$.

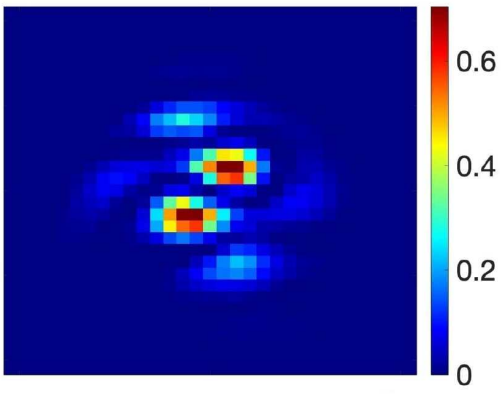

(b) Noisy data. Three-point reconstruction with regularization.

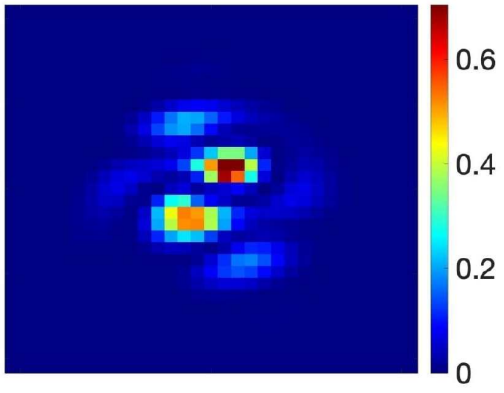

(c) Exact data. One-point reconstruction.

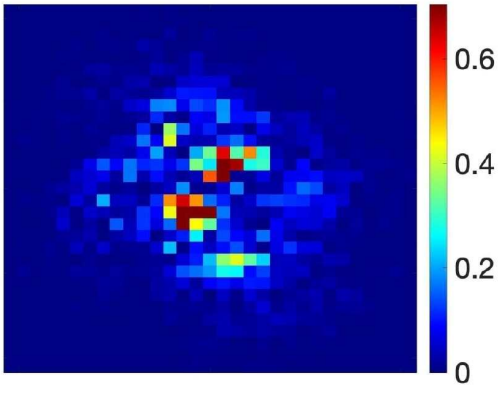

(d) Noisy data. Three-point reconstruction without regularization.

Figure VI.5: Exact $|\widehat{v}|^2$ and examples of its phaseless inverse scattering reconstructions; see Subsection 3.2, Section 5 and Subsection 7.1. (a) Exact $|\widehat{v}|^2$.
(b) Regularized reconstruction $|\widehat{v}|^{2,3,r}_{noisy}$ from noisy $|f|^2$ at $E = 25^2$, 30^2, 35^2. Regularization parameter $r = \sqrt{10}$.
(c) Reconstruction $|\widehat{v}|^{2,1}$ from $|f|^2$ at $E = 35^2$.
(d) Reconstruction $|\widehat{v}|^{2,3}_{noisy}$ from noisy $|f|^2$ at $E = 25^2$, 30^2, 35^2 without regularization.

$n = 1, 2, 3$, $E_1 = 25^2$, $E_2 = 30^2$, $E_3 = 35^2$, and $N = 572$, where N is the grid parameter mentioned in Subsection 7.1. In particular, we have that $\tau_{j+1} - \tau_j = 5$, for $n = 2, 3$.

In a similar way with Section 6, we compare $\widehat{v}_n(p, s, \vec{\tau})$ and $|\widehat{v}(p, s, \vec{\tau})|^{2,n}$ with different s for different n, and with the same maximal energy ($E = 35^2$) involved into reconstructions.

In addition, we consider $\mathcal{P}_N^{int}$ defined by (7.3), where $E = E_1$, $N \geq 2\sqrt{E_3}/\pi$.

To measure the quality of numerical reconstructions $\widehat{v}_n$ and $|\widehat{v}|^{2,n}$, we use the relative error

$$\mathfrak{E}(u, u_0, G) = \frac{\|u - u_0\|_{\ell^2(G)}}{\|u_0\|_{\ell^2(G)}}, \tag{7.4}$$

where u, u_0 are functions on some grid $G \subseteq \mathcal{P}_N^{int}$. In particular, we consider $G = \mathcal{P}_N^{small}$, where

$$\mathcal{P}_N^{small} = \{p = \frac{\pi}{2}(n_1, n_2),\ p^2 < E/4 :\ n_1, n_2 \in \mathbb{Z}_N\}. \tag{7.5}$$

The consideration of the relative error $\mathfrak{E}$ on G which is smaller than $\mathcal{P}_N^{int}$ is motivated by the fact that we cannot expect good quality of the reconstructions $\widehat{v}_n$, $|\widehat{v}|^{2,n}$ in (3.1), (3.5) near the boundary of $\mathcal{P}_N^{int}$ in view of formulas (3.4) for $|p| \approx \sqrt{E}/2$. In contrast, the approach of Subsection 4.1 overcomes this difficulty.

Our examples include multipoint reconstructions of $|\widehat{v}|^2$ from $|f|^2$ corrupted by Poisson noise. In these examples we used $N_p = 10^7$ Poisson particles per energy level.

Figure VI.5 shows exact $|\widehat{v}|^2$ and some of its multipoint reconstructions on $\mathcal{P}_N^{int}$ defined by (7.3) for $E = 25^2$. These reconstructions are based on formulas (3.1) and their regularized version suggested in Section 5.

As mentioned above, Figure VI.5(a) shows exact $|\widehat{v}|^2$.

Figure VI.5(b) shows the regularized three-point reconstruction $|\widehat{v}(p,s,\vec{\tau})|^{2,n,r}_{noisy}$, $n = 3$, $s = 25$, from noisy $|f|^2$ at $E = 25^5$, $E = 30^5$, $E = 35^5$, with regularization parameter $r = \sqrt{10}$.

Figure VI.5(c) shows the standard one-point reconstruction $|\widehat{v}|^{2,1}(p,s,\vec{\tau})$ for $s = 35$, from noiseless $|f|^2$ at $E = 35^2$.

Figure VI.5(d) shows three-point reconstruction $|\widehat{v}(p,s,\vec{\tau})|^{2,n}_{noisy}$, $n = 3$, $s = 25$, from noisy $|f|^2$ at $E = 25^5$, $E = 30^5$, $E = 35^5$ without regularization.

In particular, Figure VI.5 shows that the regularized three-point reconstruction $|\widehat{v}|^{2,3,r}_{noisy}$ even from noisy data is better than the standard one-point reconstruction $|\widehat{v}|^{2,1}$ from exact data with the same maximal energy. Besides, Figure VI.5 shows that the three-point reconstruction $|\widehat{v}|^{2,3,r}_{noisy}$ from noisy data without regularization does not work.

Note that $|y|^2 \approx 2000$ in formula (2.5), $n = 3$, $s = 25$, used for reconstructions of Figures VI.5(d). Roughly speaking, this increases the initial dispersion in noisy values of $|f|^2$ in 2000 times. This leads to very bad reconstruction shown in Figure VI.5(d). In contrast, $|y^r|^2 = 10$, which is much smaller than 2000, and leads to proper result shown in Figure VI.5(b).

In addition to Figure VI.5, we describe and compare our multipoint reconstructions in Tables VI.1, VI.2, VI.3, VI.4. The reconstructions considered in Tables VI.1 and VI.2 proceed from formulas (3.1), (3.5) and involve an input data grid based on (1.10). The reconstructions considered in Tables VI.3 and VI.4 proceed from formulas (3.1), (3.5) in their version of Subsection 5 and involve an input data grid based on (4.2).

j	1	2	3
$\mathfrak{E}(\widehat{v}_j, \widehat{v})$	0.3444	0.1570	0.0822
$\mathfrak{E}(\lvert\widehat{v}_j\rvert^2, \lvert\widehat{v}\rvert^2)$	0.3244	0.1979	0.0524

Table VI.1: Relative L_2 errors $\mathfrak{E}(\widehat{v}_j, \widehat{v})$ and $\mathfrak{E}(|\widehat{v}_j|^2, |\widehat{v}|^2)$ on $\mathcal{P}_N^{small}$ for different reconstructions $\widehat{v}_j$ of $\widehat{v}$, where data grid parameters (k,l) are defined using (1.10).

j	1	2	3
$\mathfrak{E}(\lvert\widehat{v}\rvert^{2,j}, \lvert\widehat{v}\rvert^2)$	0.3244	0.1691	0.0921
$\mathfrak{E}(\lvert\widehat{v}\rvert^{2,j}_{noisy}, \lvert\widehat{v}\rvert^2)$	0.3226	0.2590	0.6219
$\mathfrak{E}(\lvert\widehat{v}\rvert^{2,j,r}_{noisy}, \lvert\widehat{v}\rvert^2)$	0.3226	0.2468	0.1953

Table VI.2: Relative L_2 errors $\mathfrak{E}(|\widehat{v}|^{2,j}, |\widehat{v}|^2)$ on $\mathcal{P}_N^{small}$ for different non-regularized reconstructions $|\widehat{v}|^{2,j}$ of $|\widehat{v}|^2$ from exact phaseless data, noisy phaseless data, and regularized reconstructions from noisy phaseless data. Data grid parameters (k,l) are defined using (1.10). Regularization parameter $r = \sqrt{10}$.

j	1	2	3
$\mathfrak{E}(\widehat{v}_j, \widehat{v})$	0.2607	0.0840	0.0316
$\mathfrak{E}(\lvert\widehat{v}_j\rvert^2, \lvert\widehat{v}\rvert^2)$	0.2908	0.1396	0.0242

Table VI.3: Relative L_2 errors $\mathfrak{E}(\widehat{v}_j, \widehat{v})$ and $\mathfrak{E}(|\widehat{v}_j|^2, |\widehat{v}|^2)$ on $\mathcal{P}_N^{small}$ for different reconstructions $\widehat{v}_j$ of $\widehat{v}$, where data grid parameters (k,l) are defined using (4.2). This table is a version of Table VI.1, corresponding to Subsection 4.1.

j	1	2	3
$\mathfrak{E}(\lvert\widehat{v}\rvert^{2,j}, \lvert\widehat{v}\rvert^2)$	0.2908	0.1269	0.0475
$\mathfrak{E}(\lvert\widehat{v}\rvert^{2,j}_{noisy}, \lvert\widehat{v}\rvert^2)$	0.2895	0.1736	0.6552
$\mathfrak{E}(\lvert\widehat{v}\rvert^{2,j,r}_{noisy}, \lvert\widehat{v}\rvert^2)$	0.2895	0.2186	0.1536

Table VI.4: Relative L_2 errors $\mathfrak{E}(|\widehat{v}|^{2,j}, |\widehat{v}|^2)$ on $\mathcal{P}_N^{small}$ for different non-regularized reconstructions $|\widehat{v}|^{2,j}$ of $|\widehat{v}|^2$ from exact phaseless data, noisy phaseless data, and regularized reconstructions from noisy phaseless data. Data grid parameters (k, l) are defined using (4.2). Regularization parameter $r = \sqrt{10}$. This table is a version of Table VI.2, corresponding to Subsection 4.1.

As well as Figure VI.5, Tables VI.1, VI.2, VI.3, VI.4 show that our multipoint reconstructions of $\widehat{v}$ or $|\widehat{v}|^2$ are much better than the classical one-point reconstructions, under the condition that the multipoint reconstructions are properly regularized for the noisy case. These tables also show that formulas (3.1), (3.5) in their version of Subsection 4.1 lead to considerably better reconstructions than the initial formulas (3.1), (3.5).

Note that the reconstructions $|\widehat{v}|^{2,3,r}_{noisy}$, $|\widehat{v}|^{2,1}$, $|\widehat{v}|^{2,3}_{noisy}$ mentioned in Table VI.2 are shown in Figure VI.5(b), (c), (d). Note also that the three-point reconstructions $|\widehat{v}_3|^2$, $|\widehat{v}|^{2,3}$ from noiseless data mentioned in Tables VI.1–VI.4 look similar to exact $|\widehat{v}|^2$ shown in Figure VI.5(a). For more figures in connection with reconstructions considered in Tables VI.1–VI.4, see [33].

8 Conclusion

Many functions arising in direct and inverse problems admit the asymptotic expansion of the form (1.1). In many cases, the most important information is contained in the leading coefficient a_1, which can be approximately reconstructed from z at a sufficiently large point s using the standard one-point formula

$$a_1 = z(s) + \mathcal{O}(s^{-1}), \text{ as } s \to +\infty. \tag{8.1}$$

In this work we continued studies on reconstruction of the leading coefficient a_1 in expansion (1.1) from measurements of z at *several* sufficiently large points s (multipoint reconstruction approach). In particular, we presented the first numerical implementation of the recent theoretical formulas of [27] on this reconstruction. Our results include an efficient regularization of these multipoint formulas for the case of random noise.

We tested our general studies for the case of total electrical charge recovering from measurements at several remote points and for the case of inverse scattering at several high energies. In the second case, we proceed from the theoretical work [28]. We demonstrated that our numerical implementation of the aforementioned multipoint formulas essentially improves the reconstruction based on formula (8.1). We also improved and developed considerably theoretical formulas of [28] on inverse scattering at several large energies; see Section 4.

Important advantages of the aforementioned multipoint approach consist in explicit reconstruction formulas, easy and fast numerical implementation, considerable increasing in precision in comparison with (8.1) already for the two-point case, small or moderate number of measurements required for reconstruction.

In our opinion, the results of the present work open perspectives of numerical applications of the aforementioned multipoint studies to different inverse and direct problems. These issues include, in particular, further studies on:

(i) phased or phaseless inverse scattering at several high energies,
including the case of potentials v with discontinuities mentioned in Introduction;

(ii) determination of total electrical or gravitational charge from several exterior measurements;

(iii) reconstuction of far-field (scattering amplitude) from several near-field measurements;

(iv) reconstruction of phaseless far-field (scattering amplitude) from several phaseless near-field measurements;

In this respect, issues (i) and (ii) are already discussed in this work, whereas theoretical formulas for issues (iii) and (iv) are given in [27] and [32].

Bibliography

[1] F.V. Atkinson, *On Sommerfeld's 'radiation condition'*, London, Edinburgh Dublin Phil. Mag. J. Sci. 40 645–651 (1949)

[2] N.V. Alexeenko, V.A. Burov, O.D. Rumyantseva, *Solution of the three-dimensional acoustical inverse scattering problem. The modified Novikov algorithm,* Acoust. Phys. 54(3), 407–419 (2008)

[3] A.D. Agaltsov, T. Hohage, R.G. Novikov, *An iterative approach to monochromatic phaseless inverse scattering*, Inverse Problems 35, 24001 (24 pp.) (2019)

[4] M. Born, *Quantenmechanik der Stossvorgange*, Zeitschrift fur Physik 38 (11-12), 803-827 (1926)

[5] F.A. Berezin, M.A. Shubin, *The Schrödinger Equation*, Mathematics and Its Applications, Vol. 66, Kluwer Academic, Dordrecht (1991)

[6] V.A. Burov, N.V. Alekseenko, O.D. Rumyantseva, *Multifrequency generalization of the Novikov algorithm for the two-dimensional inverse scattering problem,* Acoust. Phys. 55(6), 843–856 (2009)

[7] V.S. Buslaev, *Trace formulas and certain asymptotic estimates of the resolvent kernel for the Schrödinger operator in three-dimensional space*, Topics in Mathematical Physics, Vol. 1, Plenum Press, Oxford (1967)

[8] K. Chadan, P.C. Sabatier, *Inverse Problems in Quantum Scattering Theory*, 2nd edn. Springer, Berlin, 1989

[9] L.D. Faddeev, *Uniqueness of the solution of the inverse scattering problem,* Vestn. Leningrad Univ. 7, 126–130 (1956) (in Russian)

[10] P.G. Grinevich, *The scattering transform for the two-dimensional Schrödinger operator with a potential that decreases at infinity at fixed nonzero energy,* Russian Math. Surveys 55(6), 1015-1083 (2000)

[11] P.G. Grinevich, R.G. Novikov, *Transmission eigenvalues for multipoint scatterers*, Eurasian Journal of Mathematical and Computer Applications 9(4), 17–25 (2021)

[12] P. Hähner, T. Hohage, *New stability estimates for the inverse acoustic inhomogeneous medium problem and applications*, SIAM J. Math. Anal. 33(3), 670-685 (2001)

[13] G.M. Henkin, R.G. Novikov, *The $\overline{\partial}$-equation in the multidimensional inverse scattering problem*, Russ. Math. Surv. 42(3), 109-180 (1987)

[14] T. Hohage, R.G. Novikov, V.N. Sivkin, *Reconstruction from differential scattering cross section with background information*, hal-03806616 (2022)

[15] W. Hunziker, *Potential scattering at high energies*, Helv. Phys. Acta 36, 838–856 (1963)

[16] M.I. Isaev, R.G. Novikov, *New global stability estimates for monochromatic inverse acoustic scattering*, SIAM J. Math. Anal. 45(3), 1495-1504 (2013)

[17] M.I. Isaev, R.G. Novikov, G. V. Sabinin, *Numerical reconstruction from the Fourier transform on the ball using prolate spheroidal wave functions,* Inverse Problems 38(10), 105002 (2022)

[18] A. Jollivet, *On inverse scattering at fixed energy for the multidimensional Newton equation in a non-compactly supported field,* Journal of Inverse and Ill-Posed Problems 21(6), 713-734 (2013)

[19] M.V. Klibanov, *Phaseless inverse scattering problems in three dimensions*, SIAM J.Appl. Math. 74(2), 392-410 (2014)

[20] M.V. Klibanov, N.A. Koshev, D.-L. Nguyen, L.H. Nguyen, A. Brettin, V.N. Astratov, *A numerical method to solve a phaseless coefficient inverse problem from a single measurement of experimental data*, SIAM J. Imaging Sci. 11(4), 2339-2367 (2018)

[21] L.D. Landau, E.M. Lifschitz, *The classical theory of fields,* Pergamon press, chapter 5.41 (1971)

[22] R.B. Melrose, *Geometric Scattering Theory. Stanford Lectures,* Cambridge University Press (1995)

[23] F. Natterer, *The Mathematics of Computerized Tomography*, Society for Industrial Mathematics, 184 pp. (2001)

[24] R.G. Novikov, *Multidimensional inverse spectral problem for the equation* $-\Delta\psi + (v(x) - Eu(x))\psi = 0$, Functional Analysis and Its Applications, 22(4), 263-272 (1988)

[25] R. G. Novikov, *Small angle scattering and X-ray transform in classical mechanics,* Ark. Mat. 37, 141–169 (1999)

[26] R. G. Novikov, *An iterative approach to non-overdetermined inverse scattering at fixed energy*, Sbornik: Mathematics 206(1), 120-134 (2015)

[27] R. G. Novikov, *Multipoint formulas for scattered far field in multidimensions,* Inverse Problems 36, 095001 (2020)

[28] R.G. Novikov, *Multipoint formulas for inverse scattering at high energies,* Russ. Math. Surv. 76(4), 723-725 (2021)

[29] R. G. Novikov, *Multipoint formulas for phase recovering from phaseless scattering data*, The Journal of Geometric Analysis, 31(2), 1965-1991 (2021)

[30] R.G. Novikov, *Multidimensional inverse scattering for the Schrödinger equation*, In: Cerejeiras, P., Reissig, M. (eds) Mathematical Analysis, its Applications and Computation. ISAAC 2019. Springer Proceedings in Mathematics & Statistics, vol 385, pp 75-98, Springer, Cham. (2022)

[31] R.G. Novikov, V.N. Sivkin, *Phaseless inverse scattering with background information*, Inverse Problems 37(5), 055011 (2021)

[32] R.G. Novikov, V.N. Sivkin, *Fixed-distance multipoint formulas for the scattering amplitude from phaseless measurements*, Inverse Problems 38(2), 025012 (2022)

[33] R.G. Novikov, V.N. Sivkin, G.V. Sabinin, *Multipoint formulas in inverse problems and their numerical implementation,* hal-04053473 (2023)

[34] R.G. Novikov, I.A. Taimanov, *On unitarity of the scattering operator in non-Hermitian quantum mechanics,* hal-03989986 (2023)

[35] Rakesh, M. Salo, *Fixed angle inverse scattering for almost symmetric or controlled perturbations,* SIAM J. Math. Anal. 52(6), 5467–5499 (2020)

[36] V.G. Romanov, *Inverse problems without phase information that use wave interference*, Sib. Math. J. 59(3), 494-504 (2018)

[37] V.G. Romanov, *Phaseless problem of determination of anisotropic conductivity in electrodynamic equations*, Dokl. Math. 104(3), 385-389 (2021)

[38] A.S. Shurup, *Numerical comparison of iterative and functional-analytic algorithms for inverse acoustic scattering,* Eurasian Journal of Mathematical and Computer Applications 10(1), 79-99 (2022)

[39] A.S. Shurup, *Functional-analytical reconstruction of high contrast inhomogeneities,* Eurasian Journal of Mathematical and Computer Applications 11(2), 130–143 (2023)

[40] G. Vainikko, *Fast Solvers of the Lippmann-Schwinger equation,* Direct and Inverse Problems of Mathematical Physics (eds R.P. Gilbert, J. Kajiwara, Y.S. Xu) Kluwer, Dordrecht (2000)

[41] C.H. Wilcox, *A generalization of theorems of Rellich and Atkinson,* Proc. Am. Math. Soc. 7, 271–276 (1956)

[42] D. Yafaev, *High-energy and smoothness asymptotic expansion of the scattering amplitude,* Journal of Functional Analysis 202(2), 526-570 (2003)

ECOLE
DOCTORALE
DE MATHEMATIQUES
HADAMARD

Titre : Problèmes de diffusion inverse sans information de phase

Mots clés : l'équation de Schrödinger, transformation de Fourier, diffusion inverse sans information de phase, diffuseurs de fond, formules multipoints, implémentations numériques

Résumé : Cette thèse est consacrée à différentes approches pour des problèmes de diffusion inverse sans information de phase. Nos études sont motivées par des problèmes de tomographies qui utilisent des particules élémentaires (par exemple, des électrons, des rayons X) comme outil de sondage. Dans ces tomographies, seules les valeurs absolues des données de diffusion sont mesurables.
Dans le cadre de la mécanique quantique, cette limitation est liée au principe de Born selon lequel les valeurs complexes de la fonction d'onde n'ont pas d'interprétation physique directe, alors que ses valeurs absolues carrées admettent une interprétation probabiliste et peuvent être directement mesurées. Dans le cadre de l'optique (y compris la diffusion des rayons X), cette limitation est liée aux très hautes fréquences d'onde, qui ne permettent pas de mesurer directement la phase d'onde par les dispositifs techniques modernes.
Nous contribuons à la diffusion inverse sans phase en développant la méthode des diffuseurs de fond et la méthode multipoint.
La méthode des diffuseurs de fond utilise la diffusion en présence d'objets connus a priori. Par nos résultats, à cet égard, nous contribuons également au problème de récupération de phase pour la transformation de Fourier classique.
La méthode multipoint consiste à trouver des termes dominants importants (non accessibles pour les mesures directes) dans le développement asymptotique d'une fonction à partir de plusieurs valeurs de cette fonction (accessibles pour les mesures directes).
Pour les deux méthodes, nous donnons, en particulier, de nouvelles formules explicites pour divers problèmes de diffusion inverse sans (ou avec) information de phase. De plus, nous implémentons numériquement plusiers de nos résultats théoriques. Dans ces implémentations nous utilisons, en particulier, des techniques de régularisation anciennes et nouvelles.
Nos algorithmes peuvent être appliqués, par exemple, à l'imagerie par rayons X et à la tomographie électronique.

Title : Inverse scattering problems without phase information

Keywords : Schrödinger equation, Fourier transform, phaseless inverse scattering, background scatterers, multipoint formulas, numerical implementations

Abstract : This thesis is devoted to different approaches to phaseless inverse scattering problems. Our studies are motivated by problems of tomographies which use elementary particles (for example, electrons, X-ray photons) as probing tool. In these tomographies only the absolute values of scattering data are measurable.
In the framework of quantum mechanics, this limitation is related to the Born principle that complex values of the wave function don't have direct physical interpretation, whereas its absolute values squared admit probabilistic interpretation and can be directly measured. In the framework of optics (including X-ray scattering) this limitation is related to very high wave frequencies, which don't allow to measure wave phase directly by modern technical devices.
We contribute to phaseless inverse scattering by developing the method of background scatterers and the multipoint method.
The method of background scatterers uses scattering in presence of a priori known objects. By our results, in this connection, we also contribute to the phase retrieval problem for the classical Fourier transform.
The multipoint method consists in finding important leading terms (not accessible for direct measurements) in asymptotic expansion of a function from several values of this function (accessible for direct measurements).
For both methods, we give, in particular, new explicit formulas for various phaseless and phased inverse scattering problems. In addition, we implement numerically many of our theoretical results. In these implementations we use, in particular, old and new regularisation technics.
Our algorithms can be applied, for example, to X-ray imaging and to electron tomography.

Institut Polytechnique de Paris
91120 Palaiseau, France